



Departamento de biología

# INTERACTIONS BETWEEN PHYSICAL FORCING, WATER CIRCULATION AND PHYTOPLANKTON DYNAMICS IN A MICROTIDAL ESTUARY

Tesis Doctoral

Clara Llebot Lorente

Barcelona, 2010

Illustrations of the title page and the covers of chapters 2, 3 and 4 by Carme Lorente

JUAN LUIS GOMEZ PINCHETTI, SECRETARIO DEL DEPARTAMENTO DE BIOLOGÍA DE LA UNIVERSIDAD DE LAS PALMAS DE GRAN CANARIA

**CERTIFICA**,

Que el Consejo de Doctores del Departamento, en sesión extraordinaria, tomó el acuerdo de dar el consentimiento para su tramitación a la Tesis Doctoral titulada *"Interactions between physical forcing, water circulation and phytoplankton dynamics in a microtidal estuary"* presentada por la doctoranda Dª. Clara Llebot Lorente y dirigida por los Dres. Dª. Marta Estrada Miyares y D. Jordi Solé Ollé.

Y para que así conste, y a efectos de lo previsto en el Artº 73.2 del Reglamento de Estudios de Doctorado de esta Universidad, firmo la presente en Las Palmas de Gran Canaria, a 8 de octubre de 2010.



DOCTORADO EN OCEANOGRAFÍA
DEPARTAMENTO DE BIOLOGÍA

# INTERACTIONS BETWEEN PHYSICAL FORCING, WATER CIRCULATION AND PHYTOPLANKTON DYNAMICS IN A MICROTIDAL ESTUARY

**CLARA LLEBOT LORENTE**

DIRECTORES:
**MARTA ESTRADA MIYARES**
**JORDI SOLÉ OLLÉ**

| ..... | ..... | ..... |
|---|---|---|
| **MARTA ESTRADA MIYARES** | **JORDI SOLÉ OLLÉ** | **CLARA LLEBOT LORENTE** |

BARCELONA, 2010

A tots aquells que estimo

## ABSTRACT

This thesis focuses on the interactions between water circulation dynamics, nutrient availability and the structure of the phytoplanktonic community from a mesoscale point of view. To accomplish this aim we studied the micro-tidal estuaries of Alfacs and Fangar, located in the Ebre river Delta, in the Northwestern Mediterranean. The work was developed along three main lines. First, the analysis of the variability of a 14-year long time series of the phytoplankton and environmental data showed a strong seasonality of the phytoplankton communities of both bays, characterized by an autumn diatom assemblage and a winter group of dinoflagellates in Alfacs, and a flagellate-dominated group in winter, and a mixed group of dinoflagellates and diatoms in late spring and summer in Fangar. The phytoplankton dynamics and composition was different in the two bays, a finding that could be attributed to a lower residence time of the water in Fangar, which has a smaller volume than Alfacs but receives comparable inputs of freshwater. No relevant temporal trends were detected in phytoplankton abundance or composition. Second, scale considerations and a three-dimensional circulation model of Alfacs revealed that the principal forcing factors are freshwater inflow and wind, while the tide is not relevant regarding water transport or mixing. The freshwater input is important at a seasonal scale, and is responsible for the stratified situation usually found in Alfacs. The wind is particularly important at time scales of a few days and, above a certain threshold, wind events can mix the estuary and break the stratification. Based on the strength of the stratification relative to the wind speed, as expressed by a Richardson number, and the direction of the wind, three scenarios regarding the coupling between wind forcing and hydrodynamics have been defined, demonstrating the importance of wind in controlling the exchange of water with the exterior. Finally, the third line of research approached the budget of major nutrients (nitrogen N and phosphorus P) in Alfacs. A zero-dimensional ecosystem model incorporating phytoplankton, zooplankton and the concentrations of various (organic and inorganic) N and P pools suggested that the inputs of dissolved organic phosphorus (DOP) through the discharge channels are a crucial source of phosphorus to the system, explaining the draw-down of nitrogen during the summer and the observed high primary production. Two non-exclusive mechanisms could explain DOP availability for phytoplankton: direct uptake and remineralisation to dissolved inorganic phosphorus. Input of phosphorus from sediment resuspension could be important at short time scales, but did not seem to be a substantial contribution to the total P budget from a seasonal perspective. In conclusion, this thesis shows how the physical forcing can influence the composition, timing and abundance of the phytoplanktonic community in two bays that can be taken as an example of microtidal estuarine water bodies.

# Acknowledgements

*It feels strange that during such a long time I have been looking forward to writing the acknowledgements of my thesis, and now that the time has come I don't know where to start. I have decided that I will write this part in Catalan because it is the language with which I feel more comfortable acknowledging contributions. I apologize to those of you who don't speak Catalan, but I am sure that you understand my reasons, and I will make sure that I write your part in a language that you understand.*

En primer lloc, és imprescindible agrair a la Marta i el Jordi el seu paper com a directors de tesi. La Marta, treballadora incansable, ha estat sempre al peu del canó tot i les moltes altres obligacions que té, donant idees, suggerint millores, revisant, donant referències, millorant l'anglès... la seva professionalitat, els coneixements immensos i la seva exigència en fer les coses ben fetes m'han ensenyat no només ciència, sinó com fer ciència. Al Jordi li he d'agrair els ànims que sempre m'ha sabut donar en moments difícils. El fet de ser aquella persona a qui puc preguntar allò que ja hauria de saber sense sentir-me ignorant, quin llibre consultar per treure l'entrellat d'aquella formula física que em porta de cap, o com trobar solucions quan sembla que estic en un carreró sense sortida. A tots dos, els he d'agrair que m'hagin estat guiant durant aquests cinc anys en el meu aprenentatge com a investigadora.

En segon lloc, he d'agrair també l'ajuda a dos investigadors que m'han guiat i ajudat àmpliament en parts fonamentals d'aquesta tesi, i sense els quals no hauria pogut fer aquest estudi des de punts de vista tan interdisciplinaris. A Francisco Rueda tengo que agradecerle el haberme introducido al mundo de la modelización, y haberme enseñado los conceptos básicos de dinámica de fluidos. Siempre ha estado dispuesto a ayudarme, a pesar de mis largos periodos de silencio cuando había un millón de cosas urgentes que pasaban por delante de nuestro proyecto. Agradezco también sus esfuerzos para comunicar no sólo lo que está mal, sino también lo que está bien. Gran parte de nuestra comunicación, sobretodo este último año, ha sido a distancia, y quiero agradecerle su disponibilidad por correo electrónico o

Skype, especialmente cuando debido a la diferencia horaria teníamos que comunicarnos a horas incómodas. *Yvette Spitz, on the other hand, has introduced me to biological models. She has been extremely helpful, motivating, and very pacient to teach me when I didn't know anything about biological modeling or spoke English very well. I appreciate her willingness to provide advice on any subject, even if it was not directly related to our project, and her wonderful pedagogic skills. I have always felt respected and valuated by her, and I especially want to thank Yvette for her support this last year, during which she understood how important it was to me to finish this thesis and made it a high priority without putting extra pressure on me.*

Molts altres investigadors m'han ajudat, en més o menys mesura, a dur a terme aquesta tesi. L'Antonio Turiel, que em va ensenyar bones pràctiques de programació al principi del doctorat, m'ha aconsellat sempre que he trucat a la seva porta, i sempre ha mostrat un genuí interès en què la meva carrera científica arribi a bon port. L'Elisa Berdalet, que ha treballat molt per tenir un grup de gent treballant als Alfacs, perquè tinguéssim finançament, i perquè les dades de camp fossin útils i rigoroses. Vull agrair en general als investigadors del departament de biologia que sempre han estat amistosos i disposats a ajudar i a resoldre els meus dubtes. Vull agrair també el bon ambient, i l'esforç de tots per crear un departament obert, ple de bona gent, que no només es preocupen per la feina, sinó també per les persones que els envolten. També vull agrair a tots els membres del departament de física que, tot i no ser-ho oficialment, sempre m'han acollit com si fos una estudiant més del departament, m'han donat accés als recursos de càlcul i m'han aconsellat i orientat amb dedicació.

Veureu que aquesta tesi inclou resultats experimentals. He tingut la gran sort de disposar de totes aquestes dades tot i no haver hagut d'anar al camp gaire sovint. Això representa una feina immensa que espero haver reconegut amb fidelitat en cada un dels treballs. He d'agrair, doncs, amb molt i molt de fervor a tots aquells que han posat temps i energia a recopilar aquestes dades. A la Mireia Lara i el Rubén Quesada, que han anat als Alfacs incomptables vegades, i sempre m'han tingut a mi al cap a l'hora de dissenyar l'estratègia de mostreig. Per tots els munts d'ocasions en què han intentat trobar respostes pels meus inacabables dubtes sobre l'ADCP, o els termistors, o el CTD, o qualsevol detall de les campanyes, gràcies. Gràcies també a l'Elisa Berdalet, el Jaume Piera i la Marta Estrada per les seves contribucions a fer que cada una de les campanyes fos un èxit. Gràcies al Maximino Delgado, la Margarita Fernández, el Jordi Camp i tot el personal de l'IRTA que han estat recollint dades i comptant fitoplàncton des de ben abans que jo sabés què volia dir fitoplàncton. Gràcies a totes aquelles altres persones que han dut a terme treballs de camp per una cosa o altra i que m'han acabat fet servei en algun moment de la meva tesi, com l'Esther Garcés, la Sofia Loureiro, el Jordi Camp, la Mariona Segura. Moltes gràcies a tots vosaltres.

Durant aquests cinc anys de tesi he coincidit i col·laborat amb altres estudiants, que han fet la feina molt més engrescadora i agradable i han convertit la tesi en

una experiència molt humana. Vull fer un èmfasi molt especial en els estudiants, de tots els departaments, amb qui m'he trobat a l'Institut de Ciències del Mar. Crec que a l'ICM hi ha un ambient únic, ple de gent molt llesta, molt motivada, i amb molt bon cor. Em van acollir des del primer dia i hi he fet amistats que segur que duraran molt de temps. Intentaré no deixar-me ningú, i si ho faig, si us plau, l'interessat sàpiga perdonar-me. Moltes gràcies a la Vero, per ser una persona amb qui puc compartir feina i també experiències, inquietuds i plans de futur. Per ser una d'aquelles amistats en què en retrobar-se després d'un temps de separació sembla que només hagin passat cinc minuts. A la Mariona Claret per totes les estones passades a Barcelona, a Corvallis, al Wecoma, de congrés o allà on sigui. Per totes les converses i els intercanvis de sensacions sobre tot allò que ens envolta. Al Javi, una persona amb un gran cor, tot i que li agradi amagar-ho. D'ell no només he après qui va ser Genghis Khan sinó compromís, lleialtat, i saber posar la feina en el lloc adequat en la nostra escala de valors. Al Ben, un company de despatx immillorable tot i la seva predilecció per llibres amb títols extremadament avorrits, sempre disposat a escoltar i a compartir, a fer un favor o a dir una paraula amable quan més fa falta. Ells dos, junt amb el Sergio, amant de la música de qui he après què vol dir tenir una vocació, el Martí, l'ambientòleg, meteoròleg, músic, científic... i el Marc, han format el millor despatx que mai m'hagués passat pel cap. Amb ells he passat moments fantàstics, i creieu-me quan us dic que els trobo molt, molt a faltar. Als companys de l'hora de dinar i de moltes altres coses us he de felicitar per la vostra simpatia, espontaneïtat, alegria, companyia i amistat. Al Marco, la Rocío, el Roberto, la Maria Pastor, la Maria Piles, la Vero González, la Sandra, la Sofia... I també a la Bea, la Montse, la Raquel, la Lorena, la Clara, la Pati, l'Arantxa, la Mireia, el Rubén, la Cristina, l'Estela, la Maricel, l'Enric, la Gisela, Juancho... També vull agrair a la resta del personal no científic de l'ICM el seu suport en les tasques quotidianes i burocràtiques que acompanyen tota tesi doctoral. Han estat professionals i eficients, i ho agraeixo. Gràcies, també, al Xavier per totes les converses nocturnes que feien més agradable el final d'una llarga jornada.

Respecto a mi estancia en el Instituto del Agua, en Granada, tengo que agradecer la gran acogida que tuve. Muchas gracias a Anna, Andrea, Oti, Javier, Eva. Fue un placer compartir con vosotros las tostadas con tomate del desayuno, los senderos de Sierra Nevada, la campaña en el Gergal, los moros y cristianos de Elda, y las calles y tapas de la preciosa ciudad de Granada. También quiero agradecer su compañía a mis compañeras de piso Cate, Carlotta y Katy, a Antonio por su hospitalidad mientras buscaba habitación, y a Miguel por ser un guía excepcional.

*My thesis has involved various stays at Oregon State University, in Corvallis. I want to thank Tim Cowles, who was the first person to give me the opportunity to come to the US to do research. He responded with enthusiasm to my request (which I made only two days before the deadline!), and he and Susan welcomed me to their country and their house in a wonderful way that I would have never*

*expected from people who barely knew me. Tim also helped me with the first steps of biological modeling. I also want to thank the graduate students, postdocs and technicians from COAS whom I met during my stays. Thanks to Gaby, Ata, Chris, Andrey, John, Kate, Laura, Tommo, Martín, Roberto, Yvan, Piero, Cassia... I want to acknowledge also people that I have met in other situations who have made my stays a pleasure: Vaclav, Atil, Tani, Denise, Alex, Niya, Kalin, Jill, Zak, Jake, Lisa, Adam and Jen.* I una abraçada ben especial pels catalans de Corvallis: l'Alba i el David, l'Òscar i la Mariona, i la bonica Aloma.

Finalment, tan o més important que tots aquells relacionats amb la feina, ho són aquells que no hi tenen res a veure. Que m'han fet tenir una vida plena, saludable, i que sempre, sempre m'han donat suport per poder acabar aquesta tasca que semblava ben bé inacabable.

A la Gemma, la Marta, la Sílvia, les amigues de tota la vida. Aquelles en qui puc confiar-ho tot en qualsevol moment, tot i ser a l'altra punta del món. Una abraçada immensa per tantes llocades, tantes nits a la paninoteca, tants experiments culinaris, i per tantes vegades que heu estat al meu costat aguantant la meva xerrameca sobre gent que no coneixeu, tecnicismes que no us interessen o problemes que us queden molt lluny. Al Nico, no només amic excepcional sinó també company de pis. Moltes gràcies per estar sempre a punt per escoltar-me i intentar trobar solucions, per tenir més confiança en el que puc fer que jo mateixa i, simplement, per ser un amic dels de sempre i per sempre. Als de campaments, perquè amb vosaltres he compartit moments molt intensos, i he après el valor de l'esforç que fa falta per arribar al cim, de formar part d'un grup, de la bellesa i la màgia dels Pirineus. Per totes les excursions amb la canalla o sense, per les tardes al Dada, pels caps de setmana a la muntanya, per les rutes i per tots els munts d'anècdotes entranyables que conservo amb tendresa. *I switch to English one last time to thank the tremendous help, support and love that Charles has given me during these last years. He has taught me English, helped me to fit in to a different country, been by my side (or by the other side of the computer) when everything seemed to fall apart, and laughed with me when everything was right again. I want to acknowledge here how important his help has been, especially during these last difficult months.*

En últim lloc, el lloc d'honor, vull agrair a la meva família el fet que siguin la millor família del món. Als meus tiets, cosins i recosins, a la iaia Enriqueta i la Carolina, però per sobre de tot, als meus pares i al Gerard, que m'han fet la persona que sóc, i a qui sé que sempre puc recórrer, passi el que passi, per sentir-me segura, valorada, i molt, molt estimada. Al meu pare he d'agrair, a més, tots els seus consells sobre la meva recerca i sobre la meva vida professional. La seva experiència i coneixements en aquest camp m'han ajudat, donat empenta i solucionat problemes en moltes més ocasions de les que puc recordar. A la meva mare no només li dec el seu suport i amor incondicional, sinó també les il·lustracions de la portada de la tesi i de les portades dels capítols 2, 3 i 4. Finalment, al Gerard vull agrair-li el seu bon humor, i el fet que sigui un amic a més d'un germà. Gràcies a tots tres, a més, per fer-me de secretaris i de consellers en aquestes últimes setmanes de burocràcia.

# Contents

# List of Figures

# List of Tables

# Chapter 1

# Introduction

## 1.1 Introduction and objectives

### 1.1.1 Introduction

In aquatic environments, the main primary producers are microscopic photosynthetic algae, known collectively as phytoplankton, that transform $CO_2$ and nutrients into organic molecules using solar energy. The primary production of phytoplankton in the oceans of the world is estimated to be 45-50 Gt C year$^{-1}$, of the same order than land plants and accounting for about 96% of total marine primary productivity (Longhurst et al., 1995). Phytoplankton is formed by different groups of eukariotic algae and cyanobacteria, constitutes the base of aquatic trophic food webs and its abundance and composition affects ecosystem function and biogeochemical cycles.

The structure and dynamics of the plankton communities is tightly related to the variability of the physical properties of the aquatic environment. The maintenance of a given primary productivity rate needs not only solar energy, but also an input of external energy that does not circulate through the photosynthetic path and derives from physical phenomenon such as tides, wind and other forcings that generate water movement. This movement, that covers a wide range of spatio-temporal scales and translates into advection and turbulence, has a key role in the redistribution of nutrients, in the selection of the dominant phytoplankton species and in the operation of the marine food chains. In recent times, the improvement of measuring instruments, including remote sensors, probes for salinity, temperature, fluorescence and other variables and Doppler velocimeters, has allowed the determination of water properties with high spatio-temporal resolution and has fostered new research into a variety of interactions between biology and fluid dynamics.

At relatively large scales with respect to the size of the organisms, water motion may transport them through the water column and determine the patterns of

distribution of temperature, salinity and nutrients. At smaller scales, water turbulence may have direct effects on the organisms such as altering growth rates and cell shape, may affect the establishment of aggregations and may influence the encounter rates between gametes or between predator and prey (Estrada and Berdalet, 1997). For example, several laboratory experiments (e.g., Berdalet and Estrada, 1993; Sullivan et al., 2003) have shown a decrease of dinoflagellate growth rates in the presence of certain levels of turbulence.

One of the most successful conceptual models aiming to explain the interaction between the physical environment and the phytoplanktonic community was developed by Ramon Margalef in 1978. Margalef (Margalef, 1978; Margalef et al., 1979) asserted that the best predictor of primary production and of dominant life-forms of phytoplankton is the available external energy, on which advection and turbulence depend, and devised a diagram (usually referred as Margalef's Mandala, Fig 1.1) that placed phytoplankton life-forms in an ecological space defined by nutrient concentration and intensity of turbulence. In general energy and nutrient levels are related. Situations of low energy are generally associated to substantial stratification and low nutrient concentrations are low. On the other hand, vigorous mixing of the water column will bring up nutrients to the photic zone. The mandala model suggests that phytoplankton groups are physiologically adapted to different ranges of nutrient concentrations and turbulence, and that there is a succession from diatoms, on one side, adapted to high turbulence and high nutrient conditions, to dinoflagellates, on the other, that are motile and may thrive in low nutrient and low turbulence environments. Dense dinoflagellate blooms and red tides are favored in the unusual case of high nutrient concentration in low turbulence conditions. This observation has both theoretical and practical interest, because some of these proliferations end up being harmful due either to the large accumulation of biomass or to the toxicity of the species forming the bloom. In these cases they are called Harmful Algal Blooms (HABs). Because of their potential noxious effects on humans and ecosystems, it is of great importance to understand the mechanisms that allow the creation and maintenance of HABs (Gilbert and Pitcher, 2001). Following a similar line to Margalef's mandala, a detailed conceptual model of the relationships between environmental characteristics and HAB communities has been proposed by (Smayda and Reynolds, 2001).

### 1.1.2 Objectives and structure of the thesis

This thesis aims to investigate interactions between water circulation dynamics, nutrient availability and structure of the phytoplanktonic community from a mesoscale point of view. The study, focuses on seasonal timescales (from days to months) and on spatial scales of the order of a few meters to a few kilometers in order to obtain a broad perspective of the environmental processes affecting phytoplankton dynamics in one of the main estuarine environments of the NW Mediterranean, the micro-tidal bays of the Ebre Delta system. The work will be centered in three

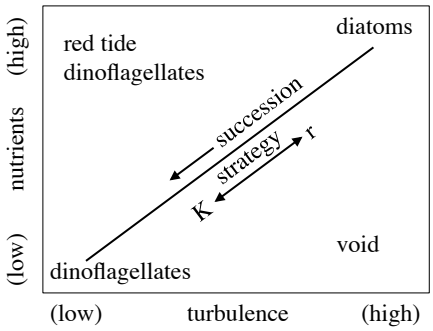


Figure 1.1: Margalef's Mandala (Margalef et al., 1979)

specific objectives:

1. To explore the coupling between the physico-chemical factors and the temporal variability of the phytoplankton assemblages

2. To study of the relationships between physical forcing, hydrodynamic processes and the transport timescales of water in the largest of the Ebre Delta bays

3. To ascertain the role of the fluxes of organic and inorganic compounds of major nutrients (N and P) on phytoplankton community succession and bloom development.

The remaining sections of this introductory chapter will present a brief account of the reasons for the choice of the region of study (Section 1.1.3) and of the methodological approaches followed in the work (Section 1.1.4). The next chapters will develop the thesis objectives, according to the following schema :

**Chapter 1** will provide background information on the ecological characteristics of the region of study.

**Chapter 2** will be devoted to the coupling between the physico-chemical factors and the temporal variability of the phytoplankton assemblages (objective 1).

**Chapter 3** will deal with the study of the relationships between physical forcing, hydrodynamic processes and the transport timescales (objective 2).

**Chapter 4** will consider the third objective, to ascertain the role of the fluxes of major nutrients on phytoplankton community succession and bloom development.

**Chapter 5** will provide a general discussion of the observations, data and modeling results, from the point of view of the importance of physical, chemical and biological interactions in shaping the dynamics of the phytoplankton community in a micro-tidal estuarine region.

**Chapter 6** will state the conclusions of the thesis

### 1.1.3 Choice of the region of study

The region of study comprises the two estuarine embayments of the deltaic system of the Ebre River, Els Alfacs to the south and El Fangar to the north (thereafter Alfacs and Fangar). The two bays share some common characteristics that make them suitable for this kind of study. In addition, each of them shows particularities that lend interest to comparative studies, a subject that will be addressed in this thesis, although the main emphases will be placed on the study of Alfacs, the largest of the bays, for which more historical data are available.

Several reasons support the particular interest of studying the relationship between the phytoplankton community and the physical forcing in Alfacs and Fangar.

On one hand, the study of the coupling between environmental forcing and biological dynamics in Alfacs and Fangar presents a strong scientific interest. Both bays receive freshwater inputs from channels draining the rice fields of the delta plain, irrigated with water from the Ebre river. Therefore, the chemical composition of the freshwater entering the bays is different from that of the Ebre River water and the input fluxes are regulated according to agricultural needs and not the climatology of the region. The bays are connected to the Mediterranean, which determines their micro-tidal conditions. In general, the circulation in estuaries is determined by a combination of freshwater inputs, tides, the effect of Earth rotation, and wind stress, interacting with circumstances such as the size, depth and geometry of the estuary. Due to these interactions, the ecological characteristics of different estuaries, even within the same geographical region, can be highly variable and although estuaries worldwide have been the subject of numerous studies (Ketchum, 1954; Gerreira et al., 2005), many of these systems, including the Ebre Delta bays, are still not well understood.

On the other hand, both bays are highly productive and provide a number of ecosystem services. For example, they provide shelter and nursery grounds for many aquatic species, contribute to the removal of excess nutrients discharged from the river and generate economical returns because of the presence of fisheries, aquaculture, and activities for tourists. The flooded rice fields create a perfect environment for birds and host a highly diverse fauna and flora, making them one of the most important wetlands of the Mediterranean (Fasola and Ruiz, 1996). Harmful algal blooms, both from diatoms and dinoflagellates, occur repeatedly in Alfacs and Fangar. Due to the presence of aquaculture activities in both bays, the

development of HABs leads to important economical loses. The present work focuses on the whole community of phytoplankton from a broad perspective rather than on specific aspects of the HAB phenomena, with the idea that improving the knowledge of the interactions between environmental conditions and phytoplankton assemblages is a basic step to understand the ecology of HAB phenomena in the bays.

Finally, Alfacs and Fangar have been the subject of several scientific research projects and due to the HAB problematics, a monitoring program including phytoplankton counts and physico-chemical measurements has been in place since 1987. Given the size of the bays, there is no need of large expensive ships of long cruises to take samples. The emplacement, dimensions and characteristics of the bays make them a perfect experimental site from which patterns observed can be potentially extrapolated to larger areas.

### 1.1.4 Methodological approach

This section will provide a brief explanation of the methodological approaches used to develop the three objectives of the thesis, taking into account that an extended description of these topics can be found in the corresponding chapters (2 to 4).

#### 1.1.4.1 Objective 1

The first objective (Chapter 2) aims to characterize the patterns of the phytoplankton variability and their relation to the physical forcing in Alfacs and Fangar. The article presented in this chapter assesses whether there are long term trends in phytoplankton abundance or composition that might have been caused by climatic patterns, the seasonal cycle of the community and its coupling with environmental forcing factors and the similarities and divergences between the two bays regarding these subjects. Special attention is devoted to the ecological response of phytoplankton taxa in order to have a better understanding of the mechanisms underlying algal community changes, and to identify if the possible causes of these changes are natural or anthropogenic.

The existence of a monitoring program since the late eighties has produced a fourteen year long series of phytoplankton species abundance data, together with basic physical measurements, such as salinity and temperature, for two different depths of stations located in the center of Alfacs and Fangar bays. The methodology applied in this objective included a) Statistical analyses to estimate the climatologies and the temporal trends of each of the variables. b) Principal Component Analyses (PCA) in order to decompose the phytoplankton data into a smaller number of meaningful dimensions (Legendre and Legendre, 1998). c) Empirical Mode

Decomposition (EMD) to quantify the relationship between the series of physico-chemical and biological variables (Huang et al., 1998). This technique decomposes a series into a number of non-linear modes, called Intrinsic Mode Functions (IMF), with time-depending frequencies. EMD does not require stationarity, an advantageous feature for cases, as the present one, in which the time series are not stationary.

#### 1.1.4.2 Objective 2

The second objective (Chapter 3) studies the relationships between physical forcing, and hydrodynamics in Alfacs. More specifically, its goals are to a) Explore the relative importance of forcing factors such as tides, wind stress and density gradients on the spatial and temporal dynamics of the estuarine circulation. b) Estimate the role of different forcing factors on the occurrence and characteristic time scales of mixing processes, and c) Describe the forcing conditions leading to selected main hydrodynamical scenarios.

The methodology of this objective is based on two different approaches. On one hand, adimensional numbers and scale arguments have been used to create a conceptual model of the forcing and mixing processes on the bay. This procedure attempts to simplify the system as much as possible in order to obtain meaningful information, and is particularly useful for systems that have not been exhaustively studied, like Alfacs Bay. On the second hand, a three-dimensional hydrodynamical model has been implemented and validated for Alfacs. The chosen model is a three-dimensional free surface hydrodynamic model that has been successfully applied to studies of estuaries and lakes (Rueda and Cowen, 2005a; Zamani et al., 2010). The model is used to determine the aspects that are too dependent on the morphology of the bay to be resolved with adimensional numbers and to relate the forcing conditions to the patterns of water circulation in the bay. The model is validated with Acoustic Doppler Current Profiler data and temperature and salinity measurements from thermistors, salinometers and CTD profiles taken as part of the project TURECOTOX (CTM2006-13884-C02-01).

#### 1.1.4.3 Objective 3

The third objective (Chapter 4) seeks to ascertain the relative importance of P or N limitation on phytoplankton community succession and bloom development in Alfacs Bay, and to explore the contribution of the different sources of these nutrients. A basic hypothesis tested is whether the high phytoplankton productivity of Alfacs may be explained by use of dissolved organic phosphorus or by the release of phosphorus from the sediment in resuspension events. These questions have been explored by means of an ecological model that takes into account the results of Chapter 3 to simulate the temporal evolution of two representative groups of phy-

toplankton as a function of physical forcing, nutrient availability and biological factors (such as the growth or mortality rate, or their dependence on light).

The model is zero-dimensional and has been constructed specially for Alfacs. The biological components are the two groups of phytoplankton (diatoms and flagellates) and one group of zooplankton grazers. The physical environment is represented as an homogeneous and rectangular mixed layer, the depth of which changes depending on wind events. The nutrients included in the model are nitrogen and phosphorus in their dissolved organic and inorganic forms, and silicon for the diatoms. There are also two pools of detritic phosphorus and nitrogen. The model uses some forcing data specific for Alfacs, and its parameters have been chosen from the literature, trying to be as close as possible to the reality of Alfacs.

## 1.2 Background

### 1.2.1 Geographical background

The Ebre Delta, the third largest Delta in the Mediterranean Sea, began developing after the last glaciation, and expanded during the Holocene due to the high sediment carrying activity of the Ebre River (Guerrero et al., 1993). The morphology of the delta is in constant change; its shape has changed remarkably during the last 1000 years and is in fact still evolving due to the variations in the river flow and sediment balance (Ibàñez et al., 1997; Palanques and Guillén, 1998). The Ebre Delta is surrounded by the Ebre Shelf, which has a surface of approximately 12000 $km^2$ and is about 60 km wide at the river mouth latitude (Salat et al., 2002). The circulation off the shelf break is influenced by the Catalan Current (the part of the Northern Current that flows in front of the Catalan Coast), which flows towards the southwest. A density front separates the dense open sea waters from the continentally-influenced waters, which have lower salinity (Font et al., 1988). Locally, the water column on the Ebre Shelf presents a thin surface layer (less than 30 m deep) of low salinity, influenced by the Ebre river discharge, the magnitude of which is controlled by the variability of the river flow and the local thermal stratification. The seasonal variation of the water mass structure and circulation is high in this region: sea surface temperature varies from 12.65°C in winter to 22.29°C in summer; average sea surface salinity is 36.54 in winter and 37.86 in autumn; and the depth of the 15°C isotherm (which can be considered as representative of the thermocline) ranges from 80–110 m in autumn, to 40–50 m in summer and surface in winter (Salat et al., 2002).

The deltaic complex comprises two estuarine bays, Alfacs to the South and Fangar to the north. Both bays are connected to the sea and receive water from the Ebre river through human-controlled drainage channels from the irrigation of rice field located in the delta plain (Fig. **??**).

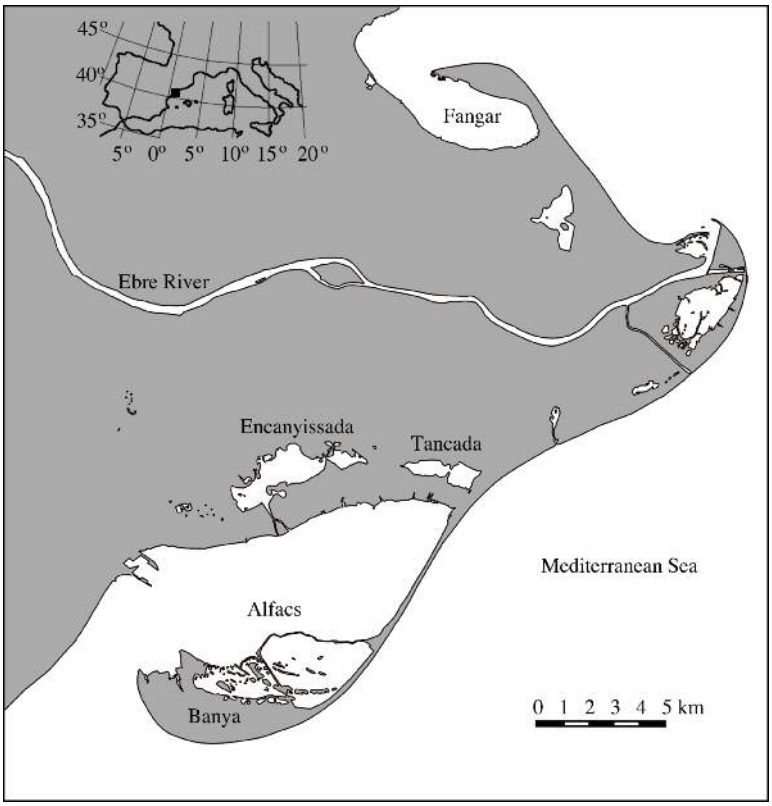


Figure 1.2: Map of the study zone

Alfacs Bay (Fig. 1.2.1) is the largest bay of the Ebre Delta (40°33'–40°38'N, 0°33–0°44'E). It is roughly 11 km long and 4 km wide, with an average depth of 3.13 m and a maximum depth of 6.5 m. The Alfacs basin is separated from the sea by a sand barrier that leaves a 2.5 km wide mouth, allowing water to be exchanged with the open sea (Camp, 1994). The shores of the bay are surrounded by shallow platforms that descend slowly from 0 to 1.5 m deep, and connect to the 4 to 6 m deep central basin (1.3). The dimensions of the bay are summarized in Table 1.1.

Fangar (Fig. 1.2.1) is the northern bay of the Ebre delta complex (40°45'–40°49'N, 0°41–0°48'E). Its dimensions are approximately 6 km long and 2 km wide, with a mean depth of 2 m and a mouth 1 km wide. It contains roughly $16 \times 10^6$ $m^3$ of water.

Both Alfacs and Fangar harbor an active finfish and shellfish aquaculture industry. The main crop is the mussel *Mytilus galloprovinvialis*, with 90 rafts in Alfacs and 76 at Fangar devoted to its culture, and an average annual yield of $3 \times 10^6$ kg (Ramón et al., 2005). Other cultured shellfish are the ostreid *Crassostrea gigas* and the clams *Ruditapes decussatus* and *R. philippinarum* (Ramón et al., 2005). Mussel culture in the delta is threatened by the sensitivity to water temperature,

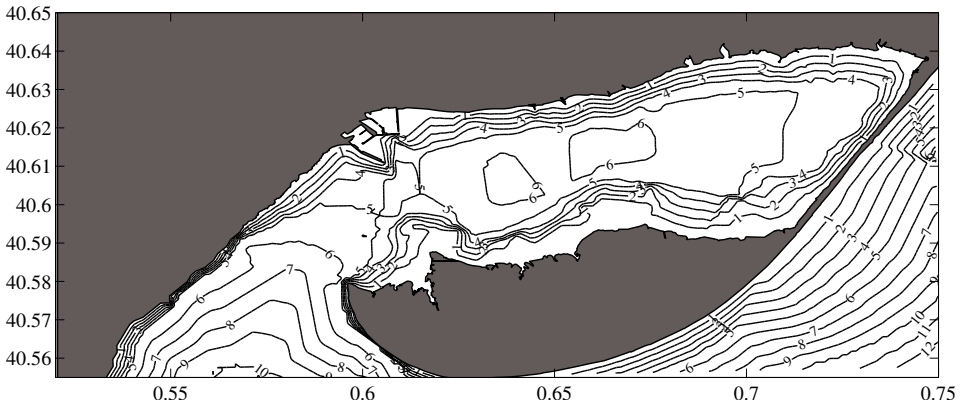


Figure 1.3: Map of the bathymetry of Alfacs Bay interpolated from bathtymetric transects (Guillén, 1992) and bathymetric charts. Latitude/Longitude units.

which causes mortalities when it raises to more than 28°C, and the occurrence of Harmful Algal Blooms, that impede mussel commercialization.

As stated above, this thesis will include a comparison of the variability of environmental and phytoplankton time series in Alfacs and Fangar (Chapter 2), but it will focus mainly physical-biological interactions in Alfacs, which is the best studied bay. Information on Fangar is limited to a few studies, performed during the seventies and eighties (López and Arté, 1973; Camp and Delgado, 1987; Delgado and Camp, 1987; Delgado, 1987), comparing the hydrology, biochemistry and phytoplanktonic community in Alfacs and Fangar, while during the two last decades about 70 studies have been devoted to Alfacs. It can be expected, however, that some of the conclusions reached in this work for Alfacs can be extrapolated to Fangar, taking into account differences such as size and water residence times.

The next sections of this introduction include a general review of the physicochemical (Section 1.2.3) and biological (Section 1.2.5) characteristics of the Ebre Delta bays, with emphasis on Alfacs.

### 1.2.2 Freshwater sources

The Ebre Delta bays contain a mixture of saltwater from the Mediterranean and freshwater of continental origin. The rainfall (which, at the neighboring weather station of Tortosa, ranges from 300 mm to more than 1000 mm), the urban waste water from towns such as Sant Carles de la Ràpita and Poblenou del Delta, and the freshwater from the Ebre that enters the bays through their mouths are relatively unimportant sources of freshwater (Delgado, 1987; Camp, 1994) compared to the irrigation channels. Underground seepage may be important too, although it is not clear to what extent.

| | | |
|---|---|---|
| Length | 11000 | m |
| Maximum width | 5200 | m |
| Minimum width | 3600 | m |
| Mouth width | 2500 | m |
| Length of the central basin | 10000 | m |
| Width of the central basin | 2500 | m |
| Maximum width of the central basin | 3000 | m |
| Width of the central basin in the mouth | 1500 | m |
| Surface area | $49 \times 10^6$ | $m^2$ |
| Surface platforms | $18 \times 10^6$ | $m^2$ |
| Surface central basin | $31 \times 10^6$ | $m^2$ |
| Mean depth | 3.13 | m |
| Maximum depth | 6.5 | m |
| Mean depth of platforms | 0.64 | m |
| Mean depth of central basin | 4.17 | m |
| Volume of water | $153 \times 10^6$ | $m^3$ |
| Extension of the fluvial basin on the north | $79 \times 10^6$ | $m^3$ |
| Extension of the fluvial basin on the south | $10 \times 10^6$ | $m^3$ |

Table 1.1: Dimensions of Alfacs Bay, from Camp (1994)

The Delta is criss-crossed by approximately 200 km of channels that transport water from the Ebre river to the rice fields. The drainage channels drive the water from the fields to the Mediterranean, the lagoons, and the bays of Alfacs and Fangar. The flow of water is mainly powered by gravity, although on some occasions, due to the flatness of the area, the use of pumps is necessary (March and Cabrera, 1997). The flux of the drainage channels depends on the agricultural needs and, in Alfacs, ranges approximately between 13 and 14.5 $m^3s^{-1}$ during the months of the rice crop, from April to September. From October to January, when the water is no longer needed for cultivation, the fields are kept flooded for environmental reasons, with a low flux rate of 7-8 $m^3s^{-1}$, and from mid January to end of March the channels are closed for maintenance and there is no flow (Farnós et al., 2007; Camp, 1994; Prat and Ibàñez, 2003). These numbers are only indicative, because farmers can control the water entering and leaving their fields and the actual fluxes are highly variable (Muñoz, 1990). When the channels open again in April all the rice fields of the right (south) side of the Ebre, about $125 \times 10^6$ $m^2$, are totally flooded in 10 days with a water height of about 0.15 m. About a 60% of this field surface empties their waters into Alfacs.

The composition of the water of the channels is highly influenced by its flow through rice fields. Rice field farmers add fertilizer one month before flooding, plant the rice one week after the flooding, and fertilize again three months after flooding, when the rice has begun developing secondary stems. After harvest, the rice straw is mixed with the soil (Christian et al., 1996). Of the total nitrogen (N) and phosphorus (P) inputs, the rice gets a 70% of the N and a 91% of the P,

| Reference | $NH_3^-$ | $NH_2^-$ | $NH_4^+$ | $PO_4^{3-}$ |
|---|---|---|---|---|
| Muñoz (1998) | 20–80 | 2–14 | 10–100 | |
| Camp and Delgado (1987) | 15–45 | 1.6–2.8 | | 0.8–1.5 |
| de Pedro (2007) 1986–1987 | 29.8±7 | 3.34±1 | 19.3±5 | 1.0±0 |
| de Pedro (2007) 1996–1997 | 85.3±16 | 6.35±2 | 76.1±29 | 0.6±0 |

Table 1.2: Measured concentrations of inorganic nutrients in the channels (mmol $m^{-3}$).

while a 15% of the N and a 3% of the P runs away with the water. The rest goes to the macrophites and other organisms that live in the rice fields (Forès, 1992). Rice fields act as filters, retaining one part of the incoming N and P and releasing the other in the form of organic N, ammonium, particulate N, soluble reactive P, and particulate P, depending on the stage of the crop (Forès, 1989, 1992). The concentrations of particulate organic nitrogen and phosphorus are higher in the channel waters than in the river, and it is likely that an important proportion of the nutrients enters Alfacs in particulate form (Prat et al., 1988). The variability of the nutrient concentrations in the channels is very poorly known (Muñoz, 1998; Camp and Delgado, 1987; de Pedro, 2007; Forès, 1989, 1992). A summary of measured concentrations of inorganic nutrients in the channels is presented in table 4.5.

The quality and magnitude of the flux of underground water discharging into Alfacs is complicated to estimate. The hydrological system of the delta is formed by three aquifers. The shallower is 5-10 m deep, porous and formed by sand, and its surface water has low salinity due to the freshwater inputs from the flooded rice fields. The lower part of the aquifer has higher salinities. The intermediate aquifer is 10 - 50 m deep and has low permeability. The deeper aquifer, multilayered, is 70 - 500 m deep. The salinity of the waters of the middle and deep aquifers is high (Bayó et al., 1997; Curcó, 2006). (Camp, 1994) calculated that in order to explain the low salinities observed during the closed channel season, the underground inputs had to be between 2 and 4 $m^3 s^{-1}$.

Camp (1994) conducted a hydrological balance of Alfacs considering freshwater inputs, evaporation and rainfall. The calculated evapotranspiration in the bay is about $6 \times 10^5$ $m^3$ per year and the precipitation $3.1 \times 10^5$ $m^3$ per year. Taking into account the annual inputs of freshwater from the channels, the bay would have a surplus of $19 \times 10^5$ $m^3$ per year, although the seasonal changes of these factors could result in lower or even negative freshwater surplus during some months, specially in autumn.

### 1.2.3 Hydrography

There are few studies about the hydrography of the bays. López and Arté (1973) studied Fangar, the northern bay, and described the seasonal range of temperature and salinity, as well as the circulation patterns of the surface waters, which were

| Reference | $NH_3^-$ | $NH_2^-$ | $NH_4^+$ | $PO_4^{3-}$ |
|---|---|---|---|---|
| Delgado and Camp (1987) | 0.40±0.39 | 0.14±0.06 | | 0.47±0.24 |
| de Pedro (2007) | 4.6±7.4 | 0.26±0.24 | 1.06±0.1 | 0.18±-0.23 |

Table 1.3: Measured concentrations of inorganic nutrients in Alfacs (mmol $m^{-3}$) and its standard deviation.

determined by means of floaters. Camp and Delgado (1987) made a first attempt to describe the hydrography of Alfacs and Fangar, classifying them as salt-wedge estuaries and using salinity balances to estimate the residence time of freshwater in Alfacs and Fangar, which were reported to be respectively 10 to 20 days and 1 to 2 days. A more complete account of the physical environment in Alfacs, including some of the results from (Camp and Delgado, 1987), was published by Camp (1994).

Camp (1994) describes Alfacs as a system that is usually stratified in a "stationary state" characterized by two water layers, a dense saline layer at the bottom that receives inputs from the sea and a surface layer of low salinity that flows out of the estuary towards the Mediterranean. Strong wind events may mix the two layers and lead to a temporal "non stationary state". After a perturbation, the system returns to the previous stratified state within 24 - 48 hours. The estimated residence time of the freshwater ranged from 7 to 14 days, depending on the season. The reduction of freshwater flux during the closed channel season reduces the exchange of water with the Mediterranean, increasing the residence time of freshwater instead of raising salinity. The water velocity and transport were determined by means of a correntimeter installed in the mouth of Alfacs at 4.5 m depth. The mean direction of the flow was along the axis of the bay. The flux was three times stronger with open than with closed channels and during strong wind events that mixed the water column, the flow direction was very variable. In general, the volume of water exchanged with the sea was ten times higher than the inputs of freshwater. A periodicity of 3 h was observed in addition to the tide signal.

### 1.2.4 Nutrients

The inorganic nutrient concentrations are related to the amount of freshwater, as the channels are the main nutrient source. In Alfacs, there is a North-South gradient in the nutrient concentration, because the areas that are closer to the channels receive more freshwater and, therefore, more nutrients. As the estimated nutrient loads explained only a fraction of the observed phytoplankton biomass buildup, Delgado and Camp (1987) suggested the existence of additional nutrient sources such as remineralization in the sediment. The ranges of nutrient concentrations published in Delgado and Camp (1987) and de Pedro (2007) are summarized in Table 1.3.

The role of the sediment in nutrient balances was addressed by Vidal et al.

(1989, 1992), who concluded that the ammonium released by the sediments was enough to supply most of the phytoplankton requirements in Alfacs. They also found that the released amounts depended on the type of bottom sediment. Phosphorus liberation is activated when the sediments are resuspended. After a resuspension event, there is a short-term release of soluble reactive phosphorus (SRP) that is followed after some minutes by a retrieval of phosphorus that lasts until the system reaches an equilibrium concentration. The final concentration is around 0.2 - 0.3 mmol SRP $m^{-3}$, and in general the whole process results in a net increase of phosphorus in the column (Vidal, 1994).

### 1.2.5 Phytoplankton

Alfacs and Fangar are very productive bays. Their average phytoplankton concentrations during the period 1982-1986 were around 3.2 mg $m^3$ in Alfacs and 3.5 mg $m^3$ in Fangar, about one order of magnitude higher than typical values (Delgado, 1987) for the open Mediterranean. As observed by means of inverted microscopy, the nano and micro phytoplanktonic community, dominated by nanoflagellates, diatoms and small dinoflagellates, is similar to that of the Mediterranean, except for the frequent presence of some benthic diatoms and freshwater species. The phytoplankton communities of Alfacs and Fangar show clear seasonal changes in response to meteorological and hydrological variability, including the yearly cycle of freshwater inputs through the drainage channels (Delgado, 1987).

Apart of Delgado (1987), the other studies of the phytoplankton community have been centered on potentially harmful species. Both Alfacs and Fangar are included in a monitoring program to determine the water quality of shellfish growing areas in Catalonia, and the detection of potential HAB producers is an important aspect of it. The reported toxic species include the dinoflagellates *Alexandrium minutum*, *A. catenella*, *Dinophysis sacculus*, *D. caudata*, *Proceratium reticulatum*, *Karlodinium veneficum*, *K. armiger* and the diatom *Pseudo-nitzschia* spp (Fernández-Tejedor et al., 2010).

*Alexandrium* is a widespread genus in the Western Mediterranean (Vila and Masó, 2005; Garcés et al., 1999b), and its occurrence in the Catalan coast appears to have increased in recent years (Vila et al., 2001b). *Alexandrium minutum*, a species associated to episodes of paralytic shellfish poisoning (PSP), was observed for the first time in Alfacs in 1989 (Delgado et al., 1990). Since then, blooms of *Alexandrium* have been recurring almost every year at the beginning of the spring. *Dinophysis sacculus* and *Dinophysis caudata* can cause Diarrhoetic Shellfish Poisoning (DSP) at very low concentrations (500 - 1200 cells $l^{-1}$), resulting in the closure of the mussel farms. *Karlodinium* spp., previously identified as *Gyrodinium corsicum* (Garcés et al., 2006), was detected for the first time in Alfacs in 1994. The blooms of *Karlodinium* spp. cause water discoloration and the death of wild fauna and cultured mussels and fish (Delgado and and, 1995). The toxic effect of these dinoflagellates on different organisms has been demonstrated by (Delgado

and Alcaraz, 1999; Fernández-Tejedor et al., 2007; Vaqué et al., 2006). The cells of *Karlodinium* spp. tend to accumulate at the bottom of the water column, although no daily migration patterns have been described (Garcés et al., 1999a). The blooms of the diatom *Pseudo-nitzschia* spp. are potential generators of amnesic shellfish poisoning (ASP) toxicity, although no cases have been reported in Alfacs. Loureiro et al. (2009a,b) suggested that organic nutrients could have an important effect on the growth of *Pseudo-nitzschia* spp. A description of the different species of the genus present in Alfacs can be found in Quijano-Sheggia et al. (2008).

### 1.2.6 Relationship between environmental forcing and phytoplankton community dynamics

There is evidence, in particular for Alfacs, of linkages between wind stress, the intensity of water column mixing and the appearance and disappearance of blooms, but the understanding of the mechanisms underlying such observations is limited. Episodes like the *Alexandrium minutum* bloom observed by (Delgado et al., 1990) and the *Karlodinium* spp. bloom described by Garcés et al. (1999a) were preceded by strong winds that supposedly could have enhanced nutrient supply to phytoplankton by resuspension of sediments, but no data could be gathered to prove this point. The blooms themselves appeared during a calm period of weak winds and strong stratification. The low turbulence conditions would reduce advection losses and, together with high nutrient availability, would provide the necessary conditions for bloom development. Finally, bloom dispersion was caused by strong winds Delgado et al. (1990) or the input of freshwater from the channels Garcés et al. (1999a) that increased the loss of phytoplankton by advection. In fact, correlation between *Karlodinium* spp. densities and a stratification index has been suggested in Fernández-Tejedor et al. (2010).

These relationships between wind speed and direction, input of freshwater and the occurrence of blooms suggest that these physical forcing factors may affect the water residence time of the bay, although the mechanisms are not clear. Camp (1994) suggested that the decrease of freshwater inputs and the reduced estuarine circulation during the winter channel closure reduced the exchange with the Mediterranean and increased the water residence time. Camp and Delgado (1987) observed also that strong wind events that mixed the Alfacs water column interrupted the estuarine circulation and increased the water residence time in the bay. However, vertical mixing would also influence phytoplankton populations by disrupting their vertical distribution.

Another meteorological feature that affects the hydrodynamics and ecology of the bays is the temperature. In Alfacs, where water residence times are higher than in Fangar, the probability of HABs or anoxia increases in summer, when high temperatures strengthen the stratification, increase evaporation and reduce the amount of freshwater in the bay (Camp, 2005). In general, although several studies in Alfacs have explored the relationships between the seasonal cycle, freshwater inputs

and wind events with the spatio-temporal variations of the phytoplankton community (Delgado, 1987), the coupling between the meteorological forcing, the hydrodynamics of Alfacs and the dynamics of its phytoplankton assemblages has not yet been addressed quantitatively.

### Box 1. Harmful Algal Blooms

Some phytoplankton species have the capacity of developing Harmful Algal Blooms (HABs), proliferations of algae with noxious consequences for animal or human health, or for human socio-economic interests. HABs appear to have increased in the recent years, although it is not clear to what extent the increment in coastal resource use and the enhanced awareness and vigilance of the problem have contributed to this perceived increase. Two main types of HABs can be distinguished, according to whether the harmful effects are due to high biomass accumulation or to toxicity. Some blooms, often dominated by one or several species, can reach concentrations of $10^4$ – $10^6$ cells $l^{-1}$ and last for a few weeks. When the bloom collapses, the degradation of organic matter can deplete the oxygen concentration in the water and cause anoxia, with important consequences for fish, shellfish and in general the whole food web. Dense blooms can also reduce the light available for other photosynthetic organisms deeper in the water column. The second group of HABs is originated by species of phytoplankton that produce toxins. Some organisms, such as *Dinophysis* spp., are able to cause toxicity problems at fairly low concentrations. The toxins generated by the algae are transferred through the food chain and may accumulate in bivalve mollusks, fish and other animals used as food by humans, which may become ill when consuming these organisms.

The main categories of toxicity that pose a risk for human health are caused basically by dinoflagellates and include Paralytic Shellfish Poisoning (PSP), Diarrhoetic Shellfish Poisoning (DSP), Neurotoxic Shellfish Poisoning (NSP), and Ciguatera Fish Poisoning (CFP). Another type of toxicity, Amnesic Shellfish Poisoning (ASP), is produced by diatoms of the genus *Pseudo-nitzschia* (see e.g., Zingone and Enevoldsen, 2000; Hallegraeff, 2003). Other health problems caused by HABs include skin irritation, allergies and respiratory affections. Some HAB species produce toxins that cause fish kills or are detrimental for other organisms of the ecosystem. A list of the harmful effects caused by HABs and examples of organisms that cause them can be found in Zingone and Enevoldsen (2000).

There is a lot of variety among HAB species. Many of them are normal components of the seasonal phytoplankton succession and it must be taken into account that the concept of harmfulness relates to human interests, not to ecological properties of the algae. One can find reports of harmful events caused

by dinoflagellates, diatoms, prymnesiophytes, raphidophytes and cyanobacteria, although the most common culprits are flagellates. Of the 60-200 reported species of noxious algae, a 90% are flagellates, and a 75% dinoflagellates (Zingone and Enevoldsen, 2000; Smayda, 1997). However, non-flagellated organisms, such as diatoms, are also important in marine waters.

Diatoms are non-motile and tend to thrive in relatively turbulent, nutrient-rich environments. Their cellular walls are made of silica, which makes them dependent on silicon in addition to other nutrients (nitrogen, phosphorus, ...) that all phytoplankton need. On the other hand, dinoflagellates can swim and tend to grow more slowly. Motility allows dinoflagellates to control their position in the water column to find nutrients or light and to avoid regions of high turbulence that could cause them physical damage, physiological impairment, or behavioral modification (Smayda, 1997). The ecophysiological variety of HAB species and the complexity of physico-chemical and biological factors influencing their proliferations make it very difficult to foresee the occurrence and consequences of blooms. However, conceptual models such a the so-called "mandala" of Margalef (1978); Margalef et al. (1979) have provided a schema to predict the dominance of major phytoplankton functional groups as a function of nutrient availability and external energy in the form of water motion. In this framework, red tides and high biomass dinoflagellate blooms are seen as a particular case of phytoplankton succession under conditions of high stratification accompanied by nutrient availability.

# Chapter 2

## HYDROGRAPHICAL FORCING AND PHYTOPLANKTON VARIABILITY IN TWO SEMI-ENCLOSED ESTUARINE BAYS.

This article is in process of revision in the Journal of Marine Systems as

Llebot, C., Solé, J., Delgado, M., Camp, J., Fernández-Tejedor, M., Estrada, M. Hydrographical forcing and phytoplankton variability in two semi-enclosed estuarine bays

## ABSTRACT

Alfacs and Fangar (North East of the Iberian peninsula) are two embayments of the Ebre Delta complex with typical Mediterranean characteristics. Both are subject to the same meteorological forcing and receive similar freshwater inputs from irrigation drainage channels. However the basin volume in Alfacs is about ten times larger than in Fangar. We studied the temporal patterns of series of chlorophyll *a* and phytoplankton counts sampled between 1990 and 2003 from two depths of a fixed station in each bay, and related them to the variability of environmental variables (water, temperature, salinity and stratification). A principal component analysis performed on the correlation matrix among the (log-transformed) abundance data of the most frequent taxa revealed three main trends of variability. The first principal component (PC1) indicated a gradient of marine (more important in Alfacs) versus freshwater (particularly in Fangar) influence. PC2 reflected the seasonal cycle of phytoplankton in Alfacs, characterized by the dominance of a diatom assemblage typical of Mediterranean coastal waters in autumn and a group of dinoflagellates, including toxic taxa, in winter – early spring. PC3 expressed mainly the seasonal changes in Fangar and opposed a mixed phytoplankton group, including mostly dinoflagellates, with population maxima between May and October, to dinoflagellates of the winter group. Empirical Mode Decomposition was applied to the environmental variables and to the principal components in order to analyze the temporal structure of the data. All the series presented strong seasonal modes; an index based on phase shift between pairs of series revealed correlations between some of the principal components and environmental variables (temperature and salinity in Alfacs and temperature, salinity and stratification in Fangar). Water temperature showed a slight increasing trend along the sampling period. Between 1997 and 2003, some phytoplankton taxa also presented a weak increasing trend, particularly in the bottom samples of Fangar. Differences among the seasonal patterns of phytoplankton variability in Alfacs and Fangar could be attributed to the lower residence times of the water in Fangar, which resulted in a stronger hydrological control of phytoplankton abundance and composition.

## 2.1 Introduction

Estuarine environments, at the boundary between freshwater and marine ecosystems, sustain high biological productivity ecosystems and provide important resources and socio-economical services. Estuaries and, in general, coastal ecosystems are subjected to numerous natural and anthropogenic stresses, acting on a variety of spatio-temporal scales. Local processes include nutrient inputs from land, which will vary as a function of land and water uses. On a large scale, estuarine and coastal waters may be particularly susceptible to the effects of climate change, which could act not only through increasing temperatures, but also through other mechanisms such as alterations of sea level or precipitation patterns on land. The effects of environmental changes include shifts in algal community, food web structure, major nutrient cycles and carbon export (Short and Neckles, 1999; Le Quéré et al., 2007; Ji et al., 2007; Noiri et al., 2005; Sarmiento et al., 1998).

To assess the relative impact of local-scale and climatic forcing on a particular ecosystem, it is necessary to know the main mechanisms and physical variables that drive its behavior. In open waters of temperate areas, much of the variability is imposed directly or indirectly by the annual cycle of solar radiation (Sverdrup, 1953; Cloern and Jassby, 2009). One of the main features triggered by the seasonal fluctuations is the winter or spring phytoplankton bloom that occurs after winter mixing has replenished nutrients in the surface layers, when increasing irradiance and stratification allow positive phytoplankton net growth. In contrast, due to their close exposure to impacts from land, ocean and atmosphere, estuarine and nearshore waters present complex seasonal patterns, with large variability both across and within ecosystems (Cloern and Jassby, 2008). In addition to seasonally occurring, somewhat predictable, phytoplankton proliferations, unusually high biomass levels of some phytoplankton populations may also occur as localized phenomena in space and time, in response to particular environmental and ecological conditions, such as high nutrient loads coupled with high water residence times (Paerl, 1988). Some of these algal blooms (harmful algal blooms or HABs) can have deleterious consequences for other organisms in the aquatic ecosystem or for human health and economy (Anderson et al., 1998; Smayda, 1990, 1997; Solé et al., 2006a,b). Coastal waters are particularly exposed to anthropogenic influences, such as nutrient inputs from point sources, acting on local and short-term time scales. Because events of proliferation and senescence of primary producers have relatively short characteristic periods, (on the order of a few weeks), the fluctuations induced by anthropogenic effects tend to occur at finer spatio-temporal scales than those arising from global climatic shifts.

In order to sort out climate change effects from direct anthropogenic impacts on phytoplankton variability, it is necessary to understand the mechanisms underlying algal population changes. With this aim, the present work will explore the patterns of phytoplankton variability and their relationship with physical forcing

in the bays of Els Alfacs and El Fangar (hereafter Alfacs and Fangar), two semi-enclosed embayments of the Ebre River delta complex (NW Mediterranean). The aim of this work is to characterize the patterns of phytoplankton variability and their relationship with physical forcing.

These bays present typical shallow coastal ecosystem (SCEs) characteristics Cloern (1996): they are influenced both by land inputs and exchanges with the sea, and are therefore characterized by marked spatial gradients, and their shallow depth implies that the interactions between the pelagic and benthic domains are strong. As in other aquatic habitats, turbulent mixing, which is modulated by the buoyancy introduced by freshwater inputs, is a key process that determines the vertical fluxes of heat, salt, nutrients and plankton. SCEs are also particle rich compared to open ocean, and many of them are also nutrient rich. Furthermore, Alfacs and Fangar share typical features of Mediterranean embayments, such as the weak tides and the lack of a strongly dominant process of physical forcing. As other estuaries, the bays of Alfacs and Fangar are very heterogeneous and dynamic systems; their water circulation patterns are complex and subject to changes at a wide range of temporal scales (including daily, seasonal and multiannual). Due to this variability, and in spite of earlier work, our knowledge of physical forcing and its interactions with the planktonic communities of Alfacs and Fangar is still limited.

Both Alfacs and Fangar host an important bivalve (mainly mussel) aquaculture industry, which is affected by the sporadic occurrence of HABs. The main toxic microalgal taxa are *Alexandrium minutum*, *Alexandrium catenella*, *Dinophysis sacculus*, *Dinophysis caudata*, *Protoceratium reticulatum*, *Karlodinium veneficum*, *Karlodinium armiger*, and *Pseudo-nitzschia* spp. (Delgado et al., 1990; Delgado and and, 1995; Fernández-Tejedor et al., 2008).

A strong coupling between the meteorological forcing and the hydrological properties of Alfacs, was demonstrated by Solé et al. (2009), who found that water temperature was correlated with air temperature, wind speed and air pressure. Delgado (1987) studied the annual cycle of the phytoplankton community in the Ebre Delta bays and concluded that the temporal and spatial variations observed in the phytoplankton were a consequence of the seasonal cycle, the inputs of freshwater and the effect of non-periodic physical factors like wind storms. However, no quantitative study has been made yet to validate the hypothesis of a strong coupling between the physical forcing and the temporal distribution of phytoplankton in the bays.

We will use time series of biological variables (phytoplankton assemblages, Chl *a*) sampled simultaneously to physico–chemical measurements (temperature, salinity, stratification) in Alfacs and Fangar in order to characterize the seasonal patterns of variability of the phytoplankton communities in both bays and to obtain insight about their coupling with environmental forcing. To carry out this goal we will first analyze the data set, calculating some statistical parameters to determine long-term evolution and trends of the variables. Secondly, we will use Principal

Component Analysis (PCA) to obtain decorrelated variables that will allow us to summarize the structure of the community and the temporal succession of phytoplankton assemblages. Finally we will use Empirical Mode Decomposition (EMD) to analyze the periodicities of the time series of biological and environmental variables and to estimate the relationship between these time series. In the following section we will describe the area of study, the observational data and the methodology used. Next, we will show the main results obtained. Finally, we will discuss the implications of our results for understanding the influence of climatic forcing on the ecology of the bays.

## 2.2 Materials and Methods

Fangar is the northern bay of the Ebre Delta (40°40'N,0°40'E, Fig. 2.1). It has a capacity of $16 \times 10^6$ m$^3$, with an extension of $12 \times 10^6$ m$^2$ and 2 m mean depth (Camp and Delgado, 1987) and a 1 km wide mouth. Alfacs is located in the southern part of the Delta complex Delta. It has a surface area of $49 \times 10^6$ m$^2$, a volume of $153 \times 10^6$ m$^3$ and an average depth of 3.13 m, with a mouth 2 km wide. The hydrography of Alfacs and Fangar is typical of slightly stratified estuaries (Hansen and Ratray, 1966). The bays are stratified throughout the year, except during strong wind events that cause mixing of the water column (Camp and Delgado, 1987; Camp, 1994; Delgado, 1987). Alfacs and Fangar are positive estuaries with a freshwater input greater than evaporation (Delgado, 1987), so that their mean salinity is always lower than that of the sea. Seawater enters the bays from the Mediterranean Sea and freshwater comes mainly from discharge channels collecting irrigation water from the rice fields and draining into the bays. Until 2001, these channels were closed in winter, approximately from November to March, and open during the rest of the year. Starting in 2001, the channels are only closed from January to March (Serra et al., 2007). Their mean flow is 13 m$^3$s$^{-1}$ at Alfacs, and 10 m$^3$s$^{-1}$ at Fangar (Camp and Delgado, 1987). The Chl *a* concentrations in the bays are high compared with those typical of coastal waters of the Mediterranean (López and Arté, 1973; Delgado, 1987). During 1982–1986, the annual mean Chl *a* concentrations of Alfacs (3.20 $\mu$g l$^{-1}$) and Fangar (3.44 $\mu$g l$^{-1}$) were one order of magnitude higher than those in the neighboring open sea (Delgado, 1987). This relatively high phytoplankton biomass is the main cause of the success of shellfish aquaculture in the bays (López and Arté, 1973).

The data used for this work were collected by IRTA–Sant Carles de la Ràpita (Institute for Food and Agricultural Research and Technology, named "Centre Nacional d'Aqüicultura" before 1999) from 1990 to 2003 as a component of the Monitoring program on water quality of the shellfish growing areas in Catalonia. Temperature, salinity and chlorophyll for Alfacs were taken also during 2004, but for the sake of simplicity, we will use 2003 when referring to the end of all the time series. The sampling sites were located in the center of the bay (40°N 46' 34"

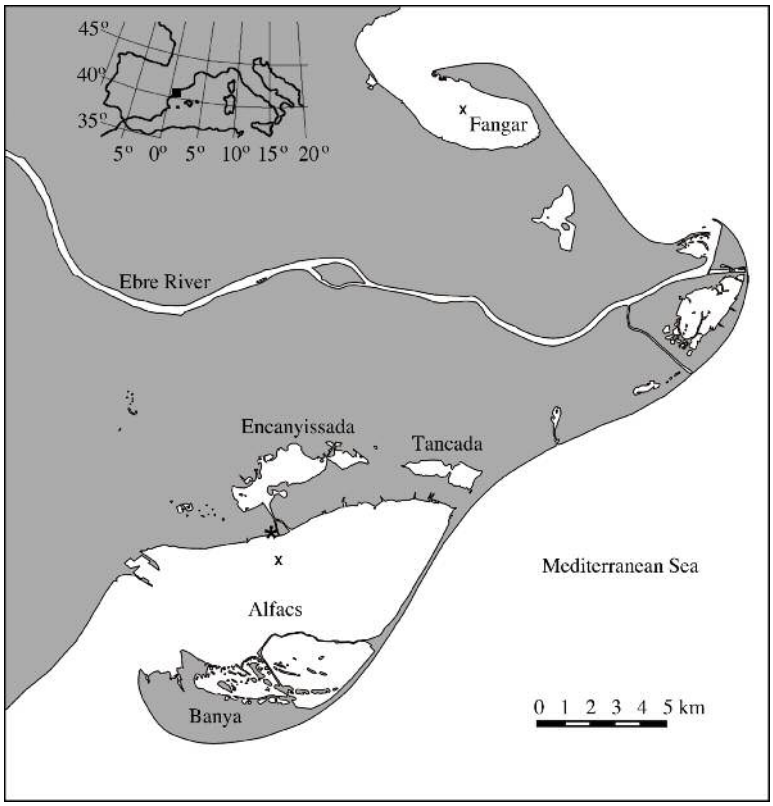


Figure 2.1: Map of the study zone. ⋆ : weather station; X : sampling site.

0°E 44' 52") in Fangar (Solé et al., 2009) and at (40° 36' 33" N, 0° 39' 22" E) in Alfacs. Water samples were taken weekly from 0.5 m depth (surface) with a Niskin bottle or with plastic containers and from 0.5 m above the bottom, at about 5.5 m depth in Alfacs and 3.5 m in Fangar (bottom), with a bottom sampling bottle. Water salinity and temperature were measured by means of a portable sonde (WTW instruments). A stratification index was calculated using the Brunt–Väisäla frequency (equation 2.1, where $\rho$ is density, $g$ is acceleration of gravity and $z$ is depth) with the measured temperature and pressure at surface and depth.

$$N = -\sqrt{\frac{g}{\rho}\frac{\mathrm{d}\rho}{\mathrm{d}z}} \tag{2.1}$$

Between 1990 and 1995, Chl *a* was measured filtering 500 ml of water on Whatman GF/F filters that were placed on acetone 90% for 6-10 hours. The Chl *a* concentration of the extract was determined, after centrifugation, from trichromatic absorbance readings (Jeffrey and Humphrey, 1975) by means of a Shimadzu UV240 spectrophotometer. After 2000, Chl *a* was estimated using a TURNER

fluorometer. The conversion factor for the *in vivo* measurements is calculated by the linear regression of the *in vivo* readings versus measured Chl *a* concentrations in acetone extracts for the same sample. For this purpose one integrated sample at the central station of each bay was analyzed every week. Water samples for phytoplankton examination were fixed with formalin solution (1% final concentration) and stored in hermetically closed bottles (Delgado et al., 2004). Phytoplankton cells were counted by means of Nikon or Leica DM–IL inverted microscopes (Utermöhl, 1958); settling chambers of 25 ml were used until 1995; thereafter, 50 ml chambers of better optical quality were adopted. The entire bottom of the chamber was scanned at 63–100x magnification to enumerate the larger organisms, and one transect at 200–400x magnification was examined to count the small, more abundant organisms. When possible, mainly in the case of large diatoms and dinoflagellates, the cells were classified down to the level of species or genus. Coccolithophores were not intensively studied, (they were not specially abundant) and only *Syracosphaera pulchra* was routinely identified. Small flagellates were not quantified.

The studied phytoplankton time-series covers the period from 1990 to 2003. However, there are some intervals without measurements. These gaps are sporadic and affect some of the taxa. Therefore, in order to obtain a long but consistent data set we had to discard some species.

Climatologies of the environmental (temperature, salinity and stratification) and biological data sets were calculated by pooling the data corresponding to each week of the year and calculating the mean for each week. The weekly seasonal variability of the variables along the sampling years was represented by means of color-coded graphs in order to visualize possible changes in timing of maxima and minima. For concision, only the time series corresponding to surface samples are shown in the figures (Figs. 2.2, 2.3).

The linear temporal trends of the environmental and phytoplankton variables were calculated as the regression lines of their weekly anomalies (the difference between the value for a particular week and the corresponding global mean) with respect to time. Only slopes (as determined by the t test) were considered. Due to the methodological changes between 1994 and 1995 and the interruption between 1996 and 1997, only the last part of the series (between 1997 and 2003) was used for the phytoplankton variables (diatoms, dinoflagellates and principal components). All the variable anomalies presented unimodal histograms, although only a few of them could be considered as normally distributed according to the Wilk–Shapiro test. In this context, we considered as significant those regressions of anomalies with respect to time in which both Spearman's $\rho$ was significant and the 95% confidence interval of the regression slope did not include 0. Chl *a* was excluded from the regression analysis because of the large interval of missing data and the short time span of available measurements with each method (acetone extracts or *in vivo*). However, the medians of the 1990–1995 and 2000–2004 subseries were compared by means of the Mann–Whitney U test.

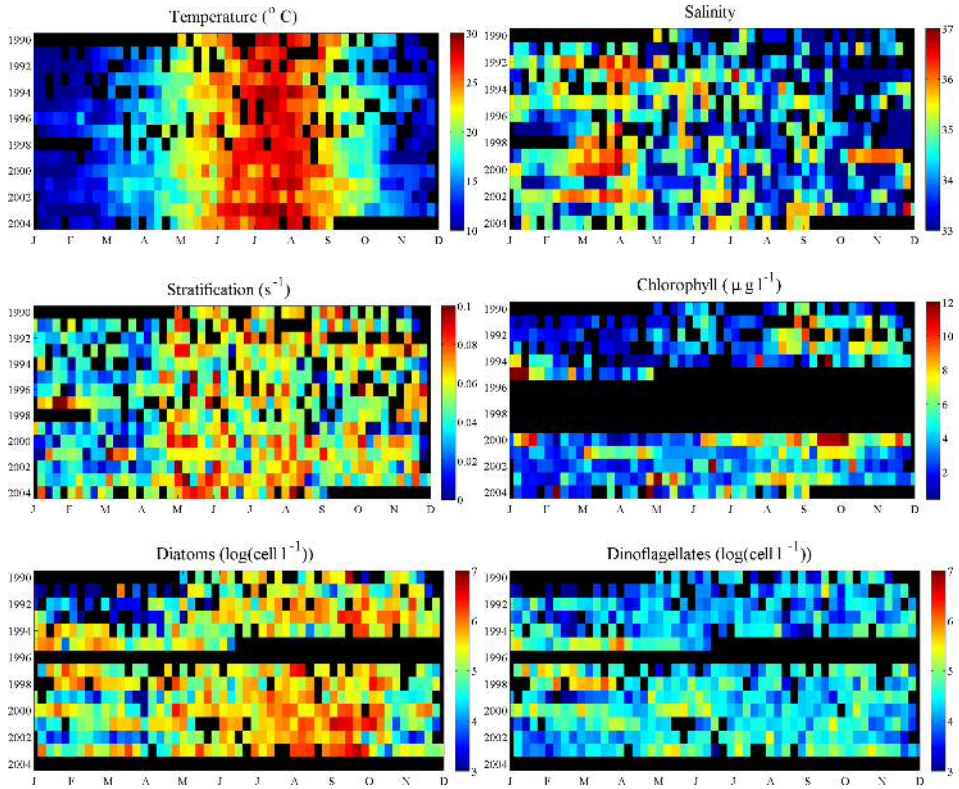


Figure 2.2: Seasonal distribution of weekly sampled environmental and phytoplankton variables at 0.5 m depth in Alfacs, during the period from 1990 to 2003.

The phytoplankton data were analyzed by means of a Principal Component Analysis (PCA). The aim of PCA is to reduce the dimensionality of a data set and provide a new set of uncorrelated variables, named Principal Components (PC), which are a linear combination of the source data and are ordered so that the successive components explain decreasing proportions of the variance present in the original variables (Legendre and Legendre, 1998).

The weights of the variables or loadings reflect the relative importance of a variable within a principal component. PCA allows to summarize in a few principal components a maximized proportion of the information contained in the original data set. As the analysis is based on the correlation or covariance matrix among all the original variables, it is also useful to extract unbiased trends from data with a large associated error, as happens with phytoplankton counts (Estrada, 1979; Delgado, 1987).

The PCA was performed on the correlation matrix among the log-transformed abundances of selected taxa from a pooled data set including the surface and bottom samples of Alfacs and Fangar. We considered a total of 36 taxa that were present

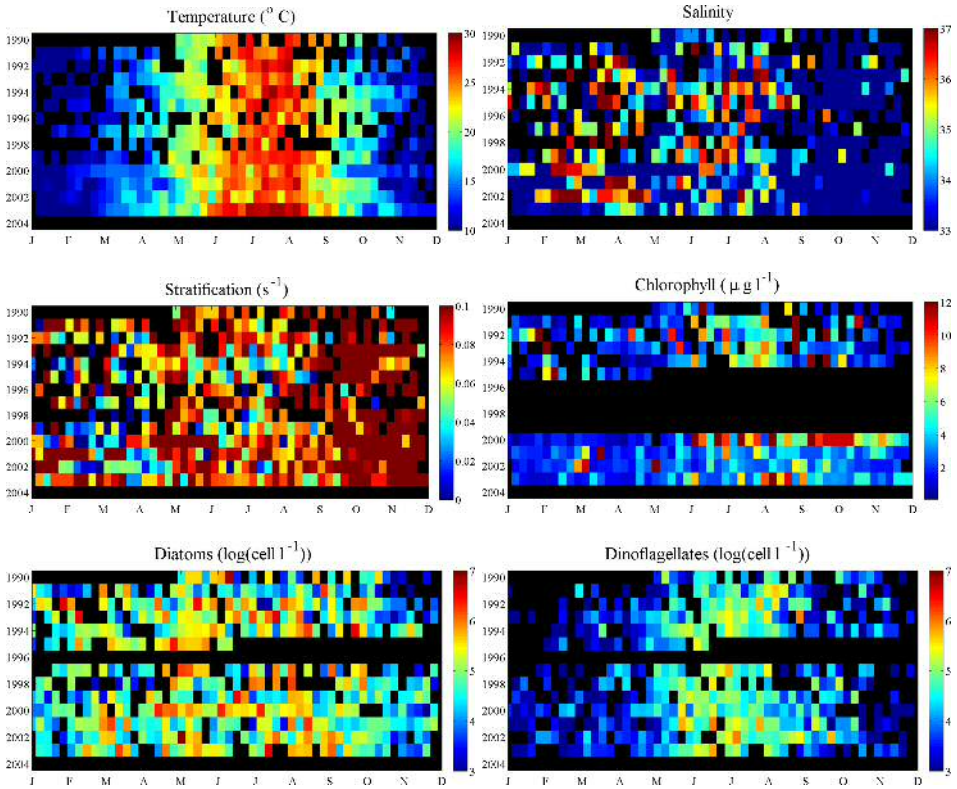


Figure 2.3: Seasonal distribution of weekly sampled environmental and phytoplankton variables at 0.5 m depth in Fangar, during the period from 1990 to 2003.

in more than 10 % of the samples of either Alfacs or Fangar. The exceptions were *Dinophysis caudata* and *Scenedesmus* sp. These taxa were found in less that 10% of the samples of both bays, but were included because of their interest (*D. caudata* is a producer of Diarrhoetic Shellfish Poisoning (DSP) and *Scenedesmus* sp. is an indicator of freshwater). The number of samples was 1103 (572 from Alfacs and 531 from Fangar). Separate analyses including the whole series or the segments between 1990 and 1994 and 1997 and 2003 (before and after the changes in counting method) gave consistent results with respect to the distribution of the taxa in the component space; for simplicity, only the whole series was considered in this work.

Grossman et al. (1991) concluded that the eigenvalue methodologies, such as PCA, can be used to detect patterns if the number of samples is at least three times the number of descriptors. In our case, the data set was 1103 samples x 36 descriptors (the taxa), with a ratio of about 30 to 1, indicating that our PCA should be stable.

In order to give a precise quantification of the timing and period of the tempo-

ral fluctuations of the environmental and biological variables, we used Empirical Mode Decomposition, a recently developed method for time series analysis (Huang et al., 1998) that is particularly well-suited for the study of phytoplankton data sets, which are typically non-linear and non-stationary.

The first step of the EMD is the decomposition of a time series into Intrinsic Mode Functions (IMF) that have well behaved Hilbert transforms and permit the calculation of instantaneous frequencies. The IMFs satisfy two conditions (Huang et al., 1998): (1) The number of extrema and the number of zero crossings must be either equal or differ at most by one and (2) at any point, the mean value of the envelope defined by the local maxima and the envelope defined by the local minima is zero. The sum of all IMFs retrieves the original data.

The EMD methodology (Huang et al. (1998)) was applied to the time series of temperature, salinity, stratification and to principal components 1 to 3 from the Alfacs and Fangar PCAs.

The degree of synchronization between the IMFs was assessed by means of an index, the quantity $\delta$ defined in (Solé et al., 2009):

$$\delta_{nm}(t) \equiv cos(\Delta\theta_{nm}(t)) = Re(e^{i\Delta\theta_{nm}(t)}) \tag{2.2}$$

being $\Delta\theta_{nm}(t)$ the phase difference between two IMF $c_n$ and $c_m$. The variance of $\delta$ is indicative of the regularity of the phase difference between the IMF that are being compared. We will call this quantity $\delta$ index.

$$\delta \text{ index} \equiv var[\delta_{nm}] \tag{2.3}$$

If the $\delta$ index is 0 both series will have a constant phase shift, while if it is high (up to a maximum of 1) they will be strongly decorrelated. We used $var[\delta_{nm}]$ = 0.25 (a slightly lower value than the 0.30 adopted by (Solé et al., 2007)) as an operational threshold to select pairs of IMF with a sufficiently constant phase shift.

## 2.3 Results

### 2.3.1 Environmental variables

The time series of temperature showed a strong seasonal cycle, while the fluctuations of salinity and stratification were more irregular (Figs. 2.4 and 2.5). Chl *a* and phytoplankton counts presented high variability at various temporal scales; only the dinoflagellates of Fangar seemed to present a well–marked seasonal signal. Figs. 2.2 and 2.3 present an overall view of the intensity and regularity of the seasonal cycles during the sampling period. Examination of these figures corroborates the periodicity of the temperature cycle; none of the series seems to present

any consistent changes in the yearly timing of maxima and minima. Comparison of Fig. 2.2 with Fig. 2.3 highlights some of the differences between the two bays concerning the fluctuations of salinity, stratification and dinoflagellate abundance.

The temperature climatologies (Figs. 2.6 and 2.7) of both Alfacs and Fangar were very similar. The highest temperatures occurred in August with weekly means of 28 °C (although in some occasions temperatures could reach 30 °C). The lowest temperatures, with means of 10 °C and extremes of 6 °C were observed in January. The deep layer was warmer than the shallow layer during the fall and winter months and colder during spring and winter. Bottom salinity ranged between 31 and 36 in the shallow layers of Alfacs, with the higher salinities during the closed channel period. At Fangar, which is the smallest bay, the inputs of freshwater had a greater effect and surface salinity ranged from 22 to 30 between October and December. The seasonal climatology of stratification (Figs. 2.6 and 2.7) reflected the differences between the salinity of the upper and lower water layers and showed a marked increase in April-May. The lowest average stratification was found between January and May in Alfacs and between February and May in Fangar.

The time series of temperature anomalies (Fig. 2.8 and Fig. 2.9) presented a slight positive slope, while those of salinity and stratification did not show any statistically significant trend except for the bottom salinity samples of Alfacs (Table 2.3).

### 2.3.2 Dynamics and composition of phytoplankton

#### 2.3.2.1 Principal component analysis

The first three principal components (PCs) of the analysis of the pooled Alfacs and Fangar data were considered for further examination. The amount of variance explained by these components was, respectively 14.95%, 7.84% and 6.85%. These relatively low values are typical of PCAs of phytoplankton data sets with a high number of variables (Legendre and Legendre, 1998).

The position of the taxa vectors in component space, based on their correlations (or loadings) with the first principal components are shown in Fig. 2.10. The species that contribute the most to the values (or scores) or each component are those with the highest loadings. The first principal component (PC1) presents positive loadings with most of the species, which is a common finding in phytoplankton PCAs. This reflects the common response of most taxa to general conditions favoring phytoplankton growth. The taxa with the highest loadings included dinoflagellates like (the numbers in parentheses refer to Fig. 2.10) *Ceratium furca* (3), *Prorocentrum minimum* (13) and *Prorocentrum micans* (12). Among the diatoms, the highest positive loadings corresponded to Centric diatoms (20), *Cerataulina pelagica* (21) and *Thalassionema nitzschioides* (31). The only negative

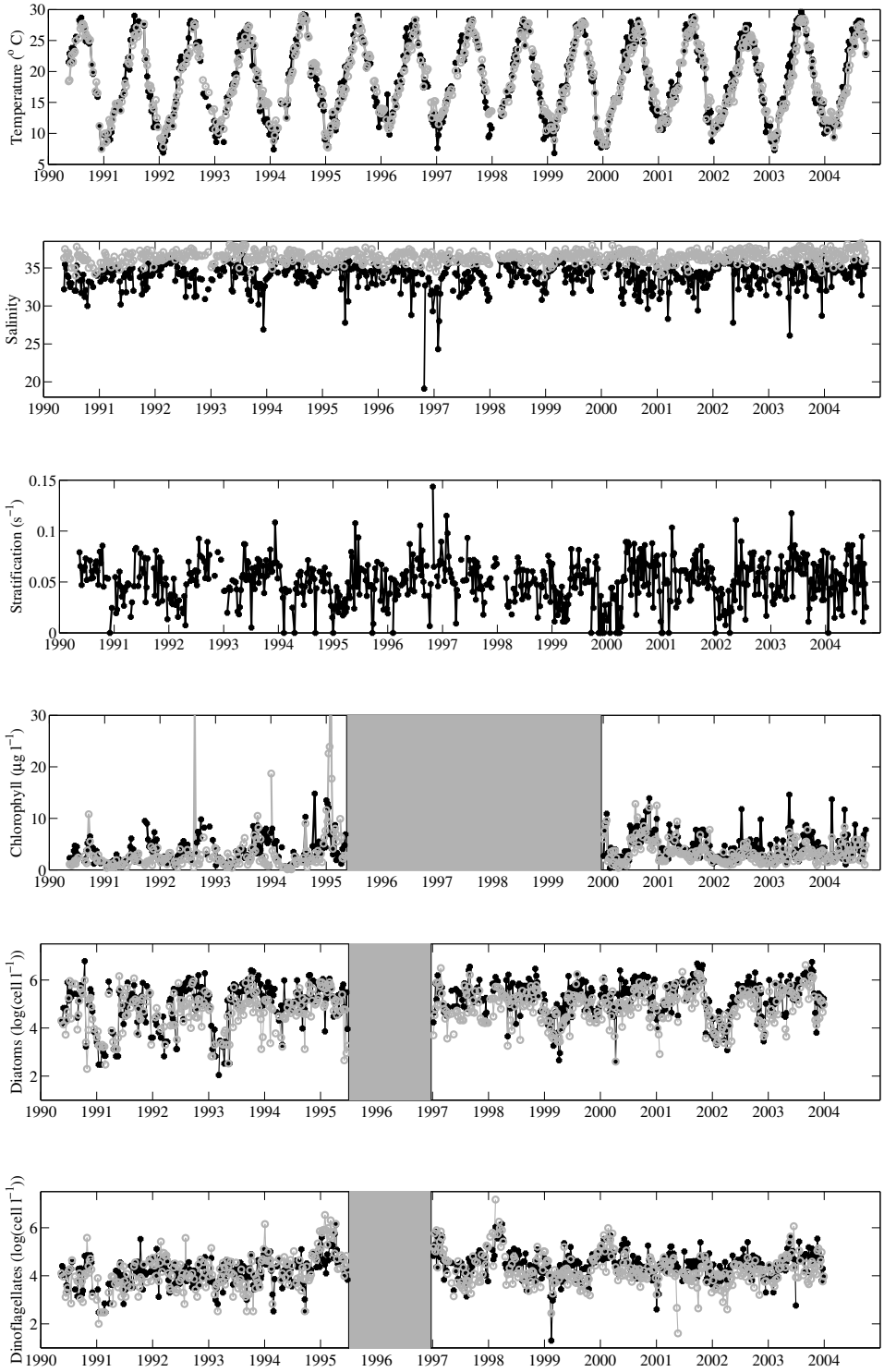


Figure 2.4: Environmental and biological data from Alfacs. *Black dots*: data at 0.5 m depth; *Grey circles*: data at 5.5 m depth. From top to bottom: temperature (°C), salinity, stratification ($s^{-1}$), Chl *a* ($\mu g\ l^{-1}$), diatoms (log(cell $l^{-1}$)), dinoflagellates (log(cell $l^{-1}$)).

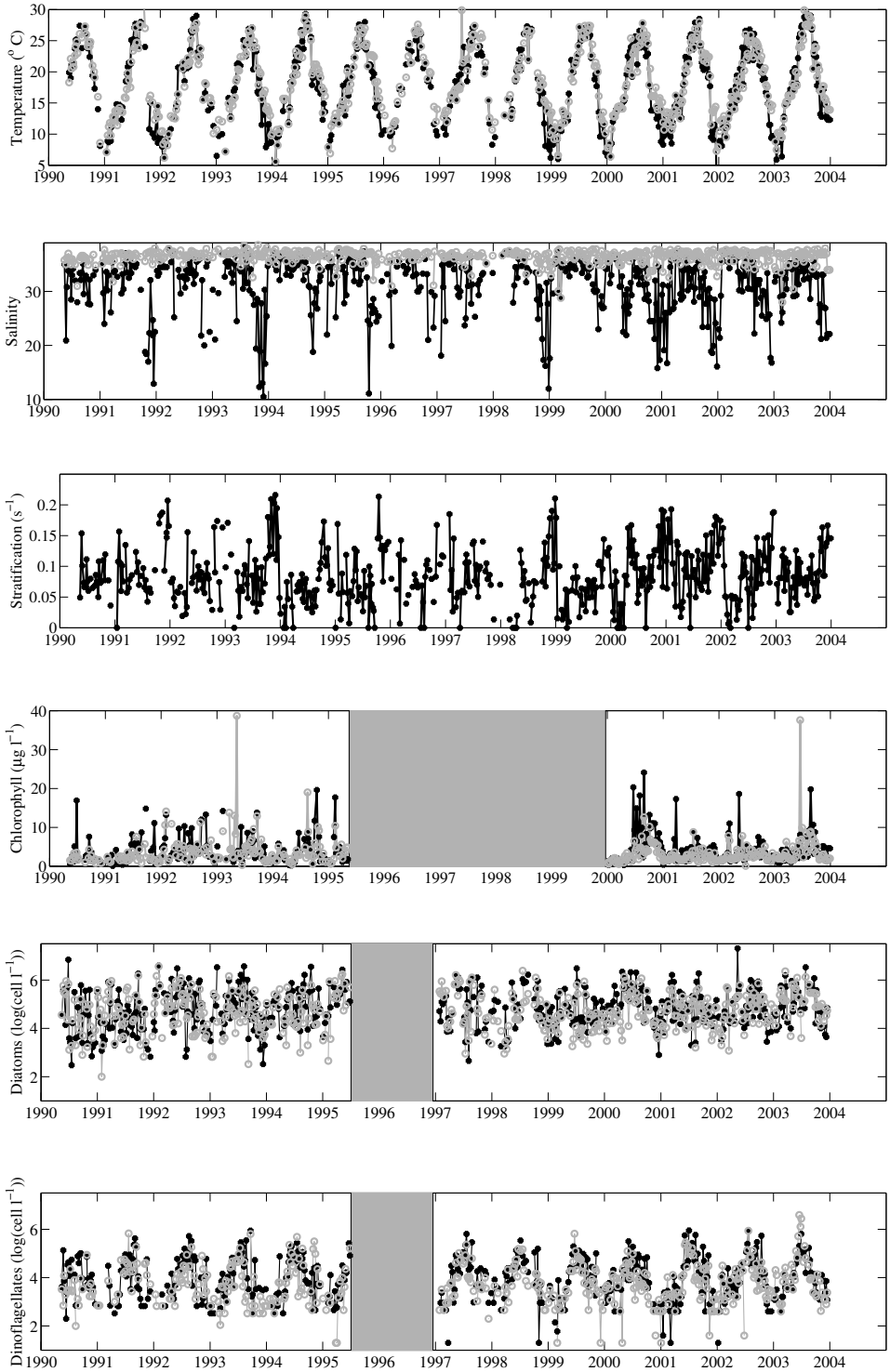


Figure 2.5: Environmental and biological data from Fangar. *Black dots*: data at 0.5 m depth; *Grey circles*: data at 5.5 m depth.; From top to bottom: temperature (°C), salinity, stratification ($s^{-1}$), Chl *a* ($\mu g\ l^{-1}$), diatoms (log(cell $l^{-1}$)), dinoflagellates (log(cell $l^{-1}$)).

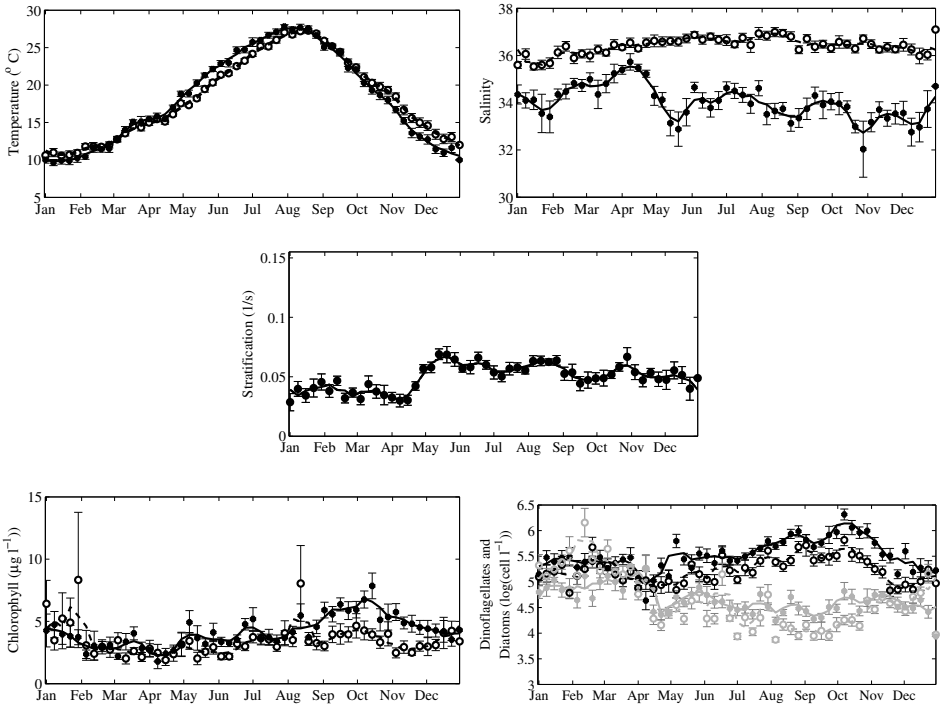


Figure 2.6: Weekly climatology of environmental and phytoplankton variables in Alfacs for the period 1990-2003. From left to right and from top to bottom: temperature, salinity, stratification, Chl *a*, and diatoms and dinoflagellates. *Filled circles* and *solid lines*: weekly mean $\pm$ standard deviation normalized by $\sqrt{n-1}$ and three point average, respectively, of data (except from stratification) from 0.5 m; *Open circles* and *broken lines*: weekly mean $\pm$ standard deviation normalized by $\sqrt{n-1}$ and three point average, respectively, of data (except from stratification) from 5.5 m depth. In the bottom right graph, *black circles* and *lines* are for diatoms and *gray circles* and *lines* for dinoflagellates.

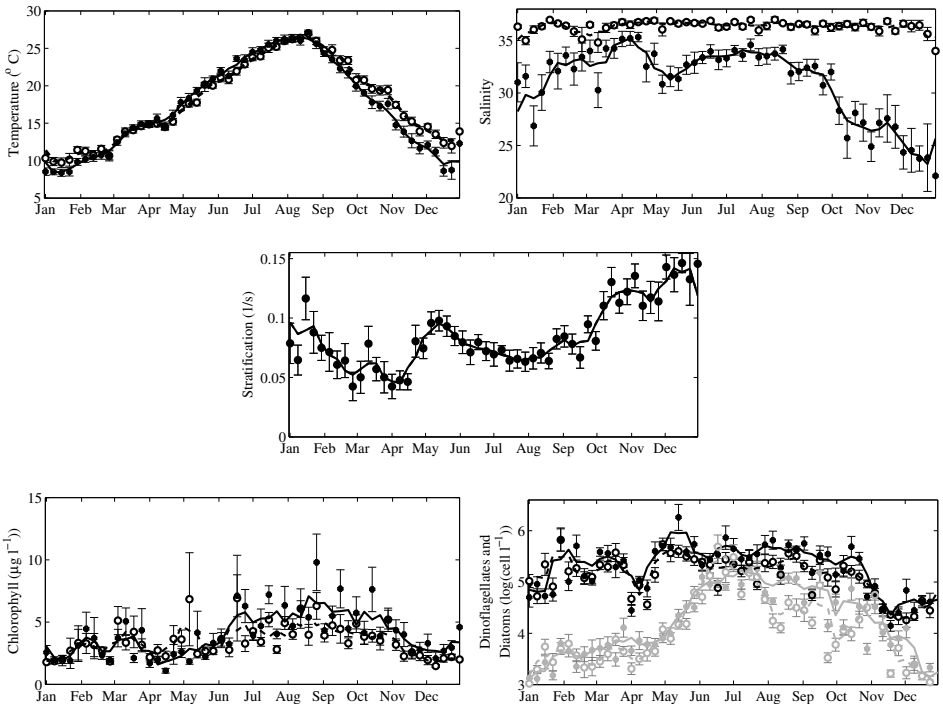


Figure 2.7: Weekly climatology of environmental and phytoplankton variables in Fangar for the period 1990-2003. From left to right and from top to bottom: temperature, salinity, stratification, Chl *a*, and diatoms and dinoflagellates. *Filled circles* and *solid lines*: weekly mean $\pm$ standard deviation normalized by $\sqrt{n-1}$ and three point average, respectively, of data (except from stratification) from 0.5 m; *Open circles* and *broken lines*: weekly mean $\pm$ standard deviation normalized by $\sqrt{n-1}$ and three point average, respectively, of data (except from stratification) from 5.5 m depth. In the bottom right graph, *black circles* and *lines* are for diatoms and *gray circles* and *lines* for dinoflagellates.

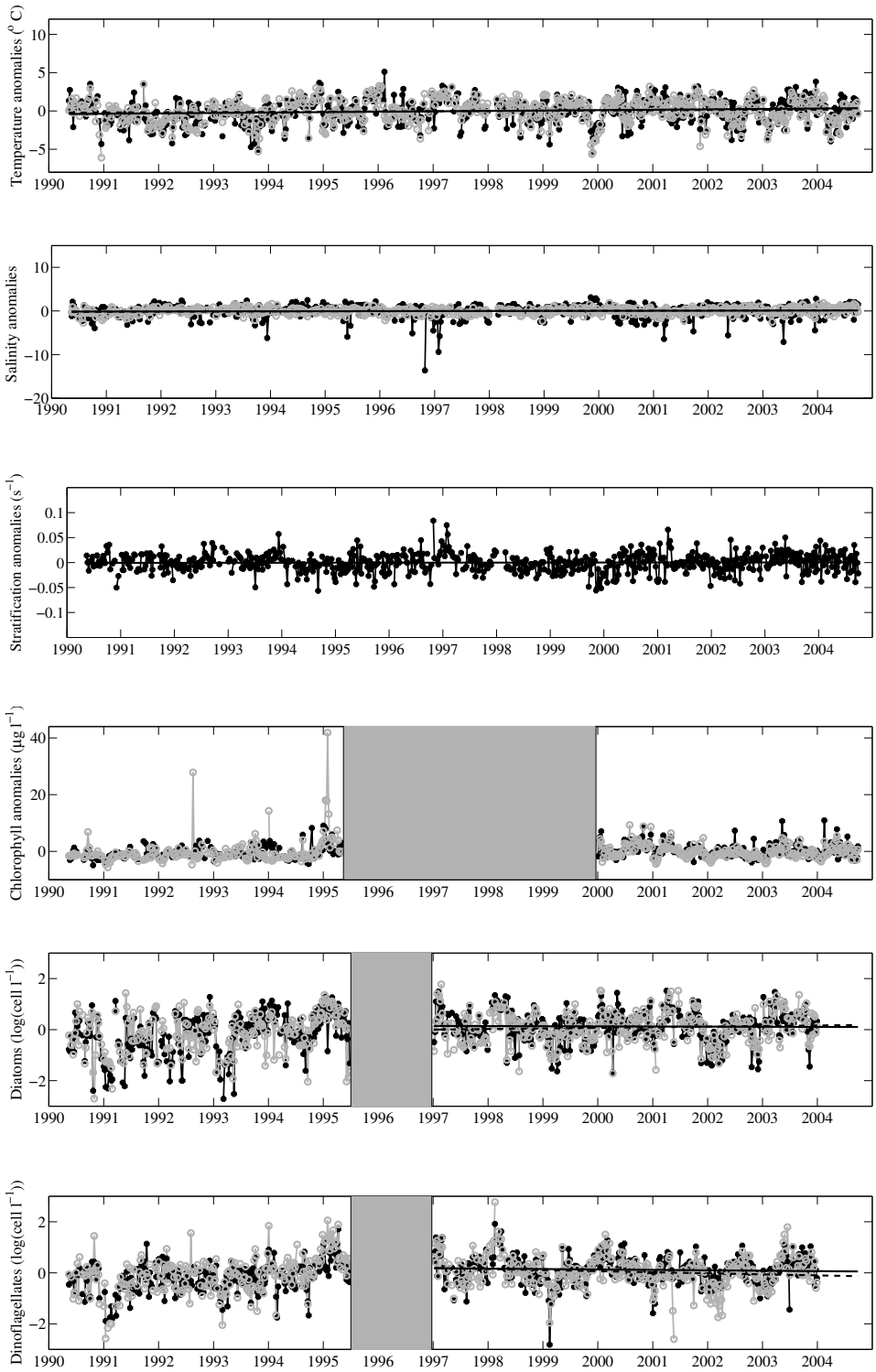


Figure 2.8: Anomalies of physical and biological data from Alfacs. *Black dots*: data at 0.5 m depth; *Grey circles*: data at 5.5 m depth. — Linear regression for 0.5 m; - - Linear regression for 5.5 m. From top to bottom: temperature (°C), salinity, stratification (s$^{-1}$), diatoms (log(cell l$^{-1}$)), dinoflagellates (log(cell l$^{-1}$)).

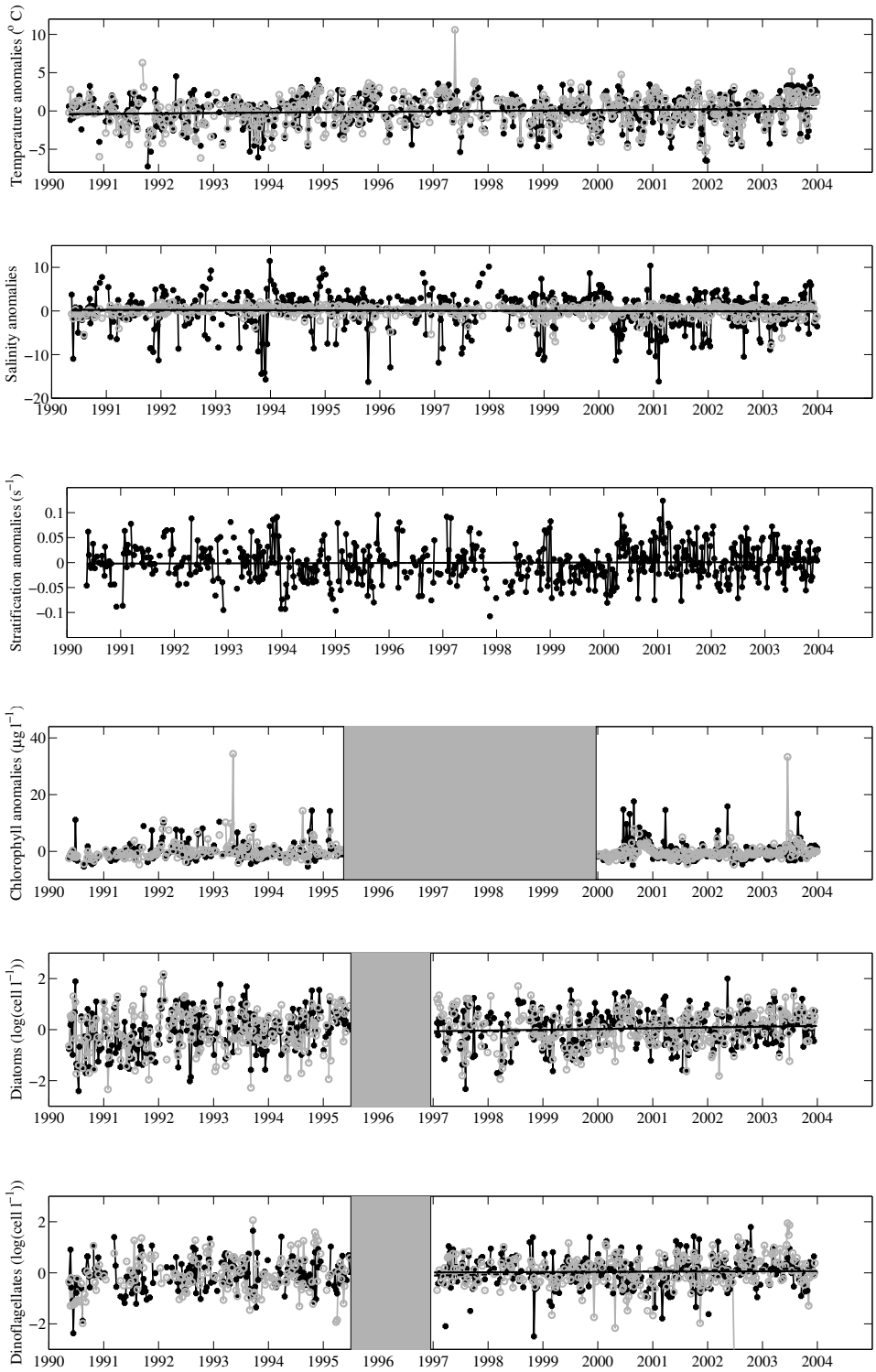


Figure 2.9: Anomalies of physical and biological data from Fangar. *Black dots*: data at 0.5 m depth; *Grey circles*: data at 5.5 m depth. — Linear regression for 0.5 m; - - Linear regression for 5.5 m. From top to bottom: temperature (°C), salinity, stratification (s$^{-1}$), diatoms (log(cell l$^{-1}$)), dinoflagellates (log(cell l$^{-1}$)).

| | | PC1 | PC2 | PC3 | DIA | DIN |
|---|---|---|---|---|---|---|
| Alfacs | Chl *a* | **0.457** | **0.256** | **0.183** | **0.394** | **0.115** |
| Fangar | Chl *a* | **0.263** | -0.093 | **0.264** | **0.391** | **0.167** |

Table 2.1: Correlations between Chl *a* and PC scores, sum of dinoflagellates (DIN), sum of diatoms (DIA). Significant correlations in bold (P>0.95)

loadings correspond to *Chaetoceros* spp. large (22), *Thalassiosira* spp. (32) and *Scenedesmus* spp. (35).

The highest positive loadings on the second principal component (PC2) were shown by a group of three diatoms: *Thalassionema nitzschioides* (31), *Lioloma pacificum* (27) and *Cylindrotheca closterium* (24), accompanied by the heterotrophic ebridian *Hermesinum adriaticum* (34). A group of dinoflagellates with *Dinophysis sacculus* (6), *Alexandrium minutum* (2), and *Karlodinium* spp.(10) presented the most negative loadings. The third principal component opposed a mixed group with high positive loadings, including *Eutreptiella* sp. (33) and the dinoflagellates (*Peridinium quinquecorne* (15), *Akashiwo sanguinea* (1) and *Protoperidinium spp.* (16) to dinoflagellates like *Karlodinium* spp. (10), (*Ceratium furca* (3), *Ceratium fusus*(4), *Prorocentrum micans* (12) and *Karenia* spp. (9), and the benthic diatom *Pleurosigma* sp. (28).

#### 2.3.2.2 Seasonal and interannual variability

The seasonality of the phytoplankton counts was very different in the two bays (Figs. 2.6 and 2.7). In Alfacs the diatom peak occurred in the fall, during the months of September and October, for both the shallow and the deep layers. The cell abundances at the bottom layer were 3-5 times smaller than those at surface. On the other hand, the peak of diatom abundance in Fangar was found during summer, and the shallow layer concentrations were only slightly higher than those of the bottom waters. Dinoflagellates were about one order of magnitude less abundant than diatoms; they reached their maximum during the first months of each year in Alfacs, but peaked in July in Fangar (Figs.2.6 and 2.7). Cell numbers were similar in shallow and deep layers, although on some occasions the deep concentrations in Alfacs were higher than those at the surface. The Chl *a* followed the diatom trend, as reflected in the higher values of the correlation of Chl *a* concentration with diatoms (Table 2.1). Chl *a* peaked in October in Alfacs, while Fangar presented high concentrations from July to November. The lower Chl *a* values for both bays occurred during late winter and early spring.

The median values of Chl *a* were 3 (Alfacs) and 2.7 (Fangar) $\mu$g $l^{-1}$ for the period 1990-1995 and 3.8 (Alfacs) and 2.7 (Fangar) $\mu$g $l^{-1}$ for 2000-2004. The difference was significant for Alfacs ($p$= 0.0002) and not significant in Fangar ($p$= 0.39) according to the Mann–Whitney U test for a 0.05 significance level. The lin-

ear temporal trends of the anomalies of bottom diatoms and dinoflagellates of Fangar were also positive for the 1997–2003. However, the magnitude of the changes was less than 0.05 (log total cells $l^{-1}$ $year^{-1}$) in all cases. None of the series of yearly minimum and maximum values presented statistically significant trends (data not shown).

The time series of the scores of the three first Principal Components can be found in Figs.2.11–2.12. In both bays, the amplitude of the fluctuations of some principal components tended to be somewhat higher from 1995 onwards. As will be discussed later, this finding may be an artifact due to changes in the counting method. All components presented somewhat marked seasonal variations, but the patterns were different in Alfacs and Fangar. The most regular fluctuations were shown by PC2 in Alfacs and by PC3 in Fangar, especially after 1995. According to the climatologies (Fig. 2.13), PC1 maxima tended to occur in November in Alfacs and between May and September in Fangar. PC2 presented a maximum in September and a minimum in March-May in Alfacs. In Fangar, PC2 was weakly positive during most of the year and had a minimum in June-July. PC3 tended to be highest between May and October in both bays, but the shape of the distribution was different in Alfacs and Fangar. There were no consistent changes in these patterns along the sampling period (Fig. 2.14). With the exception of PC2 in Fangar, all PCs were significantly correlated with Chl *a* concentration (Table 2.1). The highest correlation coefficients with Chl *a* were shown by PC1 in Alfacs and, with very similar values, by PC2 and PC3 in Fangar.

In both bays, the interannual variability of the phytoplankton variables was relatively small with respect to the seasonal fluctuations, as can be seen by comparing the ranges of the annual means of the variables (shown in Fig. 2.15 for the period 1997-2003) with the range of the seasonal maxima and minima (Figs. 2.6, 2.7 and 2.13).

### 2.3.3 Empirical Mode Decomposition

The application of Empirical Mode Decomposition to the time series of temperature, salinity, stratification, and the three first principal components gave from 7 to 9 IMFs with frequencies ranging from 0.02 $week^{-1}$ to 0.001 $week^{-1}$for each series. For simplicity, only the surface results are presented, as those for the bottom series were similar. As an example, the IMFs corresponding to PC2 are shown in Fig. 2.16. All variables presented at least an IMF with annual (seasonal) periodicity, accompanied by IMFs with higher and lower frequencies, down to the last low-frequency IMF identified as the trend. The amplitude differences between the high frequency IMF (noise), the annual IMF and most of the other IMF were relatively small, specially for the PC IMF, making it difficult to establish the significance of the IMF based on frequency criteria such as those in (Solé et al., 2007, 2009). Given that this study focuses on the influence of environment forcing on the

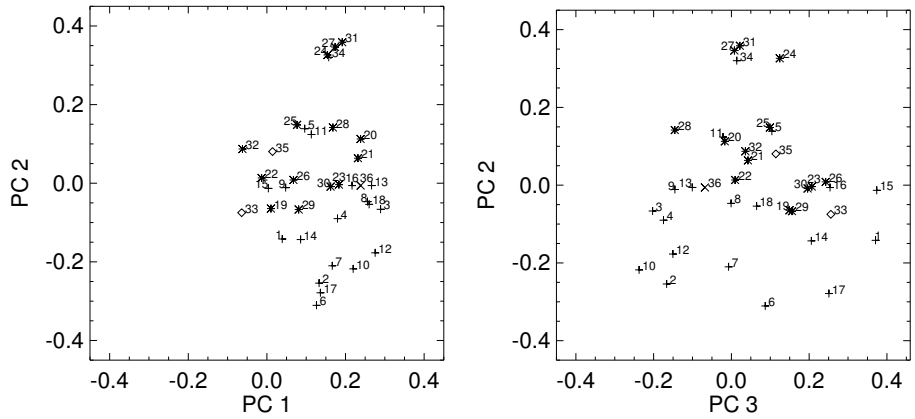


Figure 2.10: Position of the extremes of the species' vectors in two–dimensional plots of the first Principal Components. + Dinoflagellates; ∗Diatoms; × Coccolithophores; ◇ Others; △ Added species; The numbers indicate the species (see Table 2.4)

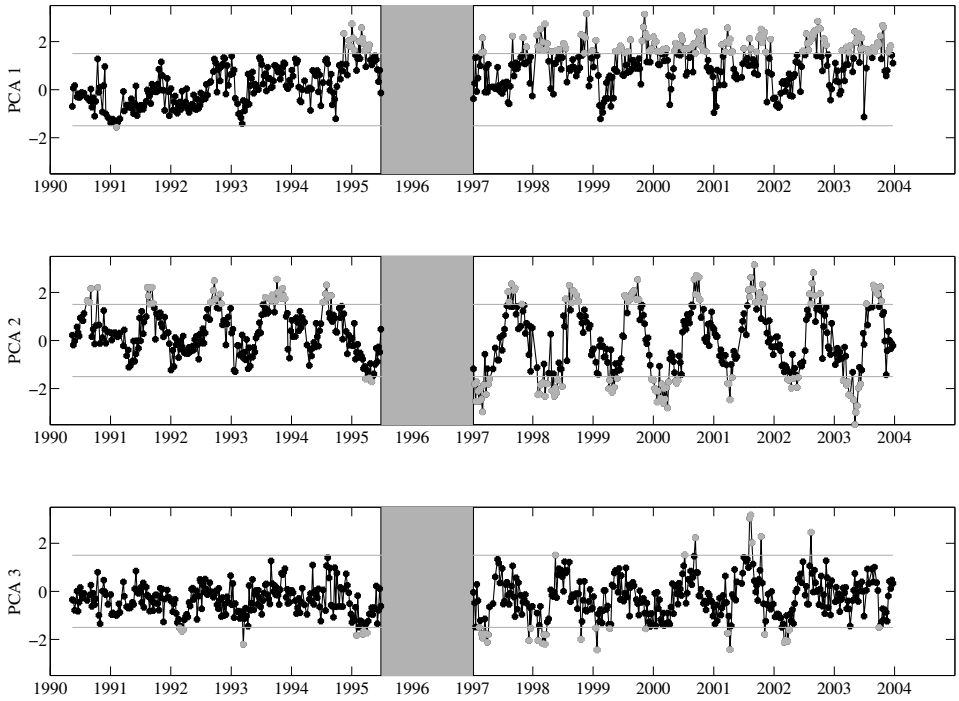


Figure 2.11: Scores of the three first principal components (PCs) for the 0.5 m depth samples of Alfacs. From top to bottom: PC1, PC2 and PC3.

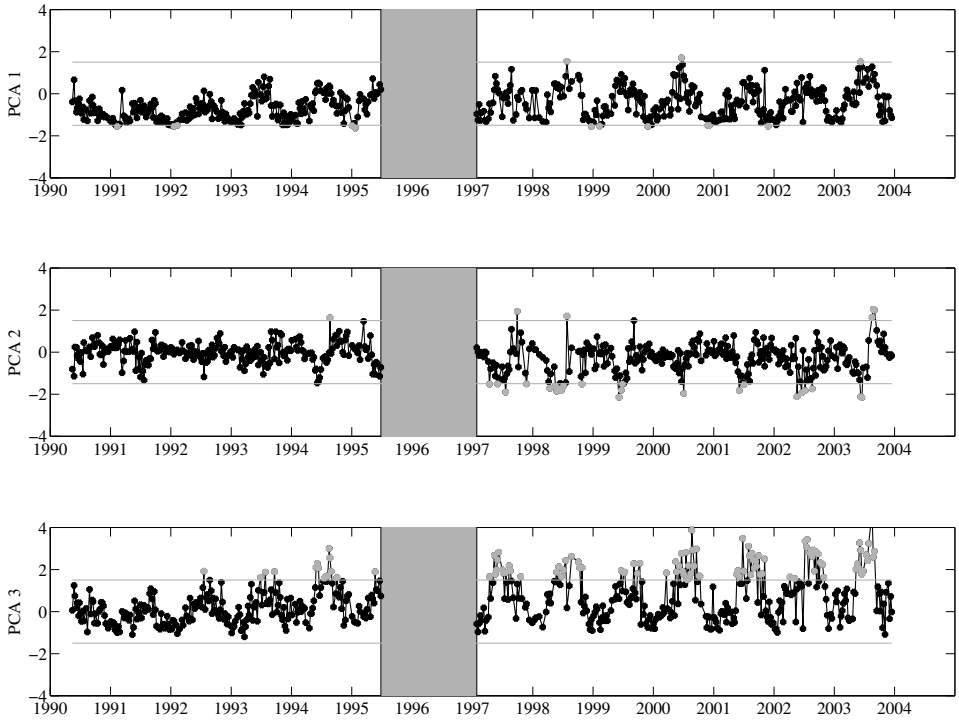


Figure 2.12: Scores of the three first principal components (PCs) for the 0.5 m depth samples of Fangar. From top to bottom: PC1, PC2 and PC3. Note change of scale for the third principal component.

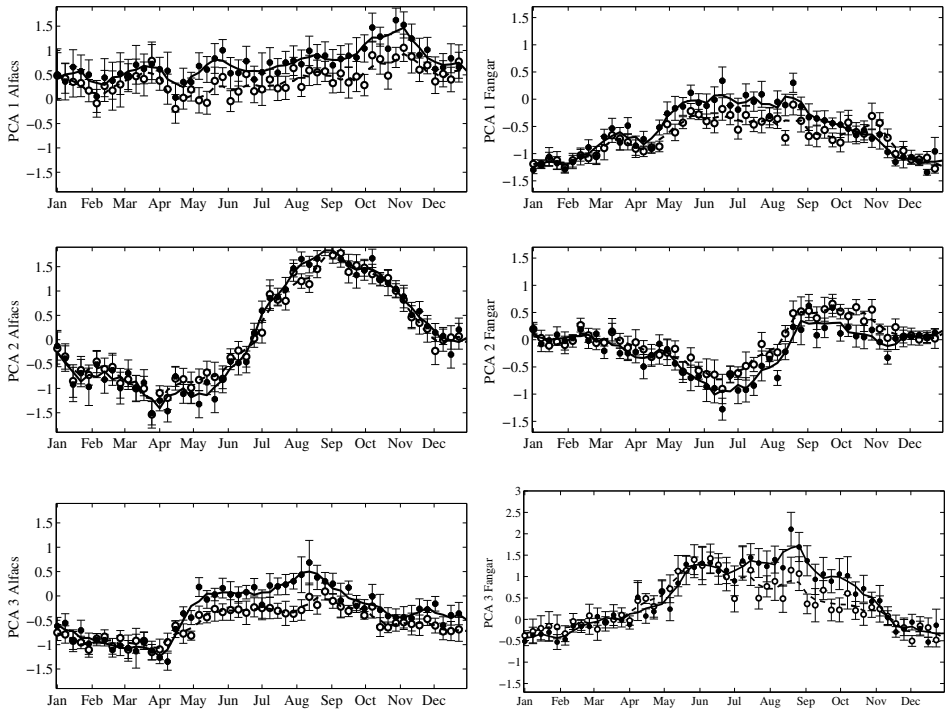


Figure 2.13: Weekly climatology of the scores of PC1, PC2 and PC3 of the 0.5 m depth samples of Alfacs (left column) and Fangar (right column) period 1990–2003. *Filled circles* and *solid lines*: weekly mean $\pm$ standard deviation normalized by $\sqrt{n-1}$ and thee point average, respectively, of data from 0.5 m depth ; *Open circles* and *broken lines*: weekly mean $\pm$ standard deviation normalized by $\sqrt{n-1}$ and three point average, respectively, of data from 5.5 m depth. Note change of scale in PC2 Alfacs and PC3 Fangar.

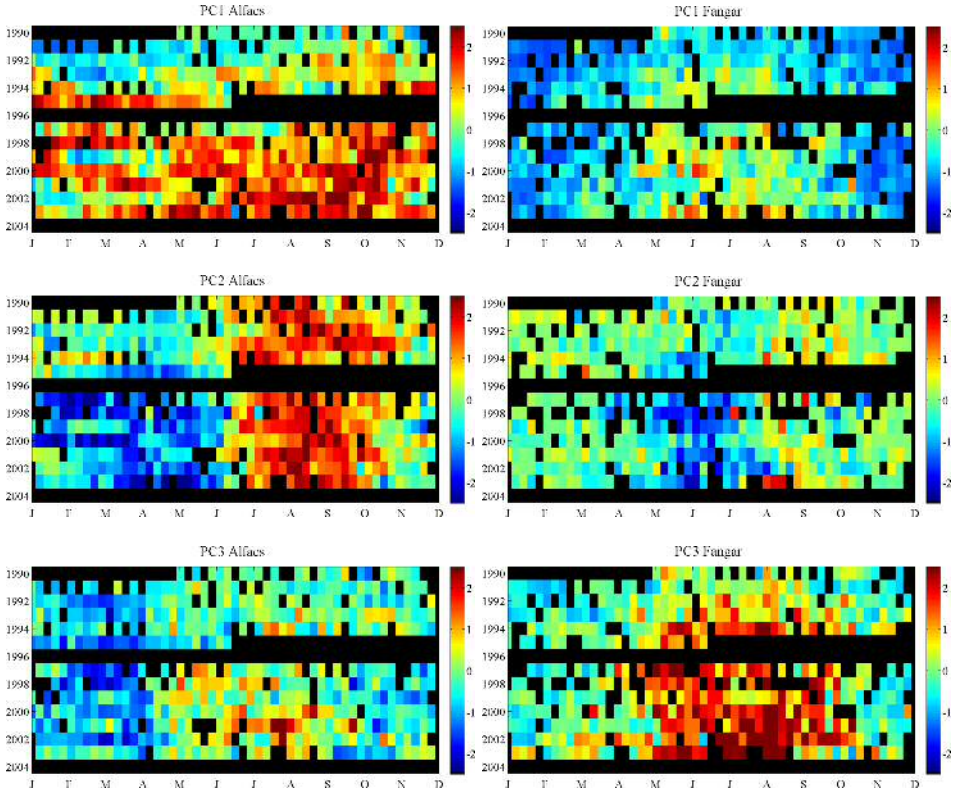


Figure 2.14: Seasonal distribution of the scores of the first three PCs at 0.5 m depth of Alfacs (left column) and Fangar (right column) during the period from 1990 to 2003.

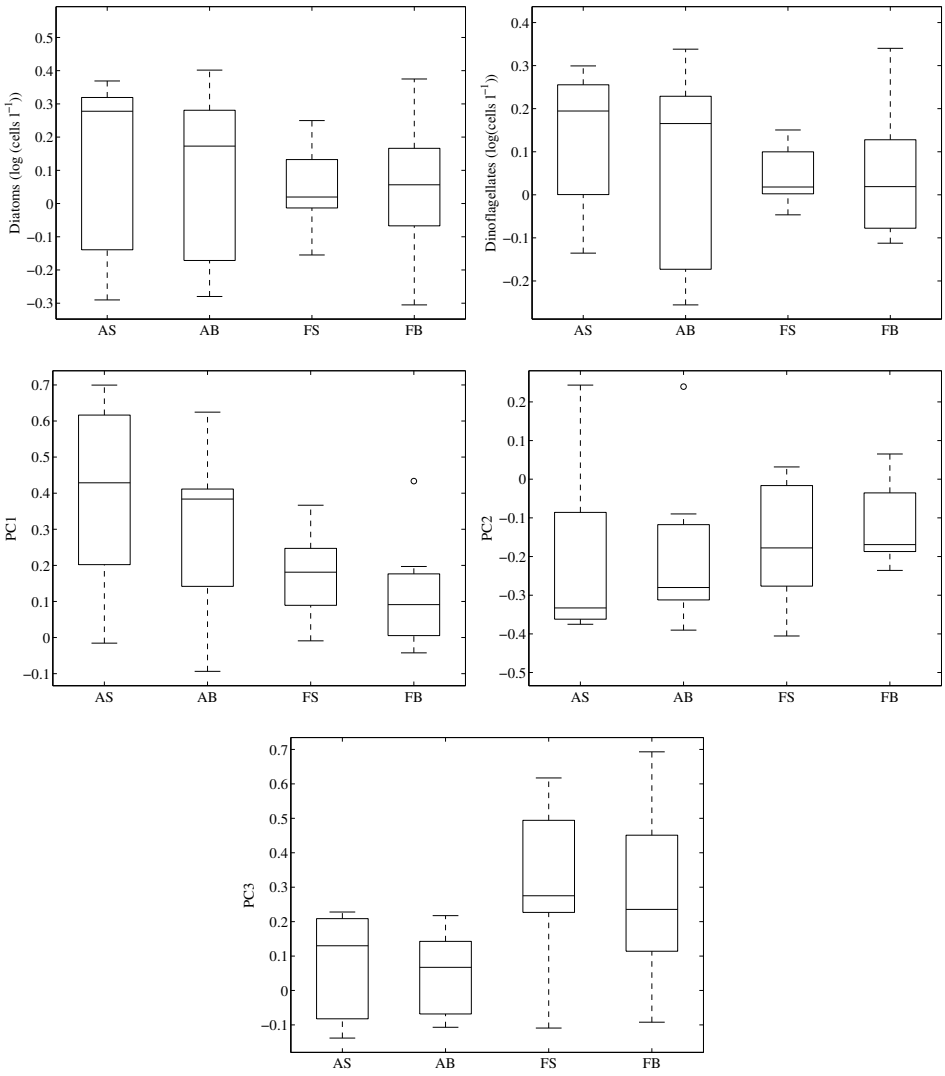


Figure 2.15: Variation of the annual means of the phytoplankton variables for the years 1997 to 2003. The central mark is the median, the edges of the box are the 25th and 75th percentiles, the whiskers extend to the most extreme data points not considered outliers, and outliers are plotted individually. AS: Alfacs Surface; AB: Alfacs Bottom; FS: Fangar Surface; FB: Fangar bottom.

| | Temperature | $var[\delta_{nm}]$ | Salinity | $var[\delta_{nm}]$ | Stratification | $var[\delta_{nm}]$ |
|---|---|---|---|---|---|---|
| Alfacs | | | | | | |
| PC1 | | | IMF 5 – IMF 5 | 0.23 | | |
| PC2 | IMF4 – IMF5 | 0.18 | | | | |
| PC3 | | | | | | |
| Fangar | | | | | | |
| PC1 | IMF4 – IMF4 | 0.08 | | | IMF5 – IMF4 | 0.30 |
| PC2 | IMF4 – IMF5 | 0.23 | IMF5 – IMF5 | 0.24 | | |
| PC3 | IMF4 – IMF4 | 0.15 | | | IMF5 – IMF4 | 0.26 |

Table 2.2: Correlations between pairs of IMF (first IMF: temperature, salinity or stratification; second IMF: PC)

seasonal dynamics of phytoplankton, we concentrated our subsequent analyses on the annual IMFs.

The results of the application of the $\delta$ index test to the annual IMF pairs are summarized in Table 2.2. The pairs of correlated IMFs and the corresponding $\delta$ index are presented in Fig. 2.17. In Alfacs, IMF5 of PC1 and IMF4 of PC2 were respectively correlated with IMF5 of both salinity and temperature. In Fangar, IMF4 of all the PCs were correlated with IMF4 or IMF5 of temperature, while IMF5 of PC2 was correlated with IMF5 of salinity.

## 2.4 Discussion

### 2.4.1 Environmental variables

The linear regression of weekly temperature anomalies showed a marginally significant positive slope for both surface and bottom samples of both bays. Solé et al. (2009), also reported a small increasing trend for monthly temperature anomalies in Alfacs; however, in their case, the slope was non-significant. Although these observations must be interpreted with caution, given the low correlation coefficients and the short time span of the measurements, they are likely to be associated with the general warming of air temperatures detected in the region (Martín-Vide, 2005). Salinity presented a weak significant increasing trend in the bottom layer of Alfacs. The magnitude of the trend is similar to that detected in coastal waters of Mallorca (0.017 and 0.031 per year at 10 and 50 m depth (Vargas-Yáñez et al., 2007). The mechanisms accounting for the salinity increase of marine waters are likely to imply circulation changes rather than direct effects of warming or evaporation (Vargas-Yáñez et al., 2007). Similarly, the trends in the bays may be related to changes in the estuarine circulation in response to effects such as the increased temperature (and decreased density) mainly affecting the shallow waters. This increasing trend of salinity contrasts with the results of de Pedro (2007), who found a slight decrease in the salinity of the deep (below the pycnocline) layers, between

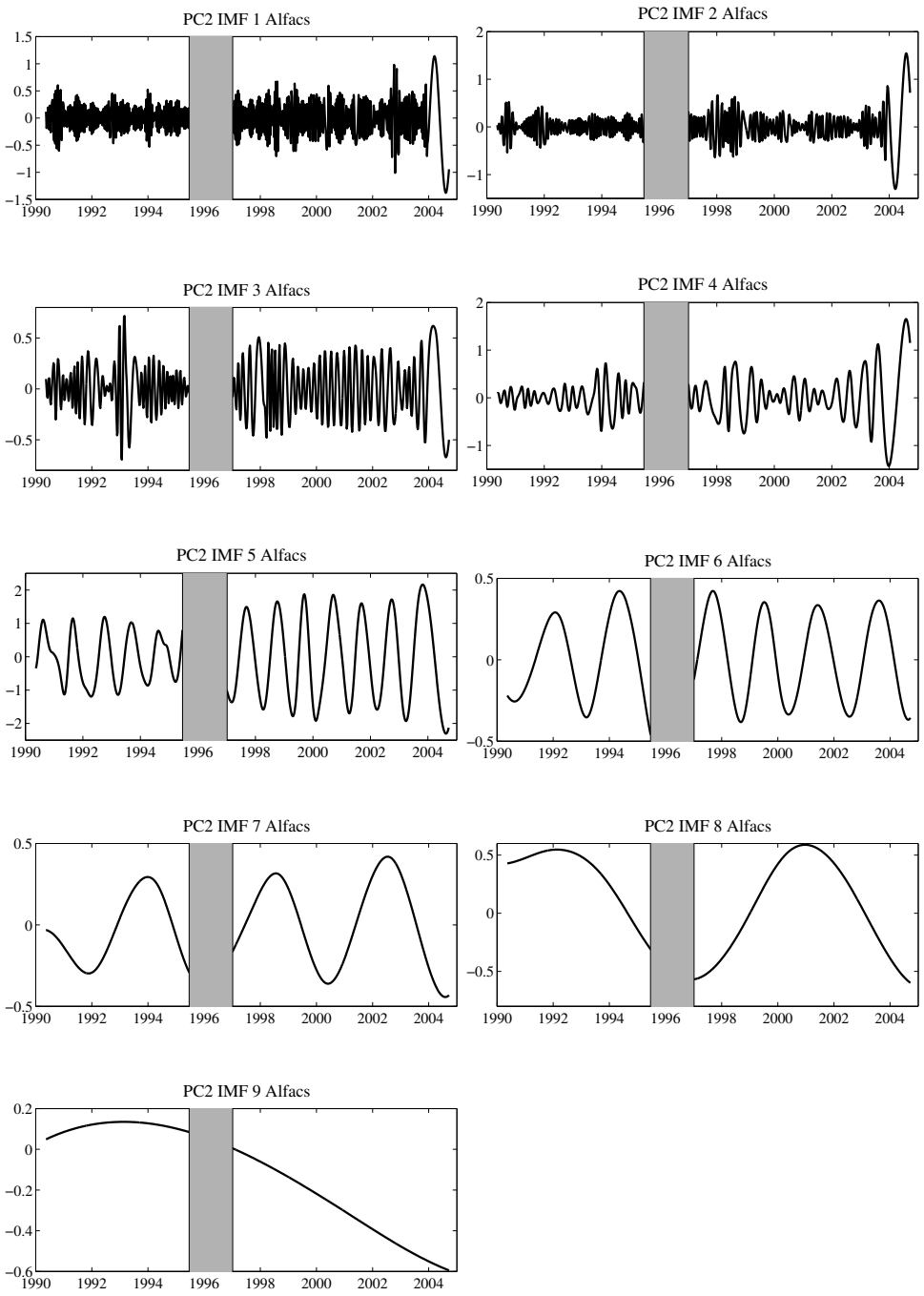


Figure 2.16: Example of IMF decomposition of the scores of PC2 of the 0.5 m depth samples of Alfacs.

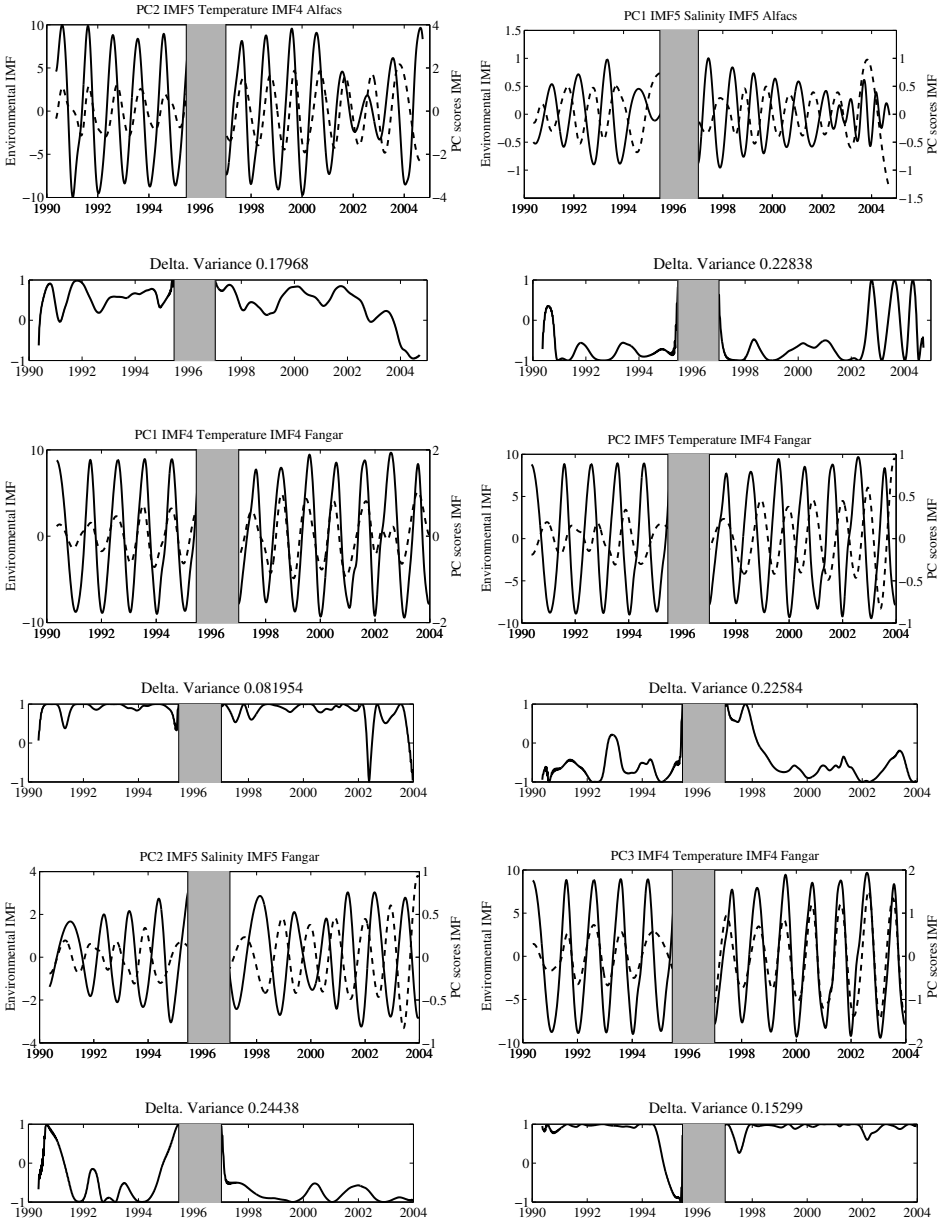


Figure 2.17: Pairs of significantly correlated annual IMFs of environmental variables and PC scores (see Table 2.2). *Solid line*: environmental IMF; *broken line*: PC scores IMF.

1990 and 1998. This discrepancy could be due to differences in the time periods considered and in the data analysis methods, and highlights the need of a longer series of data in order to make reliable conclusions.

The temperature peaks that occurred in August-September in both Alfacs and Fangar (Figs. 2.2 and 2.3) are in agreement with the evolution of air temperatures in the region, and did not show any tendency to a change in timing along the studied period. Interestingly, the lowest salinities and highest stratification values occurred in Fangar between October and December during the closed channel period, a feature that did not change (data not shown) if the climatology was performed only for the years before 2001, when the ecological freshwater flow between October and November had not been established yet. This observation may be linked to interaction between estuarine circulation and higher surface water densities due to low autumn- winter temperature (Camp, 1994). In addition, freshwater is allowed into Fangar during these months in connection with hunting and fishing activities. Unfortunately, no good data appear to be available on the actual freshwater fluxes. In addition, there is a poorly known input of underground freshwater into both bays, with significant implications for both nutrient fluxes and water column stability (Llebot et al., 2010).

### 2.4.2 Dynamics and composition of phytoplankton

The lack of differences in the median concentrations of Chl *a* in Fangar between the 1990-1995 and 2000-2004 subseries suggests that there were no trends in overall phytoplankton biomass during the studied period. In Alfacs, the differences between the two periods are significantly different, showing an increase of the Chl *a* concentration during the second period. However, these data must be interpreted with caution, due to the change in measurement method that took place in 2000.

The positive trends detected in diatoms, dinoflagellates and principal components for some of the sample subsets (Table 2.3) suggest that there may have been a slight increase in the abundance of the taxa associated positively with the principal components, but they were too small to be relevant.

Most phytoplankton taxa encountered in this study could be found in both Alfacs and Fangar, but some of them (like *Karlodinium* spp. and *Thalassionema nitzschioides*) showed striking differences in mean abundance between the two bays (see Table 2.4). An interesting feature was the qualitative and quantitative differences in the seasonality of diatoms and in particular of dinoflagellates between Alfacs and Fangar. In Alfacs, diatoms peaked in October - November, while dinoflagellates were more abundant between December and April (Fig. 2.6). In contrast, in Fangar, both diatoms and dinoflagellates were more abundant during the summer (Fig. 2.7). However, the overall behavior of dinoflagellates in Fangar masks the occurrence of two assemblages that dominate the seasonal cycle and

| Variable | Alfacs | | | | | |
|---|---|---|---|---|---|---|
| | 0.5 m. | | | 5.5 m. | | |
| | Slope | $R^2$ | $\rho$ | Slope | $R^2$ | $\rho$ |
| Temperature (°C) | 0.052±0.03 | 0.018 | 0.15 | 0.029±0.027 | 0.007 | 0.09 |
| Salinity | NS | | | 0.025 ± 0.013 | 0.023 | 0.14 |
| Stratification ($s^{-1}$) | NS | | | NS | | |
| Diatoms 1997–end (log(total cells $l^{-1}$)) | NS | | | NS | | |
| Dinoflagellates 1997 (log(total cells $l^{-1}$))–end | NS | | | NS | | |
| PC1 | 0.051±0.04 | 0.016 | 0.14 | 0.068±0.04 | 0.034 | 0.19 |
| PC2 | NS | | | NS | | |
| PC3 | 0.050±0.04 | 0.020 | 0.14 | 0.042±0.03 | 0.023 | 0.14 |
| | Fangar | | | | | |
| | 0.5 m. | | | 3.5 m. | | |
| | Slope | $R^2$ | $\rho$ | Slope | $R^2$ | $\rho$ |
| Temperature (°C) | 0,051±0,04 | 0.010 | 0.118 | 0,060 ±0,04 | 0.016 | 0.143 |
| Salinity | NS | | | NS | | |
| Stratification ($s^{-1}$) | NS | | | NS | | |
| Diatoms 1997–end (log(total cells $l^{-1}$)) | NS | | | 0.0467±0.0387 | 0.019 | 0.16 |
| Dinoflagellates 1997–end (log(total cells $l^{-1}$)) | NS | | | 0.0426± 0.037 | 0.018 | 0.15 |
| PC1 | NS | | | 0.060±0.026 | 0.064 | 0.27 |
| PC2 | NS | | | 0.039±0.031 | 0.020 | 0.14 |
| PC3 | 0.078±0.047 | 0.036 | 0.19 | 0.089±0.050 | 0.040 | 0.20 |

Table 2.3: Slope (time units are $year^{-1}$) and 95% confidence interval of regression lines of anomalies from series shown in figures 2.4 and 2.5. Only significant trends (95% confidence interval not including zero) and correlation coefficients are shown. NS: no significant. R: Pearson's linear correlation coefficient; $\rho$: Spearman's rho.

Table 2.4: Statistics for the chosen species. Period 1990–2003, samples taken every one–two weeks. (units: cells/l). A: Alfacs; F: Fangar.

| **Specie** | **Num.** | **Observations** | | **% Observations** | | **Mean** | | **St. Deviation** | | **Maximum** | |
|---|---|---|---|---|---|---|---|---|---|---|---|
| | | A | F | A | F | A | F | A | F | A | F |
| *Akashiwo sanguinea* | 1 | 75 | 206 | 6.6 | 19.7 | 695 | 1238 | 2560 | 2664 | 20800 | 20800 |
| *Alexandrium minutum* | 2 | 182 | 10 | 16.0 | 1.0 | 905 | 285 | 1260 | 203 | 8645 | 600 |
| *Ceratium furca* | 3 | 651 | 80 | 57.4 | 7.6 | 656 | 9.2 | 1362 | 180 | 25308 | 1332 |
| *Ceratium fusus* | 4 | 198 | 42 | 17.5 | 4.0 | 143 | 58 | 469 | 138 | 5460 | 1332 |
| *Dinophysis caudata* | 5 | 86 | 34 | 7.6 | 3.3 | 92 | 50 | 200 | 69 | 1300 | 333 |
| *Dinophysis sacculus* | 6 | 256 | 174 | 22.4 | 16.6 | 198 | 350 | 522 | 913 | 6200 | 9324 |
| *Gyrodinium* spp. | 7 | 201 | 70 | 17.7 | 6.7 | 1722 | 2988 | 2850 | 6766 | 2760 | 35200 |
| *Heterocapsa niei* | 8 | 498 | 123 | 43.9 | 11.8 | 10702 | 1554 | 58423 | 2703 | 917280 | 22100 |
| *Karenia* sp. | 9 | 129 | 18 | 11.4 | 1.7 | 10809 | 4877 | 41609 | 13425 | 374500 | 55944 |
| *Karlodinium* spp. | 10 | 312 | 9 | 27.5 | 0.9 | 140088 | 499 | 885032 | 155 | 14842200 | 910 |
| *Oxytoxum longiceps* | 11 | 130 | 35 | 11.5 | 3.3 | 830 | 818 | 1329 | 1471 | 8800 | 8000 |
| *Prorocentrum micans* | 12 | 756 | 174 | 66.7 | 16.6 | 2509 | 861 | 3735 | 1693 | 32760 | 15470 |
| *Prorocentrum minimum* | 13 | 497 | 80 | 43.8 | 7.6 | 10083 | 6520 | 48259 | 24857 | 641433 | 204000 |
| *Prorocentrum triestinum* | 14 | 380 | 377 | 33.5 | 36.0 | 5419 | 51745 | 16770 | 264524 | 164470 | 3780000 |
| *Protoperidinium quinquecorne* | 15 | 27 | 177 | 2.4 | 16.9 | 566 | 1638 | 473 | 4141 | 2000 | 42800 |
| *Protoperidinium* spp. | 16 | 415 | 308 | 36.6 | 29.4 | 914 | 1495 | 2590 | 2828 | 49140 | 35200 |
| *Scrippsiella* spp. | 17 | 650 | 568 | 57.3 | 54.3 | 2338 | 18805 | 3176 | 52894 | 32760 | 592000 |
| Small dinoflagellates | 18 | 1051 | 729 | 92.7 | 69.7 | 21747 | 7774 | 81578 | 17256 | 141440 | 190000 |
| *Benthic Diatoms* | 19 | 646 | 727 | 57.0 | 69.5 | 4674 | 12532 | 17550 | 25482 | 367900 | 317600 |
| *Centric Diatoms* | 20 | 586 | 259 | 51.7 | 24.8 | 68189 | 115801 | 220878 | 1276527 | 3847480 | 20408000 |
| *Cerataulina pelagica* | 21 | 338 | 104 | 29.8 | 9.9 | 19791 | 31429 | 81568 | 131366 | 1315760 | 989989 |
| *Chaetoceros* spp. large (30$\mu$m) | 22 | 265 | 320 | 23.4 | 30.6 | 9980 | 26862 | 19739 | 83678 | 163800 | 1068920 |
| *Chaetoceros* spp. small | 23 | 684 | 534 | 60.3 | 51.1 | 133273 | 193564 | 311185 | 460469 | 5760700 | 6106500 |
| *Cylindrotheca closterium* | 24 | 663 | 475 | 58.5 | 45.4 | 90227 | 12891 | 258424 | 52583 | 3449990 | 764400 |
| *Guinardia striata* | 25 | 129 | 71 | 11.4 | 6.8 | 4531 | 1518 | 10729 | 1649 | 94500 | 11322 |

Continued on next page

**Table 2.4 – continued from previous page**

| Specie | Num. | Observations | | % Observations | | Mean | | St. Deviation | | Maximum | |
|---|---|---|---|---|---|---|---|---|---|---|---|
| | | A | F | A | F | A | F | A | F | A | F |
| *Leptocylindrus danicus+minimus* | 26 | 372 | 465 | 32.8 | 44.5 | 16055 | 40966 | 34732 | 111655 | 311000 | 1440920 |
| *Lioloma pacificum* | 27 | 345 | 85 | 30.4 | 8.1 | 13867 | 14393 | 43154 | 50313 | 509600 | 302400 |
| *Pleurosigma* spp. | 28 | 385 | 76 | 34.0 | 7.3 | 2209 | 564 | 4710 | 952 | 70720 | 7200 |
| *Proboscia alata* | 29 | 232 | 187 | 20.5 | 17.9 | 16760 | 9139 | 64101 | 25093 | 601100 | 248885 |
| *Pseudo-nitzschia* spp. | 30 | 680 | 588 | 60.0 | 56.2 | 64744 | 73587 | 183018 | 236106 | 2354350 | 2680860 |
| *Thalassionema nitzschioides* | 31 | 525 | 234 | 46.3 | 22.4 | 151379 | 8338 | 440389 | 12916 | 5401760 | 89200 |
| *Thalassiosira* spp. | 32 | 112 | 214 | 9.9 | 20.5 | 19376 | 48337 | 101846 | 228505 | 907088 | 3175200 |
| *Eutreptiella* spp. | 33 | 154 | 395 | 13.6 | 37.8 | 2452 | 5371 | 7498 | 13769 | 81600 | 141050 |
| *Hermesinum adriaticum* | 34 | 249 | 18 | 22.0 | 1.7 | 6744 | 2159 | 19430 | 4415 | 234400 | 18200 |
| *Scenedesmus* spp. | 35 | 86 | 81 | 7.6 | 7.7 | 1408 | 835 | 2253 | 686 | 19565 | 3600 |
| *Syracosphaera pulchra* | 36 | 470 | 137 | 41.4 | 13.1 | 4746 | 1153 | 11577 | 1191 | 167960 | 6825 |

tend to proliferate at different times of the year (summer or winter), as will be discussed below, in connection with the PCA results.

The differences in phytoplankton composition between Alfacs and Fangar are well reflected in the ordination of samples in relationship with PC1. As can be seen in Fig. 2.18, the samples from Fangar tend to be concentrated in the negative side, while those of Alfacs also occupy the positive side. In phytoplankton analyses in general, most taxa are correlated with one of the sides (the positive one in our case) of the first PC, reflecting that many taxa tend to respond in the same way to favorable sets of environmental conditions (in a spring bloom, for example). In our case, there is also a sizable group of species negatively correlated with PC1 indicating that they favored under different conditions than those of the positive side. The occurrence of organisms like *Scenedesmus*, *P. quinquecorne* and *Eutreptiella* in the negative side (Fig. 2.10) indicates the relationship of the positive-negative direction of PC1 with a high-low freshwater influence trend. The concentration of the Fangar samples in the negative side of PC1 expresses this trend. It mus be noted that "freshwater influence" as used here is not the same as salinity; although the climatology of PC1 is comparable to that of salinity in Fangar, it is quite different in Alfacs, suggesting that the PC1 trend incorporates other ecological effects. The positive correlation of PC1 with Chl *a* (Table 2.1) indicates that the high Chl *a* situations are not associated with a strong freshwater influence. This finding may be explained by the low water residence times associated with situations of large freshwater input in Fangar, which has a smaller basin volume than Alfacs (see section 2.4.3). The low water residence times do not allow enough time for the development of large phytoplankton populations.

The obvious change of pattern shown by all series of PC scores between 1994 and 1995 can be accounted for by the changes in the counting method introduced in 1995. The higher settled cell numbers (which affect the statistical variability of the counts) and improved visibility allowed by the new settling chamber seems to have affected mainly the counts of naked dinoflagellates (data not shown). It must be noted that the changes were not easily detected in the series of untransformed values or anomalies. This observation highlights the interest of multivariate methods like PCA for the detection of variability in phytoplankton data.

As can be seen in the series and climatologies of PC2 and PC3 (Figs. 2.11, 2.12, 2.13 and 2.18), the seasonal fluctuations of PC2 are more regular and have larger amplitudes in Alfacs than Fangar, while the opposite happens with those of PC3. Both PC2 of Alfacs and PC3 of Fangar (Fig. 2.13), show a peak in August–September, coinciding with the seasonal water temperature maximum. These observations suggest that PC2 and PC3 mainly express the seasonal cycles in Alfacs and Fangar, respectively, although, of course, each of them also fluctuates in the other bay. The group of diatoms positively correlated with PC2, *Cylindrotheca closterium*, *Lioloma pacificum* and *Thalassionema nitzschioides*, which form a consistent cluster of taxa with high positive loadings on PC2, moderately positive on PC1 and close to 0 on PC3, are typical of autumn phytoplankton blooms in

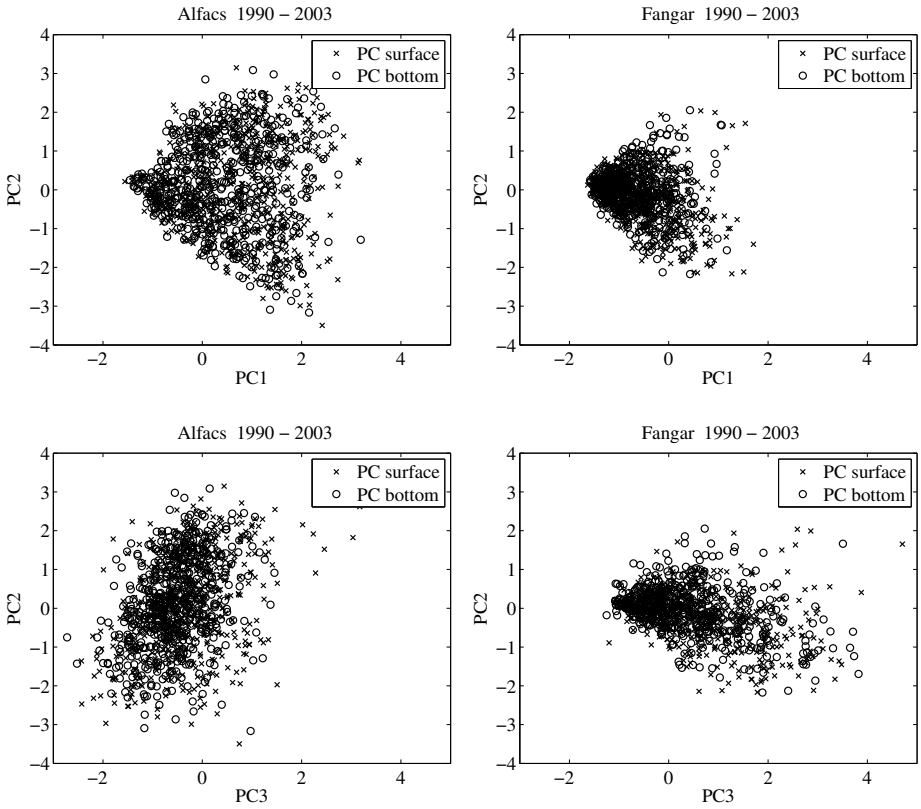


Figure 2.18: Distribution of the scores of the surface ($x$) and bottom ($\circ$) samples of Alfacs (left) and Fangar (right) in the space of PC1 and PC2 (top) and PC3 and PC2 (bottom).

the Catalan coast (Margalef, 1969); the prevalence of *Thalasionema nitzschioides* in Alfacs (Table 2.4) responds to the marine character of this bay. The late winter-early spring negative values of PC2 in Alfacs are related to the proliferation of a group of dinoflagellates including *Dinophysis sacculus*, *Alexandrium minutum*, *Karlodinium* spp. and *Scrippsiella* sp. Two of these taxa, *Alexandrium minutum* and *Karlodinium* sp., in addition to others such as *Ceratium furca* and *Ceratium fusus*, generally also with winter maxima, are typical of the winter assemblage of Fangar, as shown by their negative correlation with PC3. In contrast with PC2, the positive side of PC3 includes mainly dinoflagellates (one of them, the brackish water species *Peridinium quinquecorne*) with maxima in late spring and summer; the co-occurrence of other indicators of freshwater influence (like *Eutreptiella* sp.) may be related to the presence of these maxima during a period of relatively high freshwater inputs. The positive correlation of Chl *a* with PC2 in Alfacs and PC3 in Fangar indicate that the higher phytoplankton biomasses are associated with the assemblages characterizing the positive extreme of these PCs, the autumn blooming diatoms in Alfacs and the dinoflagellate-dominated group in Fangar.

It is important to point out that *D. sacculus* and *A. minutum* are respectively DSP and PSP (Paralytic Shellfish Poisoning) producers, while *Karlodinium* species produce fish-killing toxins. *Karlodinium* was formerly identified as *Gyrodinium corsicum* (Delgado and Alcaraz, 1999). Later studies of Alfacs strains indicated that there were, in fact, two *Karlodinium* species, *K. veneficum* and *K. armiger* (Garcés et al., 2006), both of them toxic. It is also interesting to note that *D. caudata*, another DSP producer, appears on the positive side of PC2, indicating that it tends to proliferate in autumn rather than in late winter to spring like *D. sacculus*. Another potentially toxic (ASP, Amnesic Shellfish Poisoning, producer) taxon, *Pseudo-nitzschia* spp., does not show any significant association with PC2 and is only weakly correlated with PC3. This finding may be explained because *Pseudo-nitzschia* spp. represents a mixture of species blooming at different times of the year (Quijano-Sheggia et al., 2008).

The interest of multivariate methods such as PCA is not only theoretical. As can be seen comparing Figs. 2.14 (top right), and 2.14 (bottom right) with Figs. 2.2 (middle left) and 2.3 (middle left), the seasonal patterns shown by the PCs are more regular than those of the individual taxa (data not shown) and of the taxonomically-based functional groups (diatoms or dinoflagellates) to which they belong. The use of PCs or similar multivariate methods enhances our predictive power with respect to the potential appearance of noxious taxa and can help to improve the management of aquaculture resources.

### 2.4.3 Coupling between environmental and biological variables:

The EMD analysis allowed us to establish the frequency and amplitude of the seasonal fluctuations with quantitative criteria. The method also allowed us to analyze the timing and variability of the biological variables in relationship with the physical forcing. This point has a particular importance in order to propose typical coupled physical-biological scenarios for the behavior of the two bays. The definition of these scenarios should be a starting point to implement numerical models of the bay ecosystems.

One of the main objectives of this paper was to find relationships between the main climatic and physical forcings and the ecology of Alfacs and Fangar. In both bays, we found significant couplings between trends of phytoplankton variability expressed by the first PCs, temperature and salinity (Table 2.2). However, as can be seen in Fig. 2.17, the phase relationships which were very regular for periods like 1991 to 1995 or 1997 to 2001, often broke down near the extremes of the series. This observation was probably an artifact of the method, as shown by repeated EMD analyses with slightly different parameters. Another common drawback with EMD decomposition is that it can produce IMFs with mixed frequencies. This was the cause of the decreased amplitude of Alfacs surface temperature between 2001 and 2003 (Fig.2.17 ). This type of problem can be monitored by means of the Hilbert spectrum (data not shown) of the variable (Huang et al., 1998), but

limits the interpretation of the IMFs. EMD has the important advantage over more traditional techniques that it can be applied to nonlinear and non-stationary data, but has rarely been used with ecological data. Further applications of the method should help to explore its potential.

The seasonal cycle of phytoplankton biomass in the open waters in the vicinity of the Ebre Delta is characterized, as in other Mediterranean areas, by a Chl *a* increase starting in late autumn, with the weakening and break-up of the thermocline, that culminates in a winter phytoplankton bloom in January-February (Morales-Blake, 2006; D'Ortenzio and d'Alcalà, 2009) fueled by nutrients mixed into the euphotic zone. After this peak, the Chl *a* decreases along with the progressive stratification of the water column, to a minimum around August-September. In some areas, close to the coast, the autumn increase constitutes a secondary peak (Margalef, 1969). The differences between Alfacs and Fangar are striking. As can be seen in Figs. 2.2, 2.3, 2.6 and 2.7, the seasonal cycles in Alfacs and Fangar differ among themselves and from the typical marine pattern in the region. The Chl *a* peak in Alfacs takes place in October-November, about two months later than in Fangar. In addition, the two bays show different patterns of qualitative and quantitative variability of their phytoplankton assemblages. However, it is interesting to note that, although represented by different species, the two PCs that best reflect this seasonal variability, PC2 for Alfacs and PC3 for Fangar, peak in August-September, at the time of the temperature maximum. As discussed by Cloern and Jassby (2008), phytoplankton seasonality at the land-sea interface is driven by more than a few climatic factors. In the Ebre delta bays, tidal currents are relatively weak, but freshwater discharges, both from human-controlled channels and from underground sources, affect not only the stability of the water column, but also represent an important source if nutrients, both inorganic and organic (Llebot et al., 2010).

The effects of environmental forcing (including temperature, mixed layer depth and freshwater fluxes) on the dynamics of two phytoplankton functional groups with basic properties of diatoms and dinoflagellates has been explored for Alfacs by means of a zero-dimensional ecological model (Llebot et al., 2010). The simulations show that the magnitude of the exchanges with the sea and the nutrients (including dissolved organic phosphorus, Loureiro et al. (2009a)) provided by freshwater could influence basic features of the abundance and seasonal variability of the two groups. However, these factors alone are unlikely to explain the marked fluctuations of dinoflagellate numbers at Fangar, which show autumn and winter minima, at times when the proportion of freshwater, as reflected by the low salinities, should ensure a relatively good nutrient availability. Comparison of Figs. 2.7 (salinity, top right) and 2.7 (dinoflagellates, bottom right) suggest that the decrease in dinoflagellates during the final months of the year might be related to the salinity differences between surface and bottom layers during these months. A likely possibility is that dinoflagellate growth is unable to cope with presumably vigorous estuarine circulation associated with the strong salinity gradient; this could also

explain the concomitant (although less intense) decline of diatoms and Chl *a*. Further studies of the hydrodynamics of the bays and their effect on the phytoplankton should be addressed to clarify these points.

One of the reasons for the different patterns of environmental variables such as salinity and stratification in Alfacs and Fangar may be the different size of the two basins ($16 \times 10^6$ m$^3$ Fangar, $153 \times 10^6$ Alfacs). A lower mass of water causes higher fluctuations of the physical variables such as temperature and salinity (Camp and Delgado, 1987). Assuming that the freshwater inputs are of the same order of magnitude in both bays, the resulting freshwater residence times are 1-2 days for Fangar and 10 days for Alfacs (Camp and Delgado, 1987)). These differences can account for the marine versus freshwater influence gradient in the phytoplankton composition detected by PC1. The two bays also present marked differences in the seasonal distribution of freshwater discharges, as indicated by the comparison of the corresponding salinity and stratification climatologies. In correspondence with the higher nutrient content of freshwater, Fangar shows higher nutrient loads (Delgado and Camp, 1987) and concentrations than Alfacs. However, as noted in 2.4.2, the lower residence times of water in Fangar allow for only a partial consumption of these nutrients by phytoplankton, with the result that the build-up of phytoplankton biomass, as measured by Chl a concentrations, is comparable to that found in Alfacs. Other habitat differences between Alfacs and Fangar could include factors such as circulation patterns and turbulence intensity.

Altogether, the fluctuations of the Alfacs and Fangar phytoplankton can be characterized by a large seasonal component resulting from an integration of the meteorological cycle and of anthropogenic influences linked to it (opening and closing of the irrigation drainage channels). The weakness of the temporal trends, together with the relatively low range of interannual variability indicate that during the last few years, there have not been large disturbances affecting the bay ecosystems. However, long-term monitoring will be needed in order to ascertain the response of these ecosystems to continuing global change.

## 2.5 Acknowledgments

We acknowledge the support from Projects 'Population Dynamics and Toxicity of Harmful Microalgae in Coastal Embayments', a cooperative project of the National Research Council of Canada and the Spanish Ministerio de Asuntos Exteriores; TURECOTOX (CTM2006-13884-C02-01), funded by the Spanish Ministry Education and Science, and the Grup de Recerca d'Oceanografia Mediterrània (2009/SGR/588), of the Generalitat de Catalunya; Dirección General de Pesca (Generalitat de Catalunya) and the IRTA technical staff. We thank Antonio Turiel for valuable advice. C.L. was supported by a contract (Beca CSIC Predoctoral I3P-BPD2005) from of the CSIC (Spanish Ministry of Education and Science), and during the last months by a Beca de Postgrado of la Fundación Caja Madrid.

# Chapter 3

## HYDRODYNAMIC STATES IN A WIND-DRIVEN MICROTIDAL ESTUARY

This chapter has been submitted at a refereed journal as

Llebot, C. Rueda, F.J., Solé, Artigas, M. L., J. Estrada, M. Hydrodynamic states in a wind-driven microtidal estuary

**ABSTRACT**

A conceptual model of the physical behavior of a shallow microtidal estuary (Alfacs Bay) is built using scaling arguments applied to field data and three-dimensional simulations. At seasonal time scales, the buoyancy associated to freshwater inflows dominates over tidal forcing, yielding a strongly stratified two-layered system, with the surface and the bottom layers flowing in opposite directions (classical estuarine circulation). Wind controls the physical behavior of the bay at shorter (days to weeks) time scales. Three scenarios or states have been defined, depending on the predominant direction and the strength of the wind relative to the intensity of stratification (parametrized through the Richardson number $Ri^\star$). For weak winds (scenario 1), with $Ri^\star > L/h$ (being $L$ the length of the bay and $h$ the depth of the mixed layer), mixing occurs as a consequence of stirring and convection processes, and the mixed-layer deepens very slowly. For strong winds with $Ri^\star < L/2h$ wind-driven mixing is rapid and occurs mainly as a consequence of shear at the pycnocline. In this strong wind situation, two scenarios can be identified: one for persistent northwesterly NW winds (scenario 2) and another for diurnal SW winds (scenario 3). In scenario 2, the estuarine circulation is initially strengthened. In scenario 3, in contrast, the estuarine circulation is weakened and even reversed. In both cases, the exchange of water with the Mediterranean decreases after a few hours, when the wind overturns the stratification and generates strong horizontal density gradients across the bay. Driven by these horizontal gradients, the bay relaxes quickly (within 7-14 hours) to scenario 1, after the wind ceases. These scenarios have important implications for the ecology of the bay, including the occurrence of phenomena such as harmful algal blooms.

## 3.1 Introduction

Estuaries and near-shore waters, in the boundary between land and sea, are among the most productive marine ecosystems (Underwood and Kromkamp, 1999; Kocum et al., 2002), providing fish, drinking water, navigation and recreation for people living in the adjacent areas, and other critical services, which include nutrient cycling, flood control, waste treatment and species refuge (Scavia et al., 2002). The pressure exerted on these ecosystems can be, though, overwhelming due to the large and still growing population living near them. Seven of the ten largest cities in the world (London, New York City, Tokyo, Shanghai, Buenos Aires, Osaka and Los Angeles), for example, are sited next to estuaries and depend on their resources and services (McLusky and Elliott, 2004). In consequence, a large number of estuarine ecosystems are on the brink of collapse, exhibiting serious ecological and economical problems that include the recurrent occurrence of Harmful Algal Blooms (HABs), anoxia, accumulation of chemical contaminants and overexploitation of fisheries (Kennish, 2002). Designing and implementing adequate management strategies to mitigate these problems requires a sound and quantitative understanding of how estuarine systems behave, and the ability to identify the particular processes and mechanisms leading to a given problem at a particular site.

Estuaries are partially enclosed bodies of water located in a coastal area where freshwater surface inflows mix with ocean water (Biggs and Cronin, 1981). however, mixing between fresh and marine waters in these systems is neither instantaneous nor uniform, leading to unsteady and spatially varying (Kocum et al., 2002) turbidity (Burchard and Baumert, 1998; Cloern, 1987; Gallegos and Platt, 1985), nutrient (Yin and Harrison, 2007; Vidal, 1994; Vidal et al., 1997), chemicals (Audry et al., 2007), salinity (Li et al., 1999), temperature and oxygen (Borsuk et al., 2001) fields. The spatial and temporal changes in environmental conditions result from a subtle balance between freshwater inflows, tidal and wind-driven forces varying at a wide range of time scales and interacting under a particular geometry. The rate at which estuaries are flushed out or at which vertical and horizontal mixing, and dispersion occur is relevant for the bio-geochemical behavior of the estuary as it influences its biotic communities and determines the persistence of concentration gradients of nutrient and contaminants. For example, long mixing and flushing time scales relative to reaction rates (e.g. growth) may promote the development of Harmful Algal Blooms HABs (Margalef, 1997; Reynolds, 1997). Horizontal dispersion also influences patch dynamics as it acts to reorganize and homogenize distributions of waterborne biological material (Kierstead and Slobodkin, 1953; Okubo, 1978; Martin, 2003).

The literature on the physical oceanography of estuaries has focused on systems such as the Columbia River Estuary (MacCready et al., 2009) or San Francisco Bay (Walters et al., 1985), where mixing and transport are largely controlled by the interaction between large freshwater inflows and strong tides (Uncles, 2002). However, the influence of wind on estuarine mixing dynamics and circulation can

also be important. Weisberg (1976), for example, observed that the effect of wind on the circulation of a partially mixed estuary was of equal or greater importance than that of the tide or gravitational convection. Zhong and Li (2006) used a three-dimensional hydrodynamic model to demonstrate that the wind energy input in an estuary with low tides was of the same order of magnitude than that of tidal energy. In Mobile Bay (Noble et al., 1996), wind forcing accounted for 25% of the current variance when the water column was strongly stratified. Geyer (1997) suggested, using scaling arguments and one-dimensional modeling, that wind forcing could exert a strong influence on the water residence time of microtidal estuaries. The effect of wind on estuarine circulation and mixing is potentially more important in microtidal estuaries. The dominant forcing factors in these systems, though, are not always the same, and examples can be found of microtidal estuaries dominated by freshwater inputs (Liu et al., 1997), tidal forcing (Sylaios et al., 2006), winds (Geyer, 1997) or a balance among all these variables (Niedda and Greppi, 2007). The relative magnitudes of the forcing factors could also vary in time due to seasonal or episodic changes of wind forcing and freshwater inflows. Hence, different forcing combinations and, consequently, different states or scenarios characterized by a particular combination of physico-chemical variables can be defined for a specific microtidal system. Identifying those states or scenarios, the forcing conditions under which they develop and the time needed for the transition between the states sets the stage to understand the bio-geochemical behavior of an estuary. Studies dealing with this topic are scarce.

Our goal is to construct a conceptual model of the physical behavior of a shallow microtidal estuary, and to develop a detailed description of the different scenarios or states characterizing the distribution of the physical and chemical properties of its aquatic environment. The Bay of els Alfacs (thereafter Alfacs), in the Northeastern coast of the Iberian Peninsula, is taken here as a prototypical example of microtidal embayment. Alfacs is forced by weak tides with ranges that do not exceed 0.25 m. The hydrography of Alfacs was studied in the eighties by J. Camp and M. Delgado (Camp and Delgado, 1987; Camp, 1994). Most profiles collected by (Camp and Delgado, 1987; Camp, 1994) revealed a stratified system, as a result of freshwater inflows from irrigation channels and groundwater seepage. Vertical homogenization of the water column occurred only during strong wind events. Our knowledge of mixing and transport processes in Alfacs and, in general, in other semi-enclosed Mediterranean embayments with weak tidal forcing, is still limited and very qualitative. However, a better understanding of these systems, often very important for the local and regional economy, is necessary to devise sustainable managing strategies of their resources and services. In this work, we apply scaling arguments to field data and use a three-dimensional mixing and transport model (Smith, 2006) to conduct to conduct numerical simulations of the transport and mixing processes in Alfacs. Scaling arguments provide a straightforward first-order (hence, rough) description of the dominant forces that need to be taken intro account to explain the physical state of a body of water. Hydrodynamic models of

estuarine circulation, can resolve non-linear effects and can be useful to determine the effects of forcing factors, the fate of different water constituents or the impact of anthropogenic inputs (Allanson, 2001; Niedda and Greppi, 2007; van de Kreeke and Robaczewska, 1989). They are also the first step in the development of coupled physical-biological models, which may allow a better understanding of the ecology of the estuary and of the mechanisms influencing phenomena such as phytoplankton blooms (Lucas et al., 1998).

This work is organized as follows. Section 4.2 summarizes the physical characteristics of Alfacs, describes the hydrodynamical model and reviews the field data used to run it. Section 4.3 presents the results in two subsections. In subsection 3.3.1 we introduce field observations and scale arguments, and in subsection 4.2.2 we validate the hydrodynamical model and present the results of numerical simulations. Each subsection addresses the three main forcing variables potentially affecting the bay i.e. tide, wind and freshwater inputs. In section 4.5 we discuss the results and summarize the conclusions.

## 3.2 Materials and Methods

### 3.2.1 Study site

The Ebre Delta, one of the largest estuarine habitats in the Northeastern coast of the Iberian Peninsula, comprises two embayments connected to the sea, the largest one, Alfacs to the South (Fig. 3.1) and Fangar to the north. Alfacs (Fig. 3.1) (40°33'–40°38'N, 0°33–0°44'E) is roughly 11 km long and 4 km wide, with an average depth of 3.13 m and a maximum depth of 6.5 m. A sand barrier leaves a mouth around 2.5 km wide, allowing water to be exchanged with the open sea (Camp, 1994).

According to Delgado and Camp (1987) and Camp (1994) Alfacs receives freshwater inputs from five sources which include (1) the Ebre river, mixing with seawater and entering through the mouth of the bay; (2) direct rainfall, which ranges from 300 to 1000 mm per year at the neighboring weather station of Tortosa; (3) urban waste water from the towns of Sant Carles de la Ràpita and Poblenou del Delta; (4) underground sources; and (5) irrigation channels, with flow rates that vary along the year. The three first sources are negligible compared with the last two. After flowing trough rice fields and lagoons, irrigation water is drained into the bay through a number of channels located along the northern shore. These channels are only open eight months per year (from March–April to October–November), when rice fields are irrigated. During those months, the flow is ca. 14.5 $m^3\ s^{-1}$ (Farnós et al., 2007). From November to mid January the flow is kept low (7.8 $m^3\ s^{-1}$ (Farnós et al., 2007)), and from mid January to April the channels are closed for maintenance purposes. At the time of open-channels, the largest source of freshwater into the Bay is the discharge from irrigation channels.

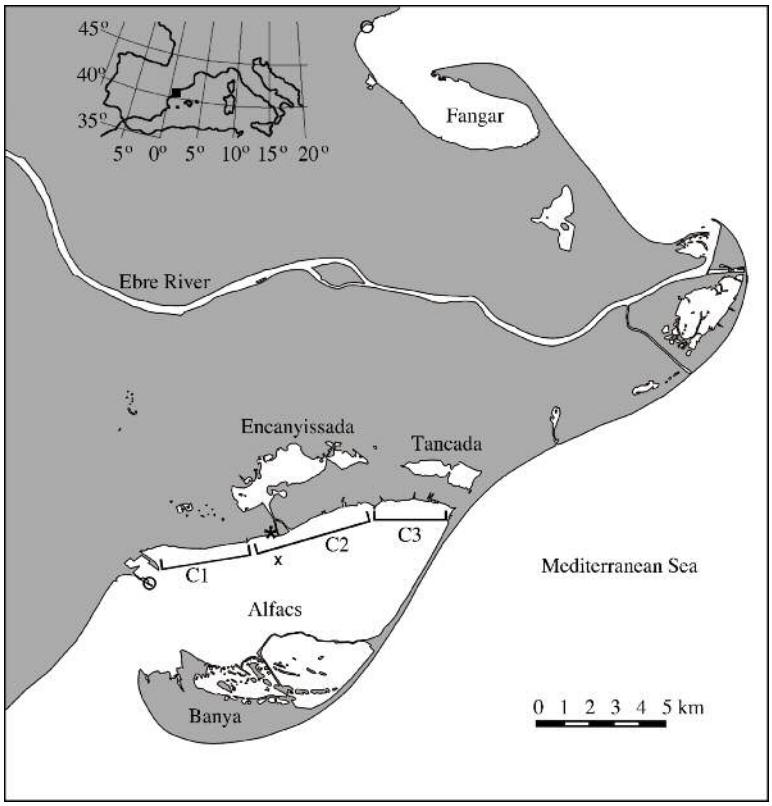


Figure 3.1: Map of the study zone. ⋆ : weather station; X: sampling site; ∘ : Gauging station; C1, C2, C3: areas defined for channel input.

For water budgeting purposes the channels are grouped into Eastern, Central and Western sections, depending on the location of their openings along the northern shore. Inflow through channels in these sections account, respectively for 74%, 15% and 10% of the total irrigation returns to the bay (Camp, 1994). The amount of groundwater flow is uncertain, but Camp (1994) estimated that it can vary from 2 to 4 $m^3/s$.

### 3.2.2 Experimental data

Water salinity and temperature data were collected from 1990 to 2004 on a weekly basis at a central station of Alfacs (40° 37.161' N 00° 39.781' E see Fig. 3.1) using a portable sonde (de Pedro, 2007). Additional temperature and conductivity profiles were taken during 2007, 2008 and 2009, with an approximate periodicity of two months, also at the central station. A climatology of water temperature, salinity and density based on the 14-year data set has been performed calculating weekly means and standard errors.

An Acoustic Doppler Current Profiler (ADCP) was deployed in April 2007 at the central sampling station (see Fig. 3.1). From May 2008 to March 2009, the ADCP was set to work at low resolution mode, recording velocities every 0.1 m and once every hour. The velocity records were continuous except for short periods of maintenance. From April 2007 to May 2008 the ADCP was set to record intermittently during short periods of time (10-15 days) at a higher resolution (about 1 sample per minute). Six thermistors (placed every 1 m) and two conductivity meters (one near the surface and another near the bottom) were also deployed at the central sampling station from July 2008 to October 2009, and recorded data once every 10 minutes. The two conductivity meters consistently malfunctioned due to bio-fouling one week after each deployment. Hence, the salinity information was taken, when necessary, from the salinity climatologies constructed as indicated above.

Meteorological data (air temperature and relative humidity, solar radiation, atmospheric pressure and wind speed and direction) were collected at 2 m above the ground near Alfacs (UTM coordinates: 302116, 4500214. See Fig. 3.1). The weather station is operated by the Meteorological Service of Catalonia (see www.meteocat.com). Tidal records were obtained from the tide gauge of Puertos del Estado in the Barcelona Harbor (3754). Puertos del Estado provides the tide harmonics in its web page (http://www.puertos.es), calculated over the period 1993–2000. Water surface elevation data were also available on-line from gauges existing at Sant Carles de la Ràpita and l'Ampolla (Fig. 3.1) and operated by XIOM (Xarxa d'Instruments Oceanogràfics i Meteorològics).

The wind records were analyzed using the methodology proposed in Guadayol and Peters (2006). An event is defined as one continuous period of time during which the wind speed is higher than a given threshold. Each wind event is characterized by the number of hours that the event lasts (persistence, $p$), and a minimum speed. The frequency $f$ of events with a minimum persistence follows a stretched exponential distribution (Guadayol and Peters, 2006) of the form

$$f = b_1 \exp\big(-p^{b_2}\big) \tag{3.1}$$

being $b_1$ and $b_2$ parameters that vary for each different threshold value.

### 3.2.3 Computational Model

Numerical simulations were conducted with a three–dimensional free surface hydrodynamic model Smith (2006). The model is based on the continuity equation for incompressible fluids, the Reynolds-averaged form of the Navier-Stokes equations for momentum, the transport equation for temperature, and an equation of state relating temperature and salinity to fluid density. The flow in the model is assumed hydrostatic (the weight of the fluid identically balances the pressure) and

the density differences are neglected unless the differences are multiplied by gravity (Boussinesq's approximation) (Rueda and Schladow, 2003). Turbulent mixing in the vertical is represented following the level 2.5 Mellor–Yamada hierarchy of turbulence closure models (Kantha and Clayson, 1994). Horizontal mixing of momentum is parametrized using a constant mixing coefficient. The model does not include any vertical movement of the bottom profile nor lateral movement of the shoreline due to sediment transport. It also assumes that the bottom is impermeable and that the effects of evaporation and precipitation are negligible. Details of the numerical algorithm can be found in Smith (2006) and Rueda and Schladow (2002); Rueda and Smith (2008). In previous studies, it has been shown that this model provides accurate results both in semi-enclosed systems that, like Alfacs (see below), are subject to weak tidal forces (Rueda et al., 2003b,a; Rueda and Cowen, 2005b), and, in systems, such as San Francisco Bay, with stronger tidal forcing (Zamani et al., 2010). Furthermore, the model has been validated against analytical solutions of the governing equations (Rueda and Schladow, 2002; Rueda and Smith, 2008), which provides solid grounds to believe on the validity of the simulations .

### 3.2.4 Simulations and model setup

The hydrodynamic model was set to simulate the transport and mixing processes in Alfacs from 2007 to 2009. The model grid (Fig. 3.2) was constructed from the shoreline, transects collected by (Guillén, 1992), and bathymetric charts. The domain covers an area of $18.8$ x $9.6$ km, and includes the Bay and a portion of the Mediterranean Sea. It has been assumed that irrigation water is discharged through three main channels (Fig. 3.2). The computational grid is structured with rectangular cells of uniform dimensions ($200$ x $200$ x $0.5$ m). It has $94$ cells on the $x$–axis, $48$ on the $y$–axis, and $19$ on the $z$. The time step was set to $60$ s.

Initial conditions for model simulations consisted of horizontally homogeneous temperature and salinity fields. The initial profiles of salinity and temperature were obtained by linearly interpolating values of salinity and temperature measured in the water column of the central sampling station (see below) during January 2009. Surface shear stress and heat fluxes were constructed from observations at a single weather station, assuming that the meteorological fields were uniform. The harmonics calculated from the Barcelona Harbor (see Section 3.2.2) were used to generate time series of water surface elevation, which were provided to the model as boundary conditions at the Mediterranean boundary. The salinity and temperature of the Mediterranean were approximated by assuming that the characteristics of the bottom layer in Alfacs are very similar to the characteristics of the neighboring sea. The climatologies of temperature and salinity measured at the bottom layer in the sampling station during a period of 14 years were slightly modified according to field observations of the Mediterranean collected in 1997 during FANS cruises (Salat et al., 2002) in the Ebre shelf, and were used to force the model.

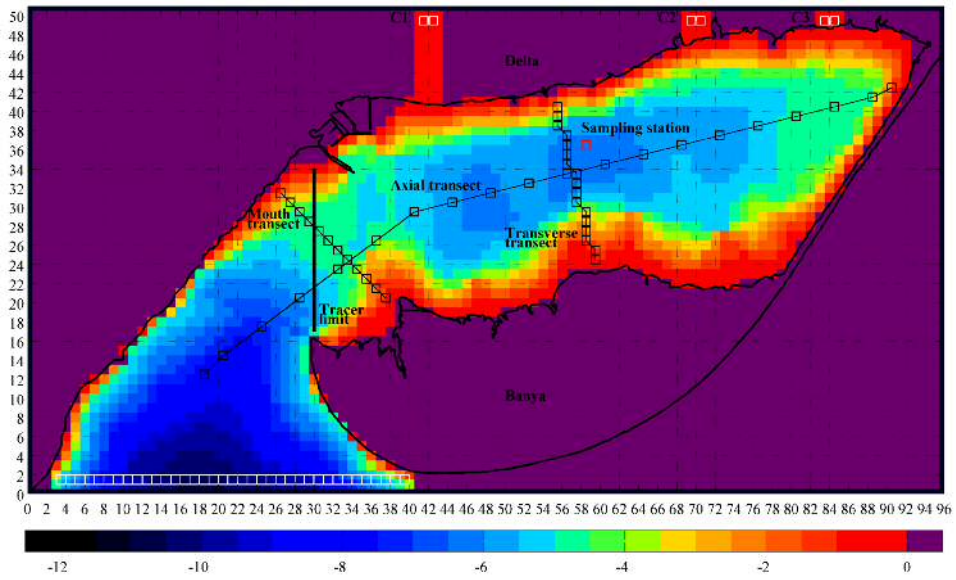


Figure 3.2: Grid of the model for Alfacs showing bathymetry. Colored squares mean depths in meters. Squares delimited by black slashed lines are groups of 4 cells. Cells delimited in white: open boundary cells. Cells delimited in black: output cells for sections. Cells delimited in red: output cells for time profiles and location of the sample station. Thick black line: boundary for tracer release. Black line: real shoreline. Each cell is 200 x 200 x 0.5 m. Flowing from the north are the three main discharge channels.

Inflow rates through the irrigation channels were assumed to be constant and equal to 14.5 $m^3s^{-1}$ during open-channel season, 7.8 $m^3s^{-1}$ during the low flow months in fall Farnós et al. (2007), and 3 $m^3s^{-1}$ during closed channel season (Camp, 1994). Freshwater inflow rate was partitioned among three irrigation channels following the areas defined by Camp (1994) (Fig. 3.1): 75% through channel C2 (at the center), 15% through the easternmost channel C3, and the remaining through C1 (see Fig. 3.2 for the location of the channels). Water temperature in the irrigation channels were constructed from observations collected in the Delta de l'Ebre in the Delta lagoons Encanyissada i Tancada by the Parc Natural del Delta de l'Ebre. Channel salinity was set equal to the average salinity of the Ebre River measured in Tortosa (data from the Catalan Water Agency, http://mediambient.gencat.net/aca), the nearest river gauging station to Alfacs.

A series of tracer experiments were simulated, driven by the velocity fields and mixing rates calculated with the hydrodynamic model. In the first set of experiments. Tracers were released every week from January 2008 to February 2009, and the distribution of tracers 8 days after the released was examined with a Principal Component Analysis. The second and third tracer experiments were designed to analyze the distribution of properties and the exchange processes between the Alfacs and the Mediterranean under specific forcing scenarios. The tracers in this

set of experiments were released every 6 and 4 hours for a period of 6 and 3 days respectively. In all cases, the tracers were instantaneously released filling the domain within Alfacs (see 3.2 to see the area considered), with a constant concentration.

## 3.3 Results

### 3.3.1 Observations and scaling arguments

#### 3.3.1.1 Stratification

Alfacs remains stratified throughout the year, with top-bottom density differences and pycnocline depths that vary according to the season. In general the profiles collected during the period of closed-channels exhibit deeper pycnoclines and weaker stratification (Fig. 3.3). The strongest density differences, in turn, occur from April to January, when irrigation channels are opened (Fig. 3.3). Top-bottom salinity differences vary from 1 psu in March, increasing to ca. 4 psu in December, towards the end of the open-channel period. Temperature differences persist also throughout the year. The bottom layer is colder than the surface mixed layer in spring and summer time, with maximum differences of ca. $4^oC$, but warmer in winter (Fig. 3.3 and 3.4). These observations suggest that stratification is mainly driven by salinity differences in the water column, and not by temperature. If we compare the change of density due to a $4^oC$ temperature variation ($\frac{\mathrm{d}\rho}{\rho_0} = \alpha\ \mathrm{d}T$, being $\alpha = 2.57 \times 10^{-4}\ ^{\circ}\mathrm{C}^{-1}$ the coefficient of thermal expansion), with the change in density due to salinity changes of ca. 4 psu ($\frac{\mathrm{d}\rho}{\rho_0} = \beta\ \mathrm{d}S$, being $\beta = 7.7 \times 10^{-3}$ the coefficient of saline expansion), it turns out that the contribution of salinity differences to stratification is almost 20-25 times larger than the contribution from temperature.

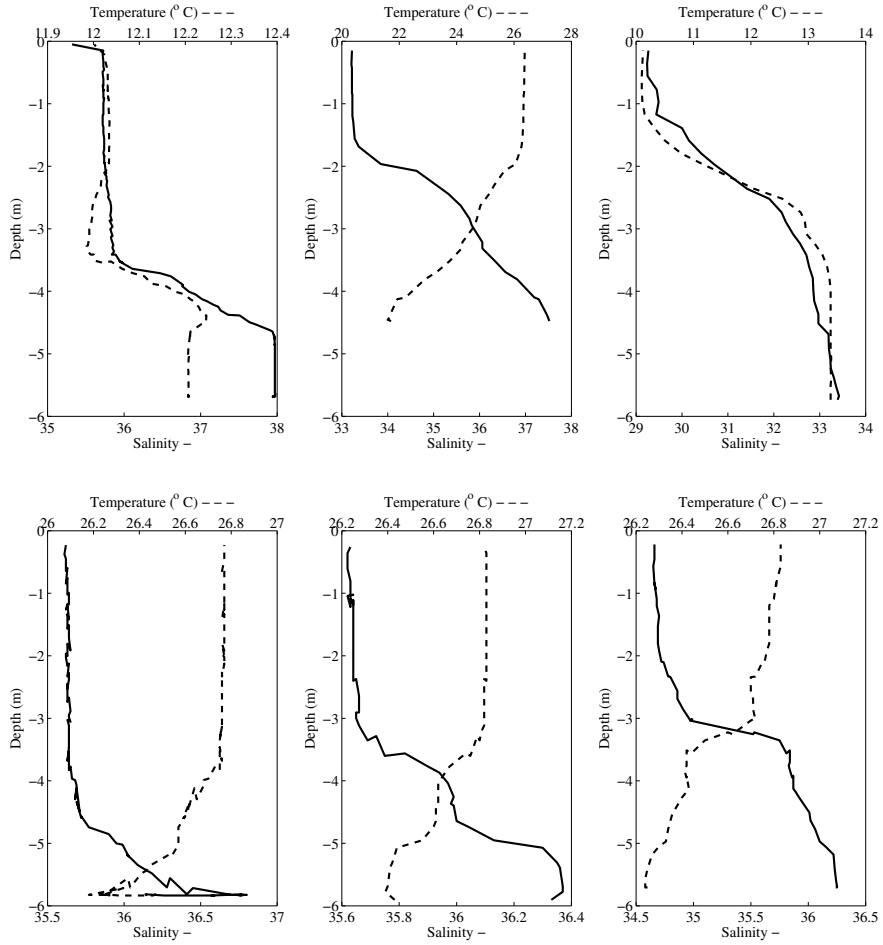


Figure 3.3: Temperature (- - -) and salinity (—) profiles at the sampling station (Fig. 3.2) of the bay. From left to right: Profile on the 2nd of March 2009. Profile on the 14th of June, 2007. Profile on the 13th of December, 2007. Profile on the 25th of July, 2007 at 14:52. Profile on the 25th of July, 2007 at 18:18. Profile on the 26th of July, 2007 at 11:16 h.

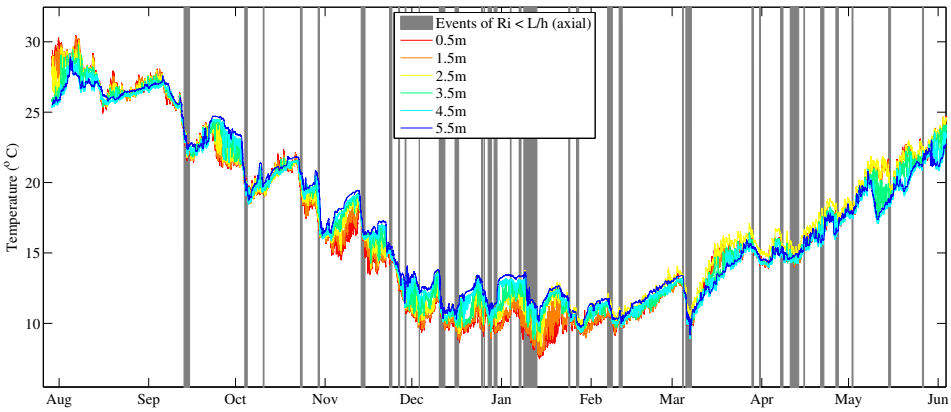


(a)

Figure 3.4: Events with presence of shear induced mixing assuming a wind in the direction of the axis of the bay (in gray) compared with thermistor data.

The fact that the presence of stratification during the closed channels months is observed in both the CTD profiles and the climatologies suggests that underground inputs of freshwater are indeed present in Alfacs and represent an essential feature contributing to the vertical structure of the bay that should be further studied. Furthermore, the fact that the magnitude of the density differences are largely controlled by salinity differences, and that these differences appear to increase in response to increasing inflow rates from the irrigation channels suggest that the seasonal evolution of stratification is to a large extent controlled by the opening and closing of the channel gates.

#### 3.3.1.2 Tides

The Mediterranean tides are characterized by small tidal amplitudes, of the order of centimeters. The harmonic analysis of the water surface elevation records collected at the Barcelona Harbor, indicate that the largest amplitude (0.046 m) corresponds to the semi-diurnal tide (period T = 12.4 h), followed by the diurnal tides (T = 23.9 h) with an amplitude of 0.037 m. The same periods appear in the analysis of the velocity and water surface elevation records collected in Alfacs. The maximum velocities induced by the sub-diurnal and diurnal tides are 0.016 m $s^{-1}$ and 0.011 m $s^{-1}$ respectively. The analysis of water surface elevation records collected within Alfacs further reveal the existence of oscillations with a period of ca. 3 hours, with amplitudes of O($1.0 \times 10^2$) m. These oscillations were also observed in previous works (Camp, 1994), and correspond to the seiching or characteristic modes of oscillation of the Bay (Wilson, 1972; Rabinovich, 2010). For semi-enclosed rectangular basin of flat bottom, the period $T$ of the lowest seiche

mode can be estimated as (Rabinovich, 2010):

$$T = \frac{4L}{\sqrt{gH}} \tag{3.2}$$

where $g$ is the acceleration of gravity, and $H$ and $L$ the depth and length of the channel. For H = 3.13 m and L = 12000 m (average depth and length of Alfacs), T is c.a. 2.4 h, similar to the average periodicity. The velocities associated with it are between 0.015 and 0.022 m $s^{-1}$.

The excursion lengths (the distance traveled by a particle during half a period due to these oscillations) are ca. 450, 150 and 70m, for the diurnal, semi-diurnal tide, and for the first seiching mode, respectively, which are small (at least 20 times smaller) compared to the length of the bay. The tidal prism was 7.0 $\times$ $10^6$ $m^3$ and 2.5 $\times$ $10^6$ $m^3$ for the diurnal and the semi-diurnal period, which correspond to 4.5% and 1.6% of the total volume of the bay respectively. The volume of water exchanged due to seiching motion is around 1% of the volume of Alfacs. These calculations suggest that tidal mixing is weak, as revealed by the persistence of well-defined and sharp pycnoclines in the CTD profiles.

#### 3.3.1.3 Tidal mixing and freshwater inflows

The balance between tidal mixing energy and the buoyancy induced by freshwater inflows determines whether the bay is well-mixed o remains stratified (Fischer et al., 1979), in the absence of other forcings. This balance is expressed by the magnitude of the *Estuarine Richardson number* (Martin and McCutcheon, 1999), calculated as

$$Ri = \frac{g' Q_R}{W U_t^3} \tag{3.3}$$

where $g' = g\ \Delta\rho/\rho_0$ is the reduced gravity, $\Delta\rho$ represents the top-bottom density difference, $\rho$ is a reference density, $Q_R$ is the freshwater inflow rates, $U_t$ the root-mean-square velocity due to tide-generated currents, and, $W$ is the estuary width. The transition between well-mixed estuaries and stratified estuaries occurs in the range $0.8 >$ Ri $> 0.08$ (Fischer et al., 1979). For $Ri < 0.08$ the estuary is expected to be well mixed, and for $Ri > 0.8$, the estuary is considered to be strongly stratified and the flow dominated by density currents. For Alfacs, $Ri$ has been calculated using the climatology of the surface and bottom densities, the freshwater inflow rates as described in Farnós et al. (2007) and an underground flow of 3 $m^3$ $s^{-1}$, and assuming that W = 2500 m, and $U_t$ = 0.017 m/s. The latter was calculated from the tidal information at the harbor of Barcelona and assuming that the area of the section connecting the bay and the Mediterranean is ca. 15625 $m^2$. The Estuarine Richardson number was always larger than 0.8, even during the periods of time when the irrigation channels are closed. Hence, the rate at which buoyancy is introduced through freshwater inputs (either channel inflows or groundwater) is

larger than the mixing rate driven by tidal currents at that time, and one expects a strongly stratified system, if other sources of mixing are ignored.

#### 3.3.1.4 Wind forcing

Wind speeds in Alfacs are typically low, with magnitudes under 2 m $s^{-1}$ during 50% of the time (Fig. 3.5). The frequency of the wind events decreases as the persistence and magnitude of the events increases (Fig. 3.6 (a)). For example, events stronger than 2 m$s^{-1}$ that last for 10 hours or more occur ca. 100 times a year. Events stronger than 5 m$s^{-1}$ with the same persistence, in turn, occur less than 20 times a year. The persistency and magnitude of the wind events vary with the season (Fig. 3.6 (b)). The length and frequency of strong winds (with wind speeds larger than 5 m$s^{-1}$ in magnitude) is similar in winter, spring and fall. In summer time, though, the frequency of the stronger events decreases.

The strongest winds are either from the Northwest NW or from the Southwest SW (Fig. 3.5). These two are also the predominant wind directions. Hence, wind forcing can be characterized as a sequence of calm and windy periods, with two types of wind events. The first corresponds to strong and persistent northwesterly winds, lasting 2-3 days and reaching velocities of up to 5 – 15 m $s^{-1}$. The second correspond to southwesterly wind events, which tend to be shorter and exhibiting daily variations during a few days. The velocities reached during the SW events reach values up to 5 - 10 m $s^{-1}$. During the calmed periods, winds are typically low (wind speeds $< 2$ m $s^{-1}$) and blowing from the NW.

#### 3.3.1.5 Residual and wind-driven circulation

Residual velocities, estimated from ADCP records, reveal the characteristic estuarine circulation with near surface water flowing towards the Mediterranean and deeper layers flowing into the bay (Fig. 3.7). The axial direction dominates in general over the transverse direction. The strength of the residual circulation changed at seasonal scales, with the strongest currents out of the bay occurring at times when the irrigation channels were open, and the weakest occurring during winter time with the channels closed. The circulation in the bay changed also on short-time scales, in response to meteorological forcing. Fig. 3.8, for example, presents a time series of along-bay currents at different depths, from April 24 to April 27 in 2007, when the bay was subject to four wind events in sequence with maximum speeds exceeding 5 m $s^{-1}$ each. These records reveal a diurnal alternation of vertically sheared exchange flows, being driven by the succession of windy and calm periods in the course of a day. Water near the surface flowed into the bay in response to south-westerly winds (first event in Fig. 3.8), and outwards towards the Mediterranean thereafter once the wind ceased. Bottom currents flowed in the opposite direction. The direction of the flows in the bay were reversed when acted upon winds with a stronger easterly component (three last events in Fig. 3.8).

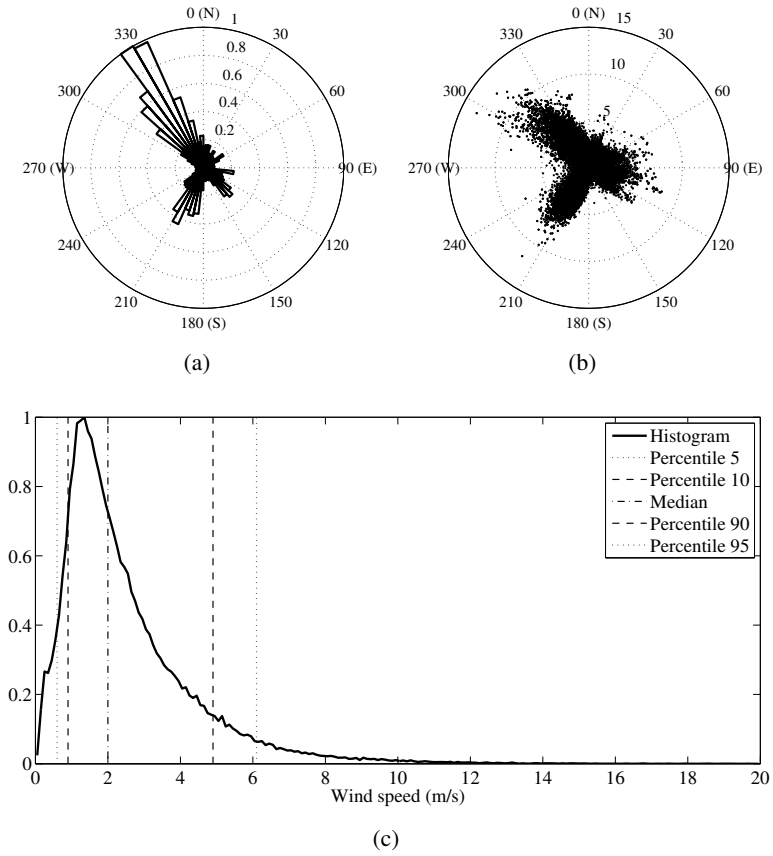


Figure 3.5: Wind statistics from the automatic weather station of Alfacs. (a) Histogram of wind direction; (b) Representation of wind speed and direction. (c) Histogram of wind speed (m/s);

#### 3.3.1.6 Wind-driven mixing

**3.3.1.6.1 Boundary shear stresses** Wind forcing in shallow estuaries generates stress and introduces turbulence in the water column directly, at the free surface surface ($\tau_s$), and indirectly, at the bottom ($\tau_b$), as a consequence of the orbital velocity associated to wind waves reaching the sediment-water interface (Carper and Bachmann, 1984; Chapra, 1984). In Alfacs, though, wave-induced bottom shear stresses are negligible compared with the magnitude of the wind shear stress at the surface. The former was calculated following the equations presented in Luettich et al. (1990) (see also Mian and Yanful (2004)). The wind stress at the free surface $\tau s$, in turn, was estimated using the bulk-aerodynamic formula

$$\tau s = \rho_0 \, C_D \, u_a^2 \tag{3.4}$$

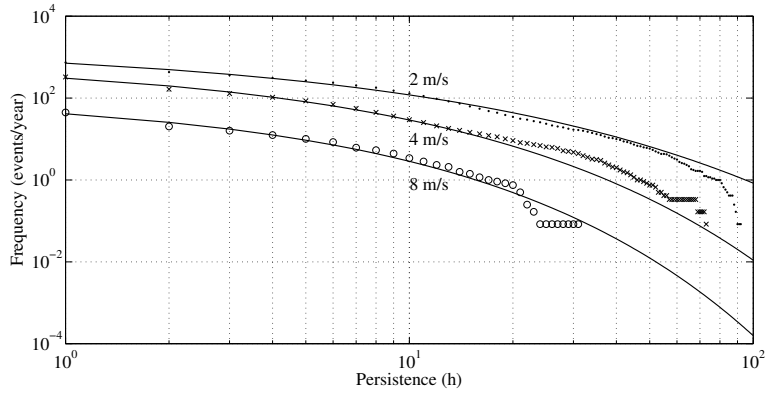


(a)

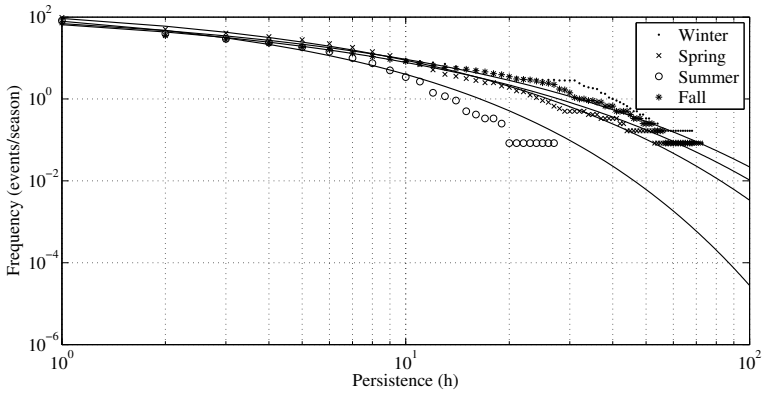


(b)

Figure 3.6: Logarithmic plot of frequency (events per year) and persistence of wind events (hours) calculated with data from Alfacs automatic weather station. (a) For events defined with different threshold values (2 m/s, 4 m/s, 8 m/s). (b) Events of 4 m$s^{-1}$ or more for different seasons.

where $u_a$ is the wind speed at 10 meters, and $C_D$ is 1.2 $\times$ $10^{-3}$ as stated by Large and Pond (1981). For $u_a$ = 2 m $s^{-1}$, the bottom wave-induced shear stress was four orders of magnitude smaller than the stress at the surface. For $u_a$ = 9 m $s^{-1}$ the surface stress is still 100 times larger than the bottom generated stress. Hence, in the analysis that follows, it will be assumed that mixing in the water column is largely associated to the wind stress at the free surface.

**3.3.1.6.2 Mixing mechanisms** Spigel and Imberger (1980) showed that mixing in the water column leading to changes in the thickness of a surface mixed layer $h$

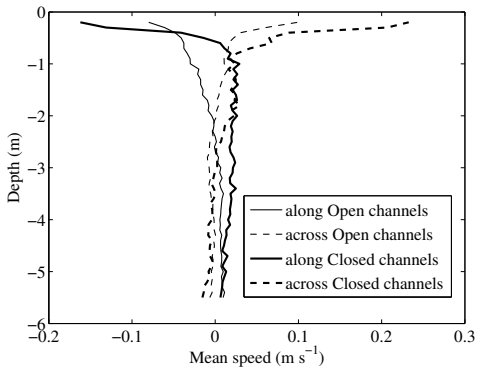


Figure 3.7: Average of water velocity in the along-coast and across-coast direction measured at the sampling station with the ADCP when the wind speed is lower than 0.5 m s$^{-1}$ for the closed channel period (15 Jan - 1 April) and the open channel period (1 April - 15 Jan).

could be represented as

$$\Big[C_T q^2 + g' h\Big] \frac{dh}{dt} = C_k^f q^3 + C_s \Big(\Delta u\Big)^2 \frac{dh}{dt} \tag{3.5}$$

where $C_T$, $C_k^f$ and $C_s$ are empirical constants, representing efficiencies of the process considered, $q$ is a velocity scale that is linear function of the wind friction velocity $u^\star$ (defined as $u^{\star 2} = \tau_s/\rho_a$, in terms of surface sear stress and $\rho_a$ the air density) and the convective velocity $u_f$ due to surface cooling, and $\Delta u$ represents the change of velocity across the bottom of the surface mixed layer. The bracketed terms on the left-hand side of 3.5 represent the energy required to entrain a parcel of water of unit depth into the surface mixed layer. The terms on the right-hand side of 3.5 represent the energy that becomes available for entrainment (mixing) as a consequence of surface stirring and surface cooling (the first term), and shear stress across the pycnocline (the second term). Following the arguments of Fischer et al. (1979) for closed basins, and adapting them for semi-enclosed bays, one can estimate whether shear or stirring dominates mixing in a semi-enclosed bay using simple scaling arguments (see Appendix). These arguments are based on the magnitude of the *bulk Richardson Number*, calculated as:

$$Ri^\star = \frac{g'\, h}{u^{*2}} \tag{3.6}$$

For $Ri^\star > L/h$, mixing is dominated by stirring. If $Ri^\star$ is smaller than $L/h$ shear will also contribute to the deepening of the pycnocline. Shear will be the dominant mixing process if $Ri^\star$ is smaller than a second threshold value equal to $L/2h$. In these scaling arguments, it is assumed that winds are of constant

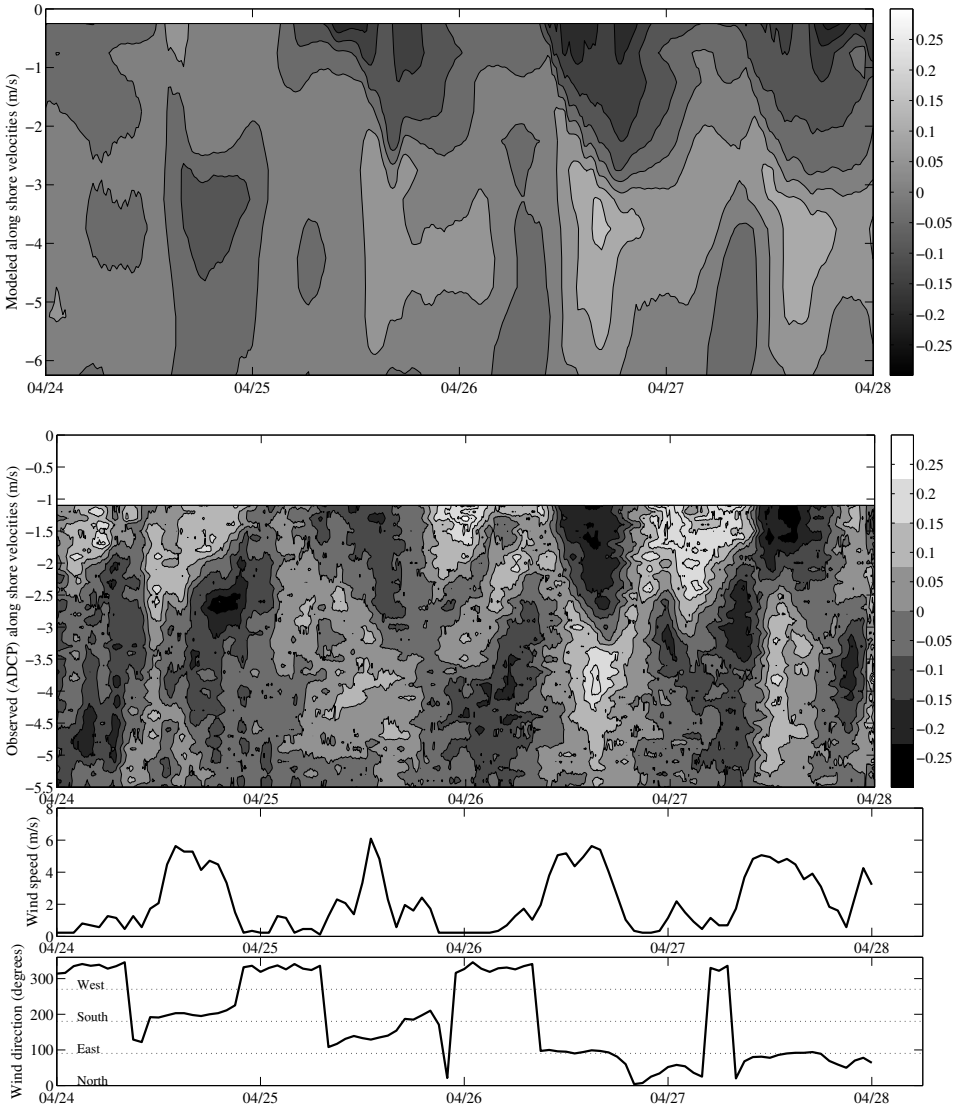


Figure 3.8: Modeled (top contour plot) and observed (bottom contour plot) water velocities in the along-coast direction at the sampling station (see Fig. 3.2) compared to wind speed and direction.

magnitude and blow for longer cut-off time, $T_c$, which is the length of time needed for the effects of the boundaries to propagate to the open end of the estuary. After $T_c$, the shear-stress will be balanced by the baroclinic pressure gradient associated with the tilting of the pycnocline, which in turn is the result of the presence of boundaries. The cut-off time can be estimated as

$$T_c = \frac{L}{\sqrt{g'h}} \tag{3.7}$$

In Alfacs, its mangitude varies in time at seasonal scale with values that range from 10 to 23 h. In winter, for example, with the irrigation channels closed, $T_c$ = 18.1 $\pm$ 0.02. In summer, with the channels opened, in turn, $T_c$ = 14.0 $\pm$ 0.1. For realistic winds, with time-varying magnitudes, one needs to filter the time series of Richardson numbers with a window of size equal to the cutoff time, before comparing the magnitude of $Ri^\star$ against threshold values (see MacIntyre et al. (2002), for example).

Richardson numbers in Alfacs were estimated for the period 2000 - 2009, assuming a mixed layer depth h = 3 m and the climatological series of top-bottom density differences $\Delta\rho$. Our filtered estimates of Richardson number, compared with $L/2h$ and $L/h$, suggest that mixing in the water column is predominantly driven by stirring. For example, stirring (turbulence generated in the surface and transported down to reach the pycnocline) was the major source of mixing during 87% of the time. Shear-driven mixing events, though, are also frequent. Shear contributed to mixing during an average of ca. 92 hours per month, and it was the dominant process an average of 43 hours a month. During shear dominated events the wind direction was between 270 (West) and 360 (North) degrees 83% of the time, although the frequency of these winds is only 43%, and the wind speed was faster than 5 m $s^{-1}$ the 67% of the occasions. Wind events of sufficient intensity to cause shear-driven mixing are very seasonal. They are most common in winter as a consequence of stronger winds and lower freshwater inputs, and a 82% of the events occur between November and April.

**3.3.1.6.3 Wind mixing and vertical stratification** Shear-driven events usually precede the development of uniform temperature conditions in the water column as observed with a thermistor chain at the center of the bay (Fig. 3.4). This can be partly explained by the energetic mixing that occurs when shear becomes the dominant mechanism (Fischer et al. (1979)). The argument of Fischer et al. (1979) is based on the comparison of the time scales necessary to deepen the pycnocline to twice the original depth by stirring $T_e^q$ or shear $T_e$. These scales can be estimated as

$$T_e^q = \frac{h}{v^\star} Ri^\star \tag{3.8}$$

$$T_e = \frac{2\eta}{C_s^{1/2}} \frac{h}{q} Ri^{\star 1/2} \tag{3.9}$$

where $\eta$ is an empirical constant $= 1.23$. In Alfacs, $T_e^q$ varied from $10^3$ to $10^5$ h, while, $T_e$ was at all times much lower, varying from 0 to 100 h and being less than 30h the 90% of the time. Hence, it is expected that the pycnocline will deepen much faster during shear-driven events than at those times when mixing is driven by stirring.

Fig. 3.3.1.1 shows a comparison between the shear-driven mixing events from August 2008 to June 2009 and the observed series of temperature at the central station. The events coincide in most cases with a mixing of the water column associated with a cooling of 2 to 5 degrees of the water, and except for a few exceptions, all the mixing events of the period can be explained by a shear related event.

#### 3.3.1.7 Large-scale response to wind forcing

The large scale response of a two-layer stratified system of small and medium-size to wind forcing can be parametrized using the ratio of $Ri^\star$ to $L/h$, also referred to in the literature as the Wedderburn $W$ number (Stevens and Imberger, 1996). For $W << 1$ (or equivalently, for $Ri^\star << L/h$), the bay overturns and bottom water upwells, with the consequent development of significant horizontal gradients in the thermal and chemical characteristics (Fig. 3.9). Temperature and salinity profiles collected in different regions of the bay (Camp, 1994), within short periods of time, reveal that water densities at the east boundary of the bay could be uniform in depth and up to 3 $\times 10^3$g m$^{-3}$ lower than at the mouth shortly after strong wind events. The system reverts to its original state, with horizontal isopycnals, after the wind ceases, as a result of baroclinic forces associated to the horizontal density gradients set up during the wind event. The time scale necessary to bring the system back to its original state can be calculated as (Monismith et al., 1990)

$$T_r = \frac{UL}{g'H} \tag{3.10}$$

where $H$ is the depth of the estuary and $U$ is the longitudinal velocity generated during the relaxation process, calculated, in turn, as

$$U = \sqrt{g'H} \tag{3.11}$$

The reduced gravity in these equations is calculated using top-bottom density differences, which become equal to the horizontal density differences across the bay during upwelling events. The time scales for relaxation in Alfacs, for density differences of 1 - 3 $\times 10^3$g m$^{-3}$, and assuming that H is the average depth of 3 m

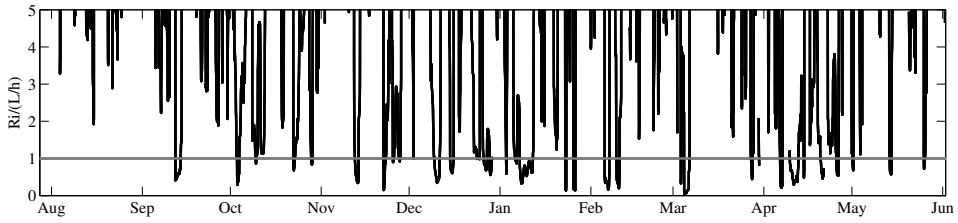


(a)

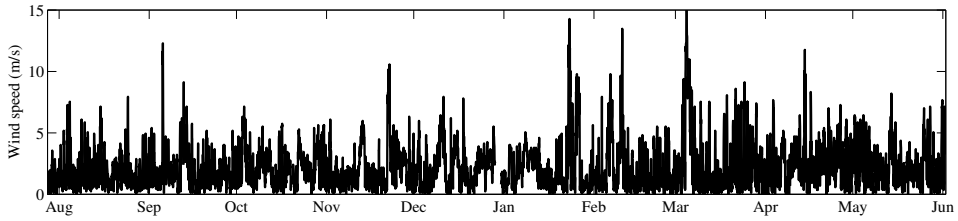


(b)

Figure 3.9: (a) Wedderburn number or threshold in which the system switches from a mixing dominated by stirring to a system with the presence of shear. (b) Wind speed.

and the length of the bay L = 11000 m, range between 10 and 18 h. These scales agree with previous observations reported in Camp (1994), and suggest that the bay re-stratifies shortly after a wind event. For example, the mixed layer raised 1.5 m in 4 hours in July 2007, after an event dominated by shear-driven mixing (Fig 3.3). The alternation of sheared flows that appear in Fig. 3.8, probably obey to the generation of horizontal density gradients during the event, following by a fast relaxation of the system to its original state.

#### 3.3.1.8 Rotational effects

Rotational effects need to be taken into account when analyzing the circulation in water bodies with horizontal dimensions larger than the Rossby radius of deformation $R_0$ and when considering processes with time scales which are on the order of $f^{-1}$ or larger, being $f$ the Coriolis parameter. The Rossby radius of deformation is estimated as the ratio between $c$, a characteristic speed at which information is propagated, and $f$, i.e. $R0 = c/f$. Rotational effects can be safely ignored in most semi-enclosed basins when analyzing free surface dynamics (Rueda et al., 2009), given the high-speed at which surface waves propagate. Internal waves, however, propagate at a speed which can be estimated as $\sqrt{g'h}$, and their Rossby radius (referred to as the internal Rossby radius) in Alfacs is of order 1000 m to 4000 m. Surface currents also are typically on the order of $10^{-1}$ m s$^{-1}$, and $R_0$ is also ca. 1000 m. Hence, it is likely that circulation and the internal dynamics is

affected by rotational effects in Alfacs. These effects have been ignored in our previous arguments. Hence, these arguments can be, at most, considered a first-order approach to understanding mixing and circulation processes in Alfacs. A more detailed description of these physical processes requires the use of more sophisticated approaches, including three-dimensional modeling.

### 3.3.2 Three dimensional model

#### 3.3.2.1 Validation

The model was validated by comparing simulations and observations of temperature, salinity and velocity at a central station in Alfacs (see Fig. 3.1). The differences between modeled and experimental values were quantified using several error norms: the root mean squared error RMSE, $I_1$ and $I_2$ norms (Table 3.3.2.1). Observed and simulated variables were averaged in time and sub-sampled every two-hours, previous to the comparison, and correspond to different depths (every 1 m for temperature and velocity, and top/bottom for salinity). The comparison between observations and simulations varied, depending on the availability of data. Modeled temperatures were validated against observations collected from July 29, 2008 to May 31, 2009. Velocity simulations, in turn, were validated against records collected from June 1, 2008 to July 28, 2008. For salinity, we only used data collected during 7 days following the installation and cleaning of the sensors. Visual inspection of the salinity records suggests that the measurements were not significantly affected by fouling in that period.

The average RMSE of the temperature predictions was 1.33 °C (Table 3.2). The $I_1$ and $I_2$ ranged between 0.042 and 0.11, and were of the same order of magnitude as those reported in other modeling studies conducted in similar environments (Rueda et al., 2003a). The errors in the temperature predictions varied in time and were larger, in general, during the spring and summer months. At that time, the model tended to simulate temperatures that are 2-3 °C lower than the observations in the lower layers. During the winter, the RMSE decreased to 0.80-1.22 °C. In general, the model captures the evolution of temperature at seasonal scales (Fig. 3.10), though it tends to under-predict the temperature near the bottom. The model also reproduces accurately the evolution of temperatures at smaller scales, like monthly, weekly and daily (Fig. 3.11). Modeled salinities agree well with the observations (Table 3.3, and Fig. 3.12), with errors of up to 1.5 salinity units. Modeled salinity follows the same trend as the climatologies (Fig. 3.10). Salinity in the surface layers increases up to ca. 2 salinity units when the channels close in mid January, and rapidly decreases in April to reach values of ca. 33 salinity units. From May to November the salinity is roughly constant, ranging from 33 to 35. The model overestimates slightly the observations during fall, and is very sensitive to the amount of underground water inputs during the closed channels period (15 January to end of April). The RMSE of velocity simulations ranged from 0.4 to

$I_1$ norm

$$I_1 = \frac{\sum_{n=1}^{N} \mid S_n - O_n \mid}{\sum_{n=1}^{N} \mid O_n \mid} \tag{3.12}$$

$I_2$ norm

$$I_1 = \frac{\left[\sum_{n=1}^{N} (S_n - O_n)^2\right]^{1/2}}{\left[\sum_{n=1}^{N} (O_n)^2\right]^{1/2}} \tag{3.13}$$

$I_\infty$ norm

$$I_\infty = \frac{\max_{\forall n} \mid S_n - O_n \mid}{\max_{\forall n} \mid O_n \mid} \tag{3.14}$$

Root Mean Squared Error

$$RMSE = \left[\frac{\sum_{n=1}^{N} (S_n - O_n)^2}{N}\right]^{1/2} \tag{3.15}$$

Root Mean Squared

$$RMS = \left[\frac{\sum_{n=1}^{N} (S_n - \overline{S})^2}{N}\right]^{1/2} \tag{3.16}$$

Table 3.1: Definition of error measures used to evaluate performance of the hydrodynamical model, where $S_n$: simulated value; $O_n$: observed value; $N$: total number of data points.

0.5 m $s^{-1}$ (Table 3.4), which is of the same order of magnitude of the RMSE reported in other modeling exercises of wind-driven systems (Rueda and Schladow, 2003; Jin et al., 2000). Modeled velocities are shown, for example, in Fig 3.8, during a period of time characterized by strong and intermittent winds, changing direction. These results indicate that the model captures the switch in the velocity direction, and it reproduces reasonably well the magnitude of the velocity in time and space.

#### 3.3.2.2 Seasonal scale changes in circulation

Fig. 3.13 and 3.14 show horizontal and longitudinal sections of the first two Empirical Orthogonal Functions EOF that result of applying a Principal Component Analysis (PCA) to the weekly series of tracer fields simulated in the first tracer transport experiment. The EOF explains a 76.5 % of the variance, and represents the average estuarine circulation, with two layers moving in opposite directions:

| | T | T Aug | T Sep | T Oct |
|---|---|---|---|---|
| Range Observations | 22.8 (7.6–30.4) | 5.2 (25.1–30.4) | 6.9 (21.1–28.0) | 7.4 (16.1–23.5) |
| Range Simulations | 23.7 (7.7–31.4) | 7.7 (23.7–31.4) | 8.3 (21.4–29.8) | 6.0 (17.2–23.2) |
| RMS Observations | 5.68 | 1.05 | 1.94 | 1.44 |
| RMSE | 1.33 | 1.84 | 1.63 | 1.02 |
| $I_1$ | 0.062 | 0.058 | 0.052 | 0.042 |
| $I_2$ | 0.074 | 0.067 | 0.067 | 0.051 |
| $I_\infty$ | 0.16 | 0.15 | 0.13 | 0.10 |
| | T Nov | T Dec | T Jan | T Feb |
| Range Observations | 8.8 (10.6–19.5) | 5.05 (8.7–13.8) | 6.0(7.6–13.6) | 4.5(9.3–13.8) |
| Range Simulations | 7.6 (11.2–18.8) | 7.0 (7.7–14.7) | 5.6(7.7–13.4) | 4.1(9.1–13.3) |
| RMS Observations | 2.03 | 1.07 | 1.25 | 0.83 |
| RMSE | 0.94 | 1.19 | 1.22 | 0.80 |
| $I_1$ | 0.049 | 0.092 | 0.090 | 0.057 |
| $I_2$ | 0.060 | 0.10 | 0.11 | 0.072 |
| $I_\infty$ | 0.14 | 0.20 | 0.26 | 0.19 |
| | T Mar | T Apr | T May | |
| Range Observations | 8.1(8.9–17.0) | 4.9(14.0–18.9) | 6.7(17.1–23.8) | |
| Range Simulations | 6.2(10.9–17.1) | 6.2(15.0–21.1) | 8.1(18.3–26.5) | |
| RMS Observations | 1.72 | 1.25 | 1.57 | |
| RMSE | 1.25 | 1.54 | 1.51 | |
| $I_1$ | 0.078 | 0.085 | 0.060 | |
| $I_2$ | 0.091 | 0.096 | 0.074 | |
| $I_\infty$ | 0.17 | 0.18 | 0.18 | |

Table 3.2: Error analysis for observed and simulated water temperature (°C).

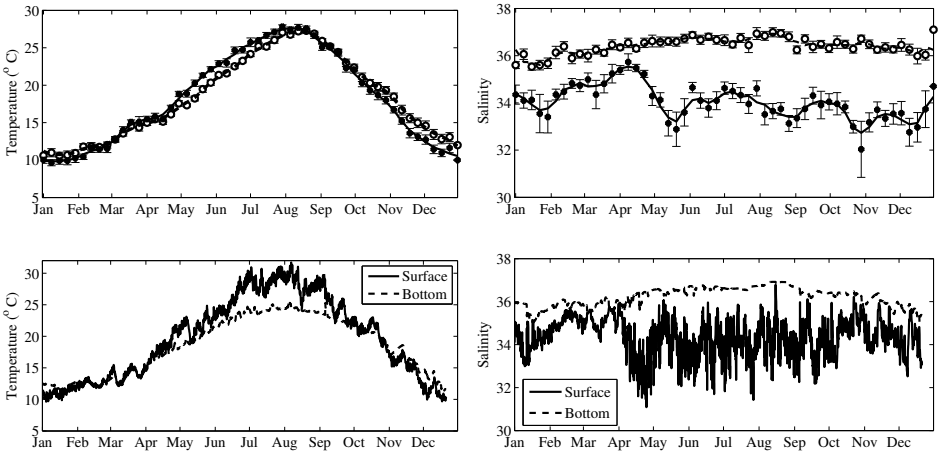


Figure 3.10: Weekly climatologies of temperature and salinity calculated over a 14 year period (top) compared to temperature and salinity results of the model (bottom). Data modeled and observed at the sampling station (Fig. 3.2)

towards the sea near the surface, while inward, into the bay, at depth. The salt wedge is identified in Fig. 3.13 by the white areas, as the salty water from the Mediterranean, free of tracers, moves inward through the bottom of the bay, replacing tracer rich water. There is an asymmetry along the north-south axis. The north side has higher concentrations at deeper depths than the south side, as can be observed in Fig 3.13(a) and 3.13(c). This asymmetry may be the result of the Coriolis effects, accumulating the westward flows at the surface towards the northern end, and the eastward currents (bottom) towards the south. The coefficients for the first component are positive at all times, with weak seasonal variations, indicating that all the tracer concentration fields after 8 days of the tracer release along the year share the same general trend.

The second EOF accounts for a 11.6 % of the variance. The coefficients of the second EOF have a strong seasonal components and are significantly correlated to the amount of freshwater emptied by the channels ($R^2$ = 0.54, P = $4\times10^{-10}$ %, not shown). They are negative at times with low freshwater inflows, including the periods with negligible inflows from the irrigation channels (15 Jan-31 March) and those others when the channels are left partially opened (1 Nov - 15 Jan). The coefficients corresponding to periods with high freshwater inflows (1 April - 31 Oct), in turn, tend to be mostly positive. Similarly to the first EOF, the second EOF exhibits has higher concentrations near the northern shore and lower concentrations near the bottom. The seasonal variations of the coefficients corresponding to the second EOF, represent the seasonal changes in stratification and the position of the salt-wedge, occurring as a consequence of changes in the inflow rates through irrigation channels. The positive values of the coefficients during periods with

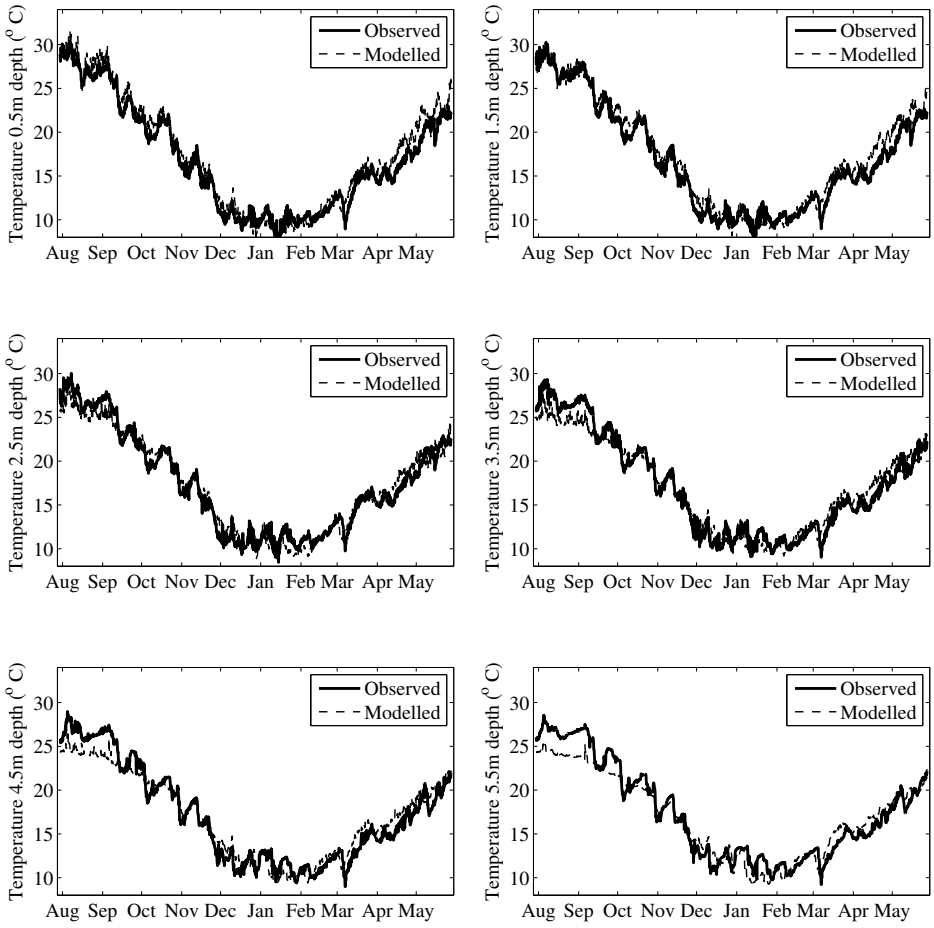


Figure 3.11: Temperature validation. Example of agreement between modeled and observed data at the sampling station (Fig. 3.2) for the period August 2008 - May 2009.

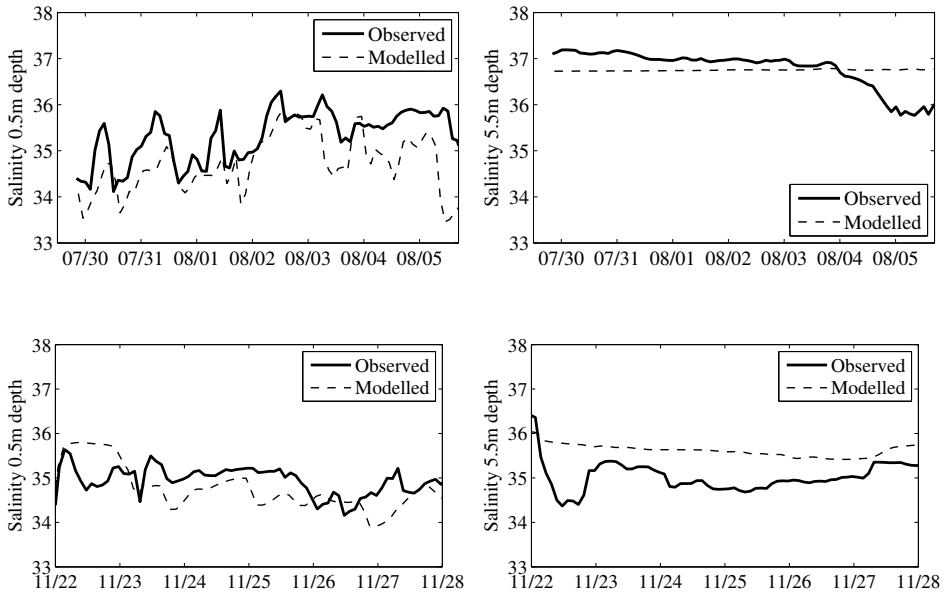


Figure 3.12: Salinity validation. Example of agreement between modeled and observed data at the sampling station (Fig. 3.2) for one week in July 2008 (top) and November 2008 (bottom).

high freshwater inputs (open channels season), will cause the vertical concentration gradients (stratification) to increase, and the salt wedge to move outwards into the sea. An example of this kind of structure is the tracer concentration on July 22nd (Fig. 3.15, which has open channels, contributes to the second EOF with high positive inputs, and shows a clear transverse gradient. On the other hand, low freshwater periods are characterized by a longitudinal gradient, specially in the mouth, where high concentrations accumulate in the east side of the bay. The lack of transverse gradient may be due to the fact that the buoyancy is weaker during these periods and, therefore, the currents are lower. The snapshot that contributes more negatively to the second EOF is shown in Fig. 3.15. It corresponds to January 13th, closed channel season, and illustrates the weakness of the transverse gradient.

Each of the remaining EOFs represents 3 % or less of the variance, hence, their results are not shown. None of these EOFs coefficients showed a clear correlation with the wind intensity, probably due to the fact that (1) the wind events are intermittent and with duration shorter than a week, which is the length of time between consecutive tracer fields used in the Principal Component Analysis, and (2) the winds are variable in speed and, also, in direction which may determine different responses in the bay.

| | S | S Jul 08 | S Sep 08 | S Oct 08 | S Nov 08 |
|---|---|---|---|---|---|
| Range Obs. | 4.4(32.8–37.2) | 3.1(34.1–37.2) | 2.9(34.4–37.3) | 4.1(32.9–37.0) | 2.3(34.1–36.4) |
| Range Sim. | 4.2(32.6–36.8) | 3.3(33.4–36.7) | 3.5(33.0–36.5) | 2.2(34.2–36.5) | 2.1(33.9–36.0) |
| RMS Obs. | 0.89 | 0.88 | 0.74 | 1.10 | 0.35 |
| RMSE | 0.75 | 0.64 | 0.83 | 0.61 | 0.60 |
| $I_1$ | 0.017 | 0.013 | 0.014 | 0.034 | 0.015 |
| $I_2$ | 0.021 | 0.018 | 0.023 | 0.017 | 0.017 |
| $I_\infty$ | 0.09 | 0.070 | 0.078 | 0.086 | 0.082 |
| | S Jan 09 | S Mar 09 | S May 09 | | |
| Range Obs. | 3.7(32.8–36.5) | 2.0(34.5–36.5) | 2.4(34.1–36.5) | | |
| Range Sim. | 2.2(33.2–35.4) | 0.9(34.8–35.7) | 4.0(32.6–36.6) | | |
| RMS Obs. | 1.17 | 0.54 | 0.52 | | |
| RMSE | 0.97 | 0.60 | 0.91 | | |
| $I_1$ | 0.024 | 0.014 | 0.020 | | |
| $I_2$ | 0.028 | 0.017 | 0.026 | | |
| $I_\infty$ | 0.13 | 0.05 | 0.11 | | |

Table 3.3: Error analysis for observed and simulated water salinity.

#### 3.3.2.3 Basin-scale response to characteristic wind events

Short-scale changes in the bay circulation are largely driven by changes in the wind forcing. Three scenarios can be defined depending on the wind forcing. The first scenario is characterized by $Ri^\star > L/h$, the wind is weak, the pycnocline deepens slowly, largely driven by stirring. This will be referred to as the *Mild wind scenario*. In this scenario the circulation is mainly estuarine, as described in section 3.3.2.2. The second and third scenarios are characterized by $Ri^\star < L/2h$, with strong mixing and rapid deepening of the mixed layer. The second scenario occurs in response to NW winds (perpendicular to the bay thalweg) with velocities of up to 5 – 15 m $s^{-1}$ lasting from 2-3 days. This will be referred to as *NW Shear Scenario*. In the third scenario, the bay is forced by diurnal SW winds (along the longitudinal axis of the bay), with speeds of up to 5 - 10 m $s^{-1}$, lasting 12-18 hours each day during 3-4 days. This third scenario will be referred to as *SW Shear Scenario*.

**3.3.2.3.1 NW Shear Scenario** Fig. 3.16 shows salinity and temperature fields before, during and after a NW wind event in November 2008. The bay was initially stratified with the pycnocline at ca. 1.5 - 2 m below the surface (11 November 18 h), with moderate longitudinal density gradients. Freshwater near the surface was flowing outward into the sea, while, the saltier seawater flowed inwards into the

| | V Across shore | V along shore |
|---|---|---|
| Range Observations | 0.29(-0.13–0.16) | 0.40(-0.19–0.21) |
| Range Simulations | 0.16(-0.07–0.09) | 0.30(-0.17–0.13) |
| RMS Observations | 0.034 | 0.041 |
| RMSE | 0.043 | 0.051 |
| $I_1$ | 1.14 | 1.17 |
| $I_2$ | 1.09 | 1.13 |
| $I_\infty$ | 2.3 | 1.77 |

Table 3.4: Error analysis for observed and simulated water velocity (m/s) for June through July 2008.

bay near the bottom, as it corresponds to the estuarine circulation. The wind started blowing on November 12th, increasing its speed from 2 to 6 m $s^{-1}$ in 24 hours. Six hours after the start of the event, strong transverse salinity and temperature gradients had developed, with a mixed layer that had deepened to 2.5 - 3 m. Driven by NW winds and as a result of the Coriolis effects, the surface layer flowed outwards in the southern half of the bay while southward at the northern half (not shown). Forty hours after the start of the event, on November 13th at 20 h, the transverse gradients persisted and the mixed layer had reached the bottom. The currents, at this point, did not show any preferred direction, probably as a consequence of the strong vertical mixing and the density gradients setup by wind counteracting the wind stress. The wind decreased progressively starting on November 14th and at the end of November 15th its maximum speed is around 2 m $s^{-1}$. The isopycnals become almost horizontal again, approximately 15 hours after the end of the event. On November 15th at 6 h, the original state before the event was almost reestablished, with the characteristic 2-layer estuarine circulation.

**3.3.2.3.2 SW Shear Scenario** Fig. 3.17 presents a sequence of fields during a strong but short SW wind event in June 2008. Previous to the event the bay was stratified with the characteristic estuarine circulation. During the wind event, the surface mixed-layer deepened to ca. 5 m and the estuarine circulation was reversed, with the surface being forced to flow inwards and the deeper layers to flow outwards. The surface layer was pushed to the north, bringing up the bottom layers near the southern end of the bay. After the wind ceases, the bay quickly returns to its original state, with horizontal isopycnals. The relaxation motions are fast, driven by the large horizontal density gradients set up by the wind acting on a water column with large vertical density differences.

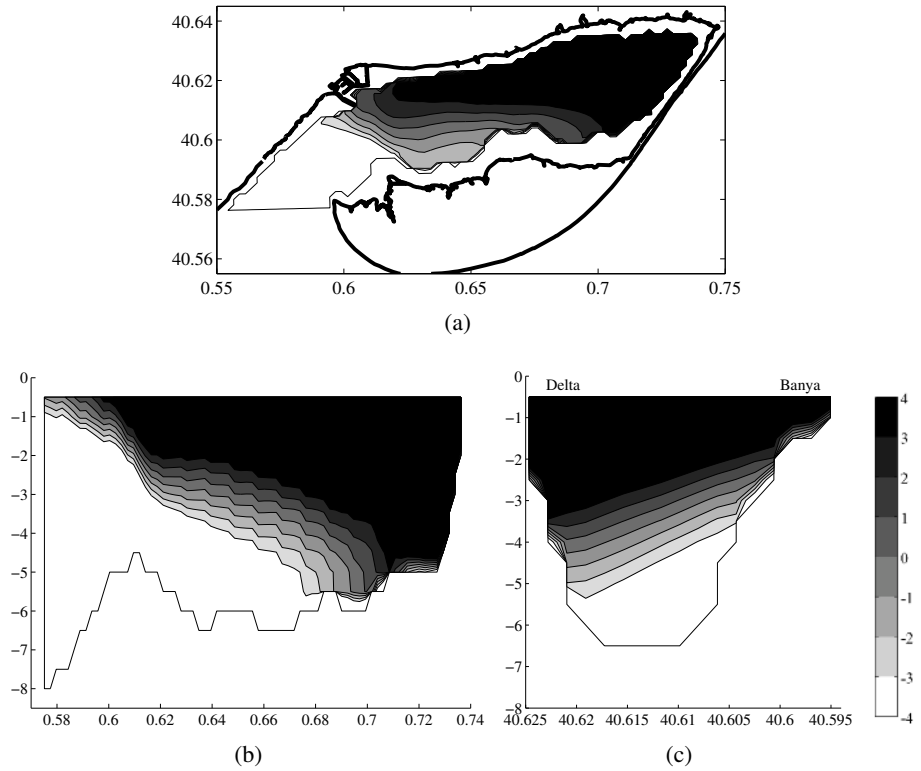


Figure 3.13: Representation of the first EOF (76.5% variance) of the tracer distribution in Alfacs eight days after the release of the tracers. a) Section at a constant depth of 3 m. b) Section along the axial transect of the bay (Fig 3.2). c) Transverse transect (Fig. 3.2).

#### 3.3.2.4 Wind-driven mass transport rates

Mass transport in and out of the bay and its evolution during the wind events were calculated from a series of tracer experiments, in which the bay was initially filled with a constant tracer concentration (see Section 4.2). A series of releases separated 4 h (November 2008) and 6 h (June 2008) in time were simulated. Fig. 3.18 shows the percentage of tracer mass removed from the bay during 12 h following the release, as a function of time during the NW and SW events in November 2008 and June 2008 analyzed above, as well as the along coast velocity profile in the mouth of the bay .

**3.3.2.4.1 NW Shear Scenario** The maximum rate of mass removal during the NW event (Fig. 3.18, left column) occurred during the first stages of the event, as a consequence of the strengthening of the estuarine circulation. The northwesterly winds induced southward currents, during the first stages of the event, veering towards the west as a result of Coriolis effects, and increasing the exchange. Wind

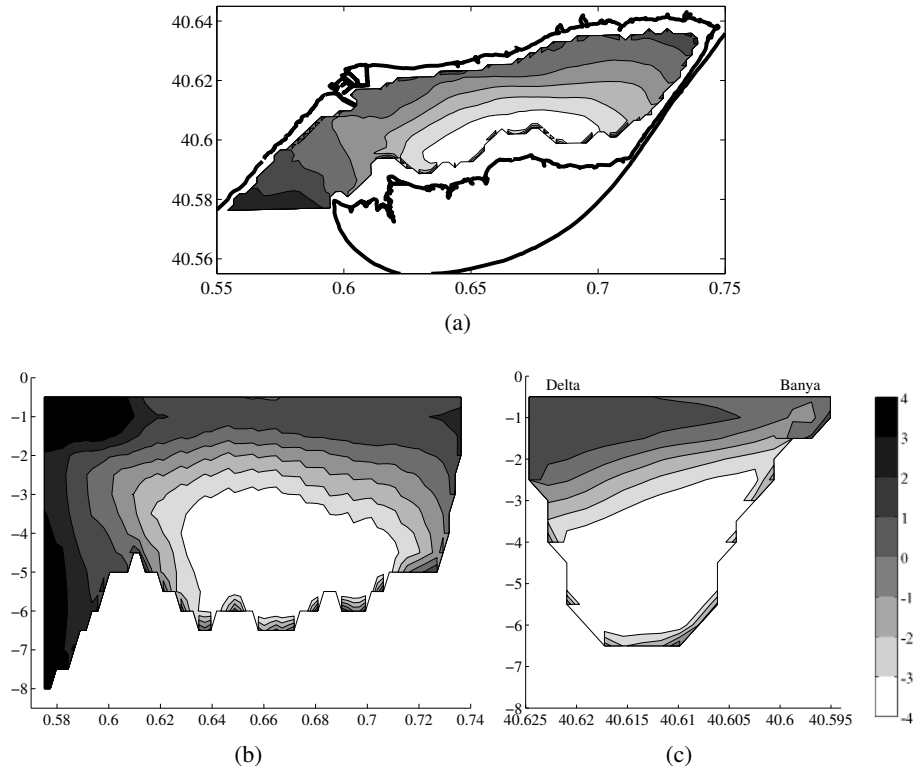


Figure 3.14: Representation the of the second EOF (11.6% variance) of the tracer distribution in Alfacs eight days after the release of the tracers. a) Section at a constant depth of 3 m. b) Section along the axial transect of the bay (Fig. 3.2). c) Transverse transect (Fig. 3.2).

forcing increases progressively the mixed layer depth, debilitating the estuarine circulation and, therefore, reducing the mass removal. During the 13th of November when the wind reaches its maximum strength the water column is mixed vertically, the estuarine circulation destroyed and the percentage of mass eliminated, minimum.

**3.3.2.4.2 SW Shear Scenario** The bay was initially subject to a short NW event at the beginning of June, 17 ((Fig. 3.18, right column), which forced the surface water to flow outwards, strengthening the estuarine circulation and increasing the exchange rate with the Mediterranean. Three SW wind events occurred during the period, separated by low winds from the NW. The three events caused a reversion of the surface layer circulation, and the rate of exchange, consequently decreased. After the short SW wind event of June 17, the estuarine circulation was re-established and rate of exchange increased again. The SW winds in on June 18 and 19 were more persistent, hence, driving a circulation opposite in sign to the

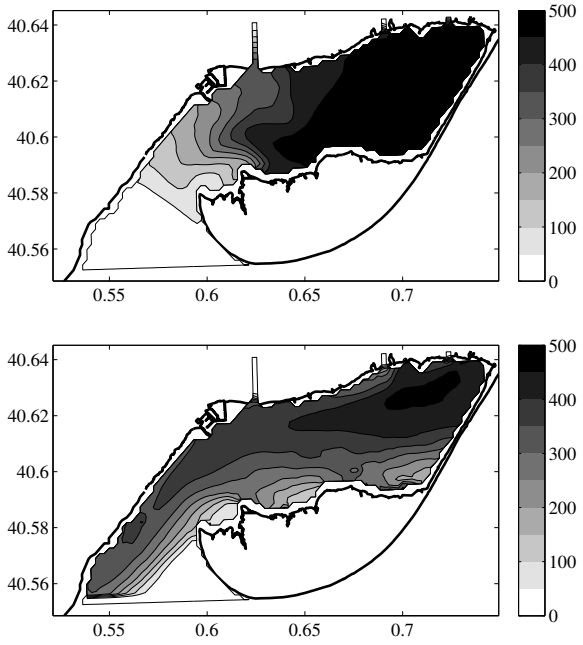


Figure 3.15: Representation of the tracer concentration after 8 days of the release in the surface layer for January 13th (top) and July 22nd (bottom).

classical estuarine exchange, and increasing the exchange rates.

## 3.4 Discussion and conclusions

The physical behavior of Alfacs, a shallow and small microtidal estuary, varies at seasonal and synoptic scales as a result of the changing force balances controlling transport and mixing processes. At seasonal scales, the variability in stratification and mixing and the large scale estuarine circulation are largely determined by changes in the freshwater inflows from groundwater sources and drainage irrigation channels. Tidal mixing is, in general, weak and, consequently, the estuary tends to remain stratified. At short time scales, however, stratification may be disrupted in response to wind forcing. Three scenarios have been defined, based on the use of the Richardson number ($Ri^{\star}$), to parametrize wind strength relative to the intensity of stratification, and on the predominant wind direction. For weak winds (scenario 1), or $Ri^{\star} > L/h$ ($L$ and $h$ denoting the length of the bay and the depth of the mixed layer, respectively), mixing occurs as a consequence of stirring and convection processes, and the mixed layer deepens very slowly. For strong winds with $Ri^{\star} < L/2h$, wind-driven mixing is rapid and occurs mainly as a consequence of shear at the pycnocline. Two scenarios can be identified in this case: one for persistent northwesterly NW winds (scenario 2), in which estuarine circulation initially

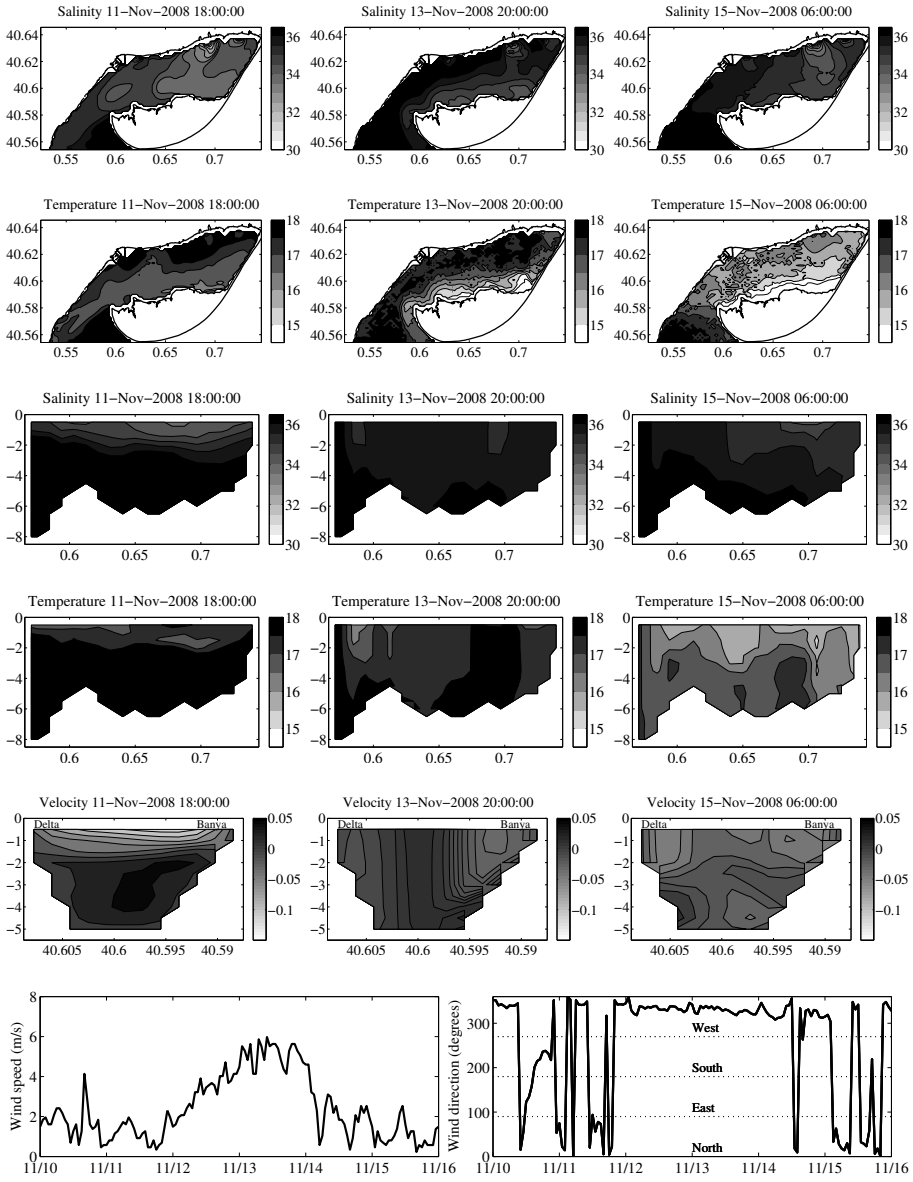


Figure 3.16: Model outputs of temperature in °C (second and fourth lines), salinity (first and third lines) and velocity in m $s^{-1}$ (fifth line) before (left column) during (middle column) and after (right column) a wind event on November 2008. Axes show longitude E and latitude N coordinates. Horizontal layers (first and second lines) represent the surface layer. Vertical sections of salinity and temperature (lines three and four) were sampled along the axial transect (Fig. 3.2. Velocity sections show the along-coast velocity along a mouth transect (Fig. 3.2). Bottom charts show the wind speed (left) and direction (right).

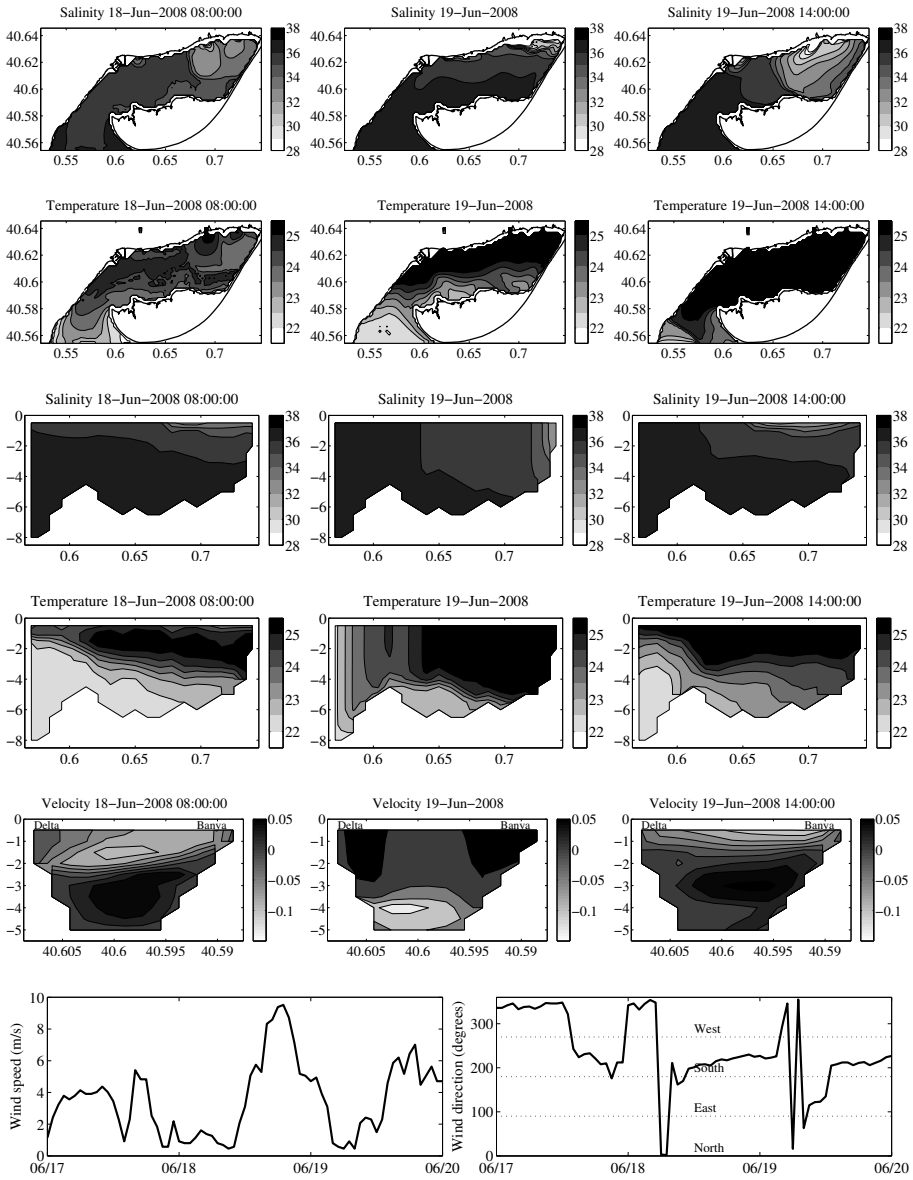


Figure 3.17: Model outputs of temperature in °C (second and fourth lines), salinity (first and third lines) and velocity in m $s^{-1}$ (fifth line) before (left column) during (middle column) and after (right column) a wind event on June 2008. Axes show longitude E and latitude N coordinates. Horizontal layers (first and second lines) represent the surface layer. Vertical sections of salinity and temperature (lines three and four) were sampled along the axial transect (Fig. 3.2. Velocity sections show the along-coast velocity along a mouth transect (Fig. 3.2). Bottom charts show the wind speed (left) and direction (right).

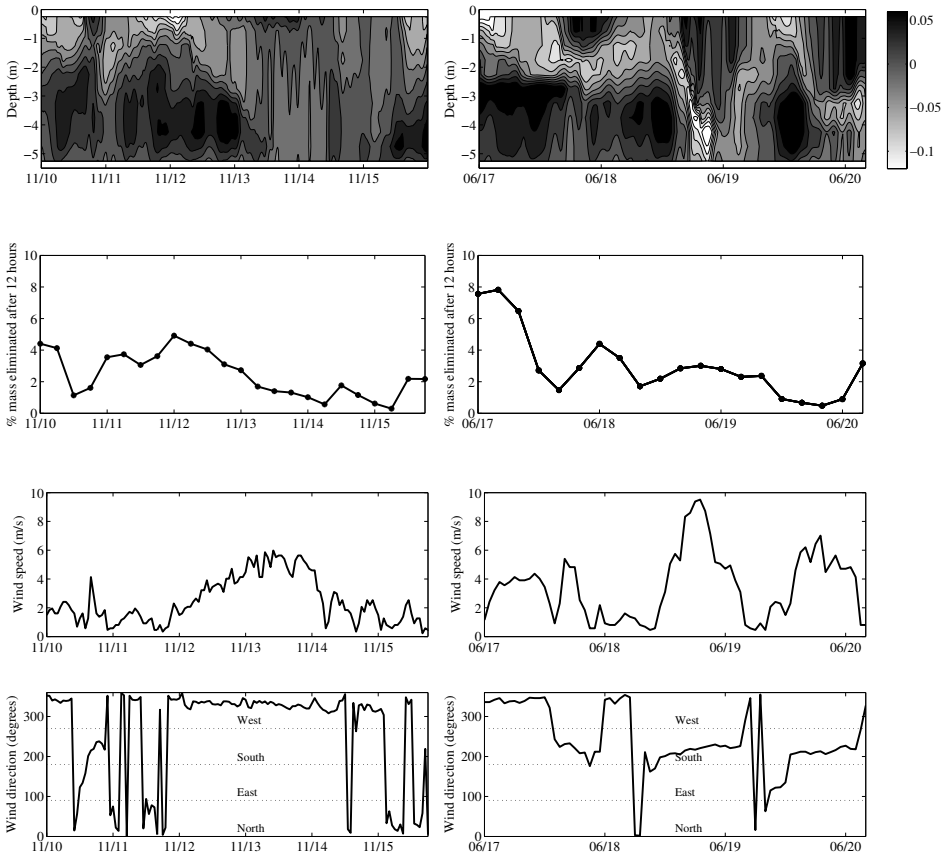


Figure 3.18: Percentage of mass eliminated after 12 hours of the tracer release during a wind event from the NW in November 2008 (top left) and a wind event from the SW June 2008 (top right). Wind speed (middle row) and wind direction (bottom row) during the same period.

strengthens, and another for diurnal SW winds (scenario 3), in which circulation weakens and may even reverse. In these scenarios, the water column overturns in response in scenarios 2-3 for winds longer than the cutoff time. In all cases, the bay re-stratifies within the 24h following the end of the wind event.

There are a few examples in the literature of work conducted to identify scenarios to describe the physical behavior of estuaries. Among them, Valle-Levinson et al. (2001) identified four scenarios describing current changes as a result of wind forcing and topography in Chesapeake Bay. Goodrich et al. (1987), working also in Chesapeake Bay, concluded that intensive mixing occurred mainly when a certain degree of shear was achieved, and they used the gradient Richardson number to define empirical thresholds for mixing events. They observed a correlation between the occurrence of wind events and the mixing episodes. These results were

supported by Blumberg and Goodrich (1990) who demonstrated through numerical simulations that the mixing observed was due to wind induced shear and not to turbulence generated at the free surface. However, the empirical thresholds that Goodrich et al. (1987) defined with the gradient Richardson number were calculated with the observed shear, which can be result of various factors. The thresholds that we propose here not only are defined analytically, but take into account only the wind generated shear, which is the variable that we are interested in, by means of calculating the bulk Richardson number instead of the gradient Richardson number. Our scenario classification is based on scaling arguments that take into account density differences and wind forcing, in a generalization to semi-enclosed systems of previous work for lakes or enclosed bodies (Fischer et al., 1979). Our arguments are based on the assumption that wind mixing is largely associated to turbulence generated at the free surface but, also and mainly, to shear-driven turbulence. This assumption, justified here on simple scaling calculations, allows a successful determination of wind speed thresholds above which the water column mixes and the estuary overturns, as demonstrated here for Alfacs (Fig. 3.4), and agrees with the results of Goodrich et al. (1987) and Blumberg and Goodrich (1990). However, it contrasts with the conclusions of other studies. For example, Schroeder et al. (1990) concluded that the mixing of Mobile Bay in response to wind was largely associated to increased bottom-drag. In Mobile Bay the bottom drag is associated to deep currents that are enhanced due to the effect of wind. The mean deep currents in Alfacs, due to its smaller dimensions and a weaker forcing, are one order of magnitude smaller than the currents in Mobile Bay, which generates a mixing power on the bottom three orders of magnitude smaller and, therefore, negligible.

In summary, this work, based on scaling arguments rather than on empirical considerations, uses the bulk Richardson number to evaluate the relative importance of wind speed and density gradients, the two most relevant forcing factors in Alfacs. To the best of our knowledge, the statement of a bulk Richardson number threshold for estuaries based on scaling arguments, and the definition of scenarios based on both mixing regimes and wind direction has not been done before.

The effect of wind direction on the hydrodynamics of the bay was explored by means of numerical experiments conducted with a three-dimensional numerical model. The obtained results were used to characterize the stratification and circulation changes occurring in response to forcing scenarios characterized by winds blowing from different directions. The level of agreement between observed and simulated temperatures, salinities and water velocities in Alfacs is comparable to that reported in other modeling studies. Deep water temperatures were under-predicted by the model in summer, probably as a result of the lack of precise boundary conditions for the marine area surrounding the bay. Improved numerical solutions could be obtained if salinity, temperatures and water surface elevation boundary conditions were either constructed from observations collected in situ or, alternatively, from simulations conducted with regional scale models of the Northwestern Mediterranean. The model results suggest that the estuarine circulation in

Alfacs is stronger during the initial stages of NW wind events. During SW events, in turn, wind forcing can induce a circulation reversal causing the surface layer to move into the bay. Such estuarine circulation reversals has also been reported in other microtidal estuaries, for example, by (Geyer, 1997; Weisberg, 1976; Stevens and Imberger, 1996). The importance of wind direction for understanding of the estuarine currents, first described analytically by Officer (1976), has also been noted in microtidal estuaries by (Valle-Levinson et al., 2001). Scaling arguments can be provided to determine whether wind forcing may reverse the estuarine circulation, by comparing the intensity of wind forcing with the baroclinic forces associated with the freshwater inflows. Using the expressions suggested by Officer (1976) and characteristic magnitudes of the bay it is possible to calculate that, in Alfacs, for winds stronger than approximately 2 m $s^{-1}$ the surface velocity due to wind forcing is stronger than the surface velocity due to density gradient. For example, for winds of 5 m $s^{-1}$ the baroclinic surface velocity can be quadrupled, supporting the idea that wind events of certain directions can intensify or reverse the estuarine circulation.

The correct identification of physical scenarios, characterized by different mixing levels and particular circulation patterns, and the time needed for the transitions between states sets the stage for understanding the bio-geochemical behavior of estuaries. In turn, this knowledge is necessary to evaluate the effect of human actions on these ecosystems and to define successful strategies to manage their resources, which have often high economical interest. Alfacs, for example, hosts a regionally important aquaculture industry, based mainly on raft cultures of the mussel *Mytilus galloprovincialis* (Delgado et al., 1990). This activity is subject to significant losses as a consequence of the development of anoxic conditions or the occurrence of Harmful Algal Blooms, when species such as *Alexandrium minutum*, which causes Paralytic Shellfish Poisoning (PSP) , *Dinophysis sacculus*, producer of Diarhetic Shellfish Poisoning (DSP) and *Karlodinium* spp., which causes fish mortality, proliferate in the water column mortality (Delgado et al., 1990; Garcés et al., 1997, 1999a; Fernández-Tejedor et al., 2004). HABs, in general, are more prone to occur when residence times are long (Margalef, 1997). Earlier studies suggest that the variability of wind speed and direction may control the evolution of HABs in Alfacs Bay. For example, frequent wind events in April mixed the water column and probably increased nutrient concentrations near the surface, precious to the bloom of *Alexandrium minutum* reported by Delgado et al. (1990). The bloom developed thereafter during a calm period when the water column re-stratified, and it lasted until late May. At that time, the bay was subject to strong winds which mixed the water column again. It is not clear, however, whether the decline of the algal population was due to wind mixing, which could disrupt the ecology of some organisms, or to dispersion by transport out of the bay. Our results support the view that sufficiently long and strong wind events could increase vertical mixing rates and enhance the input of nutrients from the sediment (Vidal, 1994). Furthermore, as explained above, wind scenarios weakening the estuarine circulation could create

favorable conditions for the occurrence of algal blooms. The increased estuarine circulation observed during the first stages of NW wind events, could increase the exchange with the Mediterranean and contribute to the demise of algal blooms. Further insight on the implications of different scenarios of physical forcing and water residence times, phytoplankton dynamics and bloom development could be obtained by coupling the hydrodynamic model developed here with a biological model including the main biotic components of the bay ecosystem.

## 3.5 Appendix

### 3.5.1 Time scales

As has been explained in the text equation 3.5 represents the changes in the thickness of a surface mixed layer $h$ due to mixing. It is a balance between the energy required to entrain a parcel of water into de surface mixed layer due to changes in kinetic energy (first term on the left-hand side of 3.5) or buoyancy (second term on the left-hand side of 3.5) and the energy available due to surface stirring and cooling (first term on the right-hand side of 3.5) and shear stress across the pycnocline (second term on the right-hand side of 3.5).

The stress caused on the surface by mild winds generates waves that interact with the present shear and generate turbulent kinetic energy and in some cases secondary movements called Langmuir cells. The time scales necessary to deepen the mixed layer from depth $h$ to $2h$ in such conditions can be calculated from equation 3.5, where the energy available for shear mixing is negligible, obtaining equation 3.8.

On the other hand, in the case of strong winds the stress on the surface induces the water to move in the direction of the wind. To compensate this movement and keep the water surface horizontal the water under the pycnocline moves in the opposite direction, creating a shear across the pycnocline. The pycnocline tilts, and the interface oscillates until it reaches an equilibrium tilt. The shear mechanism deepens the interface in an efficient way quantified by the second element in the right side of equation 3.5, where $\Delta u$ is the difference in velocity between the top and the bottom layer. The magnitude of $\Delta u$ can be estimated, in turn, from a simplified momentum balance in which the vertical gradient of shear stress, $t$, is the only source of momentum, such that

$$\frac{d(uh)}{dt} = \rho_0 u^{\star 2} \tag{3.17}$$

Baroclinic pressure gradients resulting from the tilting of the thermocline are here neglected; hence, it is strictly only applicable away from the boundaries and during the onset of the wind event. Assuming that the wind friction velocity is

constant and that the velocity below the thermocline is negligible, 3.17 can be integrated to yield an expression for $\Delta u$,

$$\Delta u \approx u = \frac{u^{\star 2} t}{h} \tag{3.18}$$

which predicts a linear increase of $\Delta$u with time. After a time period $T_c$, or cut-off time, the effects of the boundaries have propagated to the open end of the estuary, and the shear-stress in 3.17 is balanced by the baroclinic pressure gradient associated with the tilting of the pycnocline. The maximum velocity gradient will occur at $T_c$. Beyond this time, the shear will return rapidly to $u^\star$. The value of the cut-off time corresponds to one quarter of the first mode internal wave period, which depends on the geometry of the bay, and it is different for enclosed systems than for semi-enclosed systems. In our case, in which one of the boundaries is open, the cut-off time is equation 3.7.

The characteristic time scale necessary to deepen the pycnocline to twice the original depth is calculated neglecting the stirring terms in equation 3.5. Taking into account equation 3.18, evaluated at the moment of maximum velocity $T_c$, the result is equation 3.9.

### 3.5.2 Regimes

The situations that will generate shear can be identified based on the Richardson number. In order for shear to contribute to deepening, the energy available for mixing due to shear (last term in equation3.5 will have to be greater than or equal to the energy necessary for the entrainment of water given a particular buoyancy (second term in equation 3.5). Solving this balance implies that $Ri \leq C_s$, in order for shear to contribute to the deepening. Evaluating $Ri$ with the maximum velocity in equation 3.18 at a time $T_c$ reveals that the Richardson number will reach $C_s$ before a time $T_c$ if the following condition is fulfilled

$$R_i^\star \leq \frac{L C_s^{1/2}}{h} \qquad \text{if } C_s^{1/2} \sim 1 \text{ then} \qquad R_i^\star \leq \frac{L}{h} \tag{3.19}$$

which indicates that if the Richardson number evaluated with the shear velocity $v^\star$ is lower than $L/h$ shear production is contributing to deepening. A dominance of the shear production occurs if the shear is able to double the depth of the pycnocline during that period, this is, that the time-scale $T_e$ necessary for this process is lower than or equal to $T_c$.

$$R_i^\star \leq \frac{L C_s^{1/2}}{2h} \qquad \text{if } C_s^{1/2} \sim 1 \text{ then} \qquad R_i^\star \leq \frac{L}{2h} \tag{3.20}$$

Therefore, two regimes can be defined. When $Ri^\star > L/h$ the interface is sharp, energized only by wind stirring, although it becomes less defined the closer $R_i^\star$ is to the limit. The deepening is slow, and internal waves are a dominant feature. On the other hand, when $Ri^\star \leq L/h$ shear production is the main feature of this regime, although it will be dominant when $Ri^\star \leq L/2h$. In this case, shear production deepens the interface fast. Eventually the column will mix vertically, although a longitudinal gradient can be formed.

## 3.6 Acknowledgments

This work was funded by Ministerio de Ciencia y Educación (project TURECO-TOX, CTM2006-13884-CO2-00/MAR9), and is part of a collaborative agreement between University of Granada and CSIC-Institut de Ciències del Mar (ICM). Numerous public resources available online have been used to create the appropriate boundary conditions for the model. We thank Meteocat (www.meteocat.com), Puertos del Estado (www.puertos.es), XIOM (www.boiescat.org), Catalan Water Agency (http://mediambient.gencat.net/aca) as well as the Parc Natural del Delta de l'Ebre for kindly sharing their measurements. We thank Peter Smith for his support and Yvette Spitz for valuable advice and computer access. The field data has been collected by Rubén Quesada and Mireia Lara, with the advice of Elisa Berdalet and Jaume Piera. We thank Carme Lorente for her help with the maps. CL was funded by a fellowship of the Spanish National Research Council, CSIC (Beca CSIC Predoctoral I3P-BPD2005) and for a postgraduate grant of La Fundación Caja Madrid. ML was funded by a FPU program from the Spanish Government. JS was funded by Proyecto Intramural Especial del CSIC, "Desarrollo de algoritmos y validación de productos en el Centro Experto SMOS en Barcelona" (200430E530).

# Chapter 4

## The role of inorganic nutrients and dissolved organic phosphorus in the phytoplankton dynamics of a Mediterranean Bay. A modeling study.

This chapter has been published as

Llebot, C. Spitz, Y., Solé, J., Estrada, M., 2010. The role of inorganic nutrients and dissolved organic phosphorus in the phytoplankton dynamics of a Mediterranean Bay. A modeling study. Journal of Marine Systems, 83:192–209.

**ABSTRACT**

The effect of Dissolved Organic Phosphorus (DOP) availability and nutrient limitation of phytoplankton growth in an estuarine bay (Alfacs Bay, NW Mediterranean) have been studied by means of a zero-dimensional ecological model including nitrogen, phosphorus (organic and inorganic), two groups of phytoplankton (diatoms and flagellates), one group of zooplankton, and detritus. Simulations with and without DOP as an extra source of phosphorus for phytoplankton growth suggest that DOP plays an important role in the dynamics of the Alfacs Bay ecosystem. DOP is indeed necessary to simulate the observed draw-down of nitrate and build up of phytoplankton biomass. Two non-exclusive mechanisms allowing DOP availability for phytoplankton are possible: direct uptake, or remineralization to Dissolved Inorganic Phosphorus. Including both gives a better agreement with the observations. Inclusion of DOP in the model leads to predominance of phosphorus limitation of phytoplankton growth in fall and winter, and of nitrogen limitation in late spring and summer. Simulations with and without sediment resuspension suggest that this process does not significantly affect the nutrient budget in the bay.

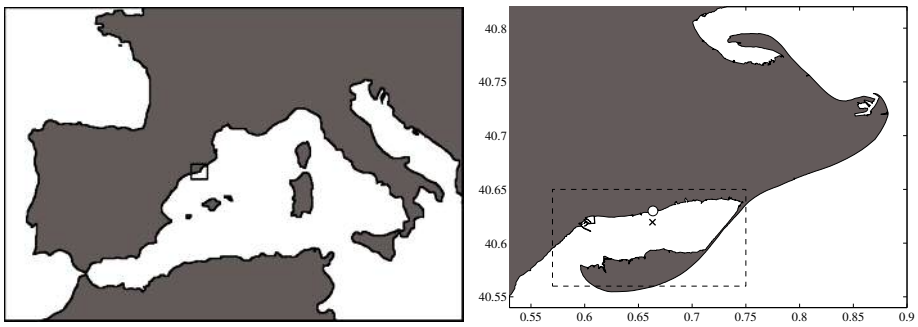


Figure 4.1: Map of the study zone in Latitude/Longitude coordinates. - - Els Alfacs Bay; ○ : weather station; x : sampling site.

## 4.1 Introduction

Coastal regions are highly dynamic and productive areas that have historically attracted human populations. In the confluence between a river mouth and the sea, estuaries hold a variety of habitats and have both a high ecological and economic value. Such areas process nutrients as they pass from the land to the sea, provide shelter and nursery grounds for many aquatic species, and support successful fisheries and aquaculture activities.

A major challenge in the study of marine coastal areas is understanding the interactions among physico-chemical variables and ecosystem behavior. Alfacs Bay represents a good case study for this challenge. Alfacs (NW Mediterranean, Fig. 4.1) is a shallow bay (3.13 m deep on average) characterized by human controlled freshwater discharge and subject to the typically small tides of the Mediterranean (less than 0.2 m). It is highly productive, and hosts successful aquaculture businesses (Camp and Delgado, 1987; Departament d'Agricultura, Alimentació i Acció Rural). However, algal blooms - some of them harmful - have been recurrent in Alfacs since 1989 (Delgado et al., 1990). Harmful algal blooms (HABs) consist of different species, such as the dinoflagellates *Alexandrium minutum* (Delgado et al., 1990), *Dinophysis sacculus* (Garcés et al., 1997) and *Karlodinium spp.* (formerly identified as *Gyrodinium corsicum*) (Fernández-Tejedor et al., 2004; Garcés et al., 1999a), and diatoms of the genus *Pseudonitzschia* (Quijano-Sheggia et al., 2008). Their frequency has increased over the years, just as it has increased in other harbors of the neighboring Catalan coast (Vila et al., 2001a). Some of these proliferations are associated with massive mortalities of cultured fish, and others cause mussel (*Mytillus galloprovincialis*) toxicity for humans (due to Diarrhetic or Paralytic Shellfish Poisoning). Because these blooms consist primarily of flagellates or diatoms, the dynamics of these groups and nutrient control of their populations will be one of the foci of this study.

The main sources of dissolved inorganic nutrients in Alfacs Bay are freshwa-

ter discharge from irrigation channels and treatment plants (Camp, 1994), ground water input, exchange with the open ocean through the mouth of the bay, flux from sediments (Delgado and Camp, 1987; Vidal, 1994), and recycling and remineralization from biological processes. Agricultural practice in the Ebre Delta, which is dominated by rice farming, delivers high inorganic nitrogen loads to the bay (of the order of 20–100 mmol N $m^{-3}$) through freshwater drainage channels. In general June and October are the months with higher nutrient concentration in the channels, because the fields are fertilized in June and emptied in October after the crop (Muñoz, 1998). Phosphorus concentrations are generally low (0.5-1.5 mmol P $m^{-3}$ ). In addition to drainage channels, ground water seepage appears to be also an important source of nutrients, given the high nitrate concentrations in the Ebre Delta aquifers, where up to 1500 mmol N $m^{-3}$ have been reported (Ministerio de Obras Públicas, Transportes y Medio Ambiente; Ministerio de Industria y Energía, 1995; Torrecilla et al., 2005). The main nutrient sinks are exchanges with the sea and consumption by phytoplankton, which can also produce detrital matter sinking to the sediment. In addition to dissolved inorganic nutrients, dissolved organic compounds have been found in high concentration in the bay, in association with freshwater discharge. Recent studies (Loureiro et al., 2009a) have documented much higher concentrations of dissolved organic phosphorus than of inorganic phosphorus concentrations during the summer.

In spite of previous work on the linkage between the phytoplankton community and the physics in Alfacs Bay (Artigas, 2008; Llebot et al., 2008), a good understanding of the main physico-chemical factors controlling the phytoplankton community is still lacking. One outstanding question concerning the ecology of Alfacs Bay is the role of nutrient fluxes on phytoplankton community succession and bloom development. Nutrient control of phytoplankton growth in Alfacs Bay has been addressed by several field studies, but with contrasting results. On one hand, Delgado and Camp (1987) reported a N:P ratio between 0.2 and 10.2, and by comparison with Redfield ratio concluded that nitrogen was the limiting nutrient of the system. On the other hand, Cruzado et al. (2002) found that phosphorus was the limiting nutrient in the Ebre Delta system and attributed this observation to the contribution of freshwater discharge, which is high in nitrogen and low in phosphorus. Freshwater input to Alfacs is indeed low in phosphorus due to its retention in the rice fields, as observed by Forès (1989). Finally, other studies point to a more complicated situation of alternating phosphorus and nitrogen limitation. Vidal (1994) considered that phosphorus was the main limiting nutrient for phytoplankton growth in Alfacs, but suggested that atmospheric and hydrodynamic forces could play key roles in alternating nitrogen and phosphorus limitation. Quijano-Sheggia et al. (2008) found that inorganic P limitation was frequent, especially during winter, while a few cases of inorganic N limitation were observed in summer. Thus, the question of the nutrient control in Alfacs remains still unanswered.

Our hypothesis is that phytoplankton production experiences a colimitation of

nitrogen and phosphorus, and that the most limiting nutrient changes during the year, depending on the variability of the sources and sinks of both nutrients. Therefore, the general aim of this work is to ascertain, by means of an ecosystem model, which nutrient or nutrients potentially limit phytoplankton production in Alfacs and to describe the main sources and sinks of these nutrients and how they affect the phytoplankton community composition. In particular, we will test two main hypotheses. 1) nitrogen or phosphorus are most limiting for phytoplankton growth in different seasons affecting the plankton community composition. 2) this alternation can be explained by two processes that affect phosphorus availability, in addition to freshwater inputs: a) phosphorus release from the sediment after resuspension events due to wind stirring (Vidal, 1994); b) availability of dissolved organic phosphorus (DOP) as a source of P to phytoplankton through two non-exclusive mechanisms: remineralization to dissolved inorganic phosphorus (DIP) and direct uptake. Although the direct uptake of DOP has been shown by several experimental studies (Bentzen et al., 1992; Currie and Kalff, 1984; Huang and Hong, 1999; Johannes, 1964; jin Oh et al., 2002; Yamamoto et al., 2004) it is only rarely taken into account by ecological models. The input of detrital particulate phosphorus (PP) from freshwater could be another source of phosphorus (Aminot et al., 1993; Némery and Garnier, 2007; Ruttenberg, 2001). Although samples of particulate matter in the channels are very scarce, the few available data suggest that the concentration of particulate phosphorus (PP) ranges between 1 and 3 mmol P $m^{-3}$ (Muñoz, 1998). We did not present this third possibility in this manuscript because the fluxes of PP to the bay and the dissolution rates seem too small to add any substantial source of phosphorus to the bay.

In order to approximate the budgets and fluxes of nitrogen and phosphorus and to address the above hypotheses, we built a zero-dimensional ecological model of the estuarine mixed layer. The model includes nine state variables: zooplankton, flagellates, diatoms, dissolved inorganic nitrogen, dissolved inorganic phosphorus, dissolved organic nitrogen, dissolved organic phosphorus, detrital phosphorus, and detrital nitrogen. The forcing variables are water density, temperature, wind intensity, freshwater input, and velocities in and out of the bay, in addition to silicon that is introduced into the model based on a time series of measured concentrations.

In section 4.2 we present the model equations and parameter values, and the choice of initial conditions and forcing used in the simulations. We also describe the field data. Section 4.3 reports the outcome of the various simulations using different sets of assumptions about the occurrence of sediment resuspension and the possibility of DOP utilization by phytoplankton, and presents the comparisons of these results with measured data. Section 4.4 presents a sensitivity analysis with respect to the fluxes and nutrient concentrations of the freshwater sources. The results are discussed in section 4.5. Finally, we summarize our conclusions in section 4.6.

## 4.2 Materials and Methods

### 4.2.1 Study site

Alfacs Bay (Fig. 4.1) is the southernmost bay of the Ebre River deltaic complex (40°33'–40°38'N, 0°33–0°44'E), and also the largest. It is roughly 11 km long and 4 km wide; its average depth is 3.13 m and the maximum depth is 6.5 m; it contains approximately $153 \times 10^6$ m$^3$ of water. A sand barrier separates the basin from the sea. The mouth of the bay is about 2.5 km wide allowing water to be exchanged with the open sea along its eastern and southern periphery (Camp, 1994).

### 4.2.2 The model

The model used in this study is a zero dimensional mixed layer model that describes the nitrogen and phosphorus cycles of a shallow non-tidal estuarine bay. The temporal rate of change of any biochemical variable of the model ($C$) follows the equation,

$$\frac{\partial C}{\partial t} = G_{(C)}, \tag{4.1}$$

where $G_{(C)}$ represents the physical and biological sources minus sinks of the model variable.

The mixed layer deepening and shallowing are calculated using buoyancy and wind stress. The model considers horizontal advection due to exchanges with the open sea across the bay mouth, and to freshwater inputs from channels and underground seepage. Advection is included in the $G_{(C)}$ term. Horizontal diffusion is neglected because it is too small compared to advective transport to warrant inclusion in the model.

The dynamics of the state variables, Zooplankton (ZOO), Diatoms (PH1), Flagellates (PH2), Dissolved Inorganic Nitrogen (DIN), Dissolved Inorganic Phosphorus (DIP), Dissolved Organic Nitrogen (DON), Dissolved Organic Phosphorus (DOP), Detrital phosphorus (DTP) and Detrital nitrogen (DTN) are described by equations 4.2 to 4.10 in Table 4.1. See Fig. 4.2 for a schematic diagram of the model and Table 4.2 for a description of the model parameters. The model is forced by six variables: water density, wind, rainfall, temperature, sea exchange, and freshwater inputs, which include discharge from channels and underground waters (Fig. 4.3, Table 4.3).

$$\frac{\partial \mathrm{PH1}}{\partial t} = \mathrm{Growth}_{(\mathrm{PH1})}\ \mathrm{PH1} - \mathrm{Death}_{(\mathrm{PH1})}\ \mathrm{PH1} - \mathrm{Exudation}_{(\mathrm{PH1})}\mathrm{PH1} - \mathrm{Grazing}_{(\mathrm{PH1})}\ \mathrm{ZOO} + \mathrm{Advection}_{(\mathrm{PH1})} \tag{4.2}$$

$$\frac{\partial \mathrm{PH2}}{\partial t} = \mathrm{Growth}_{(\mathrm{PH2})}\ \mathrm{PH2} - \mathrm{Death}_{(\mathrm{PH2})}\ \mathrm{PH2} - \mathrm{Exudation}_{(\mathrm{PH2})}\mathrm{PH2} - \mathrm{Grazing}_{(\mathrm{PH2})}\ \mathrm{ZOO} + \mathrm{Advection}_{(\mathrm{PH2})} \tag{4.3}$$

$$\frac{\partial \mathrm{ZOO}}{\partial t} = \gamma\ (\mathrm{Grazing}_{(\mathrm{PH2})} + \mathrm{Grazing}_{(\mathrm{PH1})})\ \mathrm{ZOO} - \mathrm{Death}_{(\mathrm{ZOO})}\ \mathrm{ZOO}^2 - \mathrm{Excretion}_{(\mathrm{ZOO})}\ \mathrm{ZOO} - \mathrm{Exudation}_{(\mathrm{ZOO})}\mathrm{ZOO} + \mathrm{Advection}_{(\mathrm{ZOO})} \tag{4.4}$$

$$\frac{\partial \mathrm{DIN}}{\partial t} = -\mathrm{Growth}_{(\mathrm{PH2})}\ \mathrm{PH2} - \mathrm{Growth}_{(\mathrm{PH1})}\ \mathrm{PH1} + \mathrm{Excretion}_{(\mathrm{ZOO})}\ \mathrm{ZOO} + \mathrm{Remineralization}_{(\mathrm{DON}to\mathrm{DIN})}\ \mathrm{DON} + \mathrm{FWInput}_{(\mathrm{DIN})} + \mathrm{Advection}_{(\mathrm{DIN})} \tag{4.5}$$

$$\frac{\partial \mathrm{DIP}}{\partial t} = (\mathrm{R_{NP}})^{-1}\Big( - \mathrm{Growth\_eq}_{(\mathrm{PH2})}\ \mathrm{PH2} - \mathrm{Growth\_eq}_{(\mathrm{PH1})}\ \mathrm{PH1} + \mathrm{Excretion}_{(\mathrm{ZOO})}\ \mathrm{ZOO}\Big) + \quad \mathrm{Remineralization}_{(\mathrm{DOP}to\mathrm{DIP})}\ a\ \mathrm{DOP} + \mathrm{FWInput}_{(\mathrm{DIP})} + \mathrm{Resuspension}_{(\mathrm{DIP})} + \mathrm{Advection}_{(\mathrm{DIP})} \tag{4.6}$$

$$\frac{\partial \mathrm{DTN}}{\partial t} = (1-\gamma)(\mathrm{Grazing}_{(\mathrm{PH2})} + \mathrm{Grazing}_{(\mathrm{PH1})})\ \mathrm{ZOO} + \mathrm{Death}_{(\mathrm{PH2})}\ \mathrm{PH2} + \mathrm{Death}_{(\mathrm{PH1})}\ \mathrm{PH1} + \mathrm{Death}_{(\mathrm{ZOO})}\ \mathrm{ZOO}^2 - \mathrm{Remineralization}_{(\mathrm{DTN}to\mathrm{DON})}\ \mathrm{DTN} + \mathrm{Sedimentation}_{(\mathrm{DTN})} + \mathrm{Advection}_{(\mathrm{DIN})} \tag{4.7}$$

$$\frac{\partial \mathrm{DTP}}{\partial t} = (\mathrm{R_{NP}})^{-1} \times \Big((1-\gamma) \times (\mathrm{Grazing}_{(\mathrm{PH2})} + \mathrm{Grazing}_{(\mathrm{PH1})})\ \mathrm{ZOO} + \mathrm{Death}_{(\mathrm{PH2})}\ \mathrm{PH2} + \mathrm{Death}_{(\mathrm{PH1})}\ \mathrm{PH1} - \mathrm{Death}_{(\mathrm{ZOO})}\ \mathrm{ZOO}^2\Big) - \mathrm{Remineralization}_{(\mathrm{DTP}to\mathrm{DOP})}\ \mathrm{DTP} + \mathrm{Sedimentation}_{(\mathrm{DTP})} + \mathrm{Advection}_{(\mathrm{DIN})} \tag{4.8}$$

$$\frac{\partial \mathrm{DOP}}{\partial t} = (\mathrm{R_{NP}})^{-1}\Big(\mathrm{Exudation}_{(\mathrm{PH1})}\mathrm{PH1} + \mathrm{Exudation}_{(\mathrm{PH2})}\mathrm{PH2} + \mathrm{Exudation}_{(\mathrm{ZOO})}\mathrm{ZOO} - (\mathrm{Growth}_{(\mathrm{PH2})} - \mathrm{Growth\_eq}_{(\mathrm{PH2})})\ \mathrm{PH2} - (\mathrm{Growth}_{(\mathrm{PH1})} - \mathrm{Growth\_eq}_{(\mathrm{PH1})})\ \mathrm{PH1}\Big) + \mathrm{FWInput}_{(\mathrm{DOP})} + \mathrm{Remineralization}_{(\mathrm{DTP}to\mathrm{DOP})}\mathrm{DTP} - \mathrm{Remineralization}_{(\mathrm{DOP}to\mathrm{DIP})}\ a\ \mathrm{DOP} + \mathrm{Advection}_{(\mathrm{DOP})} \tag{4.9}$$

$$\frac{\partial \mathrm{DON}}{\partial t} = \mathrm{Exudation}_{(\mathrm{PH1})}\mathrm{PH1} + \mathrm{Exudation}_{(\mathrm{PH2})}\mathrm{PH2} + \mathrm{Exudation}_{(\mathrm{ZOO})}\mathrm{ZOO} - \mathrm{Remineralization}_{(\mathrm{DONtoDIN})} + \mathrm{Remineralization}_{(\mathrm{DTNtoDON})} + \mathrm{Advection}_{(\mathrm{DON})} \tag{4.10}$$

Table 4.1: Governing equations.

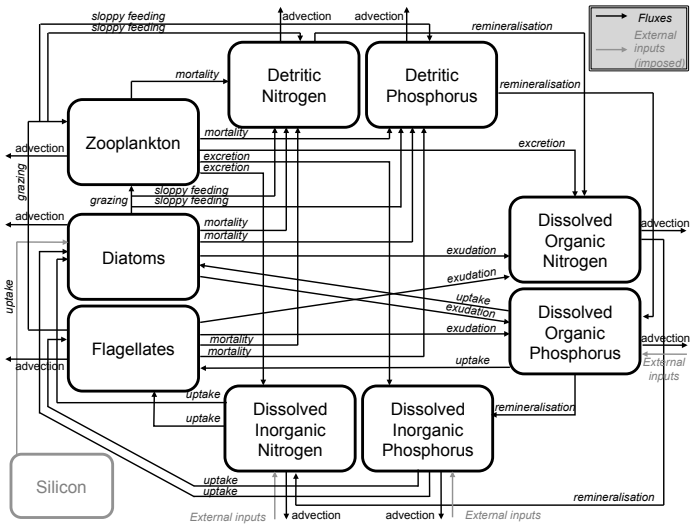


Figure 4.2: Diagram of the model fluxes and state variables.

Table 4.2: Parameters.

| Symbol | Value | Units | Description |
|---|---|---|---|
| Basic parameters of the model | | | |
| dt | 15 | min | Time step |
| Basic parameters of the plankton | | | |
| $P^B_{m(\mathrm{PH1})}$ | 1.45 | day$^{-1}$ | Maximum diatom growth rate |
| $P^B_{m(\mathrm{PH2})}$ | 1.0 | day$^{-1}$ | Maximum flagellate growth rate |
| $Kp_{(\mathrm{PH1})}$ | 0.8 | mmol N m$^{-3}$ | Diatom half saturation constant for zooplankton ingestion |
| $Kp_{(\mathrm{PH2})}$ | 0.8 | mmol N m$^{-3}$ | Flagellate half saturation constant for zooplankton ingestion |
| $m_{(\mathrm{PH1})}$ | 0.15 | day$^{-1}$ | Diatom mortality rate |
| $m_{(\mathrm{PH2})}$ | 0.15 | day$^{-1}$ | Flagellate mortality rate |
| $m_{(\mathrm{ZOO})}$ | 0.08 | day$^{-1}$ | Zooplankton mortality rate |
| $R_m$ | 1 | day$^{-1}$ | Zooplankton maximum grazing rate |
| $\chi_{(\mathrm{PH1})}$ | 0.2 | No dim | Preference of zooplankton for grazing on diatom |
| $\chi_{(\mathrm{PH2})}$ | 0.8 | No dim | Preference of zooplankton for grazing on flagellate |
| $Q_{(\mathrm{PH1})}$ | 0.04 | day$^{-1}$ | Diatom exudation rate |
| $Q_{(\mathrm{PH2})}$ | 0.04 | day$^{-1}$ | Flagellate exudation rate |
| $Q_{(\mathrm{ZOO})}$ | 0.05 | day$^{-1}$ | Zooplankton excretion rate to DON and DOP |

Table 4.2: Parameters. Continues in next page.

| Symbol | Value | Units | Description |
|---|---|---|---|
| $E$ | 0.03 | $\text{day}^{-1}$ | Zooplankton excretion rate to DTN and DTP |
| $R_{NP}$ | 16 | mole/mole | Redfield ratio |
| Basic parameters of the bay | | | |
| $A$ | 49000000 | $\text{m}^2$ | Area |
| $ML$ | 2500 | m | Mouth length |
| $\varphi$ | 40.5 | °N | Latitude |
| Light limitation | | | |
| $PAR$ | 0.48 | % | Photosynthetically active radiation |
| $I_0$ | 340 | $\text{W m}^{-2}$ | Incoming solar radiation |
| $\theta$ | 0.04 | No dim | Albedo |
| $\alpha_{(\text{PHX})}$ | 0.1 | $\text{mmolN h}^{-1}\ \text{W}^{-1}\ \text{m}^{-2}$ | Slope of the light saturation curve |
| Temperature limitation | | | |
| $T_{opt(PHU)}$ | 16 | °C | Optimal growth temperature for diatoms |
| $T_{opt(PHD)}$ | 17 | °C | Optimal growth temperature for flagellates |
| $dT_{(PHU)}$ | 12 | °C | Optimal temperature interval for diatoms |
| $dT_{(PHD)}$ | 15 | °C | Optimal temperature interval for flagellates |
| Colimitation of nutrients | | | |
| $Ks_{(\text{DIN,PH1})}$ | 0.8 | $\text{mmol N m}^{-3}$ | DIN half saturation constant for diatoms |
| $Ks_{(\text{DIP,PH1})}$ | 0.085 | $\text{mmol P m}^{-3}$ | DIP half saturation constant for diatoms |
| $Ks_{(\text{P,PH1})}$ | 0.085 | $\text{mmol P m}^{-3}$ | P half saturation constant for diatoms |
| $Ks_{(\text{DOP,PH1})}$ | 0.085 | $\text{mmol P m}^{-3}$ | DOP half saturation constant for diatoms |
| $Ks_{(\text{Si,PH1})}$ | 1 | $\text{mmol Si m}^{-3}$ | Si half saturation constant for diatoms |
| $Ks_{(\text{DIN,PH2})}$ | 0.65 | $\text{mmol N m}^{-3}$ | DIN half saturation constant for flagellates |
| $Ks_{(\text{DIP,PH2})}$ | 0.04 | $\text{mmol P m}^{-3}$ | DIP half saturation constant for flagellates |
| $Ks_{(\text{P,PH2})}$ | 0.04 | $\text{mmol P m}^{-3}$ | P half saturation constant for flagellates |
| $Ks_{(\text{DOP,PH2})}$ | 0.04 | $\text{mmol P m}^{-3}$ | DOP half saturation constant for flagellates |
| $a_{(\text{DON})}$ | 0.1 | No dim | Fraction of bioavailable DON |
| $a_{(\text{DOP})}$ | 0.5 | No dim | Fraction of bioavailable DOP |
| Sedimentation | | | |
| $\phi_{(\text{DTN})}$ | 10 | $\text{m s}^{-1}$ | Sinking velocity of DTN |
| $\phi_{(\text{DTP})}$ | 10 | $\text{m s}^{-1}$ | Sinking velocity of DTP |
| Mixed layer depth | | | |
| $L$ | 11000 | m | Length scale of the bay |
| $g$ | 9.81 | $\text{m s}^{-2}$ | Acceleration of gravity |
| $C_D$ | $1.3 \times 10^{-3}$ | No dim | Drag coefficient |

Table 4.2: Parameters. Continues in next page.

| Symbol | Value | Units | Description |
|---|---|---|---|
| $\rho_a$ | 1.2 | kg m$^{-3}$ | Air density |
| Inputs of freshwater | | | |
| $C_{(dis,\mathrm{DIN})}$ | 35 | mmol N m$^{-3}$ | Concentration of DIN in discharge channels |
| $C_{(dis,\mathrm{DIP})}$ | 0.5 | mmol P m$^{-3}$ | Concentration of DIP in discharge channels |
| $C_{(dis,\mathrm{DOP})}$ | 5 | mmol P m$^{-3}$ | Concentration of DOP in discharge channels during the months of rice cultivation (April to July) |
| $C_{(dis,\mathrm{DOP})}$ | 3 | mmol P m$^{-3}$ | Concentration of DOP in discharge channels during fallow months (August to March) |
| $C_{(dis,\mathrm{DON})}$ | 25 | mmol N m$^{-3}$ | Concentration of DON in discharge channels |
| $C_{(und,\mathrm{DIN})}$ | 300 | mmol N m$^{-3}$ | Concentration of DIN in underground water |
| $C_{(und,\mathrm{DIP})}$ | 0.5 | mmol P m$^{-3}$ | Concentration of DIP in underground water |
| $C_{(und,\mathrm{DOP})}$ | 0 | mmol P m$^{-3}$ | Concentration of DOP in underground water |
| $C_{(und,\mathrm{DON})}$ | 0 | mmol N m$^{-3}$ | Concentration of DON in underground water |
| $F_{und}$ | 60480 | m$^3$ day$^{-1}$ | Underground water flow |
| Resuspension of sediments | | | |
| $Pflow$ | 30 | mmol m$^{-2}$ h$^{-1}$ | Mean DIP flow for the first 30 min after the sediment resuspension. |
| $Peq$ | 0.2 | mmol m$^{-3}$ | Equilibrium concentration of DIP after 30 min from the sediment resuspension |
| Advection | | | |
| $dilution$ | 72 | % day$^{-1}$ | Dilution rate |
| Remineralization | | | |
| $D_{\mathrm{DTN}to\mathrm{DON}}$ | 0.1 | day$^-1$ | Detritic nitrogen remineralization rate to DON |
| $D_{\mathrm{DTP}to\mathrm{DOP}}$ | 0.2 | day$^-1$ | Detritic phosphorus remineralization rate to DOP |
| $D_{\mathrm{DON}to\mathrm{DIN}}$ | 0.1 | day$^-1$ | DON remineralization rate to DIN |
| $D_{\mathrm{DOP}to\mathrm{DIP}}$ | 0.1 | day$^-1$ | DOP remineralization rate to DIP |

Table 4.2: Parameters.

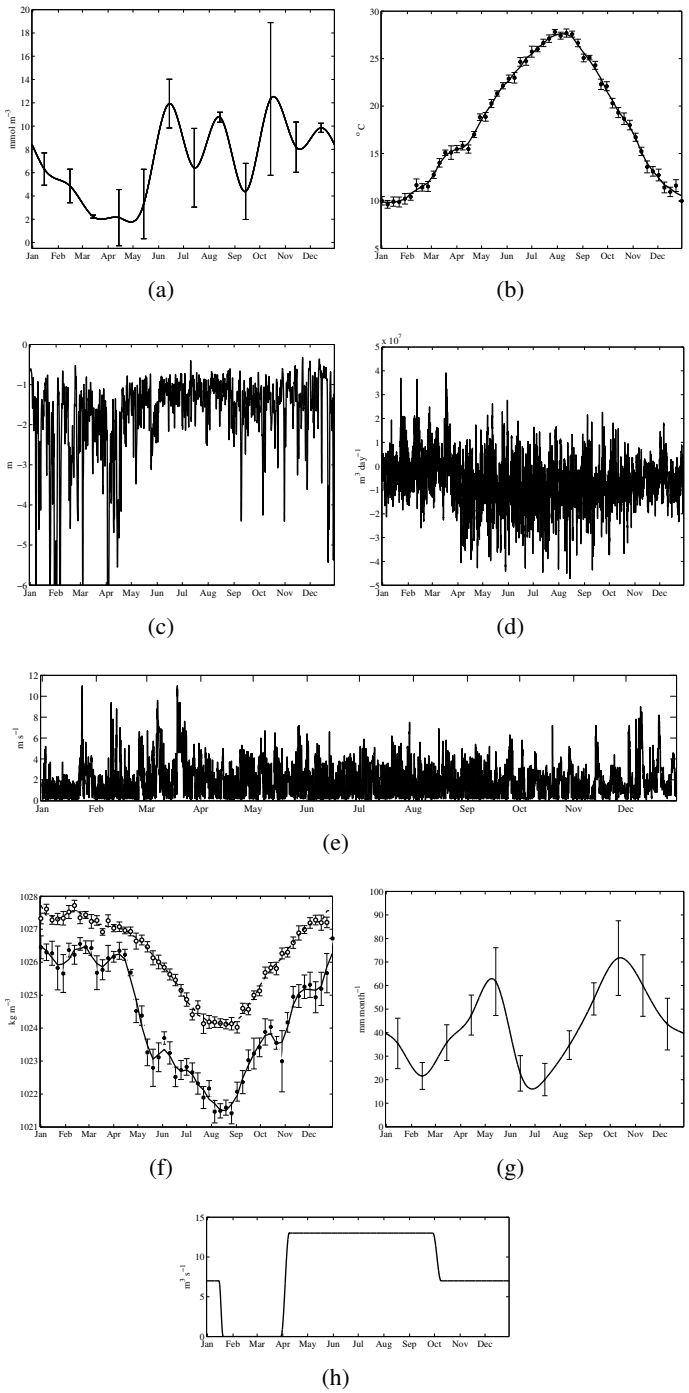


Figure 4.3: Imposed variables and forcing parameters. (a) Silicon (Redrawn from Loureiro et al. (2009a)). (b) Climatological temperature at 0.5 m over the period 1990-2003 (∘ weekly average. — three point average of the weekly averages). (c) Mixed layer depth. See text for details about the calculation. (d) Advective flow to (+) and from (-) the bay. (e) Wind speed. (f) Climatological density at 0.5 m (black) and 5.5 m (gray) over the period 1990-2003 (∘ weekly average. — three point average of the weekly averages). (g) Rainfall climatology. Vertical bars indicate standard deviation. (h) Flux from discharge channels.

| Symbol | Units | Description | Value |
|---|---|---|---|
| Si | mmol Si $m^{-3}$ | Silicon concentration | Loureiro et al. (2009a) |
| DOP | mmol P $m^{-3}$ | Dissolved organic phosphorus | Loureiro et al. (2009a) |
| R | mm $month^{-1}$ | Monthly accumulated rainfall | National Institute of Meteorology |
| $u$ | m $s^{-1}$ | Wind speed | Wind measured at an automatic meteorological station 2007 |
| $F_{(dis)}$ | $m^3$ $day^{-1}$ | Discharge channel flow | Literature (see Section 4.2.3) |
| $\rho$ | kg $m^{-3}$ | Water density | Calculated from T and salinity climatologies |
| $T$ | °C | Water temperature | T climatology |
| $V_0$ | m/s | Velocity of water in and out the bay | Physical model Si3D |

Table 4.3: Forcing variables. See Fig. 4.3 for details.

#### 4.2.2.1 Physical processes

The model includes an approximation of the basic physical processes in Alfacs, which include a calculation of the mixed layer depth, and advection.

**4.2.2.1.1 Mixed Layer Depth** The mixed layer depth represents the depth range through which the upper water column has been mixed in the recent past. It can be defined by a difference in temperature or density from the surface water, or by a gradient in temperature or density (Brainerd and Cregg, 1995). Because of the scarcity of data, we only have climatological temperature and salinity at two different depths of Alfacs. Therefore, we estimated the mixed layer depth based upon the Richardson Number and stratification relationship defined by Fischer et al. (1979). The Richardson Number indicates the potential mixing of an estuary and can be calculated as the ratio between the buoyancy due to differences of density and the kinetic energy due to the wind. Fischer et al. (1979) define four regimes (A, B, C, and D) that range from weak wind forcing and strong stratification (regime A) to strong wind forcing, causing a well mixed column (regime D). The range of winds and water densities in Alfacs suggests a transition between regime B and C when the wind is stronger than 5 m/s (Llebot, 2007). Regime B is characterized by internal waves and a sharp thermocline, while regime C has a mixed water column. The transition between regime B and C is defined by Fischer et al. (1979) to be at $Ri = (L/2h)^2$, where $L$ is the length scale of the bay, and $h$ is the mixed layer depth. By substituting this value into the Richardson Number expression,

$$Ri = \frac{\Delta\rho\ g\ h}{\rho_0\ u^{*2}} \tag{4.11}$$

$\Delta\rho$ being the difference in water density between bottom and surface layers, $g$ acceleration of gravity, $\rho_0$ a reference density, and $u^*$ surface shear velocity, we obtained equation 4.32 (Table 4.4), with which we calculated an approximation of

the mixed layer depth for the model runs. Results were smoothed with a 48h filter (Fig. 4.3).

#### 4.2.2.1.2 Advection terms

Fluxes across the mouth of the bay are called $\mathrm{Advection}$ in the equations of Table 4.1. Advection represents the flux in and out of the bay for the mixed layer and was calculated using a hydrodynamical three dimensional model. The model, referred to as Semi-Implicit Three-Dimensional Model for Estuarine Circulation (Si3D) (Smith, 2006), is a free-surface, hydrostatic, primitive equation model that has been used in studies of lacustrine systems (Rueda et al., 2003b,a; Rueda and Cowen, 2005b) and currently implemented for Alfacs (Llebot et al., 2009). The model is forced by tide, atmospheric forcing, and freshwater inputs; these are included in a similar fashion as in the present study.

In order to calculate the advective transport of the model variables, the Si3D velocity field was first averaged over the basin and then rotated in the direction parallel to the coast and perpendicular to the mouth of the bay. By using a principal component analysis of currents at the center of the bay, Artigas (2008) showed that the dominant current directions are parallel to the coast (East direction -15 $^{\circ}$) and perpendicular to the coast (North direction -15 $^{\circ}$ degrees). The calculation of $\mathrm{Advection}$ with equations 4.25, 4.26 and 4.27 (Table 4.4) is performed using the component of the current velocity that corresponds to the East–West direction minus 15 degrees. The results are shown in Fig. 4.3. Advection of the various concentrations is computed assuming that the sea concentrations are the ones in the bay recorded the previous day and multiplied by a dilution factor of 72%, which reflects a residence time of 5 to 12 days of the Alfacs waters on the Ebre shelf (Salat et al., 2002).

Freshwater inputs ($\mathrm{FWInput}$) enter the bay by two different means: discharge channels from rice fields and underground water seepage. We assume that the only non-negligible scalars carried by freshwater are nitrogen and phosphorus, in organic and inorganic forms. Freshwater sources from water treatment plants have not been included, because they only represent roughly 0.01% of the land inputs (Camp, 1994). See section 4.2.3 for information about the fluxes and equation 4.29 (Table 4.4) for details about their computation.

### 4.2.2.2 Biogeochemical processes

The growth of flagellates and diatoms is controlled by nutrients, light, and temperature. In addition to $\mathrm{DIN}$ and $\mathrm{DIP}$, nutrients include Dissolved Organic Phosphorus ($\mathrm{DOP}$) and silicon (Si) (for diatom growth). Si is imposed in the model based on monthly averages of observations carried out between April 2007 and March 2008 (Loureiro et al., 2009a). Both groups of phytoplankton are grazed by one generic group of zooplankton. Dead phytoplankton cells go to the detritus pool, as

Growth:

$$\mathrm{Growth}_{(\mathrm{PH1})} = \mathrm{Uptake}_{(\mathrm{PH1})}\mathrm{LightLim}_{(\mathrm{PH1})}\mathrm{TempLim}_{(\mathrm{PH1})} \tag{4.12}$$

$$\mathrm{Growth}_{(\mathrm{PH2})} = \mathrm{Uptake}_{(\mathrm{PH2})}\mathrm{LightLim}_{(\mathrm{PH2})}\mathrm{TempLim}_{(\mathrm{PH2})} \tag{4.13}$$

$$\mathrm{Growth\_eq}_{(\mathrm{PHX})} = \mathrm{Growth}_{(\mathrm{PHX})} - \mathrm{Growth}_{(\mathrm{PHX})}\frac{\mathrm{Upt}_{(\mathrm{DOP,PHX})}}{\mathrm{Upt}_{(\mathrm{DOP,PHX})} + \mathrm{Upt}_{(\mathrm{DIP,PHX})}} \tag{4.14}$$

Light limitation:

$$\mathrm{LightLim}_{(\mathrm{PHX})} = \frac{P^B_{m(\mathrm{PHX})}\alpha_{(\mathrm{PHX})}I}{\sqrt{(P^B_{m(\mathrm{PHX})})^2 + \alpha^2_{(\mathrm{PHX})}I^2}} \tag{4.15}$$

$$I = PAR\ I_0(1-\theta)\mathrm{DayLength} \tag{4.16}$$

Temperature limitation:

$$\mathrm{TempLim}_{(\mathrm{PHX})} = \exp\left[\frac{\left((T - T_{opt(\mathrm{PHX})}\right)^2}{dT^2_{(\mathrm{PHX})}}\right] \tag{4.17}$$

Nutrient limitation:

$$\mathrm{P} = \mathrm{DIP} + a_{(\mathrm{DOP})}\mathrm{DOP} \tag{4.18}$$

$$\mathrm{Uptake}_{(\mathrm{PH1})} = \frac{1}{1 + \frac{Ks_{(\mathrm{Si,PH1})}}{\mathrm{Si}} + \frac{Ks_{(\mathrm{DIN,PH1})}}{\mathrm{DIN}} + \frac{Ks_{(\mathrm{P,PH1})}}{\mathrm{P}}} = \tag{4.19}$$

$$\frac{\mathrm{Si\ DIN\ P}}{\mathrm{Si\ DIN\ P} + Ks_{(\mathrm{Si,PH1})}\ \mathrm{DIN\ P} + Ks_{(\mathrm{DIN,PH1})}\ \mathrm{Si\ P} + Ks_{(\mathrm{P,PH1})}\ \mathrm{DIN\ Si}}$$

$$\mathrm{Uptake}_{(\mathrm{PH2})} = \frac{1}{1 + \frac{Ks_{(\mathrm{DIN,PH2})}}{\mathrm{DIN}} + \frac{Ks_{(\mathrm{P,PH2})}}{\mathrm{P}}} = \tag{4.20}$$

$$\frac{\mathrm{DIN\ P}}{\mathrm{DIN\ P} + Ks_{(\mathrm{DIN,PH2})}\ \mathrm{P} + Ks_{(\mathrm{P,PH2})}\ \mathrm{DIN}}$$

$$\mathrm{Upt}_{(\mathrm{DIP,PHX})} = \frac{\mathrm{DIP}}{Ks_{(\mathrm{DIP,PHX})} + \mathrm{DIP}} \tag{4.21}$$

$$\mathrm{Upt}_{(\mathrm{DOP,PHX})} = (1 - \mathrm{Upt}_{(\mathrm{DIP,PHX})})\frac{a_{(\mathrm{DOP})}\ \mathrm{DOP}}{Ks_{(\mathrm{DOP,PHX})} + a_{(\mathrm{DOP})}\ \mathrm{DOP}} \tag{4.22}$$

Grazing:

$$\mathrm{Grazing}_{(\mathrm{PH1})} = \frac{R_m\chi_{(\mathrm{PH1})}\mathrm{PH1}^2}{Kp_{(\mathrm{PH1})}(\chi_{(\mathrm{PH2})}\mathrm{PH2} + \chi_{(\mathrm{PH1})}\mathrm{PH1}) + \chi_{(\mathrm{PH2})}\mathrm{PH2}^2 + \chi_{(\mathrm{PH1})}\mathrm{PH1}^2} \tag{4.23}$$

$$\mathrm{Grazing}_{(\mathrm{PH2})} = \frac{R_m\chi_{(\mathrm{PH2})}\mathrm{PH2}^2}{Kp_{(\mathrm{PH2})}(\chi_{(\mathrm{PH2})}\mathrm{PH2} + \chi_{(\mathrm{PH1})}\mathrm{PH1}) + \chi_{(\mathrm{PH2})}\mathrm{PH2}^2 + \chi_{(\mathrm{PH1})}\mathrm{PH1}^2} \tag{4.24}$$

Table 4.4: Equations. XXX means any variable, PHX any phytoplankton group, DIX any dissolved inorganic variable, DOX any dissolved organic variable, and DTX any detritus group.

Advection:

$$\text{Advection}_{(\text{XXX})} = \frac{V_0\ ML}{A}\ \Delta Conc_{(\text{XXX})} \tag{4.25}$$

$$\text{If } \text{V}_0 > 0 \quad \Delta Conc_{(\text{XXX})} = \text{XXX}_{(t-1\text{day})}\ dilution - \text{XXX} \tag{4.26}$$

$$\text{If } \text{V}_0 < 0 \quad \Delta Conc_{(\text{XXX})} = \text{XXX} - \text{XXX}_{(t-1\text{day})}\ dilution \tag{4.27}$$

Inputs of freshwater:

$$\text{FWInput}_{(\text{DIX})} = \frac{F_{(dis)}C_{(dis,\text{DIX})} + rF_{(und)}C_{(und,\text{DIX})}}{A\ MLD} \tag{4.28}$$

$$r = rain + evaporation \tag{4.29}$$

$$rain = \frac{R - min(R)}{max(R) - min(R)} + 1 \tag{4.30}$$

$$evaporation = \frac{min(T)}{T} \tag{4.31}$$

Mixed Layer Depth:

$$MLD = \sqrt{\frac{\rho L}{2\Delta\rho g}u^{\star 2}} \tag{4.32}$$

$$u^{\star 2} = C_D\frac{\rho_a}{\rho}u^2 \tag{4.33}$$

Sedimentation:

$$\text{Sedimentation}_{(\text{DTX})} = -\frac{\partial}{\partial z}(\phi_{(\text{DTX})})\text{DTX}) \tag{4.34}$$

Resuspension of sediment:

$$\text{when MLD(t)} = 6 \quad \text{Resuspension}_{(\text{DIX,t})} = Pflow \tag{4.35}$$

$$\text{Resuspension}_{(\text{DIX,t+30min})} = Pflow \tag{4.36}$$

$$\text{Resuspension}_{(\text{DIX,t+31min})} = 0; \text{DIP} = Peq \tag{4.37}$$

Death:

$$\text{Death}_{(\text{XXX})} = m_{(\text{XXX})} \tag{4.38}$$

Excretion:

$$\text{Excretion}_{(\text{ZOO})} = E \tag{4.39}$$

Remineralization:

$$\text{Remineralization}_{(\text{DTX}to\text{DOX})} = D_{(\text{DTX}to\text{DOX})} \tag{4.40}$$

$$\text{Remineralization}_{(\text{DOX}to\text{DIX})} = a_{(\text{DOX})}\ D_{(\text{DOX}to\text{DIX})} \tag{4.41}$$

Exudation:

$$\text{Exudation}_{(\text{XXX})} = Q_{(\text{XXX})} \tag{4.42}$$

Table 4.4: Equations, part 2.

do dead zooplankton, and the fraction of grazed phytoplankton that is not assimilated. Detritus pools have a loss by sinking and are metabolized to organic nitrogen and phosphorus, which also receive inputs from phytoplankton exudation. Organic nutrients are remineralized to inorganic nitrogen and phosphorus. Zooplankton excrete nitrogen and phosphorus to both the organic and inorganic pools.

#### 4.2.2.2.1 Growth

Phytoplankton growth in this model is controlled by light, temperature, and nutrients (equations 4.12 and 4.13, Table 4.4). The maximum growth rates were initially chosen following Merico et al. (2004), and further adapted by means of recursive simulations, keeping the values within the usual ranges for ecological models (Chapelle et al., 2000; Giraud, 2006; Kishi et al., 2007; Lacroix and Nival, 1998; Quéré et al., 2005; Lima et al., 2002; van den Berg et al., 1995). The maximum growth rate for diatoms is higher than the maximum growth rate for flagellates, as in Kishi et al. (2007), Lacroix and Nival (1998) or Merico et al. (2004).

Many mathematical expressions have been proposed to relate primary productivity to irradiance ($I$). Most of them (e.g., Jassby and Platt, 1976; Platt et al., 1980) use two common parameters: the slope of the light-saturation curve at low light levels ($\alpha$), and the maximum specific photosynthetic rate ($P_m^B$). As the curves obtained are very similar, we chose one of the simplest equations (Table 4.4, equation 4.15), from Smith (1936). The variable $I$ in equation 4.15 (Table 4.4) is the irradiance received by the cell and is calculated from equation 4.16 (Table 4.4), which uses the incoming solar radiation $I_0$, the percentage of Photosynthetically Active Radiation ($PAR$), albedo ($\theta$), and day length (Matlab program from Fennel and Neumann (2004)). As our model is only considering the mixed layer, which is very shallow (less than 6m deep), depth dependence was not taken in account. The photosynthetic parameters (Table 4.2) of equation 4.16 (Table 4.4) are taken from Fennel et al. (2002).

Phytoplankton growth is controlled by temperature following equation 4.17 (Table 4.4) (Lancelot et al., 2005). It is an exponential temperature dependence on the optimal growth temperature ($T_{opt}$) and a temperature interval ($dT$). Temperature dependence has not been set for the other biological processes because uncertainties in its parameterization added complexity, rather than insight, to the model. All the parameters of the model in Table 4.2 have been established according to the range of temperatures (10 – 28 °C, Fig. 4.3) observed in the bay.

Nutrient uptake is parameterized using a colimitation equation (Lancelot et al., 2005), which has been shown to represent accurately the observations in the case of multiple nutrient limitations (O'Neill et al., 1989). Diatoms are limited by nitrogen, phosphorus, and silicon (Table 4.4, equation 4.20), while flagellates are only limited by nitrogen and phosphorus (Table 4.4, equation 4.21).

Phytoplankton and bacteria can use some organic P substrates by the action of phosphomonoesterase enzymes. The most widely recognized of these enzymes in aquatic systems is the alkaline phosphatase (Bentzen et al., 1992). Particularly in situations of phosphorus stress, phytoplankton have a notable capacity for phosphorus uptake from organic sources (Currie and Kalff, 1984). Therefore, DOP is considered as a state variable and DOP uptake is taken into account in the model. The origin of DOP can be excretion from living microbes, plants and animals, or decomposition from dead organisms. Therefore, a large proportion of the DOP is formed by high molecular weight or colloidal material that is not readily available for uptake. The bioavailability fraction taken in the model ($a_{(DOP)}$ in Table 4.2) is similar to the values found in Huang and Hong (1999). In the colimitation equation used for the calculation of the nutrient uptake (Table 4.4, equation 4.18), phosphorus is entered as the sum of DIP and the bioavailable fraction of DOP (Table 4.4, equations 4.20 and 4.21), and a common half saturation constant for all phosphorus pools is used (Table 4.2). In order to calculate the proportion of phosphorus used from the DIP pool (named $\mathrm{Growth\_eq}_{(\mathrm{PHX})}$ in Table 4.1) and from the DOP pool, we use equation 4.14 (Table 4.1), following Spitz et al. (2001). We have utilized this formulation instead of a ratio of the DIP and DOP concentrations since we assume an energetic approach to phytoplankton growth. The amount of DIP required for growth is first calculated, and if more phosphorus is required then DOP uptake is allowed. Thus, equation 4.14 (Table 4.1) gives preference to DIP uptake over DOP uptake.

The half saturation constants for DIN uptake are taken from the range found in the literature (Fennel et al., 2002; Lacroix and Nival, 1998; Lima et al., 2002). The half saturation constant for flagellates is set lower, meaning that this group has a higher affinity for the substrate, as in Crispi et al. (2002), Lacroix and Nival (1998), and Merico et al. (2004). The half saturation constant for DIP uptake is taken from Tyrrell (1999), and modified according to the range measured by Taft et al. (1975). The half saturation constant for silicon uptake is taken from van den Berg et al. (1995) and slightly modified for better agreement with observations. The half saturation constant for DOP uptake is within the ranges measured in Bentzen et al. (1992) for bacteria and is similar to the values used in other models including DOP (Chen et al., 2002).

#### 4.2.2.2.2 Zooplankton grazing

As Franks (2002) states in his review of NPZ models, representation of zooplankton grazing has always presented a complex problem. The formulation can include a saturating response to increasing food, grazing thresholds, varying degrees of nonlinearity and acclimation of the grazing rate to changing food conditions. We used a saturating formulation with preferences of grazing as in Fasham et al. (1990) (see equation 4.24 and 4.25, Table 4.4).

#### 4.2.2.2.3 Other formulations

Mortality of both zooplankton and phytoplankton is expressed following a linear parameterization with a constant mortality rate $m$ (Table 4.4 equation 4.38). This rate was taken from the same literature as the phytoplankton growth rate, but in addition it includes a component that corresponds to filtering by mussels, which are cultured in about 90 rafts in the northern half of the bay. *Excretion*, *Exudation* and *Remineralization* are parameterized linearly with constant rates $E$ (Table 4.4, equation 4.39), $Q$ (Table 4.4, equation 4.42) and $D$ (Table 4.4, equation 4.41) respectively. The values of these rates are obtained from Crispi et al. (2002) and Pinazo et al. (1996). Detrital *Sedimentation* is expressed with a constant sinking velocity using equation 4.34 (Table 4.4). The effect of metabolic pathways such as denitrification (Mallo et al., 1993) is assumed to be included in the parameterization of the remineralization process.

### 4.2.3 Forcing variables

See Table 4.3 for a summary of the forcing variables, and Fig. 4.3 for graphs of the data. *Density* and *Temperature* are taken from a climatology based on 14 years of field data (de Pedro, 2007; Solé et al., 2009). *Silicon* is obtained from Loureiro et al. (2009a). They calculated monthly averages based on weekly samples taken between April 2007 and March 2008, from surface water (0.5 m depth) at a station located in the center of Alfacs Bay (40° 36' 0"N, 0° 39' 0" E). An annual composition of these data is shown in Fig. 4.3. *Wind speed and direction* are obtained from an automatic weather station (named Els Alfacs) managed by the Meteorological Service of Catalonia (SMC) located on the north shelf of the bay (40 ° 37' N, 0° 40' E ; see Fig. 4.1). Monthly accumulated *rainfall* climatology is calculated using daily data from the National Institute of Meteorology. The station, Roquetes (Tortosa), is located 10 km north from the bay, next to the Ebro River, and the data set covers a period from 1990 to 2004. A cubic spline interpolation was performed to fit the data set to the time step used in the model.

Forcing by freshwater inflow includes *discharge channel flux* and *underground water inputs*. Freshwater enters Alfacs Bay from a network of controlled drainage channels coming from the rice fields. Rice is cultivated on 57% of the surface of the Ebre Delta (about 7880 Ha), in lands flooded to a depth of 15-20 cm (Farnós et al., 2007). The growing season lasts approximately 190 days, from the beginning of April to the end of September. Rice is planted as a seed a week after flooding, which is followed by a vegetative period (95 days), a reproductive period (20 days) and a ripening period (40 days) (Forès and Comín, 1992). During these periods the freshwater flux to the bays is maximum ($1.84\times10^{-3}$ m$^3$ s$^{-1}$ Ha$^{-1}$). Since 2001, a lower flux from the channels ($1\times10^{-3}$ m$^3$ s$^{-1}$ Ha$^{-1}$) is maintained after the crop for agroenvironmental reasons. This situation lasts about 120 days, from October to mid January. Finally, from mid January to the end of March, the channels are closed, and the discharge channel flux is 0. When the water starts flowing again,

| Reference | $NH_3^-$ | $NH_2^-$ | $NH_4^+$ | $PO_4^{3-}$ |
|---|---|---|---|---|
| Muñoz (1998) | 20–80 | 2–14 | 10–100 | |
| Camp and Delgado (1987) | 15–45 | 1.6–2.8 | | 0.8–1.5 |
| de Pedro (2007) 1986–1987 | 29.8±7 | 3.34±1 | 19.3±5 | 1.0±0 |
| de Pedro (2007) 1996–1997 | 85.3±16 | 6.35±2 | 76.1±29 | 0.6±0 |

Table 4.5: Measured concentrations of inorganic nutrients in the channels (mmol $m^{-3}$).

all the fields are flooded with 15 cm of water in 10 days. The temporal evolution of the channel freshwater discharge during the year is shown in Fig. 4.3.

Nutrient concentrations in the waters entering the bay are one of the most important forcing factors that need to be specified in the model. Given the high variability of the nitrogen concentration in the channels (see Table 4.5) and the lack of data to assess its potential temporal dependence, a constant value of 35 mmol N $m^{-3}$ is adopted for DIN. The concentration of DON has been set to 25 mmol N $m^{-3}$ because, although we do not have measurements, there is evidence that the value is of the same order as DIN (Forès, 1992). The case for phosphorus is similar (Table 4.5), but even less data are available. A constant value of 0.5 mmol P $m^{-3}$ is chosen as the DIP concentration in the freshwater input. There are no direct measurements of DOP concentration in the channels. However, there is evidence that the rice field release higher DOP concentrations during the first stages of the crop (Muñoz, 1998). Therefore, a high value of DOP concentration in the channels (5 mmol P $m^{-3}$ ) is chosen from April to August, and a lower concentration (3 mmol P $m^{-3}$ ) from September to March. These values are within the range found in other rivers and estuaries (Hernández et al., 2000; Monbet et al., 2009). The DOP concentrations predicted with these inflows will be compared with measured DOP values within Alfacs.

The *underground inputs of freshwater* were suggested to be 0.7 $m^3$ $s^{-1}$ by Camp (1994). However, recent modeling studies have shown that this value is probably underestimated (Llebot, 2007). Because of the lack of data we approximate the underground input of freshwater as follows. The baseline flow is fixed to 0.7 $m^3$ $s^{-1}$, as suggested by Camp (1994). The flow is modulated by two additive factors ranging from 0 to 1, which represent the variations due to evaporation and rainfall (Boyle, 1994; Smith et al., 2008). It is assumed that the flow increases in the wet season and decreases with high temperature. In favorable conditions the flow almost doubles the baseline (as, for example, in Stalker et al. (2009)), while in dry and hot conditions it is close to zero.

There are very few observations of the concentration of nutrients in the underground water emptying into Alfacs Bay. Public records of underground water nitrate concentration at various locations in the area of the Ebre Delta (Agència Catalana de l'Aigua, available online), range from 20 mmol $m^{-3}$ to 3000 mmol $m^{-3}$. We chose a value of 300 mmol $m^{-3}$, which is close to the mean. As we do not know the phosphate concentration in these waters, we assume that it is the

| Symbol | Value | Units | Description |
|---|---|---|---|
| PH1 | 0.3 | mmol N $m^{-3}$ | First group of phytoplankton: diatoms |
| PH2 | 0.05 | mmol N $m^{-3}$ | Second group of phytoplankton: flagellates |
| ZOO | 0.2 | mmol N $m^{-3}$ | Zooplankton |
| DIN | 5.9 | mmol N $m^{-3}$ | Dissolved inorganic nitrogen |
| DIP | 0.18 | mmol P $m^{-3}$ | Dissolved inorganic phosphorus |
| DTN | 0.5 | mmol N $m^{-3}$ | Nitrogen fraction of the detritus |
| DTP | 0.15 | mmol P $m^{-3}$ | Phosphorus fraction of the detritus |
| DON | 0.1 | mmol N $m^{-3}$ | Dissolved organic nitrogen |
| DOP | 0.1 | mmol P $m^{-3}$ | Dissolved organic phosphorus pool |

Table 4.6: Initial conditions

same as in the freshwater channels (0.5 mmol P $m^{-3}$ ). Similar phosphate concentrations were found by Torrecilla et al. (2005) in underground waters in other parts of the Ebre river. We assumed that no organic nutrients in Alfacs originate from underground sources.

Theoretically, the adsorption/desorption reactions that take place in the sediment can have an important influence on the total concentration of dissolved inorganic phosphorus in the water column (Andrieux-Loyer and Aminot, 2001; Froelich, 1988; Lebo, 1991). Vidal (1994) studied the phosphate dynamics tied to sediment disturbances in Alfacs. She found a buffering effect that leads to a final concentration of about 0.2 to 0.3 mmol P $m^{-3}$ of soluble reactive phosphorus (SRP) when the sediments are resuspended. However, if the sediments were not resuspended but just gently stirred, the SRP diffusion from the sediment was undetectable. In the model, we assumed that sediment resuspension occurs when the mixed layer depth reaches the bottom. In this case, there is a flow of phosphorus (DIP) from the sediment to the water column during the first 30 min. After this 30 min period, an equilibrium concentration is reached due to the buffering system described in Vidal (1994). The amount of phosphorus released during resuspension and the equilibrium concentration were fixed using the data in Vidal (1994) (see Table 4.2). Because no strong correlation between the release of certain organic compounds and oxygen uptake with temperature has been observed in Alfacs (Vidal et al., 1997), we have not taken into account the dependence of sediment $PO_4$ diffusion on temperature or oxygen.

The initial conditions for the model variables are taken from the January observations for dissolved inorganic nitrogen, dissolved inorganic phosphorus, dissolved organic nitrogen, dissolved organic phosphorus and diatoms. A first approximation is used for flagellates, detritus, and zooplankton. See Table 4.6 for the adopted values.

### 4.2.4 Design of the simulations

In order to explore the hypotheses, i.e., phosphorus and nitrogen limitation, importance of sediment resuspension and DOP, we designed several modeling experi-

| Simulation Name | Sediment Resuspension | DOP Input from channels | DOP Uptake by phytoplankton |
|---|---|---|---|
| *Standard Simulation* | X | X | X |
| *No Resuspension Simulation* | | X | X |
| *No DOP Input Simulation* | X | | X |
| *No DOP Uptake Simulation* | X | X | |
| *No Extra P Simulation* | | | |

Table 4.7: Processes included in the five designed simulations

ments (Table 4.7). The first simulation incorporates DOP uptake for phytoplankton growth and resuspension of sediments (called *Standard Simulation* from now on). The second simulation includes DOP use but no sediment resuspension (*No Resuspension Simulation*). The third simulation comprises sediment resuspension but no DOP input from the channels (*No DOP Input Simulation*), although the option of DOP uptake by phytoplankton is still possible, since a DOP pool is formed by phytoplankton exudation, zooplankton excretion, and detrital remineralization. The fourth simulation includes sediment resuspension and DOP inputs, but not DOP uptake (*No DOP Uptake Simulation*). A fifth simulation with no DOP inputs from channels and no resuspension (*No Extra P Simulation*) has also been performed.

### 4.2.5 Observations

Weekly climatologies for temperature, salinity, and chlorophyll *a* were calculated from the data collected by the Aquaculture Center of IRTA (Institute for Food and Agricultural Research and Technology) from 1990 to 2003 and published by de Pedro (2007) and Solé et al. (2009). Additionally, nitrate concentrations (Fig. 4.4) were determined from 1991 to 1994 and phosphate concentrations from 1993 to 1994 (de Pedro, 2007). The water samples were collected weekly near the surface (0.5 m) at the center of the bay (Fig. 4.1). Phytoplankton from the same sampling site (M. Delgado, unpublished data) were counted by means of the Utermöhl technique, using 50 ml sedimentation chambers and a Nikon inverted microscope. Diatoms and dinoflagellates, as well as nano and microphytoplankton from other algal groups were identified down to the lowest possible taxonomical level and enumerated. A weekly climatology was calculated for diatoms, but not for flagellates, because the small size and poor conservation of many of these organisms make them unsuitable for the inverted microscope technique. This data set did not include measurements of organic nutrients. The data shown in Fig. 4.5 has been redrawn from Loureiro et al. (2009a).

The diatom data, given in cell numbers per unit volume, were transformed to N units for comparison purposes. We used a conversion factor of $16.2 \pm 1.8$ pg N cell$^{-1}$, calculated by Segura (2007) for diatoms from the Catalan coast, using X ray microanalysis techniques (this factor represents averages of measurements for a number of cells and can vary depending on the species and on environmental char-

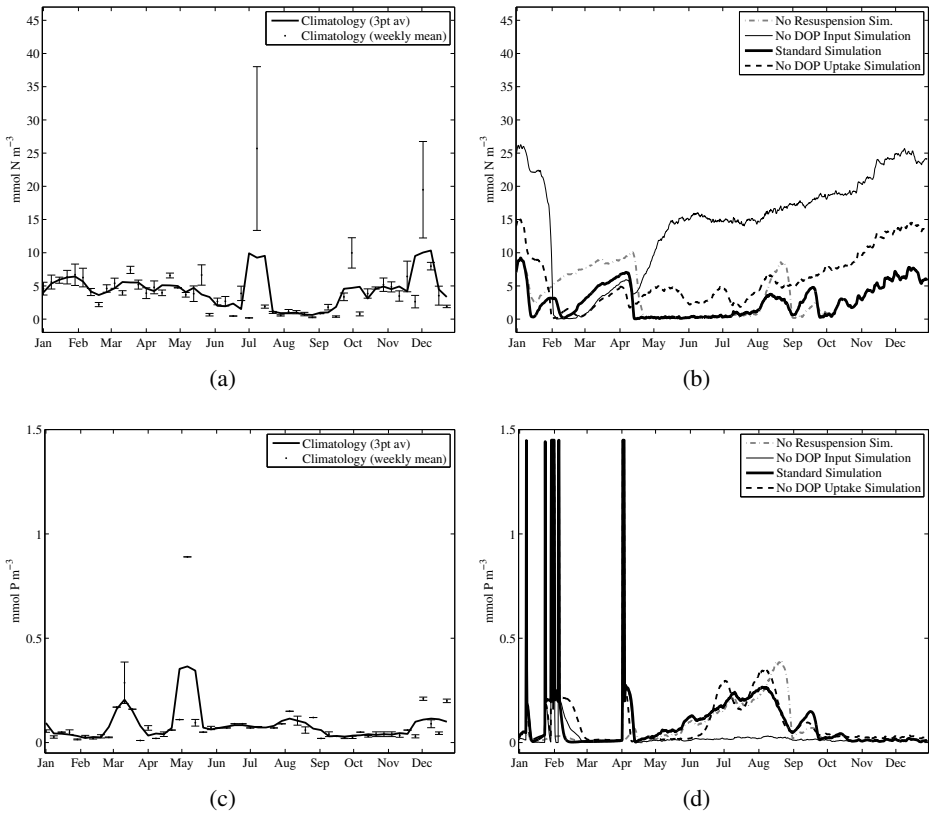


Figure 4.4: Observed and modeled inorganic nutrients for four different simulations: *Standard simulation* (including DOP inputs and resuspension), *No Resuspension Simulation* (including DOP inputs but not resuspension), *No DOP Input Simulation* (including resuspension but not DOP inputs), and *No DOP Uptake Simulation* (including DOP inputs and resuspension, but not DOP uptake). (a) Observed DIN concentration. (b) Modeled DIN concentration. (c) Observed DIP concentration. (d) Modeled DIP concentration.

acteristics). The modeled chlorophyll *a* of Fig. 4.6(e) was obtained by adding the N concentration of the two phytoplankton groups, using the Redfield ratio to calculate phytoplankton carbon and applying a carbon:chlorophyll ratio of 40 mg/mg, within the range reported by Arin et al. (2002).

Fig. 4.3-4.6 show the weekly means and the standard error of the mean of these physical, chemical, and biological data. A smoothing of the data was performed using the average of three consecutive averages.

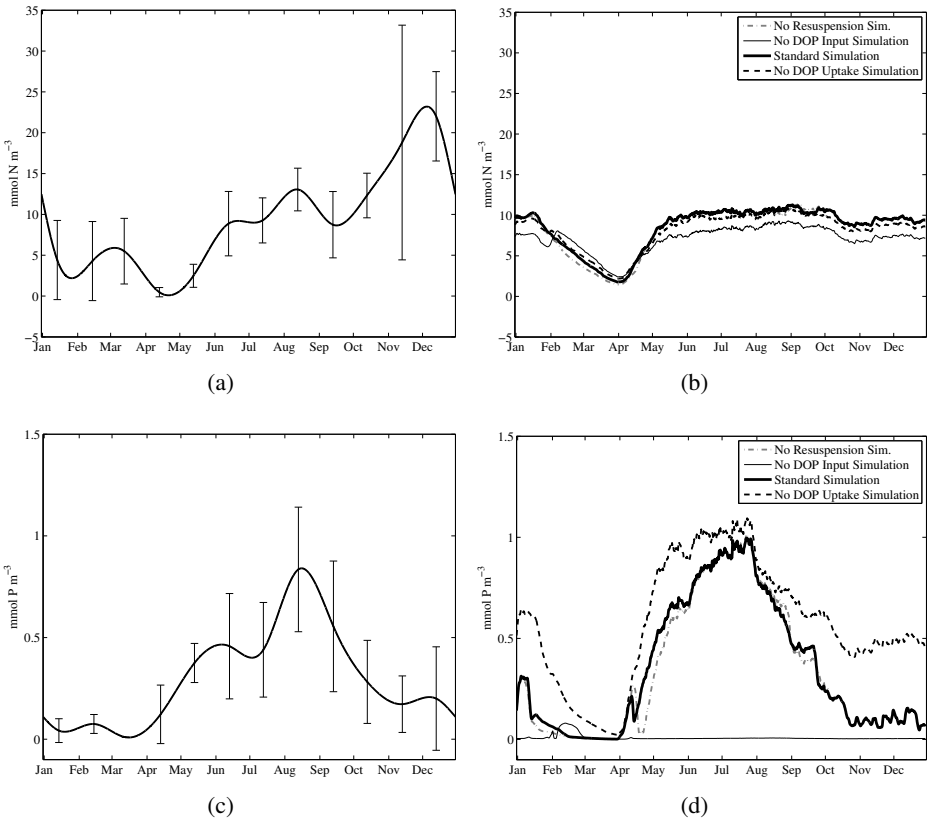


Figure 4.5: Observed and modeled organic nutrients for four different simulations: *Standard simulation* (including DOP inputs and resuspension), *No Resuspension Simulation* (including DOP inputs but not resuspension), *No DOP Input Simulation* (including resuspension but not DOP inputs), and *No DOP Uptake Simulation* (including DOP inputs and resuspension, but not DOP uptake). (a) Observed DON (Redrawn from Loureiro et al. (2009a)). (b) Modeled DON. (c) Observed DOP (Redrawn from Loureiro et al. (2009a)). (d) Modeled DOP.

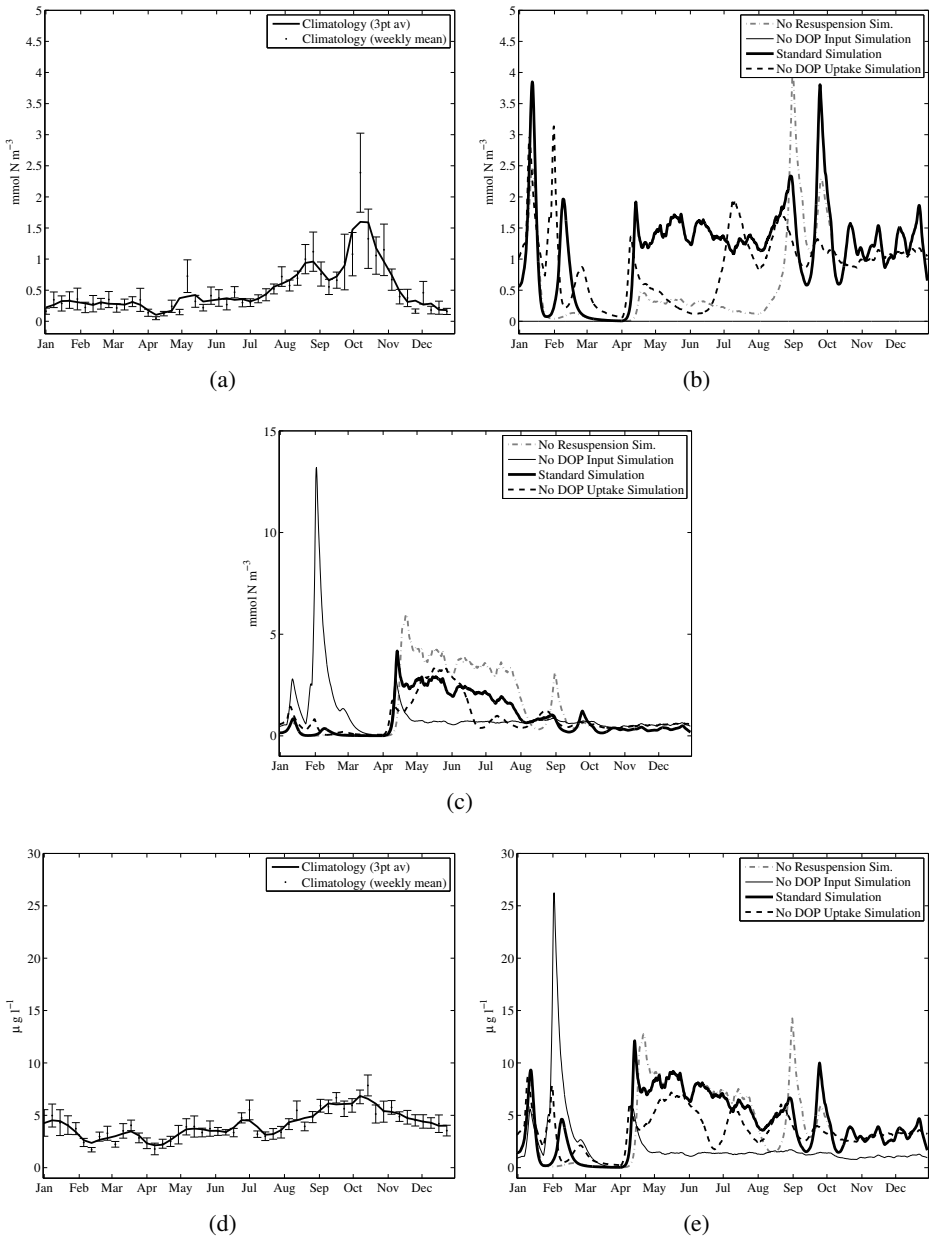


Figure 4.6: Observed and modeled phytoplankton biomass and chlorophyll *a* for four different simulations: *Standard simulation* (including DOP inputs and resuspension), *No Resuspension Simulation* (including DOP inputs but not resuspension), *No DOP Input Simulation* (including resuspension but not DOP inputs), and *No DOP Uptake Simulation* (including DOP inputs and resuspension, but not DOP uptake). (a) Observed diatom concentration. (b) Modeled PH1 (diatom) concentration. (c) Modeled PH2 (flagellate) concentration. (d) Observed chlorophyll *a* concentration. (e) Modeled chlorophyll *a* concentration.

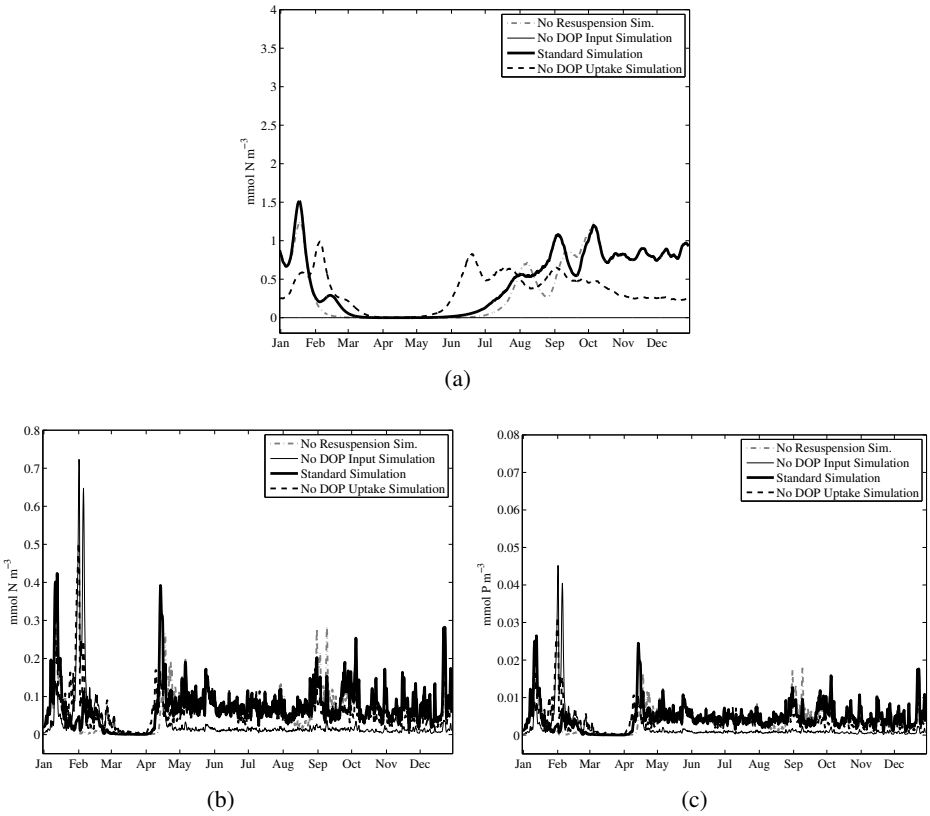


Figure 4.7: Modeled zooplankton and detritus for four different simulations: *Standard simulation* (including DOP inputs and resuspension), *No Resuspension Simulation* (including DOP inputs but not resuspension), *No DOP Input Simulation* (including resuspension but not DOP inputs), and *No DOP Uptake Simulation* (including DOP inputs and resuspension, but not DOP uptake). (a) Zooplankton (ZOO). (b) Detrital nitrogen (DTN). (c) Detrital phosphorus (DTP).

## 4.3 Results

The observations and model results are shown in Fig. 4.4, Fig. 4.5 and Fig. 4.6. The *No Extra P Simulation* (no DOP inputs from channels and no resuspension) gave generally similar results to the *No DOP Input Simulation* and has been omitted from the figures, although some of its results will be commented below. There were no observational data for zooplankton or detritus, but the model outcomes are presented in Fig. 4.7.

### 4.3.1 Dissolved inorganic nutrients

Measured DIN concentrations (Fig. 4.4(a)) are variable, as can be seen from the large standard errors of the mean for some months. DIN concentrations tend to decrease during the summer months, but there are occasional peaks of more than 40 mmol N $m^{-3}$ . The temporal evolution of the DIN concentrations for the five simulations (Fig. 4.4(b)) can be clustered into two groups. The *No DOP Input Simulation* and the *No Extra P Simulation* are characterized by values of DIN that exceed 15 mmol N $m^{-3}$ during almost two thirds of the year. These two simulations differ only from February to April, when the *No DOP Input Simulation* gives DIN values lower than 5 mmol N $m^{-3}$ while the minimum concentrations for the *No Extra P Simulation* (not shown) are always higher than 15 mmol N $m^{-3}$ . The other three simulations, which include DOP input from the channels, show higher DIN in winter, fall and the beginning of spring, and lower DIN during the end of spring and summer. Among these, the simulations with DOP uptake (*No Resuspension Simulation* and *Standard Simulation*) present a more severe DIN depletion in the summer and lower DIN concentrations in the fall than the simulations with no DOP uptake. The range and temporal evolution of DIN concentration in these simulations with uptake of DOP agrees fairly well with the observations, although the *No Resuspension Simulation* shows a higher early spring maximum than the observations.

The modeled DIP values (Fig. 4.4(c)) are similar to the observations (Fig. 4.4(d)) in all the simulations except in those that do not include DOP inputs from the channels. The observations and the simulations with DOP inputs (*Standard Simulation*, *No Resuspension Simulation*, and *No DOP Uptake Simulation*) show a DIP maximum in the summer, when DIN is depleted, and low values in fall and winter. In contrast, the simulations without DOP input (*No DOP Input Simulation* and the *No Extra P Simulation*) show DIP concentrations lower than 0.05 mmol P $m^{-3}$ during most of the year. The simulations that include resuspension (the *Standard Simulation*, the *No DOP Input Simulation*, and the *No DOP Uptake Simulation*) present some short events with DIP values reaching almost 1.5 mmol P $m^{-3}$ at the beginning of February and April. Such peaks are not present in the observations, but given their short duration and the weekly sampling interval, they could easily have been missed.

### 4.3.2 Dissolved organic nutrients

The five simulations show the same pattern regarding DON concentrations (Fig. 4.5(b)), with a minimum around 3 mmol N $m^{-3}$ in March. The observations (Fig. 4.5(c)) are of the same range. They also show a minimum in March, but rise from April to December, when there is a maximum of 20 mmol N $m^{-3}$ characterized by high variability.

As for DIN, the modeled DOP results (Fig. 4.5(d)) fall in two groups, but only the results of the simulations including DOP input from the channels resemble the observations (Fig. 4.5(c)). The simulations that do not include DOP input (*No DOP Input Simulation* and *No Extra P Simulation*) lead to concentrations close to zero during most of the year, except for a small peak in February. The rest of the simulations (*No Resuspension Simulation*, *Standard Simulation* and *No DOP Uptake Simulation*) show low values during the closed channel season, from January to March, and increase from March to reach a maximum of approximately 1 mmol P $m^{-3}$ in July, followed by low DOP concentrations during the last three months of the year. The evolution of DOP in the *No DOP Uptake Simulation* is similar to that of the two simulations that include DOP inputs from channels, but with higher concentrations, particularly during the last months of the year.

### 4.3.3 Biological variables

According to the climatological data (Fig. 4.6(a)), diatom population density rises from January to October, when it reaches a peak of about 1.5 mmol N $m^{-3}$ , although with high variability, and decreases from October to December. The three simulations (Fig. 4.6(b)) that include DOP input show a similar magnitude, variability, and some aspects of the general trend. In the *No DOP Uptake Simulation* and the *Standard Simulation* diatom biomass presents a minimum during the winter months and increases in spring months to values around 1.5 mmol N $m^{-3}$ that last until December. The population density is more variable during autumn, in agreement with the observations (largest error standard deviation) and shows a peak of 4 mmol N $m^{-3}$ . The *No Resuspension Simulation* shows the same trend as the *Standard Simulation*. The diatom abundance remains low (less than 0.5 mmol N $m^{-3}$ ) until July, and shows an earlier maximum than the other simulations and the measurements. In contrast, diatoms were not able to grow (biomass equal zero mmol N $m^{-3}$ ) in the simulations without DOP inputs from the channels, in clear discrepancy with the observations. There were no significant differences between the *No DOP Input Simulation* and the *No Extra P Simulation*.

The modeled flagellate population densities (Fig. 4.6(c)) present a sharp increase when the channels open in April, with maxima of 6 mmol N $m^{-3}$ (*No Resuspension Simulation*), 4 mmol N $m^{-3}$ (*Standard Simulation*), and 3 mmol N $m^{-3}$ (*No DOP Uptake simulation*). Flagellate abundances remain high during spring and early summer and decrease in late summer and fall while the diatom concentrations are still high. In the *No DOP Input Simulation* flagellates exhibit a high peak in February of almost 15 mmol N $m^{-3}$ and seem to outcompete the diatoms that are unable to grow. However, such a high winter maximum has not been observed (de Pedro, 2007). This simulation also shows a small peak after closing of the channels in April.

The chlorophyll climatology (Fig. 4.6(d)) displays a minimum of 3 $\mu$g $l^{-1}$ around February and March, and a maximum of 6 $\mu$g $l^{-1}$ in October. The simu-

lated chlorophyll (Fig. 4.6(e)) for the *Standard Simulation*, the *No Resuspension Simulation*, and the *No DOP Uptake Simulation* spans a larger range than the observed values, insofar as the minimum is too low because none of the modeled phytoplankton groups grows when the channels are closed. The range for the *No DOP Uptake Simulation* is similar, but the spring variability is higher than in the other simulations that include DOP input. The chlorophyll values of the simulations that do not include DOP inputs, i.e., *No DOP Input Simulation* and *No Extra P Simulation*, include a peak in February corresponding to the flagellate maximum and are low during the rest of the year, a pattern that differs from that of the other simulations and from the observations.

The zooplankton results (Fig. 4.7(a)) suggest, again, that the simulations not including DOP inputs (*No DOP Input Simulation* and *No Extra P Simulation*) are less realistic, as the zooplankton concentration goes to zero mmol N $m^{-3}$ . The other simulations (*Standard Simulation*, *No Resuspension Simulation*, and *No DOP Uptake Simulation*) are the most realistic and present a similar trend with a minimum in spring and higher values the rest of the year. No data are available to validate these modeled results.

### 4.3.4 Detritus pools

The detritus pools of both nitrogen and phosphorus (Fig. 4.7(b) and 4.7(c)) follow the same pattern. The concentrations are relatively constant throughout the year, although all the simulations display a minimum at the end of March. From March to December, there is almost no detritus remaining in the mixed layer for the simulations that do not include DOP inputs. The detrital concentrations of the *No DOP Input Simulation* are roughly 10 times smaller than those of the other simulations for both phosphorus and nitrogen. The DTN and DTP concentrations for the *No Extra P Simulation* (data not shown) are similar to those of the *No DOP Input Simulation*, with slightly lower values during the first 50 days of the year.

### 4.3.5 Most limiting nutrient

Determining the most limiting nutrient for phytoplankton growth is not a straightforward process. As explained by Flynn (ssue), the diagnostic factors for nutrient stress are cellular functions (such as the C:N:P ratio); therefore, nutrient concentrations in the environment and not their ratio are important. In the case of our model, which used a colimitation formulation (equations 4.20 - 4.21), the most limiting nutrient is the one for which the ratio of the half saturation constant to the nutrient concentration is largest, and therefore contributes the most to reduce the uptake coefficient. In the context of this work, we will consider only N and P, although Si exerts also some degree of limitation on PH1 (diatoms).

The DIN, the available phosphorus ($\mathrm{P} = \mathrm{DIP} + a_{(DOP)}\mathrm{DOP}$ for the *Standard Simulation* and $\mathrm{P} = \mathrm{DIP}$ for the *No DOP Uptake Simulation*) and the uptake coefficient for diatoms (PH1) and flagellates (PH2) are displayed in Fig. 4.8. The results of the *No Resuspension Simulation* are qualitatively similar to the *Standard Simulation* and are not shown. The ratios $Ks_{\mathrm{DIN,PHX}}/\mathrm{DIN}$ and $Ks_{\mathrm{P,PHX}}/\mathrm{P}$ were calculated to determine the periods when DIN (solid lines at top of Fig. 4.8) or P (dashed lines at top of Fig. 4.8) is the most limiting nutrient.

In the *Standard simulation* (Fig. 4.8(a)), phosphorus appears as the most limiting nutrient during fall to early spring while nitrogen is the most limiting in late spring and summer. The fall phosphorus limitation is due to low DIP and DOP, and high nitrogen concentrations from the channel discharge. In winter, the channels are closed (no DOP) but groundwater discharge is high in DIN and low in DIP; nitrogen and phosphorus limitation alternate with high frequency. The high variability of sediment resuspension during that period leads to input of high DIP concentration in the water column, which reduces phosphorus limitation. The high DOP discharge in summer seems to alleviate phosphorus limitation. In the *No DOP Uptake Simulation* (Fig. 4.8(b)), phosphorus limitation appears to be dominant for most of the year.

## 4.4 Sensitivity analysis to freshwater inputs

A sensitivity analysis was performed to evaluate the robustness of the model results. We believe that the largest uncertainty in this study resides in the freshwater inputs, i.e., channel and underground fluxes as well as their inorganic and organic concentrations. We, therefore, used a "one-at-a-time" methodology, which consists of varying one variable while holding the others fixed (Fasham, 1995; Hamby, 1994). The *Standard Simulation* was repeated by doubling and reducing by half the fluxes as well as the concentrations. That corresponds to the range that was found in the literature related to Alfacs Bay.

When perturbing the channel (Fig. 4.9) and underground (data not shown) nutrient concentrations, the temporal evolution of the modeled concentrations remains similar to the ones in the *Standard Simulation*, although their magnitudes change. More specifically, when the channel DOP is doubled, the DIP and DOP in the bay are doubled, the diatom concentration increases in the spring and their bloom lasts longer. When the channel DIN is doubled, DOP concentration remains low until early summer, DIN increases mainly in winter and fall but the summer depletion is still present. In that case, the flagellate bloom in spring lasts longer, and diatoms exhibit the highest variability in the summer instead of the fall. Raising the DIN in the underground channels has the same effect, although it is less accentuated. Reducing the channel DOP by half seems to have similar effect as doubling DIN in the channel. Doubling the underground DIP mainly affects the DIN concentration in the bay, which decreases, most notably in winter and fall.

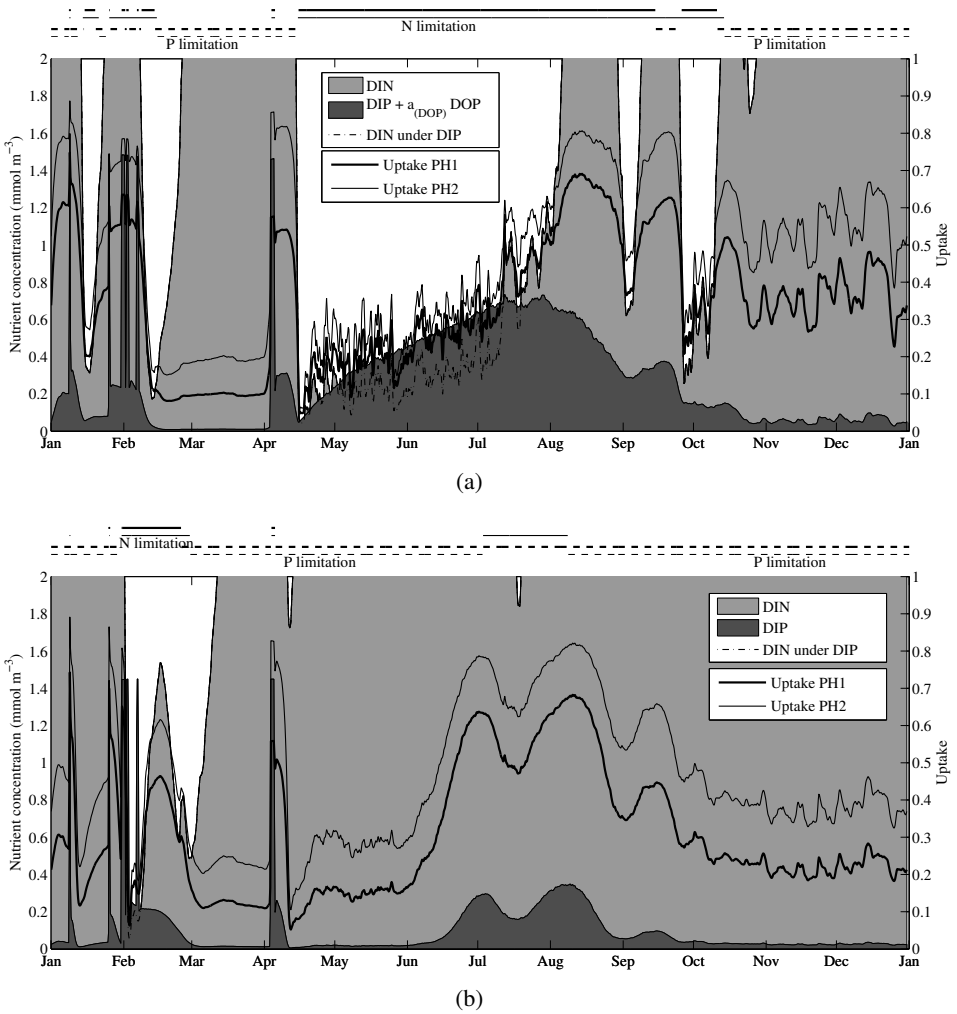


Figure 4.8: (a) Concentrations of DIN and DIP + $a_{(\mathrm{DOP})}DOP$ in the *Standard Simulation*. (b) Concentrations of DIN and DIP in the *No DOP uptake Simulation*. Only the range 0 - 2 mmol $m^{-3}$ is shown for nutrient concentration. The thick and thin lines in the graph indicate, respectively, the uptake by PH1 (diatoms) and PH2 (flagellates). The lines above the respective plots indicate the periods of nitrogen (thick solid line for diatom and thin solid line for flagellates) and phosphorus (thick dashed line for diatom and thin dashed line for flagellates) as most limiting nutrient. The most limiting nutrient was obtained by comparing the ratio of the half saturation constant to ambient concentration for each nutrient.

This addition also impacts the phytoplankton community composition, with an increase of diatoms and a decrease of flagellates in spring.

Perturbations of the channel and underground fluxes (data not shown), also conserve the trends of the *Standard Simulation*, while the nutrient concentrations change slightly in magnitude and peaks of short duration appear more frequently. The decrease of underground flow by half causes high variability in most of the variables in the bay, like the diatoms and flagellates (especially in summer and fall), the DIP concentration (which shows important peaks in summer), and the DIN concentration (which presents variability during the second part of the year). It also increases the concentration of organic nutrients. Doubling the underground flow has similar effects to doubling the DIN in the channels or in the underground flow. Doubling the channel flow has minor effect, except for a decrease of DIN and a switch between the diatom and flagellate dominance in spring similar to the one observed when increasing the phosphorus in the underground water.

The patterns of nitrogen or phosphorus limitation (not shown) are generally similar in all sensitivity experiments. Most cases show nitrogen as the most limiting nutrient in late spring and summer and phosphorus in the fall to early spring, although the length of the periods of limitation by nitrogen or phosphorus varies. The extreme cases are the simulations performed with half DOP or double DIN in the channels, in which the most limiting nutrient is phosphorus during most of the year, and the simulations with double DOP or half DIN, in which nitrogen limitation dominates most of the time. The time when phosphorus becomes the most limiting nutrient in the fall varies considerably among the experiments. In addition, the alternation between predominance of nitrogen or phosphorus limitation in January-February displays great variability.

## 4.5 Discussion

The ecological model presented here was designed with the aim of understanding the role played by different nutrient sources in the control of phytoplankton production in Alfacs Bay. As previously explained, our hypotheses were that there is an alternation in time between the limitation of nitrogen and phosphorus, and that, in addition to inorganic nutrient inputs from freshwater discharge and exchange with the sea, there are two additional processes that allow this alternation: P release by sediment resuspension and a DOP source from the channels that can be made available for phytoplankton growth either by remineralization and/or by direct uptake.

The results of the five considered simulations can be grouped into two categories: the first includes the simulations without DOP inputs from the channels (*No DOP Input Simulation* and *No Extra P Simulation*) and the second includes those with DOP input (*Standard Simulation*, *No DOP Uptake Simulation*, and *No*

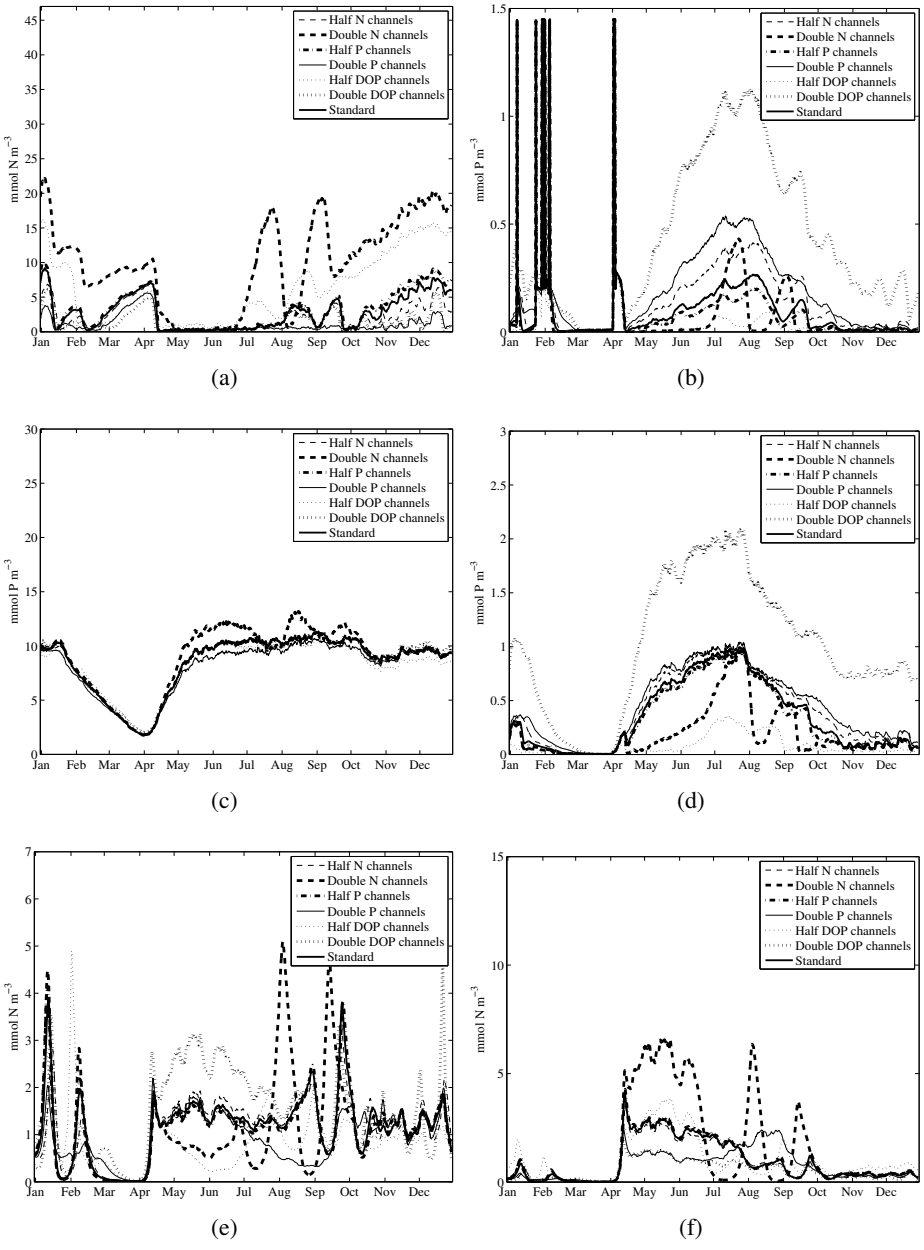


Figure 4.9: Modeled results after doubling and reducing by half the nutrient concentration in the channels. (a) Dissolved Inorganic Nitrogen (DIN). (b) Dissolved Inorganic Phosphorus (DIP). (c) Dissolved Organic Nitrogen (DON). (d) Dissolved Organic Phosphorus (DOP). (e) Diatoms (PH1). (f) Flagellates (PH2).

*Resuspension Simulation*). In the first category, the DIN, DIP and DOP concentrations during the summer reach values that are in marked disagreement with the observations. Similarly, diatom abundance and chlorophyll *a* deviate largely from the climatological observations. The second set of simulations leads to results that are in closer agreement with the temporal evolution of the nutrients, chlorophyll *a*, and phytoplankton abundance. There are no data in Alfacs to compare with zooplankton, but the modeled ZOO ranges for the simulations that include DOP are similar to measured values in Mediterranean coastal areas (Calbet et al., 2001).

Based upon the model simulations, we suggest that in order to allow the observed phytoplankton development, there must be an extra source of phosphorus in addition to DIP. As shown in the results of the *No Extra P Simulation*, without this additional phosphorus, the organisms are not capable of drawing down the DIN. As a consequence, DIN remains too high, especially during the fall and winter period, and the diatoms, zooplankton and chlorophyll stay too low. Thus, our model shows evidence that DOP inputs from freshwater sources are a key process in the ecosystem dynamics of Alfacs Bay.

The idea that resuspension of sediments plays an important role in the ecosystem response (Vidal et al., 1992) appears to need some reconsideration. The resuspension mechanism introduces phosphorus into the water column, but the amount of phosphorus in the mixed layer from this resuspension is low compared with the other DIP sources. It is, therefore, not possible to explain the magnitude of observed variables by only taking into account the resuspension mechanism, and it is not possible to find substantial differences between a simulation that includes resuspension and a simulation that does not. We recognize that there are periods during which the concentrations of the mixed layer are influenced by the resuspension of sediment. These are the periods of closed channels, with lower DIN inflow. A small addition of phosphorus could then induce a switch in the nutrient limitation. During these months, the wind is stronger than in summer and the lack of freshwater discharge from the channels weakens the stratification, making it more favorable for sediment resuspension. The results of the model show that the closed channel period is the only period where the *No Extra P Simulation* and the *No DOP Input Simulation* differ, with higher PH1 and PH2 concentrations in the *No DOP Input Simulation*. Thus, we cannot discard the possibility that resuspension has a role during the closed channel months. In addition, there might be episodic events when particularly strong resuspension of sediments can bring larger amounts of phosphorus to the water column.

Sediment resuspension in Alfacs Bay (Guillén, 1992) can be caused by currents coming from the south and entering the bay through the mouth, and by wind stirring. The model considered only the latter mechanism, which is the most common (Guillén, 1992). Sediment resuspension could be more important during periods of high currents and therefore a full three-dimensional model with sediment resuspension would be necessary to accurately simulate the phosphorus input from the sediment. While the influence of sediment resuspension on DIP concentrations of

the mixed layer was negligible, it is also possible that resuspension could affect the phosphorus and nitrogen pools of the deeper water layers. Finally, the load of phosphorus from sediments could be affected by episodes of anoxia, because the phosphorus is liberated in soluble form in anoxic environments (Golterman, 2001). Anoxia, however, rarely occurs in Alfacs Bay (Camp et al., 1991; de Pedro, 2007).

The concentrations of DOP in the bay range from 0 to 1.2 mmol $m^{-3}$ (Loureiro et al., 2009a), but the origin of this material is not well known. Loureiro et al. (2009a) associated DOP input in Alfacs Bay with freshwater discharge. Forès (1989) and Forès (1992), studied nutrient fluxes in the rice fields of the Ebre Delta, and observed a release of DOP during several phases of rice growth, from April to mid July. According to the model, DOP input from channels is, indeed, the most important source of DOP to Alfacs, ahead of exudation and detritus remineralization.

This study points towards the importance of DOP for the ecosystem of Alfacs Bay. The similarity of the results of the simulations with or without DOP uptake by both groups of phytoplankton (*Standard Simulation* and *No DOP Uptake Simulation*, respectively), indicates that DOP remineralization to DIP, a process that can occur at relatively fast rates in aquatic systems (Lomas et al., 2010), plays a substantial role. However, the fact that the agreement with the observations is better in the *Standard Simulation* than in the *No DOP Uptake Simulation* supports the occurrence of direct DOP uptake by phytoplankton. A number of studies have reported the use of DOP by phytoplankton species of various groups, albeit at different degrees. In particular, it has been shown that some HAB-forming dinoflagellates like *Alexandrium tamarense* or *Prorocentrum minimum* (which are present in Alfacs) grow well on DOP. This ability could help them to outcompete other species and cause noxious outbreaks, particularly in situations of DIP depletion (Heil et al., 2005; jin Oh et al., 2002).

Our model simulations suggest that phosphorus tends to be more limiting at the beginning and end of the year (Fig. 4.8), when its inputs are low. The highest phosphorus loads, due to DOP, tend to occur between May and October. The relationships between half saturation to nutrient concentration ratios argue for predominance of nitrogen limitation during this period. A similar seasonal pattern was observed by Fisher et al. (1992) in Chesapeake Bay, who related it to changes in the composition of freshwater inputs. A comparison of Figs. 4.3(h) and 4.8 suggests that the main driver of the changes in nitrogen and phosphorus availability are the freshwater fluxes from the channels and their associated DOP inputs.

As found in other estuaries, the switch in limiting nutrients over the year is likely to affect phytoplankton biomass, composition and seasonal cycle (D'Elia et al., 1986; Fisher et al., 1992; McComb and Others, 1981). N and P availability in general could also influence the biochemical composition of phytoplankton and could be important in relationship with food quality for grazers (Estrada et al., 2008). From a management point of view, the alternation of phosphate and nitrogen

limitation suggests the need to control the inputs of both nutrients in order to avoid potential eutrophication problems.

The results of our modeling study also highlight some key aspects that need to be addressed to improve our understanding of the nutrient budgets and the ecosystem processes in Alfacs Bay. For example, the model did not take into account the possible contribution of dissolved organic nitrogen (DON) to phytoplankton growth (Berman and Bronk, 2003). This ability could, however, favor some taxa, as suggested by Loureiro et al. (2009a) to explain *Pseudo-nitzschia* spp. dynamics. We also need to gain insight into allochthonous sources of DOP and into its metabolism in the planktonic community. Other sources of phosphorus coming from freshwater should also be considered, such as the presence of particulate organic phosphorus (POP) and particulate inorganic phosphorus (PIP). These have not been measured in detail in Alfacs, but some values given by (Muñoz, 1998) suggest that the amount of particulate phosphorus coming from freshwater ranges from 1.5 to 3.0 mmol P $m^{-3}$. The addition of this amount of particulate phosphorus (as detritus) into Alfacs Bay does not substantially change our conclusions due to the fact that the detrital matter sinks quite rapidly to the bottom. The concentration of PP would have to be more than one hundred times higher than the observations in order to see some effect in the model results (not shown). Finally, heterotrophic bacteria could play a role in the phosphorus cycle (Bentzen et al., 1992). In our model the remineralization rate was taken as constant over time, but further studies are needed to better define this process. The zero-dimensional model presented here has been useful to test our hypotheses. However, more realistic simulations should take the presence of spatial variability into account, both in the water column (Delgado and Camp, 1987) and in the sediment (Vidal et al., 1992). Three-dimensional simulations would allow a more detailed analysis of the spatio-temporal variability of the studied ecosystem.

Given the importance of the freshwater discharges as illustrated in this study, it would be desirable to have long time series of flows and nutrient content of freshwater entering the bay, both from the drainage channels and from ground water discharges. According to Llebot (2007), who used a 3D free-surface hydrostatic model of water circulation in Alfacs Bay, the existence of substantial underground water inputs was essential to explain the water column structure observed in winter. Given the potentially high nutrient concentrations in these waters it is important to better constrain their fluxes and composition.

## 4.6 Conclusions

We have used a simple ecological model to study the nutrient budget in a Mediterranean estuarine bay. Based on the simulation of five scenarios for Alfacs Bay involving the availability of DOP and its use by phytoplankton, and the presence or absence of DIP inputs from sediment resuspension, we suggest that DOP plays

a key role in providing a phosphorus source that allows draw-down of nitrate and build-up of phytoplankton biomass. Sediment resuspension does not appear to be a significant source of phosphorus, although it could have some effect during the periods of low nitrogen load. The inclusion of DOP as a phosphorus source leads to an alternation between phosphorus (winter) and nitrogen (spring and summer) limitation. The limitation during fall switches from nitrogen to phosphorus depending on the amount of DOP delivered to the bay.

## 4.7 Acknowledgments

This work was funded by projects TURECOTOX (CTM2006-13884-CO2-00/MAR9, Ministerio of Ciencia e Innovación, Spain) and CANESP (a joint project between the National Research Council of Canada and the Ministerio de Asuntos Exteriores of Spain), and by the CSIC. CL was supported by a fellowship of the Spanish National Research Council, CSIC (Beca CSIC Predoctoral I3P-BPD2005), and during the last months for a postgraduate grant of La Fundación Caja Madrid. The modeling was performed during CL's internship in the College of Oceanic and Atmospheric Sciences at Oregon State. We thank Tim Cowles for hosting CL during her first stay in the US and for his help and support during the first stages of the model development. JS was funded by Proyecto Intramural Especial del CSIC, 'Desarrollo de algoritmos y validación de productos en el Centro Experto SMOS en Barcelona' (200430E530). We are grateful to Maximinio Delgado for kindly providing phytoplankton data, to Elisa Berdalet, Esther Garcés and Mariona Segura for valuable advice and information, and Francisco Rueda for his help during the process of implementation of the physical model Si3D to Alfacs. IRTA (Institut de Recerca i Tecnologia Agroalimentàries, Generalitat de Catalunya) sponsored the collection of time series of environmental data in Alfacs Bay. The Servei Meteorològic de Catalunya and the Instituto Nacional de Meteorología provided meteorological data. We also acknowledge the valuable comments of Annie Chapelle and an anonymous reviewer.

# Chapter 5

# Discussion

This thesis studies the interaction between environmental forcing, mesoscale circulation dynamics and the phytoplankton community in two estuarine bays of the Ebre Delta, Alfacs and Fangar, which may be considered as an example of small micro-tidal estuaries. The work has been organized along three main research lines. The first one (Chapter 2) examines the variability of the phytoplankton community and its relationship with physico-chemical variables by means of the analysis of time series of data. The second one (Chapter 3) explores the key forcing factors that determine the circulation and the exchanges of water with the Mediterranean in the larger bay (Alfacs). Finally, the third line (Chapter 4) focuses on the role of organic and inorganic nutrients on phytoplankton dynamics and succession.

The analysis of 14-year long series of phytoplankton counts and physico-chemical variables (Chapter 2) revealed a clear seasonality of the phytoplankton composition in both bays, but with a different pattern in each of them, a finding that could be attributed to the shorter water residence times in Fangar, which is smaller than Alfacs but receives comparable freshwater inputs. In agreement with this interpretation, a principal component analysis pointed out a higher contribution of typical marine species in Alfacs (such as *Thalassionema nitzschioides*), and a stronger presence of freshwater-indicator species (*Peridinium quinquecorne* or *Eutreptiella* sp) in Fangar. Alfacs is characterized by a diatom assemblage typical of Mediterranean coastal waters in autumn and a group of dinoflagellates in winter, while the dominating groups in Fangar are a mixed group of flagellates and diatoms that bloom in late spring and summer, and a flagellate-dominated group in winter. The seasonal coupling between environmental and biological factors was explored more thoroughly by comparing the Intrinsic Mode Functions obtained with an Empirical Mode Decomposition of biological (principal components of the phytoplankton counts) and environmental properties (temperature, salinity and stratification). We found significant relationships of phytoplankton with temperature and salinity in both bays, and also with stratification in Fangar. Interpretation of these findings must take into account that, rather than to direct effects of temperature or salinity,

the association of these variables with phytoplankton is likely to be mediated by other environmental and biotic factors (like nutrient availability due to freshwater input or predator abundance) that have themselves a seasonal behavior and that are therefore also associated with the seasonal changes of temperature or salinity.

The study of the physical properties of Alfacs Bay (Chapter 3) by means of adimensional quantities and model simulations revealed that at seasonal timescales the tidal mixing is negligible compared to the buoyancy introduced by freshwater inputs. As a consequence the bay behaves as a strongly stratified two-layer system in which the surface layer flows outward and the bottom layer receives inputs from the Mediterranean and flows inwards. The seasonality of the freshwater inputs influences the strength of the stratification, which is weaker when the freshwater inflow is minimum. The magnitude of freshwater inputs from underground sources is uncertain, but it must be strong enough to maintain the two layer system during the closed channels period. At time scales of days to weeks, wind events influence water mixing and circulation in the bay, with effects depending on stratification strength and wind intensity. Three scenarios have been defined, using the Richardson ($Ri$) number as an indicator of the relative strengths of wind and buoyancy. For $Ri > L/h$ (first scenario), where $L$ is the bay length and $h$ the mixed layer depth, when the wind forcing is weak, the wind stress on the surface water generates stirring, which causes a very slow deepening of the mixed layer. When $Ri < L/2h$ , the wind stress induces a downwind movement of the surface, which is compensated by a movement of the bottom layer in the opposite direction. This mechanism creates a shear that rapidly deepens the mixed layer (often in a few hours). Two different scenarios can be defined for shear-dominated mixing, regarding the direction of the wind. Scenario 2 occurs when wind from the NW, which is in general strong and lasts for 2-3 days, generates $Ri < L/2h$. The NW direction induces the surface layer to move faster towards the mouth of the bay, increasing the exchange with the exterior. The third scenario is associated with low Richardson numbers ($Ri < L/2h$) caused by wind blowing from the SW, which can be strong but short (around 12 hours), as it usually has a daily oscillatory behavior. The SW direction induces the surface water to stop and move inwards contrary to its usual direction, reversing the estuarine circulation. In both cases after a few hours, when the wind has vertically mixed the bay, the exchange decreases due to the destruction of the estuarine circulation. During the mixing episodes, the formation of a transverse (N-S) gradient makes the relaxation process to be very fast, and the bay returns to a gravity-dominated state between 7 and 14 hours after the wind ceases. The mixing dynamics and water circulation of Alfacs have a tight relationship with important ecological processes, such as nutrient availability and bloom development. This chapter identifies mechanisms by which environmental forcing could affect the hydrodynamics and the ecological environment in the bay.

Finally, the third line of research (Chapter 4) uses a zero dimensional model to explore the relevance of the nitrogen (N) and phosphorus (P) pools on the dynamics of two phytoplankton groups with typical characteristics of diatoms and flagellates.

A basic hypothesis is that the productivity of Alfacs cannot be explained solely by the inputs of dissolved inorganic phosphorus (DIP) from the channels and the Mediterranean. The results of the model indicate that release due to sediment resuspension is not a significant source of phosphorus from a seasonal point of view, although it could play an important role at shorter time scales, specially during the closed channel season. On the other hand, the contributions of dissolved organic phosphorus (DOP) from the discharge channels could explain the observed phytoplankton abundance, and the summer draw-down of dissolved inorganic nitrogen. The mechanisms by which DOP enters the cycle could be the remineralization from DOP to dissolved inorganic phosphorus (DIP) and the direct uptake of DOP from phytoplankton. Including both gives a better agreement of the model results with the observations. In order to evaluate the relative importance of N and P in terms of availability for phytoplankton growth, potential co-limitation by both nutrients has been assumed. When DOP was included, phosphorus was more limiting during winter and spring, while nitrogen tended to be more limiting during summer. This chapter shows how the availability of N and P depends on physical variables, such as input of freshwater, and how, in turn, it can affect the abundance of the two groups of phytoplankton.

The results of this thesis indicate that the main physical forcing mechanisms influencing the composition, timing and abundance of the phytoplankton community in the micro-tidal estuarine bays of the Ebre Delta depend on the time scale considered.

On a seasonal time scale, freshwater inputs play a key role for the physical and biological characteristics of the bays. These inputs come mainly from drainage irrigation channels, but also from underground seepage; however, as underground flows are poorly known, the following paragraphs will focus on the channel inputs. The discharge of the channels has three important consequences. First, the freshwater that empties into the bay creates a strong stratification, which is responsible for the estuarine circulation patterns described in Chapter 3. The estuarine circulation, combined with the size of the bays, defines characteristic residence times that have a strong influence on the composition of the phytoplankton communities, as seen in Chapter 2. Second, the freshwater coming from the rice fields and discharged through the drainage channels is a crucial source of nutrients for the bay ecosystems. In particular, Chapter 4 shows that the DIN and DOP inputs from the channels are necessary for the generation of the primary production measured in Alfacs. Third, freshwater flow from the channels is high from April to October, low from November to January, and null from January to March. This marked seasonality, caused by human management of the rice fields rather than by meteorology, causes a marked annual variation of the stratification and circulation patterns (Chapter 3) and of the nutrient inputs into the bays (Chapter 4). These factors affect both the abundance and the group composition of phytoplankton, as shown in Chapter 2 and Chapter 4.

Although the channel discharge plays a key role from a seasonal point of view,

the wind is crucial for the circulation and the chemical properties of the bays at time scales of a few days. As stated in Chapter 3 for Alfacs, strong winds can cause vertical mixing of the bay. In turn, this mixing affects the amount of water exchanged with the exterior and it is possible that they affect the concentration of phosphorus too, which may be liberated from the sediment in case of resuspension events. As explained in this work, both phenomena influence the phytoplankton community. For example, wind event causing high concentration of nutrients and low levels of exchange with the sea may favor HAB development. On the other hand, certain strong wind regimes could increase the exchange with the Mediterranean and act as a trigger for the disappearance of a bloom.

Although the results presented in this thesis are based on a case study of the ecology of Alfacs and Fangar, they aim also to provide original methodology and concepts for a better understanding of micro-tidal estuaries in general.

Chapter 2 proposes a new methodology, the Empirical Mode Decomposition, as a tool to analyze biological time series. This procedure had been used before to analyze data from fields, such as acoustics (Oonincx and Hermand, 2004) and paleoclimatology (Solé et al., 2007), or as a tool to correlate meteorological and hydrographic series (Solé et al., 2009), but to the best of my knowledge, this is the first application to phytoplankton series. Although, in the study presented here, factors such as the noise inherent in phytoplankton counts or the short length of the series have made it difficult to interpret the IMFs with non-annual frequencies, we believe that Empirical Mode Decomposition, with its ability to analyze non-stationary data, has a strong potential for successful use in ecological studies.

The scale arguments developed by Fischer et al. (1979) for closed basins have been expanded to use thresholds, based on the value of the Richardson number, to identify whether mixing in an estuary is dominated by stirring or by shear in wind-driven micro-tidal estuaries. The calculation of these thresholds, together with the results of the three-dimensional model, allows the definition of circulation scenarios in response to winds of diverse strength and direction.

The results of this thesis point to several lines of future work concerning physical-biological interactions in Alfacs and Fangar.

First, given the importance of freshwater inflows from surface and underground sources for the ecology of the bays, time series data on the flux, temperature and organic and inorganic nutrient concentration of these fresh waters would represent a significant improvement for questions such as ascertaining the seasonal patterns of nutrient inputs, understanding changes occurring on scales of day to weeks, which may be strongly influenced by variations in these variables, and improving the parametrization of physical and biological models.

Second, the relationship between phytoplankton and the exchange of water in and out of the bay needs to be explored further. Chapter 3 shows the effect of two particular kinds of wind events on the circulation of Alfacs Bay, and suggest that they influence the rate of exchange with the Mediterranean, but this effect should

be addressed more thoroughly and the flushing times should be analyzed and compared with actual data. An analysis of the water residence times in particular areas of the bay could indicate which ones are the most suitable for the development of harmful algal blooms. For this purpose, the hydrodynamic model already implemented in Chapter 3 will be a very useful tool.

Finally, the implications of different scenarios of physical forcing and water residence times for phytoplankton populations could be explored by means of the coupling of a physical model such as the hydrodynamic model implemented in Chapter 3 and an ecological model such as that of Chapter 2. A coupled physical-biological model forced and validated with appropriate field measurements could provide important insights into phytoplankton dynamics and bloom development and would help to explore potential responses to climate change.

# Chapter 6

# Conclusions

1. A principal component analysis of 14 year long phytoplankton data sets for Alfacs and Fangar (two estuarine bays of the Ebre Delta) showed marked seasonal patterns and revealed that Alfacs is characterized by a diatom assemblage typical of Mediterranean coastal waters in autumn and a group of dinoflagellates in winter. In Fangar the community is dominated by a mixed group of flagellates and diatoms that bloom in late spring and summer, and a flagellate-dominated group in winter.

2. The phytoplankton community of Alfacs was characterized by typically marine species, while freshwater indicator species were also present in Fangar. These composition differences can be attributed to the shorter water residence times in Fangar, which has a smaller volume than Alfacs but receive comparable freshwater inputs.

3. An Empirical Mode Decomposition applied to environmental variables and to the principal components of phytoplankton revealed the presence of strong seasonal modes in all the series. A correlation index between pairs of series showed significant coupling between some of the principal components and environmental variables (temperature and salinity in Alfacs and temperature, salinity and stratification in Fangar). Water temperature showed a slight increasing trend along the sampling period.

4. Scale arguments indicate that, at seasonal time scales, the buoyancy associated to freshwater inflows dominates over tidal forcing in Alfacs. The system becomes strongly stratified and develops a classical estuarine circulation with a surface layer flowing into the sea and a bottom layer moving in the opposite direction.

5. At time scales of a few days, wind events are able to mix the water column of Alfacs. A threshold based on the Richardson number (Ri) has been defined. For $Ri > L/h$, where $L$ and $h$ are the length of the bay and depth of the

mixed layer respectively, the mixing is consequence of stirring and convection processes and the mixed layer deepens very slowly. For $Ri < L/2h$ shear is the dominant mixing mechanism, and acts very rapidly (at time scales of hours).

6. A three-dimensional hydrodynamic model has been implemented for Alfacs. The model has been validated and the simulation show good agreement with the observations.

7. Using the thresholds for mixing regimes and the three-dimensional simulations, three scenarios have been defined in Alfacs. Scenario 1 is characterized by weak winds causing stirring accompanied by classical estuarine circulation. Scenario 2 involves persistent NW winds that generate shear-dominated mixing. The estuarine circulation is initially strengthened. The third scenario is characterized by diurnal SW winds that produce also shear mixing and reverse the estuarine circulation. In scenarios 2 and 3, when the bay is vertically mixed the exchange with the exterior decreases.

8. A zero-dimensional ecological model has been implemented to study the effect of Dissolved Organic Phosphorus (DOP) availability and nutrient limitation of phytoplankton growth in Alfacs Bay.

9. Simulations with and without DOP as an extra source of phosphorus for phytoplankton growth suggest that DOP is necessary to simulate the observed draw-down of nitrate and build up of phytoplankton biomass in Alfacs during summer.

10. Inclusion of DOP in the model leads to predominance of phosphorus limitation of phytoplankton growth in fall and winter, and of nitrogen limitation in late spring and summer. Simulations with and without sediment resuspension suggest that this process does not significantly affect the nutrient budget in the bay, although it may be important at some points in time.

# Appendix A

# Versión en castellano

## A.1 Introducción y objetivos

### A.1.1 Introducción

En ambientes acuáticos, los productores primarios principales son las algas fotosintéticas microscópicas, conocidas colectivamente como fitoplancton, que transforman $CO_2$ y alimentos en moléculas orgánicas usando energía solar. La producción primaria de fitoplancton en los océanos del mundo se estima en 45-50 GT C año$^{-1}$, del mismo orden que las plantas terrestres, y explica cerca del 96 % de la producción primaria marina total (Longhurst et al., 1995). El fitoplancton está formado por diversos grupos de algas eucarióticas y cianobacterias, constituye la base de las redes alimentarias tróficas acuáticas, y su abundancia y composición afecta el funcionamiento de los ecosistemas y los ciclos biogeoquímicos.

La estructura y la dinámica de las comunidades de plancton están es-

trechamente relacionadas con la variabilidad de las propiedades físicas del medio acuático. El mantenimiento de una tasa de producción primaria dada necesita no sólo energía solar, sino también una entrada de energía externa que no circula a través de los canales fotosintéticos, sino que deriva de fenómenos físicos tales como las mareas, el viento y otros forzamientos que generan movimiento en el agua. Este movimiento, que cubre una amplia gama de escalas espacio-temporales y se traduce en advección y turbulencia, tiene un papel dominante en la redistribución de alimentos, en la selección de las especies de fitoplancton dominantes y en el funcionamiento de las cadenas tróficas marinas. Recientemente la mejora de los instrumentos de toma de datos, incluyendo sensores remotos, sondas de salinidad, temperatura, fluorescencia y otras variables y velocímetros Doppler, ha permitido la determinación de las propiedades del agua con una alta resolución espacio-temporal y ha fomentado nuevas líneas de investigación sobre una gran variedad de interacciones entre la biología y la dinámica de fluidos.

A escalas relativamente grandes respecto al tamaño de los organismos, el movimiento del agua puede transportarlos a través de la columna de agua y ser un factor determinante en los modelos de distribución de temperatura, salinidad y nutrientes. A escalas más pequeñas, la turbulencia del agua puede tener efectos directos sobre los organismos tales como la alteración de tasas de crecimiento y de la forma de la célula, puede afectar al establec-

imiento de agregaciones y puede influenciar las tasas de encuentro entre gametos o entre depredador y presa (Estrada and Berdalet, 1997). Por ejemplo, varios experimentos de laboratorio (e.g., Berdalet and Estrada, 1993; Sullivan et al., 2003) han mostrado una disminución de las tasas de crecimiento de dinoflagelados en presencia de ciertos niveles de turbulencia.

Uno de los modelos conceptuales más aceptados que apunta a explicar la interacción entre el ambiente físico y la comunidad fitoplanctónica fue desarrollado por Ramón Margalef en 1978. Margalef (Margalef, 1978; Margalef et al., 1979) afirmaba que el mejor indicador de la producción primaria y de las formas de vida de fitoplancton dominantes es la energía externa disponible, de la cual la advección y la turbulencia dependen. Él ideó un diagrama (referido generalmente como Mandala de Margalef, Fig. A.1) que colocaba las formas de vida fitoplanctónicas en un espacio ecológico definido por la concentración de nutrientes y la intensidad de la turbulencia. En general la energía y los niveles de nutrientes están relacionados. Las situaciones en las que la energía es baja se asocian generalmente con estratificación y las concentraciones de nutrientes son bajas. Por otra parte, la mezcla vigorosa de la columna de agua trasladará los nutrientes a la zona fótica. El modelo del Mandala sugiere que los grupos de fitoplancton están fisiológicamente adaptados a diversos rangos de concentración de nutrientes y de turbulencia, y que hay una sucesión de diatomeas, por

un lado, adaptadas a alta turbulencia y altas concentraciones de nutrientes, a dinoflagelados, por el otro, que son móviles y pueden prosperar en bajas condiciones de nutrientes y ambientes con poca turbulencia. Las altas proliferaciones de dinoflagelados y las mareas rojas están favorecidas en el caso en que se dé la inusual circunstancia de alta concentración de nutrientes en combinación con bajos niveles de turbulencia. Esta observación tiene tanto un interés teórico como práctico, ya que algunas de estas proliferaciones acaban siendo dañinas debido a la alta acumulación de biomasa o a la toxicidad de la especie que forma la floración. En estos casos se denominan proliferaciones algales nocivas (PAN o HABs en ingles, Harmful Algal Blooms). Debido a sus potenciales efectos nocivos sobre seres humanos y ecosistemas, es de gran importancia entender los mecanismos que permiten la proliferación y el mantenimiento de los PAN (Gilbert and Pitcher, 2001). Siguiendo una línea similar a la Mandala de Margalef, un modelo conceptual detallado de las relaciones entre las características ambientales y las comunidades de PAN ha sido por propuesto por Smayda and Reynolds (2001).

### A.1.2 Objetivos, planteamiento y estructura de la tesis

Esta tesis pretende investigar las interacciones entre las dinámicas de la circulación del agua, la disponibilidad de nutrientes y la estructura de la co-

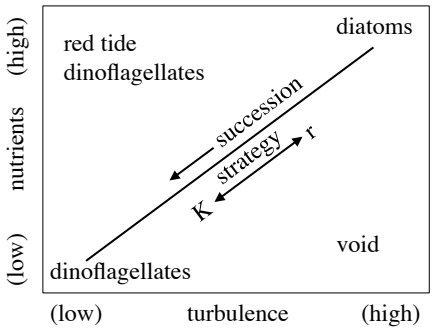


Figure A.1: La Mandala de Margalef (Margalef et al., 1979)

munidad fitoplanctónica desde el punto de vista de la mesoscala. El estudio, se concentra en escalas de tiempo estacionales y en escalas de espacio del orden de unos pocos metros a unos quilómetros para obtener una perspectiva amplia de de los procesos ambientales que afectan la dinámica del fitoplancton en uno de los ambientes estuarinos más importantes del noroeste del Mediterráneo, las bahías del sistema deltaico del río Ebro. El trabajo se centrará en tres objetivos específicos:

1. Explorar el acoplamiento entre los factores físico-químicos y la variabilidad temporal de las comunidades de fitoplancton.

2. Estudiar las relaciones entre el forzamiento físico, los procesos hidrodinámicos y las escalas de transporte de agua en la mayor de las bahías del Delta del Ebro.

3. Comprobar el papel de los flujos de los compuestos orgánicos y in-

orgánicos de los nutrientes más importantes (N y P) en la sucesión de la comunidad fitoplanctónica y el desarrollo de proliferaciones.

Las secciones restantes de este capítulo introductorio presentarán una breve explicación de las razones por las cuales se ha escogido esta región de estudio (Sección A.1.3) y de las metodologías utilizadas en el trabajo (Sección A.1.4). Los capítulos siguientes desarrollan los objetivos de la tesis, según el esquema siguiente:

**Capítulo 1** aporta información básica sobre las características ecológicas de la región de estudio.

**Capítulo 2** se dedica al acoplamiento entre los factores físico-químicos y la variabilidad temporal de las associaciones de fitoplancton (objetivo 1).

**Capítulo 3** se ocupa del estudio de las relaciones entre forzamiento físico, procesos hidrodinámicos y escalas de tiempo de transporte (objetivo 2).

**Capítulo 4** considera el tercer objetivo, comprobar el papel de los flujos de los nutrientes más importantes para la sucesión de la comunidad fitoplanctónica y el desarrollo de proliferaciones algales.

**Capítulo 5** proporciona una discusión general de las observaciones, los datos, y los resultados de los modelos desde un punto de vista de

la importancia de las interacciones físicas, químicas y biológicas para la formación de la dinámica de la comunidad fitoplanctónica en una región estuárica y micromareal.

**Capítulo 6** expone las conclusiones de la tesis.

### A.1.3 Selección de la región de estudio

La región de estudio comprende las dos bahías estuáricas del sistema deltaico del río Ebro, Els Alfacs al sur y el El Fangar al norte (en adelante Alfacs y Fangar). Las dos bahías comparten algunas características comunes que las hacen convenientes para la clase de estudio que pretendemos desarrollar. Además, cada uno de ellas muestra particularidades que prestan interés a la comparación entre ellas, tema que va a ser explorado en esta tesis, aunque el énfasis principal se pondrá en el estudio de Alfacs, la más grande de las bahías, para la cual disponemos de más datos históricos.

Hay varias razones que apoyan el interés mostrado aquí de estudiar la relación entre la comunidad del fitoplancton y el forzamiento físico en Alfacs y Fangar.

Por un lado, el estudio del acoplamiento entre el forzamiento ambiental y dinámica biológica en Alfacs y Fangar presenta un fuerte interés científico. Ambas bahías reciben entradas de agua dulce de los canales que drenan los campos de arroz del llano deltaico, irrigados con agua del río

de Ebro. Por lo tanto, la composición química del agua dulce que entra en las bahías es diferente de la del agua de río de Ebro, y los flujos de entrada están reguladas según las necesidades agrícolas y no por la climatología de la región. Las bahías están conectadas con el Mediterráneo, que determina sus condiciones micromareales. La circulación en los estuarios está determinada generalmente por una combinación de entradas de agua dulce, mareas, el efecto de la rotación de la Tierra, y el efecto del viento, conjuntamente con circunstancias tales como el tamaño, la profundidad y la geometría del estuario. Debido a estas interacciones, las características ecológicas de diversos estuarios, incluso dentro de la misma región geográfica, puede ser altamente variable y aunque los estuarios a nivel mundial han sido objeto de numerosos estudios (Ketchum, 1954; Gerreira et al., 2005), muchos de estos sistemas, incluyendo las bahías del delta del Ebro, todavía no se entienden del todo.

Por otra parte, ambas bahías son altamente productivas y proporcionan un gran número de servicios al ecosistema. Por ejemplo, proporcionan refugio y son área de desarrollo de juveniles para muchas especies acuáticas, contribuyen a la eliminación del exceso de nutrientes proporcionados por el río y generan beneficios económicos debido a la presencia de pesca, de acuicultura, y de actividades turísticas. Los campos inundados de arroz crean un ambiente perfecto para los pájaros y alojan una fauna y una flora alta-

mente diversas, convirtiéndolos en uno de los humedales más importantes del Mediterráneo (Fasola and Ruiz, 1996). Las proliferaciones algales nocivas, de diatomeas y de dinoflagelados, ocurren recurrentemente en Alfacs y Fangar. Debido a la presencia de acuicultura en ambas bahías, el desarrollo de PANs conlleva importantes pérdidas económicas. El actual trabajo se centra en toda la comunidad de fitoplancton desde una perspectiva amplia y no en aspectos específicos de los fenómenos de PAN, con la idea que la mejora del conocimiento de las interacciones entre las condiciones ambientales y las comunidades de fitoplancton es un paso básico para entender la ecología de los fenómenos de PAN en las bahías.

Finalmente, Alfacs y Fangar han sido el tema de varios proyectos de investigación científica y debido a la problemática de las PAN, se ha establecido un programa de monitorización, existente desde 1987, que incluye cuentas de fitoplancton y medidas fisicoquímicas. Dado el tamaño de las bahías, no son necesarios costosos barcos o largas campañas para recoger muestras. La situación, las dimensiones y las características de las bahías las hacen un sitio experimental perfecto del cual los modelos observados se podrían, potencialmente, extrapolar a otras áreas más extensas.

### A.1.4 Metodología

Esta sección proporcionará una breve explicación de las metodologías seguidas para desarrollar los tres objetivos de la tesis, teniendo en cuenta que una descripción extendida de estos temas se puede encontrar en los capítulos correspondientes (2 a 4).

#### A.1.4.1 Objetivo 1

El primer objetivo (Capítulo 2) pretende caracterizar los patrones de variabilidad del fitoplancton y su relación con los forzamientos físicos en Alfacs y Fangar. El artículo presentado en este capítulo evalúa si hay tendencias a largo plazo en la abundancia o composición del fitoplancton que puedan haber sido causadas por tendencias climáticas, el ciclo estacional de la comunidad y su acoplamiento con los factores de forzamiento ambientales, y las semejanzas y divergencias entre las dos bahías con respecto a estos temas. Se dedica especial atención a la respuesta ecológica de diferentes grupos de fitoplancton con el objetivo de lograr una mejor comprensión de los mecanismos que afectan los cambios en la comunidad algal, y de identificar si las posibles causas de dichos cambios son naturales o antropogénicas.

La existencia de un programa de monitorización desde finales de los años ochenta ha generado una serie de datos de catorce años con infor-

mación sobre la abundancia de especies de fitoplancton y medidas físicas básicas, tales como salinidad y temperatura, en dos profundidades distintas situadas en el centro de las bahías de Alfacs y de Fangar. La metodología aplicada en este caso incluye a) análisis estadísticos para estimar las climatologías y los patrones temporales de cada una de las variables. b) Análisis de Componentes Principales (PCA del inglés, Principal Component Analysis) para descomponer los datos de fitoplancton en un número menor de dimensiones que nos permitan obtener información (Legendre and Legendre, 1998). c) Descomposición Empírica de Modos (EMD del inglés Empirical Mode Decomposition) para cuantificar la relación entre la serie de variables fisicoquímicas y la de variables biológicas (Huang et al., 1998). Esta técnica descompone una serie en un determinado número de modos no lineales, denominados Funciones de modo intrínsecas (IMF del inglés Intrinsic Mode Functions), con frecuencias que dependen del tiempo. La EMD no requiere que las series sean estacionarias, una característica ventajosa para los casos, como el que nos ocupa, en el cual las series de tiempo no son estacionarias.

#### A.1.4.2 Objetivo 2

El segundo objetivo (Capítulo 3) pretende estudiar las relaciones entre el forzamiento físico y la hidrodinámica en Alfacs. Más específicamente, sus metas son a) explorar la importancia relativa de factores que fuerzan la bahía

tales como mareas, viento y gradientes de densidad en la dinámica espacial y temporal de la circulación estuarina. b) Estimar el papel de diversos factores de forzamiento respecto el acontecimiento y las escalas de tiempo características de los procesos de mezcla, y c) describir los forzamientos que conllevan los escenarios hidrodinámicos seleccionados.

La metodología desarrollada para alcanzar este objetivo se basa en dos técnicas distintas. Por un lado, se han usado números adimensionales y argumentos de escala para crear un modelo conceptual de los procesos de forzamiento y de mezcla en la bahía. Este procedimiento intenta simplificar el sistema tanto cuanto sea posible para obtener información significativa, y es particularmente útil para los sistemas que no se han estudiado exhaustivamente, como la bahía de Alfacs. Por otro lado, un modelo hidrodinámico tridimensional se ha implementado y validado para Alfacs. El modelo elegido es un modelo hidrodinámico tridimensional de superficie libre que ya se ha usado con éxito en estudios de lagos y estuarios (Rueda and Cowen, 2005a; Zamani et al., 2010). El modelo se utiliza para incorporar aspectos que son demasiado dependientes de la morfología de la bahía para ser resueltos con números adimensionales y para relacionar las condiciones de forzamiento con los patrones de circulación del agua en la bahía. El modelo se ha validado con datos de un Perfilador Acústico Doppler y con la temperatura y salinidad obtenidos con termistores, sal-

iómetros y perfiles de CTD (Instrumento de medición de Conductividad, Temperatura y Profundidad) registrados como parte de el proyecto TURECOTOX (CTM2006-13884-C02-01).

#### A.1.4.3 Objetivo 3

El tercer objetivo (Capítulo 4) pretende comprobar la importancia relativa de la limitación de fósforo o nitrógeno en la sucesión de la comunidad fitoplanctónica y el desarrollo de proliferaciones en la bahía de Alfacs, así como explorar la contribución de las diversas fuentes de estos nutrientes. Una hipótesis básica a comprobar es si la alta productividad del fitoplancton de Alfacs se puede explicar por medio del fósforo orgánico disuelto proveniente de los canales de riego o por la liberación de fósforo del sedimento en eventos de resuspensión. Estas cuestiones se han explorado mediante un modelo ecológico que tiene en cuenta los resultados del capítulo 3 para simular la evolución temporal de dos grupos representativos de fitoplancton en función de los forzamientos físicos, la disponibilidad de nutrientes y otros factores biológicos (tales como las tasas de crecimiento o mortalidad, o su dependencia de la luz).

El modelo tiene cero dimensiones y se ha diseñado especialmente para Alfacs. Los componentes biológicos son dos grupos de fitoplancton (diatomeas y flagelados) y un grupo de zooplancton que depreda en ellos. El

ambiente físico se representa como una capa de mezcla homogénea y rectangular, la profundidad de la cual cambia dependiendo del viento. Los nutrientes incluidos en el modelo son nitrógeno y fósforo en sus formas orgánicas e inorgánicas disueltas, y silicio para las diatomeas. Hay también dos grupos de fósforo y nitrógeno detrítico. El modelo utiliza forzamiento específico de Alfacs, y sus parámetros se han elegido de la literatura, intentando permanecer tan cerca como sea posible a la realidad de Alfacs.

## A.2 Conocimientos previos

### A.2.1 Geográficos

El delta del Ebro, el tercer delta más grande del mar Mediterráneo, comenzó a formarse después de la última glaciación, y se desarrolló durante el Holoceno debido a la gran carga de sedimento del río Ebro (Guerrero et al., 1993). La morfología del delta está en cambio constante; su forma ha cambiado notablemente durante los últimos 1000 años y de hecho está todavía el desarrollo debido a las variaciones en el balance entre el caudal del río y los aportes de sedimento (Ibàñez et al., 1997; Palanques and Guillén, 1998). El delta del Ebro está rodeado por la plataforma del Ebro, que tiene una superficie de aproximadamente 12000 $km^2$ y cuya amplitud está cerca de 60 km en la latitud correspondiente a la boca del río (Salat et al., 2002). La circulación en la zona de la plataforma está influenciada por la corriente catalana, que fluye hacia el sudoeste. Un frente de densidad separa las aguas densas de mar abierto de las aguas influenciadas por los aportes continentales, que tienen una salinidad más baja (Font et al., 1988). Localmente, la columna de agua en la plataforma del Ebro presenta una capa superficial fina (menos de 30 m de profundidad) de salinidad baja, influenciada por la descarga del río de Ebro, la profundidad de la cuál depende de la variabilidad del caudal del río y de la estratificación térmica local. La variación estacional de la

estructura y de la circulación de la masa del agua en esta región es alta: la temperatura superficial del mar varía de 12.65°C en invierno a 22.29°C en verano; la salinidad media de la superficie del mar es 36,54 en invierno y 37,86 en otoño; y la profundidad de la isoterma de 15 $^{circ}$C (que se puede considerar como representativa de la profundidad de la termoclina) se encuentra alrededor de 80–el 110 m en otoño, 40–50 m en verano y en la superfície en invierno (Salat et al., 2002).

El complejo deltaico comprende dos bahías estuáricas, Alfacs al sur y Fangar al norte. Ambas bahías están conectadas con el mar y reciben agua del río Ebro a través de los conductos de desagüe controlados por los agricultores según las necesidades de irrigación de los campos de arroz situados en el llano del delta (Fig. **??**).

La bahía de Alfacs (figura A.2.1) es la bahía más grande del delta del Ebro (40°33'–40°38'N, 0°33–0°44'E). Tiene una longitud aproximada de 11 km y una anchura de 4 km, con una profundidad media de 3.13 m y una profundidad máxima de 6.5 m. La cubeta de Alfacs está separada del mar por una barrera de arena. La boca tiene una anchura de 2.5 km, y permite que el agua sea intercambiada con el mar (Camp, 1994). Las orillas de la bahía están rodeadas por unas plataformas someras que descienden lentamente a partir 0 a 1,5 m de profundo, y conectan con la cubeta central, que tiene una profundidad de entre 4 y 6 m (A.3). Las dimensiones de la

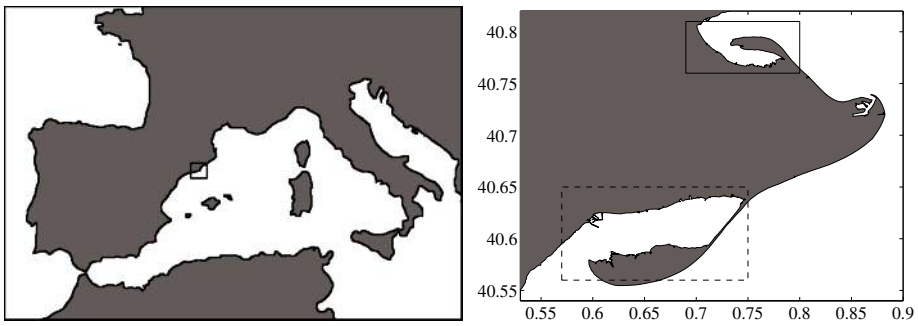


(a) (b)

Figure A.2: Mapa de la zona de estudio en coordenadas de latitud y longitud. — La Bahía de el Fangar; - - La Bahía de els Alfacs.

bahía están resumidas en la tabla A.1, obtenida de Camp (1994).

Fangar (Fig. A.2.1) es la bahía situada al norte del complejo del delta del Ebro (40°45'–40°49'N, 0°41–0°48'E). Sus dimensiones son aproximadamente 6 kilómetros de largo y 2 kilómetros de ancho, con una profundidad media de 2 m y una boca de 1 kilómetro de ancho. Contiene aproximadamente $16\times10^6$ $m^3$ de agua.

Tanto Alfacs como Fangar alojan una activa industria de acuicultura de peces y crustáceos. El cultivo principal es el del mejillón *Mytilus galloprovinvialis*, con 90 viveros en Alfacs y 76 en Fangar dedicado a su cultivo, y con una producción anual media de $3 \times 10^6$ kg (Ramón et al., 2005). Otro crustáceo cultivado son las ostras*Crassostrea gigas* y las almejas *Ruditapes decussatus* y *R. philippinarum* (Ramón et al., 2005). El cultivo del Mejillón está amenazado por la sensibilidad de estos moluscos a las altas

| | | |
|---|---|---|
| Longitud | 11000 | m |
| Anchura máxima | 5200 | m |
| Anchura mínima | 3600 | m |
| Anchura de la boca | 2500 | m |
| Longitud de la cubeta central | 10000 | m |
| Anchura de la cubeta central | 2500 | m |
| Anchura máxima de la cubeta | 3000 | m |
| Anchura de la cubeta en la boca | 1500 | m |
| Superficie bahía | $49 \times 10^6$ | $m^2$ |
| Superficie plataformas | $18 \times 10^6$ | $m^2$ |
| Superficie cubeta | $31 \times 10^6$ | $m^2$ |
| Profundidad media | 3.13 | m |
| Profundidad máxima | 6.5 | m |
| Profundidad media plataforma | 0.64 | m |
| Profundidad media cubeta | 4.17 | m |
| Volumen de agua | $153 \times 10^6$ | $m^3$ |
| Extensión cuenca receptora parte N | $79 \times 10^{\,6}$ | $m^3$ |
| Extensión cuenca receptora parte S | $10 \times 10^{\,6}$ | $m^3$ |

Table A.1: Dimensiones de la bahía de Alfacs, de Camp (1994)

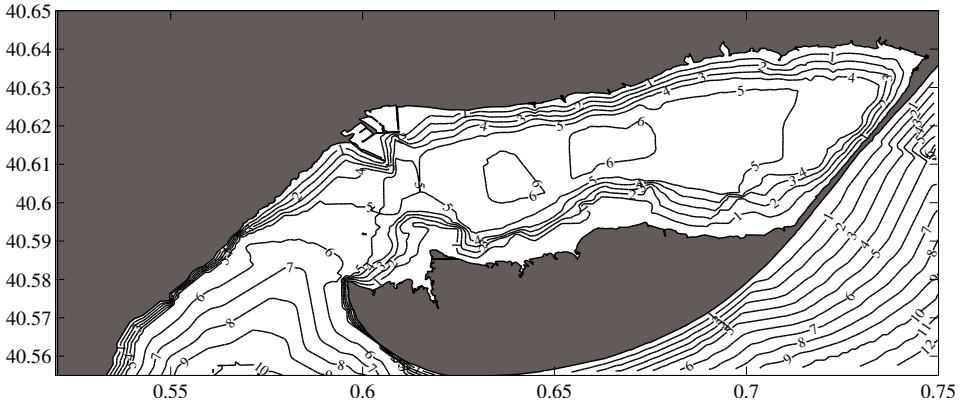


Figure A.3: Mapa de la batimetría de la bahía de Alfacs, interpolado a base de transectos batimétricos (Guillén, 1992) y cartas batimétricas. Unidades en latitud y longitud.

temperaturas del agua, y a la ocurrencia de proliferaciones algales nocivas, que impiden la comercialización del mejillón.

Tal como se declaró anteriormente, esta tesis incluye una comparación de la variabilidad de los datos ambientales y de fitoplancton en Alfacs y Fangar (Capítulo 2), aunque en general la tesis se centra en las interacciones físico-biológicas en Alfacs, que es la bahía mejor estudiada. La información sobre Fangar se limita a algunos estudios, realizados durante los años 70 y los años ochenta (López and Arté, 1973; Camp and Delgado, 1987; Delgado and Camp, 1987; Delgado, 1987), que comparan la hidrología, bioquímica y la comunidad fitoplanctónica en Alfacs y Fangar, mientras que durante las dos últimas décadas se han publicado cerca de 70 estudios sobre Alfacs. Se puede esperar, sin embargo, que algunas de las conclusiones alcanzadas en

este trabajo para Alfacs se puedan extrapolar a Fangar, teniendo en cuenta diferencias tales como su tamaño y los tiempos de residencia del agua.

Las siguientes secciones de esta introducción incluyen una revisión de las características fisicoquímicas (Sección A.2.3) y biológicas (Sección A.2.5) de las bahías del delta del Ebro, con énfasis sobre Alfacs.

### A.2.2 Fuentes de agua dulce

Las bahías del delta del Ebro contienen una mezcla de agua salada del Mediterráneo y de agua dulce de origen continental. La precipitación (que, en la estación meteorológica vecina de Tortosa, va de 300 milímetros a más de 1000 milímetros anuales), las aguas residuales urbanas de las ciudades de Sant Carlos de la Ràpita y Poblenou del Delta, y el agua dulce del río que entra en las bahías a través de sus bocas son fuentes relativamente poco importantes de agua dulce (Delgado, 1987; Camp, 1994) en comparación con las entradas de agua procedentes de los canales de irrigación. Las filtraciones subterráneas pueden ser importante también, aunque no esté claro en qué medida.

El delta está entrecruzado por aproximadamente 200 kilómetros de canales que transportan agua del río Ebro a los campos del arroz. Los canales de desagüe conducen el agua de los campos al Mediterráneo, a las lagunas, y a las bahías Alfacs y Fangar. El flujo de agua corre principalmente por

gravedad, aunque en algunas ocasiones, debido al poco desnivel del área, el uso de bombas es necesario (March and Cabrera, 1997). El caudal de los canales de desagüe depende de las necesidades agrícolas y, en Alfacs, es de aproximadamente entre 13 y 14,5 $m^3s^{-1}$ durante los meses de la cosecha del arroz, de abril a septiembre. De octubre a enero, cuando el agua ya no es necesaria para el cultivo, los campos se mantienen inundados por motivos ambientales, con un caudal de 7-8 $m^3s^{-1}$, y de mediados de enero finales de marzo los canales se cierran para hacer operaciones de mantenimiento y no hay flujo (Farnós et al., 2007; Camp, 1994; Prat and Ibàñez, 2003). Estas cifras son solamente indicativas, porque los agricultores pueden controlar el agua que entra y sale de sus campos y los caudales reales son altamente variables (Muñoz, 1990). Cuando los canales abren otra vez en abril todos los campos de arroz del lado derecho (del sur) del Ebro, alrededor de 125 $times$ $10^6$ $m^2$, se inundan totalmente en 10 días, con una altura del agua de cerca de 0,15 M. Aproximadamente un 60 % de ellos vierten sus aguas en Alfacs.

La composición del agua de los canales está altamente influenciada por el hecho de que éstos atraviesan campos de arroz. Los agricultores añaden fertilizante un mes antes de inundar los campos, plantan el arroz una semana después de la inundación, y fertilizan otra vez tres meses después de inundar, cuando el arroz ha comenzado a desarrollar tallos secundarios.

Después de la cosecha, la paja del arroz se mezcla con el suelo (Christian et al., 1996). Del total de nitrógeno (N) y de fósforo (P) introducido, el arroz retiene un 70 % del N y un 91 % del P, mientras que un 15 % del N y un 3 % del P es eliminado con el agua. El resto acaba en los macrófitos y otros organismos que viven en los campos de arroz (Forès, 1992). Los campos de arroz actúan como filtros, conservando una porción del N y del P entrantes y liberando la otra bajo la forma de N orgánico, amonio, N particulado, P reactivo disuelto, y P particulado, dependiendo de la etapa de la cosecha (Forès, 1989, 1992). Las concentraciones de nitrógeno y fósforo orgánico particulado son más altas en las aguas del canal que en el río, y es probable que una proporción importante de los nutrientes entre en Alfacs en forma particulada (Prat et al., 1988). La variabilidad de las concentraciones de nutrientes en los canales no se sabe con certeza (Muñoz, 1998; Camp and Delgado, 1987; de Pedro, 2007; Forès, 1989, 1992). Un resumen de las concentraciones medidas de nutrientes inorgánicos en los canales se presenta en la tabla A.2.

La calidad y la magnitud del caudal del agua subterránea que descarga en Alfacs es difícil de estimar. El sistema hidrológico del delta está formado por tres acuíferos. El más somero tiene una profundidad de 5-10 m, es poroso y está formado por arena, y sus agua superficiales tienen baja salinidad debido a las entradas de agua dulce desde los campos de arroz

| Referencia | $NH_3^-$ | $NH_2^-$ | $NH_4^+$ | $PO_4^{3-}$ |
|---|---|---|---|---|
| Muñoz (1998) | 20–80 | 2–14 | 10–100 | |
| Camp and Delgado (1987) | 15–45 | 1.6–2.8 | | 0.8–1.5 |
| de Pedro (2007) 1986–1987 | 29.8±7 | 3.34±1 | 19.3±5 | 1.0±0 |
| de Pedro (2007) 1996–1997 | 85.3±16 | 6.35±2 | 76.1±29 | 0.6±0 |

Table A.2: Concentraciones de nutrientes inorgánicos medidas en los canales (mmol $m^{-3}$).

inundados. La parte inferior del acuífero tiene salinidades más altas. El acuífero intermedio tiene una profundidad de entre 10 y 50 m y es muy poco permeable. El acuífero más profundo, multicapa, tiene una potencia de 70 - 500 m. La salinidad del agua de los acuíferos medios y profundos es alta (Bayó et al., 1997; Curcó, 2006). (Camp, 1994) calculó que para explicar las bajas salinidades observadas durante la época de canales cerrados, las entradas de agua subterránea tendrían que estar entre 2 y 4 $m^3 s^{-1}$.

Camp (1994) llevó a cabo balance hidrológico de Alfacs que consideraba las entradas de agua dulce, la evaporación y la precipitación. La evapotranspiración calculada en la bahía está sobre los $6 \times 10^5$ $m^3$ por año y la precipitación alrededor de $3{,}1 \times 10^5$ $m^3$ por año. Teniendo en cuenta las entradas anuales de de agua dulce de los canales, la bahía tendría un exceso de $19 \times 10^5$ $m^3$ por año, aunque los cambios estacionales de estos factores podrían dar lugar a un balance menor o hasta negativo durante algunos meses,

especialmente en otoño.

### A.2.3 Hidrografía

En general no hay muchos estudios sobre la hidrografía de las bahías. López and Arté (1973) estudió Fangar, la bahía situada en el norte, y describió los rangos estacionales de temperatura y salinidad, así como los patrones de circulación de las aguas superficiales, que estudió mediante flotadores. Camp and Delgado (1987) hizo una primera tentativa de describir la hidrografía de Alfacs y de Fangar, clasificándolos como estuarios de la cuña salina y estimando el tiempo de residencia del agua dulce en Alfacs y Fangar mediante un balance de la salinidad. Los tiempos de residencia encontrados fueron de 10-20 días para Alfacs y de 1-2 días para Fangar. Un análisis más completo del medio ambiente físico en Alfacs, incluyendo resultados de (Camp and Delgado, 1987) fue publicado por Camp (1994).

Camp (1994) describe Alfacs como un sistema que en general está estratificado en un ´´estado estacionario" caracterizado por dos capas del agua, una capa densa y salina en el fondo que recibe entradas del mar y una capa superficial de salinidad menor que sale del estuario hacia el Mediterráneo. Los eventos de viento fuerte pueden mezclar las dos capas y llevar la bahía a un ´´estado no estacionario". Al acabar la perturbación, el sistema vuelve al estado estratificado anterior en 24 - 48 horas. El tiempo de residencia del de

agua dulce estimado está entre 7 y 14 días, dependiendo de la estación del año. La disminución del caudal de agua dulce durante la estación de canales cerrados reduce el intercambio con el exterior y por lo tanto aumenta el tiempo de residencia del agua dulce, en vez de aumentar la salinidad. La velocidad y el transporte del agua se midió mediante un correntímetro instalado en la boca de Alfacs a una profundidad de 4,5 m. La dirección media del caudal en Alfacs parece estar a lo largo del eje del bahía. El flujo es tres veces más fuerte en condiciones de canales abiertos que cuando los canales están cerrados, y durante los eventos de viento fuerte que mezclan la columna de agua, el sentido de la corriente es muy variable. El volumen de agua intercambiado con el mar es generalmente diez veces mayor que las entradas de agua dulce. Una periodicidad de 3 h fue observada además de la señal de la marea.

### A.2.4 Nutrientes

Las concentraciones de nutrientes inorgánicos están relacionadas con la cantidad de agua dulce vertida, pues los canales son la fuente principal de nutrientes. En Alfacs hay un gradiente norte-sur en la concentración de nutrientes, debido a que las áreas más cercanas a los canales reciben más agua dulce y, por lo tanto, más nutrientes. Debido a que las aportaciones de nutrientes estimadas solamente explican una fracción del fitoplancton ob-

| Reference | $NH_3^-$ | $NH_2^-$ | $NH_4^+$ | $PO_4^{3-}$ |
|---|---|---|---|---|
| Delgado and Camp (1987) | 0.40±0.39 | 0.14±0.06 | | 0.47±0.24 |
| de Pedro (2007) | 4.6±7.4 | 0.26±0.24 | 1.06±0.1 | 0.18±-0.23 |

Table A.3: Concentraciones de nutrientes inorgánicos en Alfacs (mmol $m^{-3}$) y su desviación estándar.

servado, Delgado and Camp (1987) sugirieron la existencia de otras fuentes de nutrientes adicionales tales como la remineralización en los sedimentos. Los rangos de concentración de nutrientes publicados en de Pedro (2007) y Delgado and Camp (1987) se resumen en la tabla A.3.

El papel de los sedimentos en el balance de nutrientes fue estudiado por citet Vid+89, Vid+92, que concluyeron que el amonio liberado desde los sedimentos es suficiente para suministrar la mayor parte de los requisitos del fitoplancton en Alfacs. También encontraron que las cantidades liberadas dependen del tipo de sedimento del fondo. Por otro lado, la liberación de fósforo se activa cuando hay una resuspensión de sedimento en la columna de agua. Cuando se produce un evento de resuspensión, hay una liberación muy alta de fósforo reactivo soluble (SRP del inglés Soluble Reactive Phosphorus) que se sucede, después de algunos minutos, por una reabsorción del fósforo por parte del sedimento hasta que se alcanza una concentración del equilibrio. La concentración final del agua está alrededor de los 0.2 - 0.3 mmol SRP $m^{-3}$. En general el proceso implica un aumento

neto del fósforo en la columna (Vidal, 1994).

### A.2.5 Fitoplancton

Alfacs y Fangar son bahías muy productivas. Sus concentraciones medias de fitoplancton durante el período 1982-1986 fueron alrededor de 3,2 mg $m^3$ en Alfacs y 3.5 mg $m^3$ en Fangar, valores un orden de magnitud más elevados que los típicos para aguas abiertas en el Mediterráneo (Delgado, 1987). Según lo observado mediante microscopia invertida, la comunidad de nano, micro fitoplancton, dominada por nanoflagelados, diatomeas y pequeños dinoflagellados, es similar a la del Mediterráneo, a excepción de la presencia frecuente de algunas diatomeas bentónicas y especies de agua dulce. Las comunidades fitoplanctónicas de Alfacs y Fangar muestran cambios estacionales claros en respuesta a la variabilidad meteorológica e hidrológica, incluyendo el ciclo anual de entradas de agua dulce a través de los canales de desagüe (Delgado, 1987).

Aparte de Delgado (1987), los estudios sobre la comunidad fitoplanctónica en las bahías de interés se han centrado en especies potencialmente nocivas. Tanto Alfacs como Fangar están incluidos en un programa de monitoreo para determinar la calidad del agua de las zonas en las que hay cultivo de crustáceos en Cataluña, y la detección de potenciales productores de PANs es un aspecto importante de éste. Las especies tóxicas de las

cuales se ha dado noticia incluyen los dinoflagelados *Alexandrium minutum*, *A. catenella*, *Dinophysis sacculus*, *D. caudata*, *Proceratium reticulatum*, *Karlodinium veneficum*, *K. armiger* y las diatomeas *Pseudo-nitzschia* spp (Fernández-Tejedor et al., 2010).

*Alexandrium* es un género muy extendido en el Mediterráneo occidental (Vila and Masó, 2005; Garcés et al., 1999b), y su presencia en la costa catalana parece haber aumentado estos últimos años (Vila et al., 2001b). *Alexandrium minutum* es una especie asociada a episodios de intoxicación paralizante por bivalvos (PSP del inglés Paralytic Shellfish Poisoning). Fue observada por primera vez en Alfacs en 1989 (Delgado et al., 1990). Desde entonces, proliferaciones masivas de *Alexandrium* se han estado repitiendo casi cada año al principio de primavera. *Dinophysis sacculus* y *Dinophysis caudata* pueden causar intoxicación diarreica por bivalvos (DSP del inglés Dyarrhetic Shellfish Poisoning) en concentraciones muy bajas (500 - 1200 células $l^{-1}$), provocando el cierre de las explotaciones de mejillón. *Karlodinium* spp., previamente identificado como *Gyrodinium corsicum* (Garcés et al., 2006), fue detectado por primera vez en Alfacs en 1994. Las proliferaciones de *Karlodinium* spp. causan cambios en el color del agua y la muerte de fauna salvaje, mejillones y peces de las explotaciones acuícolas (Delgado and and, 1995). El efecto tóxico de estos dinoflagelados sobre diversos organismos ha sido demostrado por Delgado and Alcaraz

(1999); Fernández-Tejedor et al. (2007); Vaqué et al. (2006). Las células de *Karlodinium* spp tienden a acumularse en la parte inferior de la columna de agua, aunque no se han descrito patrones de migración diaria (Garcés et al., 1999a). Las proliferaciones de la diatomea *Pseudo-nitzschia* spp. son generadores potenciales de intoxicación amnésica por bivalvos (ASP del inglés, Amnesic Shellfish Poisoning), aunque no hay casos descritos de dicho fenómeno en Alfacs. Loureiro et al. (2009a,b) sugirió que los nutrientes orgánicos podían tener un efecto importante en el crecimiento de *Pseudo-nitzschia* spp. Una descripción de la diversas especie del género presente en Alfacs puede encontrarse en Quijano-Sheggia et al. (2008).

### A.2.6 Relación entre el forzamiento ambiental y la dinámica de la comunidad fitoplanctónica

Hay pruebas, en particular en Alfacs, de acoplamientos entre la tensión causada por el viento, la intensidad de la mezcla de la columna de agua y la aparición y desaparición de proliferaciones algales. Sin embargo, el conocimiento sobre los mecanismos en los que tales sucesos se basan es limitada. Episodios como la proliferación de *Alexandrium minutum* observada por Delgado et al. (1990) y la proliferación de *Karlodinium* spp. descrita por Garcés et al. (1999a) fueron precedidas por fuertes vientos que supuestamente habrían podido aumentar la cantidad de nutrientes accesi-

bles por el fitoplancton a través de una resuspensión de sedimentos, aunque no hay datos que puedan confirmar esta hipótesis. Las proliferaciones se desarrollaron durante un período tranquilo de vientos débiles y de estratificación fuerte. Las condiciones de baja turbulencia habrían reducido las pérdidas por advección y, junto con la alta disponibilidad de nutrientes, proporcionarían las condiciones necesarias para el desarrollo de la proliferación. Finalmente, la dispersión de la proliferación fue causada por fuertes vientos Delgado et al. (1990) o la entrada de agua dulce de los canales Garcés et al. (1999a) que aumentaron las pérdidas de fitoplancton por advección. De hecho, se ha sugerido una correlación entre las densidades de *Karlodinium* spp y un índice de estratificación Fernández-Tejedor et al. (2010).

Estas relaciones entre la velocidad y dirección del viento, la entrada de agua dulce y el desarrollo de proliferaciones sugieren que estos forzamientos físicos pueden afectar el tiempo de residencia del agua de la bahía, aunque los mecanismos no estén claros. (Camp, 1994) sugirió que la disminución de entradas de agua dulce puede causar una reducción de la circulación durante el cierre de los canales en invierno y reducir, así, el intercambio con el Mediterráneo y aumentar el tiempo de residencia. Camp and Delgado (1987) observó también que los eventos de fuerte viento que mezclan la columna de agua de Alfacs interrumpen la circulación estuarina aumentando el tiempo de residencia del agua en la bahía. Sin embargo,

la mezcla vertical también influenciaría las poblaciones del fitoplancton alterando su distribución vertical.

Otra característica meteorológica que afecta a la hidrodinámica y a la ecología de las bahías es la temperatura. En Alfacs, donde los tiempos de residencia del agua son más altos que en Fangar, la probabilidad de PANs o la presencia de anoxia aumenta en verano, cuando las temperaturas altas refuerzan la estratificación y aumentan la evaporación y reducen la cantidad de agua dulce en la bahía (Camp, 2005). Generalmente aunque varios estudios en Alfacs hayan explorado las relaciones entre el ciclo estacional, las entradas de agua dulce y los eventos de viento con las variaciones espacio-temporales de la comunidad de fitoplancton (Delgado, 1987), el acoplamiento entre el forzamiento meteorológico, la hidrodinámica de Alfacs y la dinámica de las comunidades de fitoplancton todavía no se ha estudiado cuantitativamente.

**Caja 1. Proliferaciones Algales Nocivas**

Ciertas especies de fitoplancton tienen la capacidad de desarrollar proliferaciones algales nocivas (PANs del ingés, Harmful Algal Blooms), proliferaciones de microalgas con consecuencias nocivas para la salud animal o humana, o para los intereses socioeconómicos humanos. Los

PANs parecen haber aumentado en los últimos años, aunque no está claro en qué medida el incremento del uso de recursos costeros y la mayor conciencia y la vigilancia del problema han contribuido a la percepción del aumento. Podemos distinguir dos tipos principales de PANs, según si los efectos nocivos son debidos a alta acumulación de biomasa o a toxicidad. Algunas proliferaciones, dominadas a menudo por una o varia especie, pueden alcanzar concentraciones de $10^4$ – $10^6$ células $l^{-1}$ y duran algunas semanas. Cuando se termina la proliferación, la degradación de la materia orgánica que ésta generó puede agotar el oxígeno del agua y causar anoxia, con importantes consecuencias para peces, crustáceos y en general la red trófica entera. Las proliferaciones densas pueden también reducir la luz disponible para otros organismos fotosintéticos que viven a más profundidad en la columna de agua. El segundo grupo de PANs está originado por especies de fitoplancton que producen toxinas. Algunos organismos, por ejemplo *Dinophysis* spp., pueden causar problemas de toxicidad a concentraciones muy bajas. Las toxinas generadas por las algas son transferidas a través de la cadena trófica y pueden acumularse en bivalvos, moluscos, peces y otros animales que en caso de ser ingeridos por seres humanos pueden pueden causar problemas de salud.

Las categorías principales de toxicidad que plantean un riesgo para

la salud humana son causadas básicamente por dinoflagelados e incluyen intoxicación paralizante por bivalvos (PSP del inglés Paralytic Shellfish Poisoning), intoxicación diarreica por bivalvos (DSP del inglés Dyarrhetic Shellfish Poisoning), intoxicación neurotóxica por bivalvos (NSP del inglés Neurotoxic Shellfish Poisoning) y intoxicación por Ciguatera (CFP del inglés, Ciguatera Fish Poisoning). Otro tipo de toxicidad, la intoxicación amnésica por bivalvos (ASP del inglés, Amnesic Shellfish Poisoning), es producida por diatomeas de género *Pseudo-nitzschia* (e.g. Zingone and Enevoldsen, 2000; Hallegraeff, 2003). Otros problemas de salud causados por PANs incluyen la irritación de piel, alergias y afecciones respiratorias. Algunos PANs producen toxinas que causan matanzas de pescados o son perjudiciales para otros organismos del ecosistema. Una lista de los efectos nocivos causados por PANs y ejemplos de los organismos que los causan puede encontrarse en Zingone and Enevoldsen (2000).

Hay mucha variedad entre las especie formadoras de PANs. Muchas de ellas se encuentran normalmente en el ecosistema, y son parte natural de la sucesión estacional del fitoplancton. Es importante tener en cuenta que el concepto de nocividad está relacionado con intereses humanos, no con las propiedades ecológicas de las algas. Se han descrito eventos nocivos causados por dinoflagelados, diatomeas, primnesiofíceas, y

cianobacterias, aunque los culpables mas comunes sean los flagelados. De las 60-200 especies nocivas descritas, 90 % son flagelados, y un 75% son dinoflagelados (Zingone and Enevoldsen, 2000; Smayda, 1997). Sin embargo, los organismos no flagelados, tales como diatomeas, son también importantes en aguas marinas.

Las diatomeas son organismos que no son móviles y tienden a prosperar en ambientes relativamente turbulentos, ricos en nutrientes. Sus paredes celulares están hechas de silicato, lo cual las hace dependientes del silicato además de otros nutrientes (nitrógeno, fósforo, ...) de los que el fitoplancton depende en general. Por otra parte, los dinoflagelados pueden nadar y tienden a crecer más lentamente. Su movilidad permite que los dinoflagelados controlen su posición en la columna de agua, de tal forma que pueden encontrar alimento o luz y evitar las regiones de alta turbulencia que podrían causarles daños físicos, debilitarlos fisiológicamente, o modificar su comportamiento (Smayda, 1997). La variedad ecofisiológica de las especies generadoras de PANs y la complejidad de los factores fisicoquímicos y biológicos que influencian sus proliferaciones hacen muy difícil prever el momento en el que se desarrollará una proliferación algal nociva y sus consecuencias. Sin embargo, los modelos conceptuales propuestos hasta el momento, como el Mandala de Margalef (Margalef, 1978; Margalef et al.,

1979) han proporcionado un esquema que permite predecir la especie dominante de los grupos funcionales de fitoplancton en función de la disponibilidad de energía y nutrientes. En este marco, las mareas rojas y las proliferaciones de alta biomasa de dinoflagelados se consideran un caso particular de la sucesión del fitoplancton bajo condiciones de alta estratificación acompañada de alta disponibilidad de nutrientes.

## A.3 Forzamiento hidrográfico y variabilidad fitoplanctónica en dos bahías estuáricas semi-confinadas

Alfacs y Fangar (noreste de la Península Ibérica) son dos bahías del complejo del delta del Ebro de típicas características mediterráneas. Ambas están forzadas por similares condiciones meteorológicas y reciben entradas de agua dulce parecidas de los canales de desagüe provenientes de la irrigación de campos de arroz. Sin embargo el volumen de Alfacs es cerca de diez veces más grande que el de Fangar. Estudiamos los patrones temporales de series de clorofila *a* y de fitoplancton muestreados entre 1990 y 2003 en dos profundidades distintas en una estación fija en cada bahía. Relacionamos estos patrones con la variabilidad de variables ambientales (temperatura del agua,salinidad y estratificación). Un análisis de componentes principales realizado sobre la matriz de correlaciones entre los datos (logarítmicos) de abundancia de los taxones más frecuentes reveló tres tendencias principales de la variabilidad. El primer componente principal (PC1) indicó un gradiente de aguas saladas (más importante en Alfacs) a aguas dulces (particularmente en Fangar). El PC2 reflejó el ciclo estacional del fitoplancton en Alfacs, dominado por un grupo de diatomeas típicas de aguas costeras mediterráneas en otoño y un grupo de dinoflagelados, que incluye especies tóxicas, en invierno - principio de primavera. El PC3 expresó principalmente los cambios estacionales en Fangar caracterizado por un grupo

mixto de fitoplancton, predominado por dinoflagelados, con máximos de población entre mayo y octubre, opuesto a un grupo de dinoflagelados de invierno. Una Descomposición Empírica de Modos fue aplicada a las variables ambientales y a los componentes principales para analizar la estructura temporal de los datos. Todas las variables presentaron modos estacionales fuertes; un índice basado en desplazamiento de fase entre pares de series reveló correlaciones entre algunos de los componentes principales y las variables ambientales (temperatura y salinidad en Alfacs y temperatura, salinidad y estratificación en Fangar). La temperatura del agua mostró una tendencia leve al aumento a lo largo del período de muestreo. Entre 1997 y 2003, algunos taxones de fitoplancton también presentaron una tendencia débil al aumento, particularmente en las muestras profundas de Fangar. Las diferencias entre los patrones estacionales de variabilidad del fitoplancton en Alfacs y Fangar se podrían atribuir a los tiempos de residencia más bajos del agua en Fangar, que darían lugar a un control hidrológico más fuerte de la abundancia y composición del fitoplancton.

## A.4 Estados hidrodinámicos en un estuario micromareal dominado por el viento

Un modelo conceptual del comportamiento físico de un estuario micromareal somero (Bahía de Alfacs) se ha construido usando argumentos de escala aplicados a datos de campo, y simulaciones en tres dimensiones. A escalas de tiempo estacionales la flotabilidad asociada a las entradas de agua dulce domina sobre el forzamiento mareal, creando un sistema fuertemente estratificado en dos capas, en el que la capa superficial y la capa profunda fluyen en direcciones opuestas (circulación estuarina clásica). El viento controla el comportamiento de la bahía a más corto plazo (de días a semanas). Se han definido tres escenarios o estados dependiendo de la dirección predominante del viento y de la fuerza de éste en relación a la intensidad de la estratificación (parametrización hecha a partir del número de Richardson $Ri^\star$). Para vientos débiles (escenario 1), con $Ri^\star > L/h$ (en donde $L$ y $h$ son la longitud de la bahía y la profundidad de la capa de mezcla respectivamente), la mezcla ocurre a consecuencia de mezcla turbulenta y procesos convectivos, y la capa de mezcla se hunde muy lentamente. Para vientos fuertes con $Ri^\star < L/2h$ la mezcla dominada por el viento es rápida y ocurre básicamente como consecuencia de la cizalla a la picnoclina. En esta situación de viento fuerte, se pueden identificar dos escenarios: uno por vientos persistentes del noroeste (escenario 2) y otro por vientos diurnos

del suroeste (escenario 3). En el escenario 2, la circulación estuarina inicialmente es reforzada. En el escenario 3, por contra, la circulación estuarina se debilita e incluso se invierte. En ambos casos, el intercambio de agua con el Mediterráneo disminuye después de unas cuantas horas, cuando el viento rompe la estratificación y genera fuertes gradientes horizontales a lo largo de la bahía. Debido a dichos gradientes longitudinales la relajación de la bahía es rápida (alrededor de 7-14 horas) hasta el escenario 1 cuando el viento cesa. Estos escenarios podrían tener implicaciones importantes para la ecología de la bahía, incluyendo la ocurrencia de fenómenos tales como las proliferaciones algales nocivas.

## A.5 El papel de los nutrientes inorgánicos y el fósforo orgánico disuelto en la dinámica fitoplanctónica de una bahía mediterránea. Un estudio de modelización.

El efecto de la disponibilidad de fósforo orgánico disuelto (POD) y la limitación por nutrientes en una bahía estuárica (Bahía de Alfacs, noroeste del Mediterráneo) han sido estudiados mediante un modelo ecológico cero-dimensional que incluye nitrógeno y fósforo (orgánicos e inorgánicos), dos grupos de fitoplancton (diatomeas y flagelados), un grupo de zooplancton, y detritos. Las simulaciones con y sin POD como fuente adicional de fósforo para el crecimiento del fitoplacton sugieren que el POD desempeña un papel importante en la dinámica del ecosistema. El POD es, de hecho, necesario para explicar la reducción observada del nitrato en verano y las magnitudes de biomasa fitoplanctónica registradas. Dos mecanismos no excluyentes permiten explicar el mecanismo mediante el cual el POD es disponible para el fitoplancton: la absorción directa, o la remineralización a fósforo inorgánico disuelto. La inclusión de ambos coincide en mayor medida con las observaciones. La inclusión de POD en el modelo conlleva el predominio de la limitación de crecimiento por fósforo durante el invierno, y del nitrógeno a finales de primavera y verano. Las simulaciones con y sin la inclusión de fósforo debido a resuspensión de sedimentos sugieren que

este proceso no afecta perceptiblemente el balance de nutrientes en la bahía.

## A.6 Discusión

Esta tesis estudia la interacción entre el forzamiento ambiental, la dinámica de circulación estuarina, y la comunidad fitoplanctónica en dos bahías estuáricas del Delta del Ebro, Alfacs y Fangar, las cuales se pueden considerar como un ejemplo de bahías pequeñas y micromareales. El trabajo se ha organizado a lo largo de tres líneas de investigación. La primera (Capítulo 2) examina la variabilidad de la comunidad de fitoplacton y su relación con con las variables físico-químicas mediante el análisis de series temporales de datos. El segundo, (Capítulo 3) explora los forzamientos clave que determinan la circulación y el intercambio de agua con el Mediterráneo en la bahía más grande (Alfacs). Finalmente, la tercera línea (Capítulo 4) se centra en el papel de los nutrientes orgánicos y inorgánicos en la sucesión y dinámica fitoplanctónica.

El análisis de 14 años de datos de contajes de fitoplancton y variables físico-químicas (Capítulo 2) reveló una estacionalidad clara en la composición de fitoplancton en ambas bahías, pero con un patrón diferente en cada una de ellas, lo que puede atribuirse al menor tiempo de residencia del Fangar, que es más pequeño que Alfacs pero recibe entradas de agua dulce comparables. Confirmando esta interpretación, un análisis de componentes principales indicó que la contribución de especies marinas (como *Thalassionema nitzschioides*) era más alta en Alfacs, mientras que había

una presencia mayor de especies indicadoras de agua dulce (*Peridinium quinquecorne* o *Eutreptiella* sp) en Fangar. Alfacs se caracteriza por un grupo de diatomeas típico de aguas costeras mediterráneas en otoño y un grupo de dinoflagelados en invierno, mientras que los grupos dominantes en Fangar son un grupo mixto de dinoflagelados y diatomeas que proliferan a finales de primavera y verano, y un grupo dominado por flagelados en invierno. El acoplamiento estacional entre factores ambientales y biológicos fue explorado más profundamente mediante la comparación de Funciones de Modo Intrínsecas obtenidas con una Descomposición Empírica de Modos de propiedades biológicas (los componentes principales del fitoplancton) y ambientales (temperatura, salinidad y estratificación). Encontramos relaciones significativa entre temperatura y salinidad y fitoplancton en ambas bahías, y también entre fitoplancton y estratificación en el Fangar. Para interpretar estos hallazgos debe tenerse en cuenta que más que un efecto directo de la temperatura o la salinidad, es probable que la relación entre estas variables y el fitoplancton sea mediada por otros factores ambientales y bióticos (tales como la disponibilidad de nutrientes debido a entradas de agua dulce o la abundancia de depredadores) que tienen un comportamiento estacional y que, por lo tanto, están asociados con cambios estacionales de temperatura o salinidad.

El estudio de las propiedades físicas de Alfacs (Capítulo 3) con números

adimensionales y simulaciones reveló que a escala estacional la mezcla debida a la marea es negligible comparada con la flotabilidad introducida por entradas de agua dulce. Como consecuencia la bahía se comporta como un sistema fuertemente estratificado en dos capas, en el cual la capa superficial fluye hacia fuera y la capa del fondo recibe entradas del Mediterráneo y fluye hacia dentro. La estacionalidad de las entradas de agua dulce influye en la fuerza de la estratificación, que es más débil cuando la afluencia de agua es mínima. La magnitud de las entradas de agua dulce subterráneas es incierta, pero debe ser suficientemente alta como para mantener el sistema de dos capas durante el periodo de canales cerrados. A escalas de tiempo de días a semanas, los eventos de viento influyen en la mezcla de agua y la circulación de la bahía, con efectos que dependen de la fuerza de la estratificación y la intensidad del viento. Tres escenarios se han definido usando el número de Richardson ($Ri^\star$) como indicador de las fuerzas relativas del viento y la flotabilidad. Para $Ri^\star > L/h$ (primer escenario), donde $L$ es la longitud de la bahía y $h$ la profundidad de la capa de mezcla, el viento es débil, la tensión del viento en la superficie genera turbulencia, la cual genera un hundimiento muy lento de la capa de mezcla. Cuando $Ri^\star < L/2h$, la tensión del viento induce un movimiento en la dirección del viento en la superficie, que se compensa por un movimiento de la capa profunda en la dirección opuesta. Este mecanismo crea una cizalla que hunde rápidamente

la capa de mezcla (a menudo en unas cuantas horas). Podemos definir dos escenarios en relación a las situaciones en las que la mezcla está dominada por la cizalla, en relación a la dirección del viento. El escenario 2 ocurre cuando el viento del noroeste, en general fuerte y de una duración de unos 2-3 días, genera $Ri^{\star} < L/2h$. La dirección del noroeste induce la capa superficial a moverse más rápidamente hacia la boca de la bahía, aumentando el intercambio con el exterior. El tercer escenario está asociados con números de Richardson bajos ($Ri^{\star} < L/2h$) causados por viento proveniente del suroeste, que puede ser fuerte pero suele ser corto (alrededor de 12 horas), puesto que normalmente tiene un comportamiento oscilatorio diario. La dirección del suroeste induce el agua de la superficie a pararse y moverse hacia dentro, en la dirección contraria a la dirección habitual, invirtiendo la circulación estuarina. En ambos casos después de unas cuantas horas, cuando el viento ha mezclado verticalmente la bahía, el intercambio disminuye debido a la destrucción de la circulación estuarina. Durante los episodios de mezcla la formación de un gradiente trasversal (N-S) hace que el proceso de relajación sea muy rápido, y la bahía retorna a un estado dominado por procesos gravitacionales en un periodo entre 7 y 14 horas después de que el viento pare. La dinámica de mezcla y circulación del agua en Alfacs tienen una relación estrecha con importantes procesos ecológicos tales como anoxia, disponibilidad de nutrientes y el desarrollo de proliferaciones.

Este capítulo identifica mecanismos por los cuales el forzamiento ambiental podría afectar la hidrodinámica y el ambiente ecológico en la bahía.

Finalmente la tercera línea de investigación (Capítulo 4) utiliza un modelo de cero dimensiones para explorar la relevancia del nitrógeno (N) y el fósforo (P) en la dinámica de dos grupos de fitoplancton con características típicas de diatomeas y flagelados. Una hipótesis básica es que la productividad de Alfacs no se puede explicar solamente por las entradas del fósforo inorgánico disuelto (PID) de los canales y del Mediterráneo. Los resultados del modelo indican que la liberación debido a la resuspensión del sedimento no es una fuente significativa de fósforo desde un punto de vista estacional, aunque podría desempeñar un papel importante a escalas de tiempo más cortas, especialmente durante la estación de canales cerrados. Por otra parte, las contribuciones de fósforo orgánico disuelto (POD) de los canales de descarga podían explicar la abundancia observada del plancton, y la reducción de nitrógeno inorgánico disuelto en verano. Los mecanismos por los cuales el POD se incorpora en el ciclo podrían ser tanto la remineralización de POD a fósforo inorgánico disuelto (PID) como la absorción directa de POD por parte del fitoplancton. La inclusión de ambos da un mejor acuerdo de los resultados modelo con las observaciones. Para evaluar la importancia relativa del N y el P en términos de la disponibilidad para el crecimiento del fitoplancton, se ha asumido que existe una colimitación

potencial por parte de ambos nutrientes. Cuando se incluye el POD en el modelo, el fósforo acaba siendo el nutriente más limitante durante invierno y primavera, mientras que el nitrógeno tiende a ser más limitador durante verano. Este capítulo muestra cómo la disponibilidad de N y de P depende de variables físicas, tales como entrada de de agua dulce, y cómo, a su vez, puede afectar la abundancia de dos grupos de fitoplancton.

Los resultados de esta tesis indican que los principales mecanismos de forzamiento que influyen en la composición y la abundancia de la comunidad de fitoplancton en las bahías de los estuarios micromareales del delta de Ebro dependen de la escala de tiempo considerada.

A escala de tiempo estacional, las entradas de agua dulce desempeñan un papel dominante respecto a las características físicas y biológicas de las bahías. Estas entradas vienen principalmente de los canales de irrigación del drenaje, pero también de la filtración de aguas subterráneas; sin embargo, como los flujos subterráneos no son conocidos, los párrafos siguientes se centrarán en las entradas de los canales. La descarga de los canales tiene tres consecuencias importantes. Primero, el agua dulce que descarga en la bahía crea una estratificación fuerte, que es responsable de los modelos de estuario de circulación descritos en el Capítulo 3. La circulación estuarina, combinada con el tamaño de las bahías, define los tiempos de residencia característicos que influyen fuertemente en la composición de

las comunidades de fitoplancton, según lo considerado en el Capítulo 2. En segundo lugar, el agua dulce que viene de los campos del arroz y descarga a través de los canales de desagüe es una fuente crucial de nutrientes para el ecosistema de la bahía. En particular, el Capítulo 4 muestra que las entradas de nitrógeno inorgánico disuelto (NID) y POD de los canales son necesarias para la generación de la producción primaria observada en Alfacs. Tercero, el flujo de agua dulce de los canales es alto de abril a octubre, bajo de noviembre a enero, y nulo de enero a marzo. Esta estacionalidad marcada, causada por la gestión humana de los campos de arroz y no por la meteorología, causa una marcada variación anual de los modelos de estratificación y de circulación (Capítulo 3) y de las entradas de nutrientes en las bahías (Capítulo 4). Estos factores afectan a la abundancia y a la composición del fitoplacton, tal y como se muestra en el Capítulo 2 y el Capítulo 4.

Aunque la descarga de los canales desempeñe un papel dominante desde un punto de vista estacional, el viento es crucial para la circulación y las propiedades químicas de las bahías a escalas de tiempo de algunos días. Según lo indicado en el Capítulo 2 para Alfacs, vientos fuertes pueden causar la mezcla vertical de la bahía. A su vez, esta mezcla afecta a la cantidad de agua intercambiada con el exterior y es posible que afecte también la concentración de fósforo, que puede ser liberado del sedimento en caso de

resuspension. Según lo explicado en este trabajo, ambos fenómenos pueden influir la comunidad de fitoplancton. Por ejemplo, eventos de viento podrían causar altas concentración de nutrientes y niveles bajos de intercambio con el mar que podrían favorecer el desarrollo de PANs. Por otra parte, ciertos regímenes de fuerte viento podían aumentar el intercambio con el Mediterráneo y actuar como detonantes de la desaparición de proliferaciones.

Aunque los resultados de esta tesis están basados en un caso de estudio de la ecología de Alfacs y Fangar, también pretenden proveer metodología y conceptos originales para un conocimiento mejor de los estuarios micromareales en general.

El Capítulo 2 propone una nueva metodología, la Descomposición Empírica de Modos, como una herramienta para analizar series temporales biológicas. Este procedimiento ha sido utilizado anteriormente para analizar datos de otros campos, tales como datos acústicos (Oonincx and Hermand, 2004) y paleoclimatológicos (Solé et al., 2007), o como herramienta para correlacionar series meteorológicas e hidrográficas (Solé et al., 2009), pero por lo que yo conozco, ésta es la primera vez que esta metodología se aplica a series de fitoplancton. Aunque, en el estudio presentado aquí, factores tales como el ruido inherente en los datos de fitoplancton o la corta longitud de las series ha hecho difícil interpretar IMFs de frecuencias no anuales, la Descomposición Empírica de Modos, con su capacidad de analizar datos no

estacionarios, tiene potencial para su uso en estudios ecológicos.

Los argumentos de escala desarrollados por (Fischer et al., 1979) para cuerpos de agua cerrados han sido adaptados para definir umbrales, basados en el valor del número de Richardson, para identificar si la mezcla en un estuario está dominado por cizalla o no en estuarios micromareales dominados por el viento. Los cálculos de estos umbrales, junto con los resultados de un modelo tridimensional han hecho posible la definición de escenarios de circulación en respuesta a vientos de distinta fuerza y dirección.

Los resultados de esta tesis apuntan a distintas líneas de trabajo futuro en relación a interacciones físico-biológicas en Alfacs y Fangar.

En primer lugar, dada la importancia de las entradas de agua dulce por superficie y subterráneas para la ecología de las bahías, el obtener series de datos de flujo, temperatura, y concentración de nutrientes orgánicos e inorgánicos en dichas aguas representaría una mejora significativa para cuestiones como por ejemplo determinar patrones estacionales de entradas de nutrientes, entender los cambios que suceden a escalas de días a semanas, las cuales pueden estar muy influenciadas por la variabilidad intrínseca de las variables, y la mejora de la parametrización de modelos físicos y biológicos.

En segundo lugar, la relación entre el fitoplancton y el intercambio de agua dentro y fuera de la bahía debe ser explorado con más detenimiento. El

Capítulo 3 muestra el efecto de dos clases particulares de eventos de viento sobre la circulación de Alfacs, y sugiere que éstos tienen un efecto en la tasa de intercambio con el Mediterráneo, pero este efecto debería ser abordado con más profundidad y los tiempos de residencia deberían ser analizados y comparados con observaciones. Un análisis del tiempo de residencia en áreas particulares de la bahía podría indicar cuáles son las más adecuadas para el desarrollo de proliferaciones algales nocivas. Para tal objeto, el modelo hidrodinámico que se ha implementado en el Capítulo 3 sería una herramienta muy útil.

Finalmente, las implicaciones de diferentes escenarios de forzamiento físico y tiempos de residencia para las poblaciones de fitoplancton podría ser explorada con el acoplamiento de un modelo físico, tal como el modelo hidrodinámico usado en el Capítulo 3 y un modelo ecológico como el del Capítulo 2. Un modelo acoplado físico-biológico validado y forzado con datos de campo adecuados podría proporcionar información sobre la dinámica del fitoplancton y el desarrollo de proliferaciones y ayudaría a explorar respuestas potenciales a cambios climáticos.

## A.7 Conclusiones

1. Un análisis de componentes principales de un conjunto de datos de fitoplancton de 14 años para Alfacs y Fangar (dos bahías estuáricas del

Delta del Ebro) mostraron patrones estacionales y revelaron que Alfacs se caracteriza por un grupo de diatomeas típicas de aguas costeras mediterráneas en otoño y un grupo de dinoflagelados en invierno. En Fangar la comunidad está dominada por un grupo mixto de flagelados y diatomeas que proliferan a finales de primavera y verano, y un grupo dominado por flagelados en invierno.

2. La comunidad de fitoplancton de Alfacs se caracterizó por especies marinas típicas, mientras que especies indicadoras de agua dulce estaban presentes también en Fangar. Estas diferencias en composición pueden ser atribuidas a tiempos de residencia más cortos en el Fangar, el cual tiene un volumen inferior a Alfacs pero recibe unas entradas de agua dulce comparables.

3. Una Descomposición Empírica de Modos aplicada a las variables ambientales y a los componentes principales del fitoplancton reveló la presencia de modos fuertemente estacionales en todas las series. Un índice de correlación entre pares de series mostró un acoplamiento significativo entre algunos de los componentes principales y las variables ambientales (temperatura, y salinidad en Alfacs y temperatura, salinidad y estratificación en Fangar). La temperatura del agua mostró una ligera tendencia al aumento durante el periodo de muestreo.

4. Argumentos de escala indican que, a escalas de tiempo estacionales, la

flotabilidad asociada a entradas de agua dulce domina el forzamiento mareal en Alfacs. El sistema pasa a ser fuertemente estratificado y desarrolla una circulación estuarina clásica, con una capa superficial que fluye hacia el mar, y una capa profunda que se mueve en la dirección opuesta.

5. A escalas de tiempo de unos pocos días, los eventos de viento son capaces de mezclar la columna de agua en Alfacs. Se ha definido un umbral basado en el número de Richardson ($Ri^{\star}$). Para $Ri^{\star} > L/h$, donde $L$ y $h$ son la longitud y profundidad de la bahía respectivamente, la mezcla es una consecuencia de los procesos convectivos y de mezcla turbulenta y la capa de mezcla se hunde muy lentamente. Para $Ri^{\star} < L/2h$, la cizalla es el mecanismo dominante, y actúa muy rápido (a escalas de tiempo de unas horas).

6. Un modelo hidrodinámico en tres dimensiones ha sido implementado para Alfacs. La validación del modelo ha mostrado un buen acuerdo entre los resultados de las simulaciones y las observaciones.

7. Usando los umbrales para regímenes de mezcla y simulaciones en tres dimensiones, tres escenarios han sido definidos en Alfacs. El escenario número 1 se caracteriza por vientos débiles que causan mezcla turbulenta, y está asociado a la circulación estuarina clásica. El escenario 2 implica vientos persistentes del noroeste que generan mez-

cla dominada por cizalla. La circulación estuarina inicialmente se fortalece. El tercer escenario se caracteriza por vientos diurnos del suroeste que también producen mezcla dominada por cizalla e invierten la circulación estuarina. En los escenarios 2 y 3, cuando la mezcla vertical es completa, el intercambio de agua con el exterior se ve reducido.

8. Un modelo ecológico en cero dimensiones ha sido implementado para estudiar el efecto de la disponibilidad de fósforo orgánico disuelto (POD) y la limitación de nutrientes en el crecimiento de fitoplancton en Alfacs.

9. Las simulaciones con y sin POD como fuente extra de fósforo para el crecimiento del fitoplancton sugieren que el POD es necesario para obtener la bajada de nitrato y el incremento de biomasa fitoplanctónica observados en Alfacs en verano.

10. La inclusión de POD en el modelo conlleva el predominio de limitación del crecimiento de fitoplancton por fósforo en otoño e invierno mientras que la limitación predominante es de nitrógeno durante finales de primavera y verano. Las simulaciones con y sin resuspensión de sedimentos sugieren que este proceso no afecta significativamente el balance de nutrientes en la bahía, aunque podría ser importante puntualmente.

# Bibliography


Allanson, B. (2001). Some factors governing the water quality of microtidal estuaries in south africa. *Water SA*, 27(3):373–386.

Aminot, A., Guillaud, J.-F., and Andrieux, F. (1993). Spéciaion du phosphore et apports en baie de seine orientale. *Oceanologica acta*, 16(5–6):617–623.

Anderson, D., Cembela, A., and Hallegraeff, G., editors (1998). *Physiological ecology of harmful algal blooms*. Springer-Verlag.

Andrieux-Loyer, F. and Aminot, A. (2001). Phosphorus forms related to sediment grain size and geochemical characteristics in french coastal areas. *Estuarine, Coastal and Shelf Science*, 52:617–629.

Arin, L., Anxelu, X., Moran, G., and Estrada, M. (2002). Phytoplankton size distribution and growth rates in the Alboran Sea (SW Mediterranean): short term variability related to mesoscale hydrodynamics. *Journal of Plankton Research*, 24(10):1019–1033.

Artigas, M. L. (2008). Estudi de la comunitat fitoplanctònica en relació amb la hidrodinàmica de la columna d'aigua a la badia dels Alfacs (NO Mediterrani). Master's thesis, Universitat de Barcelona.

Audry, S., Blanc, G., Schäfer, J., and Robert, S. (2007). Effect of estuarine sediment resuspension on early diagenesis, sulfide oxidation and dissolved molybdenum and uranium distribution in the gironde estuary, france. *Chemical Geology*, 238(3–4):149–167.

Bayó, A., Custodio, E., and Loaso, C. (1997). Las aguas subterráneas en el delta del ebro. *Revista de obras públicas*, 3368:47–65.

Bentzen, E., Taylor, W. D., and Millard, E. S. (1992). The importance of dissolved organic phosphorus to phosphorus uptake by limnetic plankton. *Limnology and Oceeanography*, 37(2):217–231.

Berdalet, E. and Estrada, M. (1993). Effects of turbulence on several dinoflagellate species. In *Toxic phytoplankton blooms in the sea*, pages 737–740. Proc. 5th Int. Conf. on Toxic Marine Phytoplankton, Elsevier.

Berman, T. and Bronk, D. A. (2003). Dissolved organic nitrogen: a dynamic participant in aquatic ecosystems. *Aquatic Microbial Ecology*, 31:279–305.

Biggs, R. B. and Cronin, E. L. (1981). Special characteristics of estuaries. In Nelson, B. J. and Cronin, E. L., editors, *Estuaries and nutrients*, pages 3–21. Humana Press, N. J. USA.

Blumberg, A. F. and Goodrich, D. M. (1990). Modeling of wind-induced destratification in chesapeake bay. *Estuaries*, 13(3):236–249.

Borsuk, M. E., Stow, C. A., Jr., R. A. L., Paerl, H. W., and Pinckney, J. L. (2001). Modelling oxygen dynamics in an intermittently stratified estuary: estimation of process rates using field data. *Estuarine, Coastal and Shelf Science*, 52:33–49.

Boyle, D. R. (1994). Design of a seepage meter for measuring groundwater fluxes in the nonlittoral zones of lakes – evaluation in a boreal forest lake. *Limnol. Oceanogr.*, 39(3):670–681.

Brainerd, K. E. and Cregg, M. C. (1995). Surface mixed and mixing layer depths. *Deep-Sea Research I*, 42(9):1521–1543.

Burchard, H. and Baumert, H. (1998). The formation of estuarine turbidity maxima due to density effects in the salt wedge. a hydrodynamic process study. *Journal of Physical Oceanography*, 28:309–321.

Calbet, A., Garrido, S., Saiz, E., Alcaraz, M., and Duarte, C. M. (2001). Annual zooplankton succession in coastal NP Mediterranean waters: the importance of the smaller size fractions. *Journal of Plankton research*, 23(3):319–331.

Camp, J. (1994). *Aproximaciones a la dinámica ecológica de una bahía estuárica mediterránea*. PhD thesis, Universitat de Barcelona.

Camp, J. (2005). Una aproximació quantitativa a la dinàmica de l'ecosistema deltaic. In *El delta de l'Ebre i la seva prblemàtica*, volume 929, Vol 55, Num 3, pages 123–130. Memorias de la real academia de ciencias y artes de Barcelona.

Camp, J. and Delgado, M. (1987). Hidrografía de las bahías del delta del ebro. *Inv.Pesq.*, 51(3):351–369.

Camp, J., Romero, J., Pérez, M., Vidal, M., Delgado, M., and Martínez, A. (1991). Production – consumption budget in an estuarine bay: how anoxia is prevented in a forced system. *Oceologia aquatica*, 10:145–152.

Carper, G. L. and Bachmann, R. W. (1984). Wind resuspension of sediments in a prairie lake. *Can. J. Fish. Aquat. Sci*, 41(12):1763–1767.

Chapelle, A., Ménesguen, A., Deslous-Paoli, J.-M., Souchu, P., Mazouni, N., Vaquer, A., and Millet, B. (2000). Modelling nitrogen, primary production and oxygen in a mediterranean lagoon. impact of oysters farming and inputs from the watershed. *Ecological modelling*, 127:161–181.

Chapra, S. C. (1984). *Surface water quality modeling*. McGraw-Hill Companies Inc. U.S.A.

Chen, C., Ji, R., Schwab, D. J., Beletsky, D., Fahnenstiel, G. L., Jiang, M., Johengen, T. H., Vanderploeg, H., Eadie, B., Budd, J. W., Bundy, M. H., Gardner, W., Cotner, J., and Lavrentyev, P. J. (2002). A model study of the coupled biological and physical dynamics in lake michigan. *Ecological Modelling*, 152:145–168.

Christian, R. R., Forés, E., Comín, F., Viaroli, P., Naldi, M., and Ferriari, I. (1996). Nitrogen cycling networks of coastal ecosystems: influence of trophic status and primary producer form. *Ecological modelling*, 87:111–129.

Cloern, J. E. (1987). Turbidity as a contro on phytoplankton biomass and productivity in estuaries. *Continental Shelf Research*, 7(11–12):1367–1381.

Cloern, J. E. (1996). Phytoplankton bloom dynamics in coastal ecosystems: a review with some general lessons from sustained investigation of San Francisco Bay, California. *Reviews of Geophysics*, 32(2):127–168.

Cloern, J. E. and Jassby, A. D. (2008). Complex seasonal patterns of primary producers at the land–sea interface. *Ecology Letters*, 11:1294–1303.

Cloern, J. E. and Jassby, A. D. (2009). Patterns and scales of phytoplankton variability in estuarine–coastal ecosystems. *Estuaries and Coasts*.

Crispi, G., Crise, A., and Solidoro, C. (2002). Coupled mediterranean ecomodel of the phosphorus and nitrogen cycles. *Journal of Marine Systems*, 33–34:497–521.

Cruzado, A., Velásquez, Z., del Carmen Pérez, M., Bahamón, N., Grimaldo, N. S., and Ridolfi, F. (2002). Nutrient fluxes from the ebro river and subsequent across-shelf dispersion. *Continental Shelf Research*, 22:349–360.

Curcó, A. (2006). Aiguamolls litorals: el Delta de l'Ebre. Síntesi del medi físic d'una zona humida litoral. *L'Atzavara*, 14.

Currie, D. J. and Kalff, J. (1984). A comparison of the abilities of freshwater algae and bacteria to acquire and retain phosphorus. *Limnol. Oceanogr.*, 29(2):298–310.

de Pedro, X. (2007). *Anoxic situations in estuarine zones without tidal forcing. An approach to the oxygen production/consumption budgets*. PhD thesis, Ecology department, University of Barcelona, Barcelona.

Delgado, M. (1987). Fitoplancton de las bahías del delta del Ebro. *Inv.Pesq.*, 51(4):517–548.

Delgado, M. and Alcaraz, M. (1999). Interactions between red tide microalgae and herbivorous zooplankton: the noxious effects of *Gyrodinium corsicum* (dinophyceae) on *Acartia grani* (copepoda: Calanoida). *Journal of Plankton Research*, 21(12):2361–2371.

Delgado, M. and and, J. V. F. (1995). Proliferación de un dinoflagelado del género *Gyrodinium* an la bahía de Alfacs (Delta del Ebro) asociado a mortandad de peces. In Castelló, F. and Calderer, A., editors, *Actas del V Congreso Nacional de Acuicultura*, pages 700–704.

Delgado, M. and Camp, J. (1987). Abundancia y distribución de nutrientes inorgánicos disueltos en las bahías del delta del Ebro. *Inv.Pesq.*, 51(3):527–441.

Delgado, M., Estrada, M., Camp, J., Fernández, J. V., Santmartí, M., and Lletí, C. (1990). Development of a toxic *Alexandrium minutum* Halim (Dinophyceae) bloom in the harbour of Sant Carles de la Ràpita (Ebro Delta, Northwestern Mediterranean). *Sci. Mar.*, 54(1):1–7.

Delgado, M., Fernández, M., Diogène, J., and Furones, D. (2004). Seguimiento del fitoplancton tóxico en las bahías del delta del ebro en los años 2001–2003. In Norte, M. and Fernández, J., editors, *Actas de la VIII Reunión Ibérica sobre fitoplancton tóxico y biotoxinas November 2003*, pages 159–166.

D'Elia, C. F., Sanders, J. G., and Boynton, W. R. (1986). Nutrient enrichment studies in a coastal plain estuary: phytoplankton growth in large-scale continuous cultures. *Canadian Journal of Fisheries and Aquatic Sciences*, 43:397–406.

Departament d'Agricultura, Alimentació i Acció Rural, 2008, Generalitat de Catalunya (2008). *Estadística de producció d'aqüicultura 2008*.

D'Ortenzio, F. and d'Alcalà, M. R. (2009). On the trophic regimes of the Mediterranean Sea: a satellite analysis. *Biogeosciences*, 6:139–148.

Estrada, M. (1979). Observaciones sobre la heterogeneidad del fitoplancton en una zona costera del mar Catalán. *Inv. Pesq.*, 43(3):637–666.

Estrada, M. and Berdalet, E. (1997). Phytoplankton in a turbulent world. *Scientia Marina*, 61 Suppl.:125–140.

Estrada, M., Sala, M. M., van Lenning, K., Alcaraz, M., Felipe, J., and Veldhuis, M. J. W. (2008). Biological interactions in enclosed plankton communities including *Alexandrium catenella* and copepods: Role of phosphorus. *J. Exp. Mar. Biol. Ecol.*, 355:1–11.

Farnós, A., Ribas, X., and Reverté, J. T. (2007). El Canal Porta Vida. Exhibition, Museu Comarcal del Montsià.

Fasham, M. (1995). Variations in the seasonal cycle of biological production in subarctic oceans: A model sensitivity analysis. *Deep-Sea Res.*, 42:1111–1149.

Fasham, M. J. R., Ducklow, H. W., and McKelvie, S. M. (1990). A nitrogen-based model of plankton dynamics in the oceanic mixed layer. *Journal of Marine Research*, 48:591–639.

Fasola, M. and Ruiz, X. (1996). The value of rice ields as substitute wetlands for waterbirds in the Mediterranean region. *Colonial waterbirds*, 19:122–128. Special Publication 1: Ecology, Conservation, and Management of Colonial Waterbirds in the Mediterranean region.

Fennel, K., Spitz, Y., Letelier, R. M., Abbott, M. R., and Karl, D. M. (2002). A deterministic model for $N_2$ Fixation at stn. ALOHA in the subtropical North Pacific Ocean. *Deep-Sea Research II*, 49:149–174.

Fennel, W. and Neumann, T. (2004). *Introduction to the modelling of marine ecosystems*. Elsevier, illustrated edition.

Fernández-Tejedor, M., Delgado, M., Garcés, E., Camp, J., and Diogène, J. (2010). Phytoplankton response to warming in two Mediterranean Bays of the Ebro Delta. CIESM Workshop 40 Phytoplankton Response to Mediterranean Environmental Change.

Fernández-Tejedor, M., Delgado, M., Vila, M., Sampedro, N., Camp, J., Furones, D., and Diogène, J. (2008). Resultados del programa de seguimiento de fitoplancton tóxico y biotoxinas en las zonas de producción de bivalvos de Cataluña: años 2003–2006 y primer trimestre del 2007. In Gilabert, J., editor, *Actas de la IX Reunión Ibérica sobre fitoplancton tóxico y biotoxinas Cartagena 7–10 May 2007*, pages 37–46.

Fernández-Tejedor, M., Soubrier-Pedreño, M. A., and Furones, M. D. (2004). Acute $LD_{50}$ of a *Gyrodinium corsicum* natural population for *Sparus aurata* and *Dicentratchus labrax*. *Harmful Algae*, 3:1–9.

Fernández-Tejedor, M., Soubrier-Pedreño, M. A., and Furones, M. D. (2007). Mitigation of lethal effects of *Karlodinium veneficum* and *K. armiger* on *Sparus aurata*: changes in haematocrit and plasma osmolality. *Diseases of aquatic organisms*, 77:53–59.

Fischer, H. B., List, E. J., Koh, R. C. Y., Imberger, J., and Brooks, N. H. (1979). *Mixing in inland and coastal waters*. Academic Press.

Fisher, T. R., Peele, E. R., Ammerman, J. W., and Harding, L. W. (1992). Nutrient limitation of phytoplankton in Chesapeake Bay. *Marine Ecology Progress Series*, 82:51–63.

Flynn, K. J. (this issue). Do external resource ratios matter? implications for modelling eutrophication events and controlling harmful algal blooms. *Journal of Marine Systems*.

Font, J., Salat, J., and Tintoré, J. (1988). Permanent features in the circulation of the Catalan sea. *Oceanol. Acta, Special issue*, 9:51–57.

Forès, E. (1989). Ricefields as filters. *Arch. Hydrobiol*, 116(4):517–527.

Forès, E. (1992). Nutrient loading and drainage channel response in a ricefield system. *Hydrobiologia*, 230:193–200.

Forès, E. and Comín, F. A. (1992). Ricefields, a limnological perspective. *Limnetica*, 10:101–109.

Franks, P. J. S. (2002). NPZ models of plankton dynamics: their construction, coupling to physiscs and application. *Journal of Oceanography*, 58:379–378.

Froelich, P. N. (1988). Kinetic control of dissolved phosphate in natural rivers and estuaries. *Limnol. Oceanogr.*, 33(4, part 2):649–668.

Gallegos, C. L. and Platt, T. (1985). Vertical advection of phytoplankton and productivity estimates: a dimensional analysis. *Marine Ecology Progress Series*, 26:125–134.

Garcés, E., Delgado, M., and Camp, J. (1997). Phased cell division in a natural population of *Dinophysis sacculus* and the *in situ* measurement of potential growth rate. *Journal of Plankton Research*, 19(12):2067–2077.

Garcés, E., Delgado, M., Masó, M., and Camp, J. (1999a). *In situ* growth rate and distribution of the ichthyotoxic dinoflagellate *Gyrodinium corsicum* paulmier in an estuarine embayment (Alfacs Bay, NW Mediterranean Sea). *Journal of Plankton Research*, 21(10):1977–1991.

Garcés, E., Fernández, M., Penna, A., Lenning, K. V., Gutiérrez, A., Camp, J., and Zapata, M. (2006). Characterization of NW Mediterranean *Karlodinium* spp. (Dinophyceae) strains using morphological, molecular, chemical and physiological methodologies. *J. Phycol.*, 42:1096–1112.

Garcés, E., Masó, M., and Camp, J. (1999b). A recurrent and localized dinoflagellate bloom in a mediterranean beach. *Journal of Plankton Research*, 21(12):2373–2391.

Gerreira, J. G., Wolff, W. J., Simas, T. C., and Bricker, S. B. (2005). Does biodiversity of estuarine phytoplankton depend on hydrology? *Ecological modelling*, 187:513–523.

Geyer, W. R. (1997). Influence of wind on dynamics and flushing of shallow estuaries. *Estuarine, coastal and shelf science*, 44:713–722.

Gilbert, P. M. and Pitcher, G., editors (2001). *GEOHAB. Global Ecology and Oceanography of Harmful Algal Blooms*. SCOR–IOC (UNESCO), Baltimore, Paris.

Giraud, X. (2006). Modelling an alkenone-like proxy record in the nw african upwelling. *Biogeosciences*, 3:251–269.

Golterman, H. L. (2001). Phosphate release from anoxic sediments or 'what did mortimer really write?'. *Hidrobiologia*, 450:99–106.

Goodrich, D. M., Boicourt, W. C., Hamilton, P., and Pritchard, D. (1987). Wind-induced destratification in Chesapeake Bay. *Journal of Physical Oceanography*, 17:2232–2240.

Grossman, G. D., Nickerson, D. M., and Freeman, M. C. (1991). Principal component analyses of assemblage structure data: utility of tests based on eigenvalues. *Ecology*, 72(1):341–347.

Guadayol, O. and Peters, F. (2006). Analysis of wind events in a coastal area: a tool for assessing turbulence variability for studies on plankton. *Scientia Marina*, 1(70):9–20.

Guerrero, R., Urmeneta, J., and Rampone, G. (1993). Distribution of types of microbial mats at the Ebro Delta, Spain. *BioSystems*, 31:135–144.

Guillén, J. (1992). *Dinámica y balance sedimentario en los ambientes fluvial y litoral del Delta del Ebro*. PhD thesis, Universitat Politècnica de Catalunya.

Hallegraeff, G. M. (2003). Harmful algal blooms: a global overview. In Hallegraeff, G., Anderson, D., and Cembella, A., editors, *Manual on Harmful Marine Microalgae, Monographs on Oceanographic Methodology*, 11, pages 25–49. UNESCO.

Hamby, D. M. (1994). A review of techniques for parameter sensitivity analysis of environmental models. *Environmental Monitoring Assessment*, 32:135–154.

Hansen, D. V. and Ratray, M. J. (1966). New dimensions in estuary classification. *Limnol. Oceanogr.*, 11(3):319–326.

Heil, C. A., Glibert, P. M., and Fan, C. (2005). *Prorocentrum minimum* (pavillard) schiller a review of a harmful algal bloom species of growing worldwide importance. *Harmful Algae*, 4:449–470.

Hernández, I., Pérez-Pastor, A., and Lloréns, J. L. P. (2000). Ecological significance of phosphomonoesters and phosphomonoesterase activity in a small mediterranean river and its estuary. *Aquatic Ecology*, 34:107–117.

Huang, B. and Hong, H. (1999). Alkaline phosphatase activity and utilization of dissolved organic phosphorus by algae in subtropical coastal waters. *Marine Pollution Bulletin*, 39(1–12):205–211.

Huang, N. E., Shen, Z., Long, S. R., Wu, M. C., Shih, H. H., Zheng, Q., Yen, N., Tung, C. C., and Liu, H. H. (1998). The empirical mode decomposition and the Hilbert spectrum for nonlinear and non-stationary time series analysis. *Proc. R. Soc. Lond. A*, 454:903–995.

Ibàñez, C., Canicio, A., Day, J. W., and Curcó, A. (1997). Morphologic deelopment, relative sea level rise and sustainable management of water and sediment in the ebre delta, spain. *Journal of Coastal Conservation*, 3:191–202.

Jassby, A. D. and Platt, T. (1976). Mathematical formulation of the relationship between photosynthesis and light for phytoplankton. *Limnology and oceanography*, 21:540–547.

Jeffrey, S. W. and Humphrey, G. F. (1975). New spectrophotometric equations for determining chlorophylls $a$, $b$,$c_1$ and $c_2$ in higher plants, algae and natural phytoplankton. *Biochem. Physiol. Pflanz.*, 167:191–194.

Ji, R., Davis, C. S., Chen, C., Townsend, D. W., Mountain, D. G., and Beardsley, R. C. (2007). Influence of ocean freshening on shelf phytoplankton dynamics. *Geophys. Res. Lett.*, 34:L24607.

Jin, B. K.-R., Hamrick, J. H., and Tisdale, T. (2000). Application of three–dimensional hydrodynamic model for lake okeechobee. *Journal of Hidraulic engineering*, 126(10):758–771.

jin Oh, S., Yamamoto, T., Kataoka, Y., Matsuda, O., Matsuyama, Y., and Kotani, Y. (2002). Utilization of dissolved organic phosphorus by the two toxic dinoflagellates *Alexandrium tamarense* and *Gymnodinium catenatum* (dinophyceae). *Fisheries Science*, 68(2):416–424.

Johannes, R. E. (1964). Uptake and release of dissolved organic phosphorus by representatves of a coastal marine ecosystems. *Limnology and Oceanography*, 9(2):224–234.

Kantha, L. H. and Clayson, C. A. (1994). An improved mixed layer model for geophysical applications. *J. Geophys. Res.*, 99:25235–25266.

Kennish, M. J. (2002). Environmental threats and environmental future of estuaries. *Environmental conservation*, 29(1):78–107.

Ketchum, B. H. (1954). Relation between circulation and planktonic populations in estuaries. *Evology*, 35(2):191–200.

Kierstead, H. and Slobodkin, L. (1953). The size of water masses containing plankton blooms. *J. Mar. Res.*, 12:141–147.

Kishi, M. J., Kashiwai, M., Ware, D. M., Megrey, B. A., Eslinger, D. L., Werner, F. E., Noguchi-Aita, M., Azumaya, T., Fujii, M., Hashimoto, S., Huang, D., Iizumi, H., Ishida, Y., Kang, S., Kantakov, G. A., cheol Kim, H., Komatsu, K., Navrotsky, V. V., Smith, S. L., Tadokoro, K., Tsuda, A., Yamamura, O., Yamanaka, Y., Yokouchi, K., Yoshie, N., Zuenko, J. Z. Y. I., and Zvalinsky, V. I. (2007). NEMURO – a lower trophic level model for the North Pacific marine ecosystem. *Ecological modelling*, 202:12–25.

Kocum, E., Underwood, G. J. C., and Nedwell, D. B. (2002). Simultaneous measurement of phytoplanktonic primary production, nutrient and light availability along a turbid, eutrophic uk east coast estuary (the colne estuary). *Marine Ecology Progress Series*, 231:1–12.

Lacroix, G. and Nival, P. (1998). Influence of meteorological variabilitu on primary production dynamics in the Ligurian Sea (NW Mediterranean Sea) with a 1D hydrodynamic/biological model. *Journal of Marine Systems*, 16:23–50.

Lancelot, C., Spitz, Y., Gypens, N., Ruddick, K., Becquevort, S., Rousseau, V., Lacroix, G., and Billen, G. (2005). Modelling diatom and *Phaeocystis* blooms and nutrient cycles in the southern bight of the north sea: the miro model. *Marine Ecology Progress Series*, 289:63–78.

Large, W. G. and Pond, S. (1981). Open ocean momentum flux measurements in moderate to strong winds. *Journal of physical oceanography*, 11:324–336.

Le Quéré, C., Rödenbeck, C., Buitenhuis, E. T., Conway, T. J., Langenfelds, R., Gomez, A., Labuschagne, C., Ramonet, M., Nakazawa, T., Metzl, N., Gillett, N., and Heimann, M. (2007). Saturation of the southern ocean $CO_2$ sink due to recent climate change. *Science*, 316:1735.

Lebo, M. E. (1991). Particle–bound phosphorus along an urbanized coastal plain estuary. *Marine Chemistry*, 34:225–246.

Legendre, P. and Legendre, L. (1998). *Numerical ecology*. Elsevier Science BV, Amsterdam, second english edition.

Li, M., Gargett, A., and Denman, K. (1999). Seasonal and Interannual variability of estuarine circulation in abox model of the Strait of Georgia and Juan de Fuca Strait. *Atmosphere–Ocean*, 37:1–19.

Lima, I. D., Olson, D. B., and Doney, S. C. (2002). Intrinsic dynamics and stability properties of size-structured pelagic ecosystem models. *Journal of Plankton Research*, 24(6):533–556.

Liu, J. T., Zarillo, G. A., and Surak, C. R. (1997). The influence of river discharge on hydrodynamics and mixing in a subtropical lagoon. *Journal of Coastal Research*, 13(4):1016–1034.

Llebot, C. (2007). Hydrodynamic characterization of a Mediterranean bay using Si3D, a three–dimensional model for estuarine circulation. Master's thesis, Universidad de las Palmas de Gran Canaria.

Llebot, C., Delgado, M., Turiel, A., Fernández-Tejedor, M., jorge diog ène, Camp, J., Solé, J., and Estrada, M. (2008). Coupling phytoplankton and hydrography in alfacs bay using principal component analysis and empirical mode decomposition. In *European Geosciences Union. General Assembly 2008*. Poster.

Llebot, C., Rueda, F., Solé, J., and Estrada, M. (2009). Stratification and mixing in dynamics in a mediterranean estuarine bay. In *ASLO Aquatic Sciences Meeting*. Poster.

Llebot, C., Spitz, Y., Solé, J., and Estrada, M. (2010). The role of inorganic nutrients and dissolved organic phosphorus in the phytoplankton dynamics of a Mediterranean Bay. A modeling study. *Journal of Marine Systems*, in press.

Lomas, M. W., Burke, A. L., Lomas, D. A., Bell, D. W., Shen, C., Dyhrman, S. T., and Ammerman, J. W. (2010). Sargasso Sea phosphorus biogeochemistry: an important role for dissolved organic phosphorus (DOP). *Biogeosciences*, 7:695–710.

Longhurst, A., Sathyendranath, S., Platt, T., and Caverhill, C. (1995). An estimate of global primary production in the ocean from satellite radiometer data. *Journal of Plankton Research*, 17(6):1245–1271.

López, J. and Arté, P. (1973). Hidrografía y fitoplancton del puerto del Fangar (delta del Ebro). *Inv.Pesq.*, 37(1):17–56.

Loureiro, S., Garcés, E., Fernández-Tejedor, M., Vaqué, D., and Camp, J. (2009a). *Pseudo-nitzschia* spp. (Bacillariophyceae) and dissolved organic matter (DOM) dynamics in the Ebro Delta (Alfacs Bay, NW Mediterranean Sea). *Estuarine, Coastal and Shelf Science*, 83:539–549.

Loureiro, S., Jauzein, C., Garcés, E., Collos, Y., Camp, J., and Vaqué, D. (2009b). The significance of organic nutrients in the nutrietion of *Pseudo-nitzschia delicatissima* (bacillariophyceae). *Journal of Plankton Research*, 31(4):399–410.

Lucas, L. V., Cloern, J. E., Koseff, J. R., Monismith, S. G., and Thompson, J. K. (1998). Does the sverdrup critical depth model explain bloom dynamics in estuaries? *Journal of Marine Research*, 56:375–415.

Luettich, R. A., Harleman, D. R., and Somlyódy, L. (1990). Dynamic behavior of suspended sediment concentrations in a shallow lake perturbed by episodic wind events. *Limnol Oceanogr.*, 35(5):1050–1067.

MacCready, P., Banas, N. S., Hickey, B. M., Denver, E. P., and Liu, Y. (2009). A model study of tide- and wind-induced mixing in the columbia river estuary and plume. *Continental Shelf Research*, 29:278–291.

MacIntyre, S., Romero, J. R., and Kling, G. W. (2002). Spatial-temporal variability in surgace layer deepening and lateral advection in an embayment of lake victoria, east africa. *Limnol. Oceanogr.*, 47:656–671.

Mallo, S., Vallespinós, F., Ferrer, S., and Vaqué, D. (1993). Microbial activities in estuarine sediments (ebro delta, spain) influenced by organic matter influx. *Scientia Marina*, 57(1):31–40.

March, J. and Cabrera, J. (1997). La infraestructura hidráulica, motor de desarrollo del delta. *Revista de Obras Públicas*, 3368:73–82.

Margalef, R. (1969). Composición específica del fitoplancton de la costa catalano–levantina (Mediterráneo occidental) en 1962–1967. *Investigación Pesquera*, 33:345–380.

Margalef, R. (1978). Life–forms of phytoplankton as survival alternatives in an unstable environment. *Oceanologica Acta*, 1(4):493–509.

Margalef, R. (1997). *Our biosphere*, volume 10 of *Excellence in Ecology*. Oldendorf/Luhe (Germany): Ecology Institute.

Margalef, R., Estrada, M., and Blasco, D. (1979). Functional morphology of organisms involved in red tides, as adapted to devaying turbulence. In Taylor, D. L. and Seliger, H. H., editors, *Toxic dinoflagellate blooms*. Proceedings of the second international conference ion Toxic Dinoflagellate Blooms.

Martin, A. P. (2003). Phytoplankton patchiness: the role of lateral stirring and mixing. *Progress in oceanography*, 57(2):125–174.

Martin, J. L. and McCutcheon, S. C. (1999). *Hydrodynamics and transport for water quality modeling*. Lewis Publishers.

Martín-Vide, J. (2005). Factors geogràfics, regionalització climàtica i tendències de les sèries climàtiques a Catalunya. In Llebot, J. E., editor, *Informe sobre el canvi climàtic a Catalunya*, pages 81–111. Generalitat de Catalunya. Institut d'Estudis Catalans, Barcelona.

McComb, A. J. and Others (1981). Eutrophication in the peel-harvey estuarine system, western australia. In Neilson, B. J. and Cronin, L. E., editors, *Estuaries and nutrients*, pages 323–342. N. J. Cifton and Humana Press.

McLusky, D. S. and Elliott, M. (2004). *The estuarine ecosystem: ecology, threats & management*. Oxford University Press, New York, NY (USA), third edition.

Merico, A., Tyrrell, T., Lessard, E. J., Oguz, T., Stabeno, P. J., Zeeman, S. I., and Whitledge, T. E. (2004). Modelling phytoplankton succession on the Bering Sea shelf: role of climate influences and trophic interactions in generating *Emiliana huxleyi* blooms 1997-2000. *Deep-Sea Research I*, 51:1803–1826.

Mian, M. H. and Yanful, E. K. (2004). Analysis of wind-driven resuspension of metal mine sludge in a tailings pond. *J. Environ. Eng. Sci.*, 3(2):119–135.

Ministerio de Obras Públicas, Transportes y Medio Ambiente; Ministerio de Industria y Energía (1995). *Libro blanco de las aguas subterráneas*.

Monbet, P., McKelvie, I. D., and Worsfold, P. J. (2009). Dissolved organic phosphorus speciation in the waters of the Tamar estuary (SW England). *Geochimica et Cosmochimica Acta*, 73:1027–1038.

Monismith, S. G., Imberger, J., and Morison, M. L. (1990). Convective motions in the sidearm of a small reservoir. *Limnology and oceanography*, 35(8):1676–1702.

Morales-Blake, A. R. (2006). *Estudio Multitemporal de la clorofila superficial en el mar Mediterráneo Noroccidental, evaluada a partir de datos SeaWIFS: Septiembre de 1997 a agosto del 2004*. PhD thesis, University de Barcelona, Barcelona.

Muñoz, I. (1990). *Limnologia de la part baixa del riu Ebre i els canals de reg: els factors físico-químics, el fitoplàncton i els macroinvertebrats bentònics*. PhD thesis, Universitat de Barcelona.

Muñoz, I. (1998). Carbono, nitrógeno y fósforo en la parte baja del río Ebro y en los canales de riego del Delta. *Oceologia aquatica*, 11:23–25.

Némery, J. and Garnier, J. (2007). Typical features of particulate phosphorus in the Seine estuary (France). *Hydrobiologia*, 588(1):271–290.

Niedda, M. and Greppi, M. (2007). Tidal, seiche and wind dynamics in a small lagoon in the Mediterranean Sea. *Estuarine, Coastal and Shelf Science*, 74:21–30.

Noble, M. A., Schroeder, W. W., Wiseman, W. J., Ryan, H. F., and Gelfenbaum, G. (1996). Subtidal circulation patterns in a shallow, highly stratified estuary: Mobile bay, alabama. *Journal of Geophysical Research*, 10(C11):25689–25703.

Noiri, Y., Kudo, I., Kiyosawa, H., Nishioka, J., and Tsuda, A. (2005). Influence of iron and temperature on growth, nutrient utilization ratios and phytoplankton species composition in the western subarctic Pacific Ocean during the SEEDS experiment. *Progress in Oceanography*, 64:149–166.

Officer, C. B. (1976). *Physical ocenography for estuaries (and associated coastal waters)*. J. Wiley and Sons.

Okubo, A. (1978). Horizontal dispersion and critical scales for phytoplankton patches. In Steele, J. H., editor, *Spatial pattern in plankton communities*, Series IV: Marine Sciences, pages 21–42. Nato conference on Marine biology, Erice, Italy 1977, Nato conference series.

O'Neill, R. V., DeAngelis, D. L., Pastor, J. J., Jackson, B. J., and Post, W. M. (1989). Multiple nutrient limitations in ecological models. *Ecological Modelling*, 46:174–163.

Oonincx, P. J. and Hermand, J. P. (2004). Empirical mode decomposition of ocean acoustic data with constraint on the frequency range. In *Proceedings of the Seventh European Conference on Underwater Acoustics*, Delft, The Netherlands. ECUA.

Paerl, H. W. (1988). Nuisance phytoplankton blooms in coastal, estuarine, and inland waters. *Limnol. Oceanogr.*, 33(4, part 2):823–847.

Palanques, A. and Guillén, J. (1998). Coastal changes in the ebro delta: natural and human factors. *Journal of Coastal Conservation*, 4:17–26.

Pinazo, C., Marsaleix, P., Millet, B., Estournel, C., and Véhil, R. (1996). Spatial and temporal variability of phytoplnkton biomass in upwelling areas of the northwestern Mediterranean: s coupled physical and biogeochmical modelling approach. *Journal of Marine Systems*, 7(2–4):161–191.

Platt, T., Callegos, C. L., and Harrison, W. G. (1980). Photoinhibition of photosynthesis in natural assemblages of marine phytoplankton. *Journal of Marine Research*, 38(4):687–701.

Prat, N. and Ibàñez, C. (2003). *Avaluació crítica del Pla Hidrològic Nacional i proposta per a una gestió sostenible de l'aigua del Baix Ebre*, page 127. Institut d'Estudis Catalans, Secció de Ciències Biològiques.

Prat, N., Muñoz, I., Comín, F. A., Lucena, J. R., Romero, J., and Vidal, M. (1988). Seasonal changes in particulate organic carbon and nitrogen in the river and drainage channels of the Ebro Delta (N.E. Spain). *Verh. Internat. Verein. Limnol.*, 23:1344–1349.

Quéré, C. L., Harrison, S. P., Prentice, I. C., Buitenhuis, E. T., Aumont, O., Bopp, L., Claustre, H., Cunha, L. C. D., Geider, R., Giraud, X., Klaas, C., Kohfeld, K. E., Legendre, L., Manizza, M., Platt, T., Rivkin, R. B., Sathyendranath, S., Uitz, J., Watson, A., and Wolf-Gladrow, D. (2005). Ecosystem dynamics based on plankton functional types for global ocean biogeochemistry. *Global Change Biology*, 11:2016–2040.

Quijano-Sheggia, S., Garcés, E., Flo, E., Fernández-Tejedor, M., Diogène, J., and Camp, J. (2008). Bloom dynamics of the genus *Pseudo nitzschia* (Bacillariophyceae) in two coastal bays (NW Mediterranean Sea). *Sci. Mar.*, 72(3):577–590.

Rabinovich, A. B. (2010). Seiches and harbor oscillations. In Kim, Y. C., editor, *Handbook of coastal and ocean engineering*, pages 193–236. World Scientific Publishing Co. Pte. Ltd.

Ramón, M., Cano, J., Peña, J. B., and Campos, M. J. (2005). Current status and perspectives of mollusc (bivalves and gastropods) culture in the Spanish Mediterranean. *Boletín. Instituto Español de Oceanografía*, 21(1–4):361–373.

Reynolds, C. S. (1997). *Vegetation processes in the pelagic: a model for ecosystem theory*, volume 9 of *Excellence in Ecology*. Oldendorf/Luhe (Germany): Ecology Institute.

Rueda, F., Vidal, J., and Schladow, G. (2009). Modeling the effect of size reduction on the stratification of a large wind-driven lake using an uncertainty-based approach. *Water Resources Research*, 45(3):15.

Rueda, F. J. and Cowen, E. A. (2005a). Exchange between a freshwater embayment and a large lake through a long, shallow channel. *Limnol. Oceanogr.*, 50(1):169–183.

Rueda, F. J. and Cowen, E. A. (2005b). The residence time of a freshwater embayment connected to a large lake. *Limnology and Oceanography*, 50(5):1638–1653.

Rueda, F. J. and Schladow, S. G. (2002). Quantitative comparison of models for barotropic response of homogeneous basins. *Journal of Hydraulic Engineering*, 128(2):201–213.

Rueda, F. J. and Schladow, S. G. (2003). Dynamics of large polymictic lake. II: Numerical simulations. *Journal of Hydraulic Engineering*, 129(2):92–101.

Rueda, F. J., Schladow, S. G., Monismith, S. G., and Stacey, M. T. (2003a). Dynamics of large polymictic lake. I: Field observations. *Journal of Hydraulic Engineering*, 129(2):82–91.

Rueda, F. J., Schladow, S. G., and Pálmarsson, S. O. (2003b). Basin–scale internal wave dynamics during a winter cooling period in a large lake. *J. Geophys. Res.*, 108(C3).

Rueda, F. J. and Smith, P. (2008). Analytical solutions for mathematical verification, chapter 3, test cases 1-4 and 6. In Wang, S. S., j. Roche, P., Schmalz, R. A., Jia, Y., and Smith, P. E., editors, *Verification and validation of 3D Free-surface flow models*. American Society of Civil Engineers.

Ruttenberg, K. C. (2001). Phosphorus cycle. In Steele, J. H., editor, *Encyclopedia of Ocean Sciences*, pages 2149–2162. Academic Press, Oxford.

Salat, J., Garcia, M. A., Cruzado, A., Palanques, A., Arin, L., Gomis, D., Guillén, J., de León, A., Puigdefàbregas, J., Sospedra, J., and Velásquez, Z. R. (2002). Seasonal changes of water mass structure and shelf slope exchanges at the Ebro Shelf (NW Mediteranean). *Continental Shelf Research*, 22:327–348.

Sarmiento, J. L., Hugues, T. M. C., Stouffer, R. J., and Manabe, S. (1998). Simulated response of the ocean carbon cycle to anthropogenic climate warming. *Nature*, 393:245.

Scavia, D., Field, J. C., Boesch, D. F., Buddemeier, R. W., Burkett, V., Cayan, D. R., Fogarty, M., Harwell, M. A., Howarth, R. W., Mason, C., Reed, D. J., Royer, T. C., Sallenger, A. H., and Titus, J. G. (2002). Climate change impacts on U.S. coastal and marine ecosystems. *Estuaries*, 25(2):149–164.

Schroeder, W. W., Dinnel, S. P., and Jr, W. J. W. (1990). Salinity stratification in a river-dominated estuary. *Estuaries*, 13(2):145–154.

Segura, M. (2007). *Relació entre la distribució de nutrients i oxigen dissolt i la composició elemental del fitoplàncton a la Mar Catalana (N–O Mar Mediterrània)*. PhD thesis, Universitat Politècnica de Catalunya.

Serra, P., Moré, G., and Pons, X. (2007). Monitoring winter flooding of rice fields on the coastal wetland of Ebre delta with multitemporal remote sensing images. In *International Geoscience and Remote Sensing Symposium, IGARSS*, pages 1–4, Barcelona.

Short, F. T. and Neckles, H. A. (1999). The effects of global climate change on seagrasses. *Aquatic Botany*, 63:169–196.

Smayda, T. (1990). *Novel and nuisance phytoplankton blooms in the sea: evidence for a global epidemic*. Elsevier, New York.

Smayda, T. (1997). Harmful algal blooms: their ecophysiology and general relevance to phytoplankton blooms in the sea. *Limnol. Oceanogr.*, 42:1137–1153.

Smayda, T. J. and Reynolds, C. S. (2001). Community assembly in marine phytoplankton: application of recent models to harmful dinoflagellate blooms. *Journal of Plankton Research*, 23(5):447–461.

Smith, C. G., Cable, J. E., Martin, J. B., and , M. R. (2008). Evaluating the source and seasonality of submarine groundwater discharge using a radon-222 pore water transport model. *Earth and Planetary Science Letters*, 273:312–322.

Smith, E. L. (1936). Photosynthesis in relation to light and carbon dioxide. *Proc. Natl. Acad. Sci*, 22:504–511.

Smith, P. E. (2006). A semi-implicit, three-dimensional model for estuarine circulation. Open-File report 2006–1004, U.S. Geological Survey.

Solé, J., Estrada, M., and García-Ladona, E. (2006a). Biological controls of Harmful Algal Blooms: A modelling study. *J. Mar. Syst.*, 61:165–179.

Solé, J., García-Ladona, E., and Estrada, M. (2006b). The role of selective predation in Harmful Algal Blooms. *J. Mar. Syst.*, 62:46–64.

Solé, J., Turiel, A., Estrada, M., Llebot, C., Blasco, D., Camp, J., Delgado, M., Fernández-Tejedor, M., and Diogène, J. (2009). Climatic forcing on hydrography of a Mediterranean bay (Alfacs Bay). *Continental Shelf Research*, 29:1786–1800.

Solé, J., Turiel, A., and Llebot, J. (2007). Using Empirical Mode Decomposition to correlate paleoclimatic time-series. *Natural Hazards and Earth System Sciences*, 62:46–64.

Spigel, R. H. and Imberger, J. (1980). The classification of mixed layer dynamics in lakes of small to medium size. *Journal of Physical Oceanography*, 10:1104–1120.

Spitz, Y. H., Moisan, J. R., and Abbott, M. (2001). Configuring an ecsystem model using data from the Bermuda Atlantic Time Series (BATS). *Deep-sea Research II*, 48:1733–1768.

Stalker, J. C., Price, R. M., and Swart, P. K. (2009). Determining spatial and temporal inputs of freshwater, including submarine groundwater discharge, to a subtropical estuary using geochemical tracers, biscayne bay, south florida. *Estuaries and Coasts*, 32:694–708.

Stevens, C. and Imberger, J. (1996). The initial response of a stratified lake to a surface shear stress. *Journal of Fluid Mechanics*, 312:39–66.

Sullivan, J. M., Swift, E., Donaghay, P. L., and Rines, J. E. (2003). Small-scale turbulence affects the division rate and morphology of two red tide dinoflagellates. *Harmful Algae*, 2:183–199.

Sverdrup, H. U. (1953). On conditions for the vernal blooming of phytoplankton. *ICES J. Mar. Sci.*, 18(3):287–295.

Sylaios, G. K., Tsihrintzis, V. A., Akratos, C., and Haralambidou, K. (2006). Quantification of water, salt and nutrient exchange processes at the mouth of a mediterranean coastal lagoon. *Environmental Monitoring and Assessment*, 119:275–301.

Taft, J. L., Taylor, W. R., and McCarthy, J. J. (1975). Uptke and release pf phosphorus by phytoplankton in the Chesapeake Bay Estuary, USA. *Marine Biology*, 33:21–32.

Torrecilla, N. J., Galve, J. P., Zaera, L. G., Retamar, J. F., and Álvarez, A. N. (2005). Nutrient sources and dynamics in a mediterranean fluvial regime (ebro river, ne spain) and their implications for water management. *Journal of Hydrology*, 304:166–182.

Tyrrell, T. (1999). The relative influences of nitrogen and phosphorus on oceanic primary production. *Nature*, 400:525–531.

Uncles, R. J. (2002). Estuarine physical processes research: some recent studies and progress. *Estuarine, coastal and shelf science*, 55:829–856.

Underwood, G. and Kromkamp, J. (1999). Primary production by phytoplankton and microphytobenthos in estuaries. *Advances in ecological research*, 29:93–153.

Utermöhl, H. (1958). Zur Vervollkommung der quantitativen Phytoplankton. *Methodik. Mitt. Inter. Ver. Limonol.*, 9:1–38.

Valle-Levinson, A., Wong, K.-C., and Bosley, K. T. (2001). Observations og the wind-induced exchange at the entrance to chesapeake bay. *Journal of Marine Research*, 59:391–416.

van de Kreeke, J. and Robaczewska, K. (1989). Effect of wind on the vertical circulation and stratification in the Volkerak Estuary. *Netherlands Journal of Sea Research*, 23(3):239–253.

van den Berg, A. J., Ridderinkhof, H., Riegman, R., Ruardij, P., and Lenhart, H. (1995). Influence of variability in water transport on phytoplankton biomass and composition in the southern North Sea: a modelling apporach (FYFY). *Continental Shelf Research*, 16(7):907–931.

Vaqué, D., Felipe, J., Sala, M. M., Calbet, A., Estrada, M., and Alcaraz, M. (2006). Effects of the toxic dinoflagellate *Karlodinium* sp. (cultured at different N/P ratios) on micro and mesozooplankton). *Scientia Marina*, 70(1):59–65.

Vargas-Yáñez, M., Martínez, M. C. G., Ruiz, F. M., Tel, E., Parrilla, G., Plaza, F., and Lavín, A. (2007). *Cambio climático en el Mediterráneo Español*. Instituto Español de Oceanografía, Ministerio de Educación y Ciencia, Madrid.

Vidal, M. (1994). Phosphate dynamics tied to sediment disturbances in Alfacs Bay (NW Mediterranean). *Mar. Ecol. Prog. Ser.*, 110:211–221.

Vidal, M., Morguí, J., Latasa, M., Romero, J., and Camp, J. (1992). Factors controlling spatial variability in ammonium release within an estuarine bay (Alfacs Bay, Ebro Delta,NW Mediterranean). *Hydrobiologia*, 235/236:519–525.

Vidal, M., Morguí, J.-A., Latasa, M., Romero, J., and Camp, J. (1997). Factors controlling seasonal variability of benthic ammonium release oxygen uptake in Alfacs Bay (Ebro Delta, NW Mediterranean). *Hydrobiologia*, 350:169–178.

Vidal, M., Romero, J., and Camp, J. (1989). Sediment-water nutrient fluxes. preliminary results of *in situ* measurements in alfaques bay, ebro river delta. *Scientia Marina*, 53:505 – 511.

Vila, M., Garcés, E., Masó, M., , and Camp, J. (2001a). Is the distribution of the toxic dinoflagellate *Alexandrium catenella* expanding along the NW Mediterranean coast? *Marine Ecology Progress Series*, 222:73–83.

Vila, M., Garcés, E., Masó, M., and Camp, J. (2001b). Is the distribution of the toxic dinoflagellate *Alexandrium catenella* expanding along the NW Mediterranean coast? *Marine Ecology Progress Series*, 222:73–83.

Vila, M. and Masó, M. (2005). Phytoplankton functional groups and harmful algal species in anthropogenically impacted waters of the NW Mediterranean Sea. *Sci. Mar.*, 69:31–45.

Walters, R. A., Cheng, R. T., and Conomos, T. J. (1985). Time scales of circulation and mixing processes of san francisco bay waters. *Hydrobiologia*, 129:13–36. 10.1007/BF00048685.

Weisberg, R. H. (1976). The nontidal flow in the Providence River of Narragansett Bay: a stochastic approach to estuarine circulation. *Journal of physical oceanography*, 6:721–734.

Wilson, B. W. (1972). Seiches. In Chow, V. T., editor, *Advances in hydrosciences*, 8, pages 1–94. Academic Press.

Yamamoto, T., Oh, S. J., and Kataoka, Y. (2004). Growth and uptake kinetics for nitrate, ammonium and phosphate by the toxic dinoflagellate *Gymnodinium catenatum* isolated from Hiroshima Bay, Japan. *Fisheries Science*, 70:108–115.

Yin, K. and Harrison, P. J. (2007). Influence of the Pearl River estuary and vertical mixing in Victoria Harbor on water quality in relation to eutrophication impacts in Hong Kong waters. *Marine Pollution Bulletin*, 54:646–656.

Zamani, K., Bombardelli, F. A., Wuertz, S., and Smith, P. E. (2010). Toward a 3-dimensional numerical modeling of tidal currents in san francisco bay. In *Proceedings of the World Environmental and Water Resources Congress 2010*, pages 1385–1394, Providence, RI. Environmental and Water Resources Institute, Anerucab Sicuety of Civil Engineers.

Zhong, L. and Li, M. (2006). Tidal energy fluxes and dissipation in the chesapeake bay. *Continental Shelf Research*, 26:752–770.

Zingone, A. and Enevoldsen, H. O. (2000). The diversity of harmgul algal blooms: a challenge for science abd management. *Ocean & Coastal Management*, 43:725–748.